THE UNIVERSITY
of EDINBURGH

ANALYSING MANGROVE FOREST STRUCTURE AND BIOMASS IN THE NIGER DELTA

Chukwuebuka Josephat Nwobi

THE UNIVERSITY *of* EDINBURGH

Thesis submitted for the degree of

Doctor of Philosophy

University of Edinburgh

School of Geosciences

Year of Submission 2019

Declaration

I declare that this thesis has been composed solely by myself and that it has not been submitted, in whole or in part, in any previous application for a degree. Except where states otherwise by reference or acknowledgment, the work presented is entirely my own.

Chukwuebuka Josephat Nwobi

9th of October, 2019.

Abstract

Mangrove forests are important in providing a range of ecosystem services, including food provision to local communities and carbon storage, while being globally restricted to tropical coastlines. The conservation and sustainability of mangrove forests is thus a globally important topic. Mangrove forests in the Niger Delta are known to be under high pressure from urbanisation, development, logging and oil pollution, and invasive species such as nipa palm (*Nypa fruticans*). These mangrove forests are poorly understood as a result of difficulty of access, social unrest and security restrictions. For example, there is no data on the relationship between disturbance and mangrove structure in the Delta, current area extent and biomass stocks of mangrove forest, its rate of loss, or the rate of nipa palm colonisation in the Niger Delta. The overall objective of this thesis is to utilise a combination of field data and earth observation to resolve these knowledge gaps. This work will estimate area and biomass of mangrove forests in the Niger Delta, and their changes over recent years through disturbance and invasive species.

I used an extensive field data collection in 2016-17 to establish 25 geo-referenced 0.25-ha plots across the Niger Delta and collected 567 ground control points. I estimated aboveground biomass (AGB) from a general allometric equation based on stem surveys. Leaf area index (LAI) was recorded using hemispherical photos. I performed and evaluated a land cover classification using a combination of Advanced Land Observatory Satellite Phased Array L-band SAR (ALOS PALSAR), Landsat ETM+ and the Shuttle Radar Topography Mission Digital Elevation Model (SRTM DEM) data. I also compared two supervised classification methods: Maximum Likelihood (ML) and Support Vector machine (SVM) classifiers. I established a relationship between field estimates of AGB and Advanced Land Observatory Satellite (ALOS) L-band radar backscatter. I also estimated the area of nipa palm and

mangrove forests in the Niger Delta and generated the first mangrove biomass map for the region, for 2007 and 2017 to obtain change information.

Plot estimated mean AGB was 83.7 Mg ha^{-1} and I found significantly higher plot biomass in close proximity to protected sites and tidal influence, and the lowest in the sites where urbanisation was actively taking place. The mean LAI was 1.45 and there was a significant positive correlation between AGB and LAI (R^2= 0.28). Satellite observations of NDVI for the growing season correlated positively with in-situ LAI (R^2= 0.63) and AGB (R^2= 0.8). Lower stem sizes (5-15cm) accounted for 70% contribution to the total biomass in disturbed plots, while undisturbed plots had a more even contribution of different size classes to AGB. Nipa palm invasion was significantly correlated to plots with larger variations in LAI (i.e. more patchy cover) and proportion of basal area removed within plots. The classification results showed SVM (overall accuracy 99.9 %) performed better than ML (98.7%) across the Niger Delta. I estimated a 2017 mangrove area of 794 561 ha and nipa extent of 11,419 ha. I discovered a 12% decrease in mangrove area and 694 % increase in nipa palm between 2007 and 2017. The highest radar-AGB relationship was from the combination of HH: HV and HV bands (R^2= 0.62, p-value < 0.001). Using this relationship, I estimated a mean and total AGB of 90.5 Mg ha^{-1} and 82 X 10^6 Mg in 2007; 83.4 Mg ha^{-1} and 65 X 10^6 Mg in 2017.

Local wood exploitation is removing larger stems (> 15 cm DBH) preferentially from these mangroves and creates an avenue for nipa palm colonisation. I identified opportunities to use remote sensing to estimate biomass, based on the LAI-AGB-NDVI relationship I found, and can serve as a calibration dataset for radar data to provide effective monitoring of mangrove forest degradation. It is clear from these results that remote sensing can be used to map the extent and changes in these land cover types, and thus such mapping efforts should continue for policy targeting and monitoring. I was able to show that mangroves of

the Niger Delta are at risk, from rapid clearance as well as from the invasive species nipa palm. I also provide evidence of mangrove cover loss of 11 000 ha yr^{-1} over a decade, resulting in biomass loss rate of 100 Mg ha^{-1} yr^{-1} while mangrove degradation rate of 56 Mg ha^{-1} yr^{-1} in the Niger Delta. Assessing carbon stock of mangrove forests in the Niger Delta can create a baseline for regional conservation and regeneration plans. These plans can create opportunities for generating carbon credits under reducing emissions from deforestation and forest degradation (REDD+).

Lay Summary

Mangrove forests are coastal forests located in tropical and sub-tropical regions of the world. These environments are important in providing services such as food provision, storm protection to local communications and carbon stock. Because of this, the conservation and sustainability of mangrove forests is globally important. Mangrove forests in the Niger Delta are faced with deforestation and degradation due to urbanisation, development, wood exploitation and oil pollution. This paves the way for the invasion of an alien species called nipa palm native to Asia which replaces cleared mangrove forests. Mangroves forests in the Niger Delta are poorly understood because of difficulties with access, social unrest, and security restrictions. There is no information on (i) the relationship between disturbance and mangrove forest structure in the Delta, (ii) the current area extent of mangrove forest in the Niger Delta, its rate of loss, nor the rate of nipa palm invasion and (iii) regional biomass map based on local field data. The overall objective of this thesis is to use a combination of field data and satellite imagery to monitor the effects of disturbance on mangrove forest structure and estimate current area and aboveground biomass (AGB) of mangrove forests in the Niger Delta.

Biomass is the biological weight of a living organism. I considered biomass of trees from the soil surface to the canopy, this excludes the biomass of the roots (belowground biomass). During fieldwork in 2016-17, I measured the diameter at breast height (DBH) of all mangrove trees in 25 plots across the Niger Delta, counted the number of nipa palm in each plot and collected ground control points (GPS). I used the DBH to estimate the AGB of mangroves trees. I also classified the plots into different disturbance classes namely: heavily exploited, medium exploited and undisturbed regimes. This was used to check the effect of mangrove wood cutting on the biomass and structure of mangrove forests in the Niger Delta. Using satellite imagery, I carried out a land cover classification of the Niger Delta. These land cover

classes were designated as urban regions, agricultural land, surface water, tropical forests, nipa palm, and mangrove forests. The classification was to estimate the area and change. I established a relationship between measurements of AGB from the field plots and 2017 satellite imagery. This relationship was used to predict the AGB of mangrove forests in the entire Niger Delta for 2007 and 2017. I generated the first mangrove biomass map for the region which shows how the biomass has changed over a decade.

My results showed that mangrove forests in the Niger Delta closer to the ocean had more biomass than forests closer to inland regions. I also showed that wood exploitation for fuelwood was changing the structure of mangrove forests in the region. The satellite classification results showed that mangrove area in the Niger Delta have been underestimated compared to other studies. I recorded a 12% decrease in mangrove area and a 7 fold increase in nipa palm between 2007 and 2017. My estimated total biomass of mangrove forests in the Niger Delta was lower than other studies. 2017 biomass estimates of mangrove forests in the Niger Delta showed a 33% reduction from 2007. 69% of biomass loss was due to deforestation (clearance of mangrove forests) and 28% was due to degradation (wood exploitation).

In conclusion, local wood cutting and clearance is removing larger stems from mangrove forests and creates an avenue for nipa palm invasion in the Niger Delta. There are opportunities to use satellite images to estimate biomass and land cover. It is clear from these results that satellite imagery can be used to map the extent and changes in these land cover types, and thus such mapping efforts should continue for policy targeting and monitoring. Mangroves of the Niger Delta are at risk, from rapid clearance as well as from the invasive species nipa palm. Assessing the biomass of mangrove forests in the Niger Delta can create a baseline for regional conservation and regeneration plans.

Acknowledgement

This PhD would not have been possible without the acceptance of my research by Mathew Williams, my principal supervisor. He has been a source of support and mentorship. He filled me with confidence and kept me on track anytime I lost focus. I also want to appreciate my second supervisor, Edward Mitchard, who guided me through the world of remote sensing and spatial analysis. I would also want to appreciate the entire Global Change Research Institute team for their listening ear and ready to assist attitude towards my research. I want to appreciate the Elizabeth Sinclair Fund for their assistance in field work and conferences during my research. I also want to thank the Federal Ministry of Education, Nigeria and President Goodluck Jonathan for the initiative of the Scholarship under which I am funded.

I want to appreciate Asuquo, Major, Goodluck, Davies, Francis, Martins and other field assistants during my field work. Your dedication to my work was a source of encouragement to me on days when the tide was not in our favour. I appreciate the warm reception of the Ete Kingdom, Kono and Oproama Communities which paved way for a smooth access to my field locations during my field work.

I would also want to thank all those who have gone before me and assisted me in various ways when I was only starting: Pedro and Sam. I also want to appreciate Keiko for her assistance in learning the Google Earth Engine for spatial analysis. I want to appreciate my mother's Bertha and Charity Nwobi for their moral support especially when it got rough. I want to appreciate my siblings especially Evelyn Nwobi for always being ready to sacrifice something for my thesis. I want to appreciate my extended family and friends who assisted me in various occasion during my field work. I dedicate my PhD to my late father whose early teaching has brought me thus far.

Table of Contents

List of Figures

List of Tables

List of Abbreviations

AGB: Aboveground Biomass

DBH: Diameter at breast height

LAI: Leaf Area Index

SRTM: Shuttle Radar Topography Mission

DEM: Digital Elevation Model

ALOS: Advanced Land Observing Satellite

PALSAR: Phased Array type L-band Synthetic Aperture Radar

GCP: Ground Control Point

GEE: Google earth engine

GEP: Google earth Pro

Und: Undisturbed

ME: Medium Exploitation

HE: Heavy Exploitation

NI: No Invasion

MI: Medium Invasion

HI: Heavy Invasion

NPP: Net Primary Productivity

CDM: Clean Development Mechanisms

LULUCF: Land Use, Land Use Change and Forestry

REDD+: Reduce Emissions from Deforestation and Degradation plus

dB: decibels

CASI: Compact Airborne Spectrographic Imager

SPOT: Systeme Pour l'Observation de la Terre

SVM: Support Vector machine

ML: Maximum Likelihood

RF: Random Forest

OBIA: Object Based Image Analysis

DF: Data Fusion

MMFR: Matang Mangrove Forest Reserve

Chapter 1

Introduction

1.1 Thesis Overview

This thesis aims to provide new insights into mangrove forest structure, cover and biomass in the Niger Delta using field surveys and remote sensing. This aim was motivated by the gaps in the knowledge of the following: (i) field plot data of mangroves in the Delta on local disturbance relations to biomass, canopy properties and size distributions of stems, (ii) supervised land cover classification based on ground control points collected in the region and; (iii) biomass map of the region based on the relationship of radar and field estimates of biomass. Furthermore, knowledge about how land cover and biomass change over time are also lacking. Such information is crucial for effective management and conservation of these important ecosystems. Hence, my thesis asks the following questions: (i) how do mangroves stand and canopy properties of mangrove forests in the Niger Delta relate to distance gradient and disturbance regime? (ii) what is the current area and change in cover of coastal vegetation in the Delta using optical and radar sensors?, and (iii) what is the current estimate and change in biomass of Niger Delta mangroves?

This thesis is based on work carried out in mangrove forests of the Niger Delta in southern Nigeria. Setting the framework in this chapter, I develop the terminology mangrove forests and the importance of mangrove research, describing these forests within the context of my study region and the reason for my focus in the Niger Delta. These forests are important as a result of their huge carbon potential but also the intersection with coastal population put them in a high vulnerability region for deforestation. I go further in setting the scene for the monitoring of mangrove forest structure, disturbance and productivity within the context of field work and remote sensing. I then summarise available mangrove research in Nigeria. Hence, providing the foundation to the rationale of this thesis and its relevance to Nigeria. The next chapter discusses the methodology I use in addressing my research questions

(Chapter 2). I then, present the results of my studies on wood exploitation effects on mangrove structure (Chapter 3), estimating mangrove and nipa palm area and change detection over a decade (Chapter 4) and generation of a mangrove aboveground biomass (AGB) over the same time period (Chapter 5). I then cumulate and summarize the major findings, its implication for mangrove research and future avenues for research and policy (Chapter 6).

1.2 Global importance of coastal ecosystems

Coastal ecosystems are an important sink in the global carbon budget due to their role in biogeochemical cycles and their connectivity to both land and the ocean. Blue carbon is a term coined for carbon sink in the oceans including coastal vegetation such as sea grasses, tidal marshes and mangrove forests. These ecosystems have the ability to sequester more carbon per unit area than terrestrial forests and are beneficial to climate change adaptation to sea level rise (IUCN, 2017). AGB of mangrove forests ranges from 7 and 312 t C ha^{-1} while belowground carbon storage ranges from 325 and 1893 t C ha^{-1} (Alongi, 2012). This recognition of blue carbon as an important tool in the mitigation of climate change has increased the study of carbon stock within these ecosystems (Crooks *et al.,* 2011; Herr and Pidgeon, 2011). This recognition has also increased the debate on the inclusion of coastal ecosystems in the reporting of carbon fluxes from countries in the Kyoto protocol and mechanisms in mitigating climate change impact (Grimsditch, 2011; Murray and Vegh, 2012). According to Lucas *et al.,* (2014); there are three main reasons why mangrove ecosystems should be studied extensively: 1) their potential as a carbon sink, 2) as indicators of climate change, and 3) as habitat to high plant and animal diversity. Information on mangrove biomass and carbon stocks is needed in order to analyse and add to the scarce information on carbon emissions from changes in mangrove ecosystems. New research information on how mangrove forests play a role in carbon storage and mitigation; and its inclusion in the

carbon market through the Clean Development Mechanisms (CDM), Land Use, Land Use Change and Forestry (LULUCF); and Reduce Emissions from Deforestation and Degradation plus (REDD+) has increased the need for further research on this ecosystem (Murray and Vegh, 2012). However, the relationship between regional mangrove productivity and human interaction is poorly understood. Increased study into this relationship and the means of conservation and restoration of mangroves is needed in order to protect this ecosystem by analysing the patterns of productivity and causes of their loss.

Mangroves are very productive ecosystems located in tropical and sub-tropical coasts (**Figure 1.1**). Reports of global coverage of mangrove forests shows the large uncertainty in estimating their coverage, however, a recent estimate gives a global extent of 137,600 km^2 (Bunting *et al.*, 2018). Mangroves are peculiar as a result of their geomorphology, salinity and tidal regime. They structurally and functionally adapt to their harsh environment through nutrient retention, vivparity and aerial roots enabling them survive water logged conditions (Alongi, 2014). Mangrove ecosystems in the world are of great ecological, economic and social importance (Bouillon *et al.,* 2008; Kauffman *et al.,* 2011; Mcleod and Salm, 2006) because they are both supportive of the lives of coastal population who depend on fisheries and also serve as an direct means of coastal protection from storm surges. One of the ecosystem services of mangroves is their ability to store carbon in their woody biomass and soil; making them important ecosystems in climate change reduction by preventing emissions and strengthening carbon storage (Sitoe *et al.,* 2014). However, this carbon sink is easily converted to a source due to coastal land use changes. Hence, the need to understand the effects of these land use changes to mangrove productivity in order to mediate mangrove deforestation.

The coastal location of mangroves makes them vulnerable to population stress and climate change. This vulnerability has made them more prone to degradation when compared to

other ecosystems (UNEP, 2009). These ecosystems are vulnerable to both climate change: such as sea level rise, erosion and salt water intrusion; and anthropogenic sources of stress: such as pollution, land use change and overexploitation of resources. Hence, they require ecological understanding in order manage the impact of these stressors (Scavia *et al.,* 2002). Sea level rise has been shown to be a threat to mangroves, due to its effects on sediment elevation and limited area for landward migration (Mcleod and Salm, 2006). Mangrove forests are affected by population concentration and growth driven by coastal development, aquaculture expansion and over-harvesting due to the location of mangroves on the coast (Alongi 2002; Okpiliya *et al.,* 2013); leading to the loss of carbon stored for decades at a faster rate than it is being accumulated. This has led to 12% reduction in mangroves over the past between 1996 and 2010 (Thomas *et al.*, 2017). Combined research into mangrove forest carbon potential and the cause of mangrove loss can create a platform in managing the rapid conversion of mangrove forests into a carbon source. One of the hindrance to this goal is the remote location of mangrove forests and the difficulty in assessing this ecosystem.

Figure 1.1: Mangrove forests distribution in the world from Giri et al., 2010 using Landsat imagery. Green areas represent mangrove distribution where Asia, West Africa and Australia with significantly more mangrove area.

1.3 Knowledge Gaps in Mangrove Research

Mangrove research should encompass both internal properties and external factors that structure this coastal vegetation. The study of the spatial and temporal characteristics of mangrove in terms of productivity and land use change increases the knowledge on their complex ecology, conservation; and importance in the global carbon cycle (Alongi, 2009). Information on mangrove cover, productivity and change can provide a benchmark on which restoration and conservation efforts are based. Methods employed in mangrove research involve field surveys which are important for temporal and spatial studies over small regions. However, in order to understand trends in the flow of nutrients, extent of disturbance and the biomass dynamics, the use of earth observation satellite data offers a means for global and regional mangrove research (Fatoyinbo and Simard, 2011). Globally, there is information on mangroves productivity and conservation dynamics. Komiyama *et al.* (2008) reported a range above-ground net primary productivity (NPP) between 3.99 and 26.7 t ha^{-1} $year^{-1}$ while Alongi (2009) reported a range of 0.5 to 112.1 t ha^{-1} $year^{-1}$ from different methodologies including gas exchange, light attenuation, litter fall, harvesting and incremental growth. However, regional and local research needs to be intensified in order to understand site specific mangrove properties.

The regional characteristics of mangrove forest stand structure, biomass and distribution over a landscape is an area of mangrove research lacking better understating especially in terms of disturbance. The lack of regional studies of mangrove biomass and local disturbance could be the reason for poor results in mangrove restoration plans being undertaken. The understanding of mangrove resources over-exploitation by coastal population may trigger a more concentrated plan for management and restoration. Global and regional studies have linked the rate of productivity in mangroves to their height and latitudinal location (Alongi, 2009; Saenger and Snedaker, 1993), structure of forest ecosystem (Day *et al.,* 1987; Day Jr.

et al., 1996; Sherman *et al.,* 2003), nutrient availability (Castañeda-Moya *et al.,* 2013) and ratio between litter fall and wood increment (Hossain *et al.,* 2008; Ross *et al.,* 2001). Lack of understanding between regional mangrove structure and disturbance can result in conservation and restoration efforts yielding less results leading to coastal invasive species replacing mangrove forests.

Alien invasive species are a threat to natural ecosystem function and service provision of a region. These are non-native species that tend to proliferate in areas where they were not intended to through introduction, naturalisation and invasion (Biswas *et al.,* 2007; Richardson *et al.,* 2000). Initially, they may have been introduced for other purposes, however, they have spread to other areas due to poor management. The Secretariat of the Convention on Biologival Diversity, (2010) has reiterated that the threat to biodiversity of invasive alien species; along with habitat change, climate change, exploitation and pollution; continues to be an increasing condition despite success in controlling it in some areas locally. A cause and effect system could also be the cause of increased colonisation of invasive species such as deforestation and natural hazards (Biswas *et al.,* 2007). The colonisation of invasive species can lead to a change in community structure and biodiversity by altering the function of the ecosystem (Hawthorne *et al.,* 2015). Monitoring the extent and spread of invasive and native species can provide a key to control the widespread colonisation and manage the conservation of alien and native species (Myint *et al.,* 2008), control the spread or utilise the species as a resource for the environment (Niphadkar and Nagendra, 2016). However, there is little information on the extent of local invasive alien species especially in coastal ecosystems.

1.4 Why the Niger Delta Mangrove Forests?

Nigeria's coastal ecosystem is endowed with mangroves which occupy nine out of thirty-six states of the country located on the East Atlantic West African coast. Nigeria has the largest

mangrove area in West and Central Africa (accounting for about 65.54% of the total mangrove area in the region); and the African continent (International Tropical Timber Organization, 2012; USAID, 2014). Nigeria's mangrove ecosystem is currently ranked fifth largest in the world after Indonesia, Brazil, Australia and Mexico (Bunting *et al.,* 2018). Nigerian mangroves are also of great economic and ecological importance to the coastal area of Nigeria despite the low species diversity (Feka and Ajonina, 2011), providing shoreline protection, fishery resources, fuel wood and cultural services (Abere and Ekeke, 2011). These ecosystem services can be divided into regulatory, provisioning, cultural and supporting services (Akanni *et al.*, 2017). Supporting services includes providing a habitat for biodiversity including native and transient species. In terms of regulation, mangrove forests in Nigeria provides shoreline protection from storm and erosion, water flow regulation, soil fertility and pollination. Mangroves also provide avenue for aesthetics, recreation and education. Lastly, mangrove forests provide food crops including sugar cane, rice and palm fruits while they improve fisheries from fin fishes to shell fish (Akanni *et al.*, 2017). There are five main mangrove species that have been identified along the coasts of Nigeria including red mangrove- *Rhizophora racemosa*, *R. mangle*, *R. harisonii*, white mangrove- *Avicienna germinans* and black mangrove- *Laguncularia racemosa* (Saenger and Bellan 1995; Ukpong 1991; Jackson 2011; FAO 2005).

Nigerian mangroves face degradation from pollution, urbanisation, wood over-exploitation and nipa palm (*Nypa fruticans*) invasion. The effects of these causes of degradation on mangrove forests are however poorly quantified. This coastal ecosystem in Nigeria have been involved in oil pollution since the onset of oil exploration in the Niger Delta in 1956 (Jack *et al.,* 2016). Globally, oil spills have resulted in the destruction of over 100 000 ha of mangrove vegetation since the 1950s (Duke, 2016). Oil spills results in clogged mangrove roots, increased anaerobic condition of mangroves and heavy metal pollution (IPIECA, 2002).

However, other subtle effects of urbanization and wood exploitation such as stem size structure have been overlooked resulting in scarce data on their effects on mangrove structure and function. One of the results is the colonization of cleared mangrove forests by a rapidly generating alien invasive species. Understanding the effects of these stressors on mangrove structure and biomass can create a baseline for mitigating their effects.

Nypa fruticans is an invasive palm species introduced in 1902 which have become a nuisance to the natural mangrove ecosystem in Nigeria. The proliferation of the palm results in a change to the soil characteristics, making it suitable for its proliferation (Ukpong, 2015). Characteristics of nipa vegetation includes lack of stilt roots, lack of litter fall and growth of dense monospecific stands resulting in a reduction of some of the ecosystem services provided by mangroves including sediment trapping, habitat for biodiversity, buffer effect from storms and fish production (Okugbo *et al.,* 2012). Mechanical and chemical methods have been used to reduce the growth of nipa palm, however both methods have issues with difficulty of execution and pollution (Invasive Species Compendium, 2011). Hence, one of the best means of managing its proliferation would be from cultural means by utilising its resources ranging from bio-energy, ethanol production and jewellery production (Global Invasive Species Database (GISD), 2015). However, studies have shown that lack of local market of these products reduces the efficiency of the method (Yang and Lo, 2002). Although various nipa invasion control programmes, in 1992 and 2002 have been established, there has been no positive result in managing its spread, while its utilisation is overlooked (Sunderland and Morakinyo, 2002). Reports have shown the important use of nipa palm in roof construction, cigarette wrapping, medicine and alcohol (Tsuji *et al.,* 2011). There is also a lack of information on nipa area extent over the years. Isebor *et al.,* (2003) reported that nipa palm had an area coverage of 851 km^2, however, the extent of invasion over time has seldom been probed and nipa palm is rapidly colonising cleared mangroves

along eastern coastal Nigeria. Information on nipa palm invasion over time could provide areas of high risk of mangrove threat, thereby, creating a strategy for mangrove conservation.

Restoration projects in coastal Nigeria have been largely unsuccessful due to a lack of relevant information to inform rehabilitation projects. Unfortunately, very little study has been done on mangrove productivity in Nigeria, evident from lack of a site specific allometric equations, relevant database of biomass information and reference data on losses and emissions. One of the reasons for the lack of mangrove biomass monitoring in Nigeria could be due to the harsh environment of mangroves. The root system of mangrove tree species and the regular inundation of tide along the coast of Nigeria makes it difficult to access mangrove environments for studies (**Figure 1.2**). Secondly, clashes between the local communities, private oil companies and the government makes the area a very volatile and high risk area. The security in the region is also low due to the activities of militants and illegal oil bunkering. The providence of basic biomass and growth patterns can increase the baseline data used to plan mangrove conservation projects in Nigeria.

Figure 1.2: Difficulty navigating mangrove forests as a result of the intricate root system and muddy substrate.

1.5 Methodologies in Mangrove Forests Monitoring

1.5.1 Field Survey of Mangrove Forest Structure

There is a lingering question on the effects of wood exploitation on mangrove forests productivity. Mangrove forest studies are primarily focused on productivity studies as a result of their carbon potential. Field surveys offer an intricate means of estimating ecosystem parameters in understanding nutrient dynamics, productivity, effects of anthropogenic disturbance and how these relate to one another. Stem diameter, leaf area index and soil properties are the major factors measured in understanding forest structure. Canopy features in mangrove forests are difficult to obtain because of the limited space for

access and equipment risk of salt water. Soil nutrients are also intricate in understanding nutrient dynamics in mangrove forests, however, tidal frequencies make soil properties difficult to investigate. On the other hand, stand characteristics can be used as a measure of biomass and stand structure dynamics.

Extensive mangrove biomass studies have been done globally using various approaches. According to Fatoyinbo and Armstrong, (2010); Lucas *et al.,* (2014) and Sessa, (2009), there are four main means of assessing carbon stocks in forest ecosystems, including: in-situ destructive biomass measurement, in-situ non-destructive biomass estimates, remote sensing inference and modelling. Of all these, non-destructive means of estimating biomass in mangroves is the most reported methodology of estimating biomass (Sessa, 2009). This involves the use of allometric equations to estimate the biomass of mangroves after measurement of other characteristics including trunk diameter and tree height. Allometry involves estimating the biomass of stands using proxies such as height, crown diameter and stem girth. One major advantage of allometric equations is in reducing the time and energy of carrying out a tree to tree analysis of biomass, and destruction of an already threatened ecosystem. Abib and Appadoo, (2012) reported that cutting down of mangroves trees in Mauritius was protected by law during their study of biomass and productivity of *R. mucronata*. The importance of allometric equations has also triggered the development of an international web platform on tree allometric equations called GlobAllomeTree (Henry *et al.,* 2013). According to Komiyama *et al.,* (2005); common allometric equations for all mangrove species lessens the burden of carrying out allometric equation studies for all mangrove species in all sites of the world. However, the problem of species or site variation in the relationship between the biomass and the measured parameters poses a problem in accurately estimating regional mangrove biomass.

The absence of a regional allometry in some regions may hinder estimation of mangrove biomass. This absence of regional allometric equations is largely a result of the time consuming and resource depreciative method of destructive sampling. Other complications include methodologies used in measurements, mangrove species similarities and the need for large datasets in the generation of allometric equations to cover a wide range of species and sizes (Ebuy *et al.,* 2011). These large data sets are scarcely available in most mangroves on the Atlantic coasts of Africa. Hence, the use of a general allometric equation in estimating AGB in mangrove forests creates a baseline for regions with regional allometry. My thesis will make use of a general allometric equation to estimate AGB in this study using diameter at breast height (DBH) as proxy (Komiyama *et al.,* 2005). General allometric equations are beneficial for mangrove biomass studies especially in regions like the Niger Delta where destructive sampling is detrimental to mangrove forests.

1.5.2 Environmental factors Affecting Mangrove Biomass

Environmental gradients are an integral component of mangrove productivity and this varies with proximity to tide, human influence and fresh water. Tidal influence and water chemistry are the two major factors affecting mangrove productivity (Lugo and Snedaker, 1974). Global factors affecting mangrove productivity include temperature and latitude while local conditions further act to modify the rate of productivity in mangroves (Alongi, 2009). There are various factors that are responsible for the variation of productivity across mangrove ecosystems. Saenger and Snedaker (1993) and Alongi (2009) have shown that mangrove biomass and productivity increases away from the equator from plots of biomass/ litter fall and productivity (light attenuation method) against latitude. This variation in mangrove productivity with latitude could be as a result of soil nutrient availability and use efficiency. Lugo and Snedaker, (1974) classified mangrove types based on their geomorphology including riverine, over wash, fringe, dwarf and basin mangroves forests. This could affect

the rate of productivity due to the relative influence of the riverine input, tidal flow and flooding period. Day *et al.,* (1996) showed that riverine mangrove forests, with higher nutrient inputs and lower soil salinities, had a higher wood biomass when compared to basin and fringe mangroves due to greater influence from nutrient-laden riverine runoff (Day *et al.,* 1996). Simard *et al.* (2019) also gave evidence of AGB decreasing with distance from tidal channel. Fromard *et al.,* (1998) has shown that different maturity stages in mangrove ecosystems in French Guiana result in different biomass and productivity status (Fromard *et al.,* 1998). Hossain *et al.,* (2008) also established that the rate of biomass increment in species depends on the age of the individual. Soil and water nutrients combined, provide the platform for mangrove structure and productivity but this can be modified by anthropogenic disturbance. This disturbance could affect the mangrove community in terms of structure and biomass, changing the normal trajectory of ecological succession.

1.5.3 Mangrove Forest Disturbance Effect on Mangrove Structure and Biomass

Mangrove forests are faced with natural disturbance such as hurricane and storm surges while anthropogenic sources of perturbation range from wood over exploitation to pollution. Natural disturbances cause uprooting of mangrove stands, alter the canopy cover of mangrove forests and modifying the sediment dynamics (Amir and Duke, 2009; Barr *et al.*, 2012; Clarke and Kerrigan, 2000). Amir and Duke, (2009) gave evidence of increase of forest gaps in mangrove forests of Moreton bay, Australia between 1978 and 2007 as a result of the increase in storm surges. Barr *et al.,* (2012) reported a complete removal of tree canopy and stand mortality in Florida Everglades following a Hurricane Wilma in 2005. Anthropogenic disturbances alter the nutrient composition of mangrove sediments, modify community structure or reduce the biomass and area of these forests (Clarke, 2004; Urrego *et al.,* 2014; Norilani *et al.,* 2014). Urrego *et al.,* (2014) gave evidence of wood exploitation

and poor conservation from asymmetric unimodal distribution of tree diameter and height in mangrove forests of the Gulf of Urabá. Norilani *et al.,* (2014), using basal area and biomass, gave evidence that anthropogenic disturbances from over-harvesting had a greater effect on mangrove structure than natural disturbance from lightening. These effects are evident from field assessments of basal area, leaf area index (LAI) and biomass.

Field surveys can detect the effects of disturbance on mangrove forests from analysis of stand diameter, basal area, canopy cover and biomass. The importance of establishing the rate and dynamics of biomass productivity in relation to nutrients and disturbance is important in long term monitoring. Management can use field survey information to give more attention to more productive regions in mangrove rehabilitation projects and also reduce the spread of invasive species (Cox and Allen, 1999; Kairo *et al.,* 2008). However, due to the harsh conditions of mangrove ecosystems, in situ measurements are difficult, hindering efforts to carry out spatial analysis of mangrove ecosystems (Fatoyinbo and Armstrong, 2010). The international community is therefore embracing other methods of monitoring mangrove health with digital image processing, modelling methods and remote sensing tools of choice are in use to provide spatial and temporal information on forest ecosystems including mangrove ecosystem biomass and carbon studies (Rabiatul and Mohd, 2012; Ryan *et al.,* 2011). Despite the intricacy of field surveys in mangrove forest monitoring, the spatial extent of mangroves requires the use of tools that can cover a wider mangrove region.

1.5.4 Remote Sensing Detection of Mangrove Forests Cover

Remote sensing is an important tool for mangrove research as it enables regional analysis on area and biomass patterns. Remote sensing methodology is less labour intensive and time consuming means of estimating cover and biomass of mangrove forests, and has the potential to generate and update maps of cover, biomass and vulnerability. There are two

main types of sensors used in forest monitoring: passive (optical) and active remote sensing. Passive or indirect remote sensing uses the radiation emitted from objects from earth in order to form images while active sensors uses the reflection of a radiation sent by a sensor to a target. The drawback of using passive remote sensing method is cloud cover- which obscures some of the properties of the land area (Fatoyinbo and Armstrong, 2010; Green *et al.,* 1998). However, active sensors are not affected by cloud cover but saturation of forest structure. Both sensors are used for forests mapping and biomass studies amongst others.

Mangrove ecosystems can be detected along the coast, as they are the first type of forest ecosystem encountered along tropical coasts with seagrasses and tidal marshes; however determining their inland extent is difficult using remote sensing methods. Optical remote sensors such as the Landsat ETM utilizes the characteristics of the reflectance of land structures while the active remote sensors such as SAR bands make use of the geometric properties in classifying mangroves (Li *et al.,* 2006; Lucas *et al.,* 2007). Although these two sensors can be used separately, more recent studies have used a mixture of the two to achieve higher accuracy in classification due to their combined individual strengths. Mangrove area classification is best achieved by considering sensor type, image processing method and adequate ground truthing data. Fassnacht *et al.,* (2014) deduced that the sensor type was the most important factor affecting accuracy followed by image processing method. According to Green *et al.,* (1998); they used three different optical data- hyperspectral (CASI: Compact Airborne Spectrographic Imager) and multispectral (SPOT XS: multispectral Systeme Pour l'Observation de la Terre and Landsat) to analyse various methods of classifying mangroves from the Turks and Caicos Islands, British West Indies. The analysis established that the best classification was derived from CASI and Landsat using PCA with accuracies 96% and 92% respectively as a result of the multispectral nature of CASI with better accuracy in mangrove differentiation. They concluded that differentiation between

mangrove and non-mangrove areas was best described by PCA/ band ratio analysis of Landsat data while differentiation between mangrove classes was best characterised using the same method but with CASI. Li *et al.,* (2006) also used three different data sets in classifying mangrove forest type (Landsat imagery alone, Landsat bands and C band Radar data; and new bands from fused Radar and Landsat imagery) with accuracy of 44.4%, 73.2% and 84.4% respectively. Hence, different sensors and image processing capabilities have different predictive qualities and combination of remote sensing data increases classification accuracy. The results of land cover classification can then be used as input to study specific characteristics of different land cover types such as biomass.

1.5.5 Radar Estimate of Mangrove Aboveground Biomass

Remote sensing is an effective tool in estimating biomass of forests as a result of the detecting capability of the sensors. Synthetic Aperture Radar (SAR) is the one of the widely used active remote sensing system in biomass monitoring of two methods- polarimetry and interferometry (Lucas *et al.,* 2007). In Polarimetric SAR (PolSAR), the microwave signal sent and received can be horizontal (H) or vertical (V) resulting in combined polarised data (HH, HV, VV or VH) after it has been reflected by an object in the form of backscatter (Mitchard *et al.,* 2009, 2012; Proisy *et al.,* 2000). There are various microwaves with different penetration capabilities X-band (3cm), C-band (6cm), S-band (9cm), L-band (24cm) and P-band (64cm) (Bamler and Hartl, 1999; Lucas *et al.,* 2007). The L and P-bands have the highest penetration power in forest ecosystems and have been used in the estimation of biomass (Hamdan *et al.,* 2014; Li *et al.,* 2003; R. Lucas *et al.,* 2014; Mougin *et al.,* 1999; Proisy *et al.,* 2000).

The backscatter coefficient (σ^0) in decibels (dB) is a measure of the reflected wave from a vegetation structure resulting from its interaction with the microwave. This value informs us of the wood structure of the area being measured. Hence, the measure of the back scatter

can be a measure of the biomass of a forest. The σ^0 has been shown in studies to have a significant relationship with the above ground biomass, hence, the structural diversity of the ecosystem affects the backscatter value (Fatoyinbo and Armstrong, 2010; Fatoyinbo and Simard, 2011; Hamdan *et al.,* 2014; Quiñones and Hoekman, 2004). Hamdan *et al.,* (2014) showed that ALOS PALSAR L-bands had low significant correlation with AGB with HV having the highest correlation of 40%. However, upon separation into AGB classes, they observed increased correlation to about 60% for AGB < 100 *Mg* ha^{-1} and reduced to very low values for AGB >150 *Mg* ha^{-1}.

The radar backscatter tends to have a saturation limit in effectively estimating the biomass of a region. This is the major hindrance of PolSAR in estimating biomass (Balzter *et al.,* 2007). The threshold is dependent on the polarisation and the wavelength of the radar signal. Various studies have given threshold limits of polarised wave forms. According to Proisy *et al.,* (1996), the saturation levels are about 50 Mg ha^{-1} at C-band, 130 Mg ha^{-1} at L-band, and 160 Mg ha^{-1} at P-band, while the maximum dynamics were observed in the HV- polarized bands of about 6 dB at P-band. This saturation levels show that various combinations of radar data bands react to different mangrove characteristics. The advantage of remote sensing is that it gives a spatial distribution or analysis of an area of interest. It is also important in change in time analysis of mangrove ecosystems (Sessa, 2009). The availability of remote sensing data over space and time means that this can be queried in terms of the change of land cover types and their characteristics over time.

1.5.6 Change Detection Analysis of Mangrove Cover and Structure

Analysis on the change of mangrove area and biomass is a crucial aspect of mangrove conservation because it gives an overview of the effects of land use change caused by different factors in the ecosystem. Coastal ecosystems around the world are deteriorating

rapidly due to population pressure, sea level rise and storm surges (Polidoro *et al.,* 2010); hence the need for a means of assessing this ecosystem without further compromising its state. Remote sensing application in mangrove change detection is important because it gives a spatial and temporal dimension to coastal change, which is an important aspect of climate change due to its high risk impact from sea level rise (Blasco *et al.,* 1996). In terms of change detection, Lucas *et al.,* (2014) explained that change in radar back scatter over a period of time in an area can form a basis to monitor mangrove ecosystem change which could be as a result of sea level rise or storm surges, sedimentation or erosion. The system of change detection involves extraction of features and the decisive function (Hussain *et al.,* 2013). The extraction of features includes classification of land cover types in terms of cover and biomass to be queried, while the key element in change detection involves the decision function which could be in different levels- temporal or spatial change. The process of change detection involves pre-processing of the remote sensing data; change detection technique to be used and accuracy assessment. Choosing a technique for change detection is dependent on the objective of the study, which includes the type of imagery available, size of study area and spatial resolution.

There are different processing methods used in classifying mangroves and change detection. According to (Hussain *et al.,* 2013), there are three main techniques in change detection analysis using remote sensing including 1) pixel-based; 2) object-based and 3) spatial data mining techniques. Change detection for detailed changes have employed mostly pixel and object based techniques in extracting features. The most reported approaches in mangrove change detection have been pixel-based including artificial neural network, support vector machine (SVM), random forest, maximum likelihood and decision tree (Jhonnerie *et al.,* 2015; Sambodo and Indriasari, 2013; Wijaya and Gloaguen, 2009). Random forest (RF) classification is a type of object based image analysis that uses a non-parametric

classification algorithm which has been shown to be better at mangrove classification. However, RF has the problem of object misclassification especially in transition areas; time difference of field observation and satellite imagery which results in object misinterpretation and change in land cover classes (Jhonnerie *et al.,* 2015). The Support Vector Machine (SVM) is a supervised non-parametric statistical learning technique and makes no assumption about the underlying data distribution. The algorithm learns from training data and automatically finds a threshold values from the spectral features for classifying change from no-change (Hussain *et al.,* 2013).

According to Heumann, (2011), data fusion (DF) approach and object based image analysis (OBIA) are new means of estimating change in mangrove area using remote sensing. OBIA uses grouped pixels based on image properties for analysis but DF uses different data sources to maximise the extent of available information. Sambodo and Indriasari, (2013) used a support vector machine method (SVM) to carry out a land cover classification using ALOS PALSAR data with an accuracy of 87.79% which was higher when compared to the Maximum Likelihood (ML) method. Jhonnerie *et al.,* (2015) compared two methods of classifying mangrove area using Landsat 5, ALOS PALSAR bands and spectral transformations. The results showed that the random forest methods had a higher accuracy (81.7% using a combination of Landsat, Radar and spectral transformations such as NDVI) than the ML method (76.8% using a combination of Landsat and Radar). However, the decision tree system (Tian *et al.*, 2016) of a RF classification results in misclassification when there is insufficient training data and this is where SVM performs better when there is reduced number of training pixels for classification.

The literature above shows that while there are various data sources used in classifying and carrying out change detection analysis, using the right combination of data source and image processing method provides options of retrieving structural features for mangrove forest

monitoring. Hence, optical remote sensing alone is insufficient in describing biomass of mangroves as a majority of the biomass exist in the woody part of the tree. Accuracy improvements in classification and change detection can be done using variations of datasets and methodology comparison. Propagating the error in estimating the characteristics of forests creates a baseline for predicting current and future trends in mangrove forests using modelling tools.

1.6 Mangrove Forest Biomass Research in Africa and Nigeria

There have been extensive studies on mangrove productivity and change detection in some East and West African countries, but limited information is available in Nigeria. Kauffman and Bhomia (2014) carried out training and carbon stock assessment in Gabon, Liberia and Senegal under the Blue Carbon Initiative (CIFOR, 2014). In 2014, they reported carbon stock range of 154 – 1337 Mg C ha^{-1}, with an average of 728 Mg C ha^{-1} in 20 to 30 stands of mangroves across the three countries. Ajonina *et al.,* (2014) estimated mean biomass of 1 520 ± 164 Mg C ha^{-1} with 65 % soils and roots and 35.0 % in the AGB in four Central African countries- Cameroon, Gabon, Republic of Congo (RoC) and Democratic Republic of Congo (DRC) (Ajonina *et al.,* 2014). They also estimated that between 2000 and 2010, 77,107 ha of mangrove forest was cleared in Central Africa which is equivalent to over 100,000,000 tonnes of carbon dioxide emitted. This was an attempt to inform policy makers to include mangroves in future REDD+ programs.

Flores De Santiago *et al.,* (2013) used an object based image analysis (OBIA) method to classify mangroves in Guinea, West Africa using ALOS PALSAR bands reporting an accuracy of up to 92.3% to classify mangrove from non-mangrove and differentiated three classes of mangroves with accuracy of 64.9% (Flores De Santiago *et al.*, 2013). Carreiras *et al.,* (2012) also examined the accuracy of two methods of estimating AGB of forests in Guinea Bissau using ALOS PALSAR and found that the machine learning algorithm (based on bagging

stochastic gradient boosting) outperformed a semi empirical algorithm, with correlation coefficient between observed and predicted forest AGB values of 0.95 and in a root mean square error of 26.62 *Mg* ha^{-1} (Carreiras *et al.,* 2012). The total mangrove forest AGB carbon stock of 9.08 Mt C was obtained with a mean biomass of 56.16 Mg ha^{-1}. These studies have shown that the use of ALOS PALSAR is valuable in both change detection, classification and biomass estimation of biomass in West Africa.

The Nigerian coastline can be divided into three regions- the Lagos lagoon complex, the Niger Delta region and the Cross River estuary- **Figure 1.3** (Saenger and Bellan, 1995). The Niger Delta is the largest delta in Africa and one of the largest in the world. The region has been known to support high biodiversity, commercial fisheries and timber production (Ndidi *et al.,* 2015). The Nigerian coastline is widely known for its incidence of oil spills, urbanisation and deforestation rates with little information of the documentation of the effects of these activities on the carbon balance in the environment (Langeveld and Delany, 2014). Although there have been various published and unpublished studies on mangroves in Nigeria on community structure, pollution, disease, restoration, soil vegetation relationships (Ukpong, 1994); soil salinity and mangroves (Ukpong, 1991); change in mangrove coverage (Okpiliya et al, 2013); carbon credits (Edu *et al.,* 2014); remote sensing and oil spill (Balogun, 2015); remote sensing and mangrove management (Adedeji *et al.,* 2011; Mmom and Arokoyu 2010); leaf litter dynamics (Edu *et al.*, 2014); mangrove vegetation survey (Amadi *et al.*, 2014); allometry (Nwigbo *et al.,* 2013) and remote sensing in biomass monitoring (Fatoyinbo and Simard 2013); very little information exists on mangrove productivity.

The only reported study on productivity was done by Edu *et al.,* (2014) who studied litter fall dynamics in the Cross River estuarine area of the south eastern Nigerian coastline (Edu *et al.*, 2014). They estimated annual rate of litter fall as 4.49 Mg ha^{-1} yr^{-1} which falls within the range of reported litter fall production 4.10-12.52 Mg ha^{-1} yr^{-1} (Komiyama *et al.,* 2008) while

turnover rates of leaf litter indicated export of nutrients during ebbing tide into the estuary. They also reported that leaf litter was the highest contributor of this production (64%). These production estimates are important in understanding production dynamics across tidal gradients although, more research is needed to incorporate wood production to this estimate. Elaborate classification analysis has been done on the mangrove ecosystems in Cross River estuary in south eastern Nigeria based on soil salinity and nutrient gradient (Ukpong, 1991, 1994, 2000a, 2000b). Ukpong (1991) reported negative correlation between mangrove species and soil salinity with *Laguncularia racemosa* occurring in high salinity areas and *Avicennia germinans* having the widest ecological range for salinity. Contrary to other studies which have reported strong correlations of mangrove species to phosphorus limitation (Castaneda, 2010); Ukpong, (2000) reported that mangrove species best correlated with cat-ions with Magnesium, Potassium and Calcium with *Avicennia* species occurring in high calcium regions (Ukpong, 2000a). These studies gave us a clear relationship between soil properties and mangrove species distribution, however, there was no relationship of these parameters with mangrove biomass. There have also been reports on spatial analysis of mangrove forests in Nigeria (Fatoyinbo and Simard, 2013; James *et al.*, 2007). In the absence of field data on biomass in mangrove ecosystems, remote sensing is the best approach at regional level (Anaya *et al.,* 2009). James *et al.,* (2007) reported that between 1986 and 2002, the Niger Delta lost about 21 342ha of mangrove using ISODATA classification of Landsat data. They attributed this loss of mangroves to nipa palm invasion, oil pollution, dredging, and urbanisation. Fatoyinbo and Simard, (2013) also carried out the first systematic study of estimating mangrove area, height and biomass in Africa. The study states that the best measurement tool in spatial distribution and 3D structure of mangroves is the use of remote sensing from LiDAR and InSAR. The study estimated mangrove area, above ground biomass and mean biomass for Nigeria as 8573km^2, 94 788 000 Mg and 111

Mg ha^{-1} respectively. The various reports on mangrove including litter fall, change detection and biomass estimates in Nigeria is insufficient to inform stakeholders on regional conservation of this ecosystem resulting in poor management and abandoned mangrove restoration projects. Some mangrove protected areas in the Niger Delta have been abandoned by some management organisations although partly due to security but also as a result of poor knowledge on productivity patterns of mangroves. The rapid increase of nipa palm is also encroaching a mangrove protected site in Rivers State. Hence, increased research in the Niger Delta on landscape mangrove biomass patterns should be spurred on with the involvement of various stakeholders. Knowledge on these will improve the understanding on how the Niger delta is contributing to the regional and global carbon cycle.

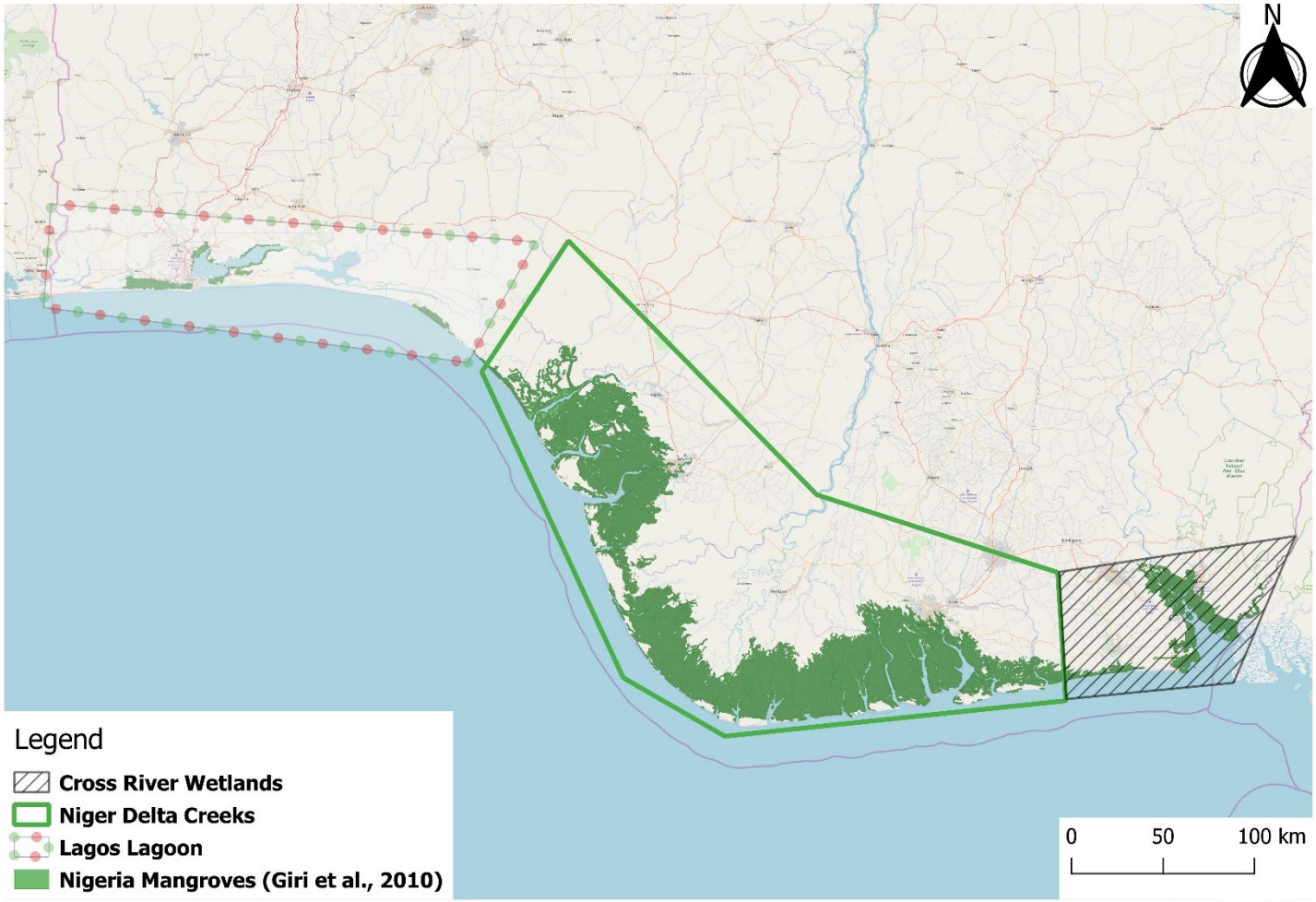

Figure 1.3: A mangrove map of Coastal Nigeria showing the divisions of the coast.

1.7 Rationale: Understanding the Effect of Wood Exploitation on Mangrove Structure and Remote Sensing Application in Monitoring Mangrove Forests in Nigeria.

Fuel wood is one of the ecosystem services provided by mangrove forests in the Niger Delta (**Figure 1.4**). However, unsustainable harvesting coupled with non-existent laws for control results in a detrimental feedback of this service to mangrove forests. Recently, at the Matang Mangrove Forest Reserve (MMFR) in Peninsular Malaysia, a suggested sustainable wood production from a 30 years old stand was 372 t ha^{-1} (Goessens *et al.*, 2014). Feka and Ajonina, (2011) estimated a volume of 4 million m^3 wood was harvested from mangrove forests in Nigeria in 1993. Although there has been no report of what a sustainable mangrove harvest may mean in Nigeria, Kinako, (1977) estimated a 600 000 tonnes of mangrove per year as sustainable in the Niger Delta (Feka and Ajonina, 2011). These values, though outdated (which also reflects the limited research in mangrove harvesting in Nigeria), shows how much pressure the mangrove forests in the Niger Delta have faced in the past decades. The problem arises where there has been no ongoing replanting of harvested mangrove resource over the decades until recently in Cross River and River states where the United Nations and locals are collaborating to replant mangrove trees. The continuous unsustainable harvesting results in a modification of the mangrove forest structure and possible change in mangrove ecosystem in the region. One of the motivation of this thesis is to bridge the information gap on the effects of development and wood exploitation, especially by local communities who depend on this ecosystem for fuel wood; on mangrove forest biomass, stand structure and canopy properties. The information generated in filling this gap can also form a foundation to generating mangrove forests management plan in Nigeria.

There is limited information on carbon stock in Africa, despite the availability of mangrove biomass studies across the world. There is however, more mangrove research being carried out in Madagascar, Kenya, Gabon, Sierra Leone and Cameroon (Alemayehu *et al.,* 2014;

Carreiras *et al.,* 2012; Flores De Santiago *et al.,* 2013; Jones *et al.,* 2015; Sitoe *et al.,* 2014). Nigeria, having the largest mangrove area in Africa and the fourth largest in the world has scarce information on biomass. The importance of embarking on biomass studies in Nigeria is to enable a relationship to be formed between mangrove forest structure and climate change effects, anthropogenic feedbacks and monitor forest loss. Also, there is very little data on the area coverage of one of the major threats to mangrove- Nipa palm (*Nypa fruticans*) invasion. Hence there is need to update the current area coverage of mangroves in some regions in coastal Nigeria and the extent of Nipa palm invasion. The integration of mangrove structure and biomass studies with its relation to local disturbance over temporal and spatial scale in Nigeria can help inform restoration projects by directing plans to high vulnerable regions.

Knowledge on mangrove structure and function can inform scientists involved in mangrove restoration projects in Nigeria leading to success in conservation plans. Productivity studies can aid in monitoring the growth of replanted mangroves and check its feasibility before any rehabilitation project is done (Chindah *et al.,* 2007). Nigerian mangrove ecosystem productivity have been seldom studied and hence very little is known on the growth trends of mangrove species in the region. This lack of studies is as a result of difficulty in assessing mangrove forests especially as a result of their intricate root system (**Figure 1.2**). The spatial and temporal changes in mangrove extent is also an important baseline information needed for conservation, and its absence, poses a challenge in the progress of conservation projects. This motivated me to embark on utilising earth observation satellites to estimate mangrove area, levels of nipa invasion and AGB in mangrove forests of the Niger delta. Hence, the outcome of this study can inform future plans in planning conservation efforts, restoration plans and carbon financing in mangrove forests of the Niger Delta.

1.8 Thesis Objectives and Scope

Mangrove forest conservation and restoration is a globally important means of mitigating climate change. However, there is still a huge uncertainty in the effects of wood exploitation on mangrove structure and the dynamics of AGB temporally and spatially in Nigeria. Despite their global contribution to global mangrove area and biomass, mangrove forests are faced with threats and scarce scientific knowledge to inform national decisions. The chapters of this thesis will help address some of the knowledge gaps and grey areas highlighted in preceding sections. The field work for this research is limited to the mangrove forests of the Niger Delta Region of coastal Nigeria, covering over 70% of the mangrove area in Nigeria. A common theme in this thesis is to understand the spatial and temporal extent of mangrove deforestation including establishing the effects of local wood harvesting on forest structure, predicting AGB from canopy structures, understanding the predictive power of optical and radar sensors to mangrove vegetation and biomass; and finally estimating mangrove area and AGB change over the Niger Delta. The main objective of the research is to provide pioneer data on regional assessment of disturbance, species invasion, mangrove cover and biomass patterns of Niger Delta mangrove forests (**Figure 1.5**). Research questions include:

- What is the trend in mangrove structure and biomass across the tidal and disturbance gradients?
- What is the relationship between canopy features and biomass?
- What is the current area extent of mangrove and nipa palm areas and changes between 2007 and 2017?
- What are the AGB estimates in Niger Delta mangrove forests and how do they change between 2007 and 2017?

The second chapter gives a general overview of the methodology used in the thesis. The third chapter titled "**Stand, Biomass and Canopy Properties across Disturbance Gradients in**

Mangrove Forests of the Niger Delta"; will provide a survey of the relationship between mangrove stand, canopy and biomass patterns in the Niger Delta; and provide the first report on the effect of local disturbance on forest structure. I aimed to: (1) establish the trend in mangrove forest structure and biomass across the tidal and disturbance gradients, (2) establish the relationship between LAI, AGB and surface reflectance, and (3) establish a relationship between nipa palm invasion and mangrove wood exploitation in the Niger Delta.

The fourth chapter titled "**Rapid Loss of Mangroves and 7-fold Expansion in the Area of the Non-Native Invasive Nipa Palm (Nypa fruticans) in the Niger Delta over 10 years**"; will focus on comparing two types of supervised classification and provides a new regional estimate of mangrove and nipa palm area in the Niger Delta. Specifically, I aimed to (1) compare the two different types of classification (MLC and SVM) in estimating mangrove area, (2) estimate current area extent of mangrove and nipa; and (3) carry out a change detection of mangrove area over a decade from 2007 and 2017.

The fifth chapter titled "**Mapping Aboveground Biomass and Decadal Biomass Change of Mangrove Forests in the Niger Delta**"; will focus on generating, for the first time, a biomass map of mangrove forests in the Niger Delta utilising ALOS PALSAR products. I aimed to (1) establish an empirical relationship between AGB and SAR data in mangrove forests of the Niger Delta; (2) generate woody biomass map of mangrove forests in the Niger Delta and; (3) detect a change of mangrove biomass from 2007 to 2017. The sixth chapter will be a review and discussion of the implications of the research.

Figure 1.4: Mangrove forests in the Niger Delta under threat by local commercial fuel wood exploitation.

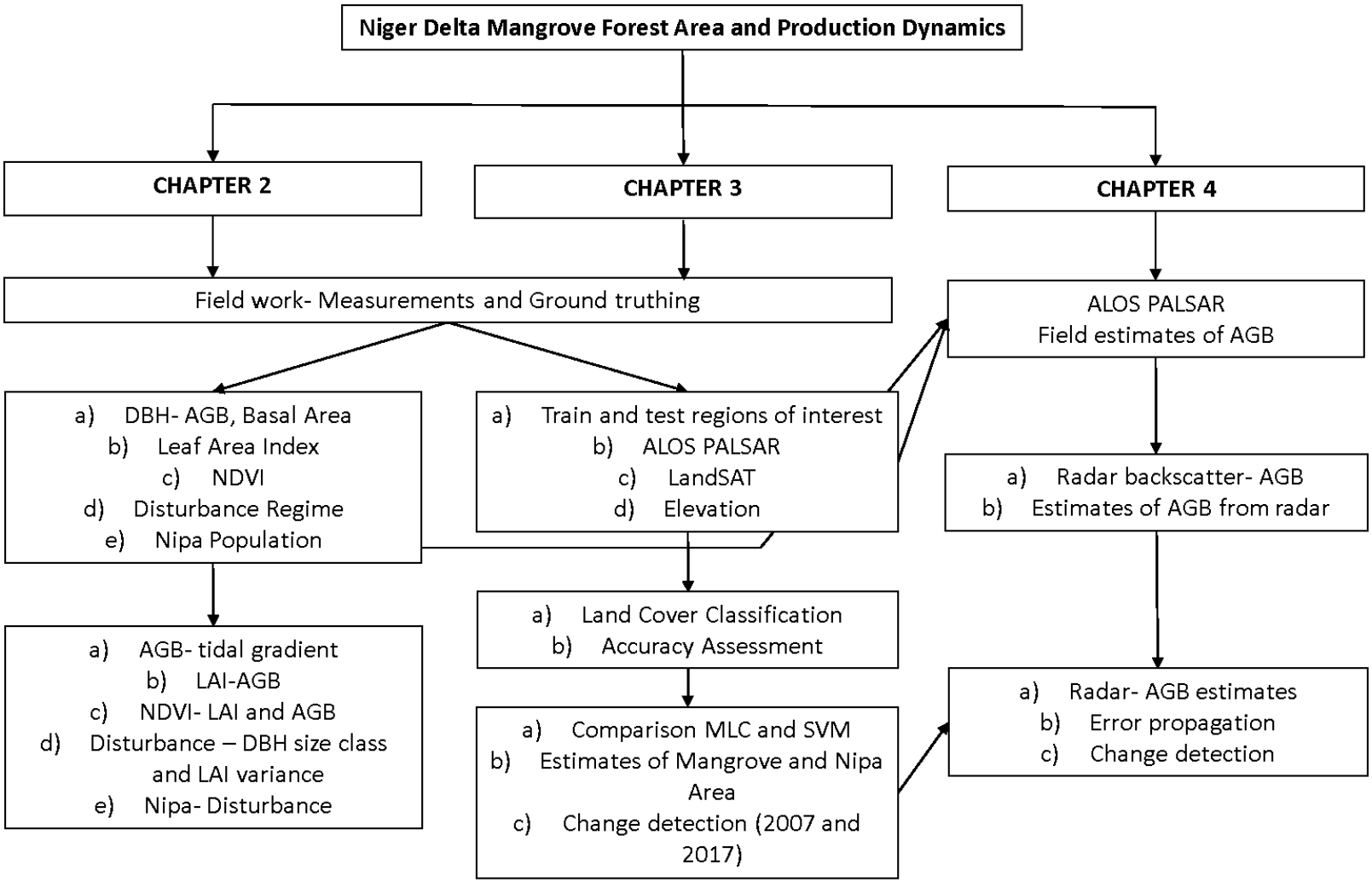

Figure 1.5: Schematic overview of thesis structure and connectivity. Arrows show flow of data through the divisions of my thesis.

1.9 References

Abere, S. A., & Ekeke, B. A. (2011). The Nigerian Mangrove and Wildlife Development. *Mediterranean Journal of Social Sciences*, *2*(7), 107–116.

Abib, S., & Appadoo, C. (2012). A PILOT STUDY FOR THE ESTIMATION OF ABOVE GROUND BIOMASS AND LITTER PRODUCTION IN Rhizophora mucronata. *Journal of Coastal Development*, *16*(1), 40–49.

Adedeji, O. H., Ibeh, L., & Oyebanji, F. F. (2011). Sustainable Management of Mangrove Coastal Environments in the Niger Delta Region of Nigeria: Role of Remote Sensing and GIS. *Proceedings of the Environmental Management Conference, Federal University of Agriculture, Abeokuta, Nigeria*, 308–326.

Ajonina, G., Kairo, J. G., Grimsditch, G., Sembres, T., Chuyong, G., Mibog, D. E., … FitzGerald, C. (2014). *Carbon pools and multiple benefits of mangroves in Central Africa: Assessment for REDD+*. *United Nations Environment Programme*.

Ajonina, G. N. (2008). Inventory and Modelling Mangrove Forest Stand Dynamics Following Different Levels of Wood Exploitation Pressures in the Douala-Edea Atlantic Coast of Cameroon, Central Africa, 215. Retrieved from http://www.freidok.uni-freiburg.de/volltexte/6132/pdf/Gordon_N._Ajonina_Thesis.pdf

Akanni, A., Onwuteaka, J., Uwagbae, M., Mulwa, R., & Elegbede, I. O. (2017). *The Values of Mangrove Ecosystem Services in the Niger Delta Region of Nigeria*. *The Political Ecology of Oil and Gas Activities in the Nigerian Aquatic Ecosystem* (Vol. 1980). Elsevier Inc. https://doi.org/10.1016/B978-0-12-809399-3.00025-2

Alemayehu, F., Richard, O., James, K. M., & Wasonga, O. (2014). Assessment of mangrove covers change and biomass in Mida creek, Kenya. *Open Journal of Forestry*, *4*(July),

398–413.

Alongi, D M. (2012). Carbon sequestration in mangrove forests. *Carbon Management*, *3*(3), 313–322. https://doi.org/Doi 10.4155/Cmt.12.20

Alongi, Daniel M. (2002). Present state and future of the world's mangrove forests. *Environmental Conservation*, *29*(03), 331–349. https://doi.org/10.1017/S0376892902000231

Alongi, Daniel M. (2014). Carbon Cycling and Storage in Mangrove Forests. *Annual Review of Marine Science*, *6*(1), 195–219. https://doi.org/10.1146/annurev-marine-010213-135020

Alongi, Daniel M. (2009). *The energetics of mangrove forests*. *The Energetics of Mangrove Forests*. https://doi.org/10.1007/978-1-4020-4271-3

Amadi, J.E. Adebola, M.O. and Eze, C. S. (2014). A Survey of the Mangrove Vegetation in the Niger Delta Region of Nigeria. *International Journal of Research (IJR)*, *1*(8), 1129–1138.

Amir, A., & Duke, N. (2009). A forever young ecosystem: light gap creation and turnover of subtropical mangrove forests in Moreton Bay, Southeast Queensland, Australia. *11th Pacific Science Inter-Congress in Conjunction with the 2nd Symposium on French Research in the Pacific*, 1–5.

Anaya, J. a., Chuvieco, E., & Palacios-Orueta, A. (2009). Aboveground biomass assessment in Colombia: A remote sensing approach. *Forest Ecology and Management*, *257*(4), 1237–1246. https://doi.org/10.1016/j.foreco.2008.11.016

Balogun, T. F. (2015). Utility of Microwave and Optical Remote Sensing in Oil Spill Detection in the Mangrove Region of Nigeria. *Journal of Geoscience and Environment Protection*, *3*, 16–21.

Balzter, H., Rowland, C., & Saich, P. (2007). Forest canopy height and carbon estimation at Monks Wood National Nature Reserve, UK, using dual-wavelength SAR interferometry. *Remote Sensing of Environment*, *108*(3), 224–239. https://doi.org/10.1016/j.rse.2006.11.014

Bamler, R., & Hartl, P. (1999). Synthetic aperture radar interferometry. *Inverse Problems*, *14*, R1–R54. https://doi.org/10.1088/0266-5611/14/4/001

Barbier, E. B., Hacker, S. D., Kennedy, C., Koch, E. W., Stier, a. C., & Silliman, B. R. (2011). The value of estuarine and coastal ecosystem services. *Ecological Monographs*, *81*(2), 169–193. https://doi.org/10.1890/10-1510.1

Barr, J. G., Engel, V., Smith, T. J., & Fuentes, J. D. (2012). Hurricane disturbance and recovery of energy balance, CO 2 fluxes and canopy structure in a mangrove forest of the Florida Everglades. *Agricultural and Forest Meteorology*, *153*, 54–66. https://doi.org/10.1016/j.agrformet.2011.07.022

Biswas, S. R., Choudhury, J. K., Nishat, A., & Rahman, M. M. (2007). Do invasive plants threaten the Sundarbans mangrove forest of Bangladesh? *Forest Ecology and Management*, *245*(1–3), 1–9. https://doi.org/10.1016/j.foreco.2007.02.011

Blasco, F., Saenger, P., & Janodet, E. (1996). Mangroves as indicator of coastal change. *Catena*, *27*, 167–178. https://doi.org/10.1016/0341-8162(96)00013-6

Bouillon, S., Borges, A. V., Castañeda-Moya, E., Diele, K., Dittmar, T., Duke, N. C., … Twilley, R. R. (2008). Mangrove production and carbon sinks: A revision of global budget estimates. *Global Biogeochemical Cycles*, *22*(2), 12. https://doi.org/10.1029/2007GB003052

Bunting, P., Rosenqvist, A., Lucas, R. M., Rebelo, L.-M., Hilarides, L., Thomas, N., …

Finlayson, C. M. (2018). The Global Mangrove Watch-A New 2010 Global Baseline of Mangrove Extent, *10*, 1669. https://doi.org/10.3390/rs10101669

Carreiras, J. M. B., Vasconcelos, M. J., & Lucas, R. M. (2012). Understanding the relationship between aboveground biomass and ALOS PALSAR data in the forests of Guinea-Bissau (West Africa). *Remote Sensing of Environment*, *121*, 426–442. https://doi.org/10.1016/j.rse.2012.02.012

Castañeda-Moya, E., Twilley, R. R., & Rivera-Monroy, V. H. (2013). Allocation of biomass and net primary productivity of mangrove forests along environmental gradients in the Florida Coastal Everglades, USA. *Forest Ecology and Management*, *307*, 226–241. https://doi.org/10.1016/j.foreco.2013.07.011

Castaneda, E. (2010). Landscape patterns of community structure, biomass and net primary productivity of mangrove forests in the Florida Coastal Everglades as a function of resources, regulators, hydroperiod, and hurricane disturbance. *Oceanography and Coastal Sciences*, *Ph.D.*(August), 171.

Chindah, A. C., Braide, S. A., Makiri, J. A., & Onokurhefe, J. (2007). Effect of crude oil on the development of mangrove (Rhizophora mangle L .) seedlings from Niger. *Revista UDO Agricola*, *7*(1), 181–194.

CIFOR, USFS, & OSU. (2014). *Sustainable Wetlands Adaptation and Mitigation Program (SWAMP)*.

Clarke, P J, & Kerrigan, R. A. (2000). Do forest gaps influence the population structure and species composition of mangrove stands in northern Australia? *Biotropica*, *32*(4), 642–652. https://doi.org/10.1111/j.1744-7429.2000.tb00511.x

Clarke, Peter J. (2004). Effects of experimental canopy gaps on mangrove recruitment: lack

of habitat partitioning may explain stand dominance. *Journal of Ecology*, *92*(2), 203–213.

Cox, E. F., & Allen, J. A. (1999). Stand Structure and Productivity of the Introduced Rhizophora mangle in Hawaii. *Estuaries*, *22*(2), 276. https://doi.org/10.2307/1352983

Crooks, S., Tamelander, J., Laffoley, D., Vandever, J., Development, S., & Presidency, V. (2011). Mitigating Climate Change through Restoration and Management of Coastal Wetlands and Near-shore Marine Ecosystems Challenges and Opportunities through Restoration and Management of Coastal Wetlands and Near-shore Marine Ecosystems Challenges and Opportuni, (121).

Day, J. W., Conner, W., Ley-Lou, F., Day, R., And, & Navarro, A. (1987). The productivity and composition of mangrove forests, Laguna de Términos, Mexico. *Aquatic Botany*, *27*, 267–284. https://doi.org/10.1016/0304-3770(87)90046-5

Day, J. W., Coronado-Molina, C., Vera-Herrera, F. R., Twilley, R. R., Rivera-Monroy, V. H., Alvarez-Guillen, H., … Conner, W. (1996). A 7 year record of above-ground net primary production in a southeastern Mexicann mangrove forest. *Aquatic Botany*, *55*, 39–60. https://doi.org/10.1016/0304-3770(96)01063-7

Duke, N. C. (2016). Oil spill impacts on mangroves: Recommendations for operational planning and action based on a global review. *Marine Pollution Bulletin*, *109*(2), 700–715. https://doi.org/10.1016/j.marpolbul.2016.06.082

Ebuy, J., Lokombe, J. P., Ponette, Q., Sonwa, D., & Picard, N. (2011). Allometric equation for predicting aboveground biomass of three tree species. *Journal of Tropical Forest Science*, *23*(2), 125–132.

Edu, E. A., Edwin-Wosu, N. L., Ononyume, M. O., & Nkang, a. E. (2014). Carbon credits

assessment in a mixed mangrove forest vegetation of. *Asian Journal of Plant Science and Research*, *4*(4), 1–12.

FAO. (2005). *Global Forest Resources Assessment 2005: Thematic Study on Mangroves. Nigeria Country Profile*. *Forest Resources Development Service Forest Resources Division Forestry, Forestry Department FAO, Rome (Italy)*.

Fassnacht, F. E., Hartig, F., Latifi, H., Berger, C., Hernández, J., Corvalán, P., & Koch, B. (2014). Importance of sample size, data type and prediction method for remote sensing-based estimations of aboveground forest biomass. *Remote Sensing of Environment*, *154*, 102–114. https://doi.org/10.1016/j.rse.2014.07.028

Fatoyinbo, T. E., & Armstrong, A. H. (2010). Remote Characterization of Biomass Measurements: Case Study of Mangrove Forests. In M. N. B. Momba (Ed.), *Biomass* (1st ed., pp. 65–78). Retrieved from http://www.intechopen.com/books/biomass/remote-characterization-of-biomass-measurements-case-study-of- mangrove-forests

Fatoyinbo, T. E., & Simard, M. (2013). Height and biomass of mangroves in Africa from ICESat/GLAS and SRTM. *International Journal of Remote Sensing*, *34*(2), 668–681. https://doi.org/10.1080/01431161.2012.712224

Fatoyinbo, T., & Simard, M. (2011). Remote Sensing of Mangrove Structure and Biomass. *Workshop on Tropical Wetland Ecosystems on Indonesia: Science Needs to Address Climate Change Adaption and Mitigation. Sanur Beach Hotel, Bali 11-14th April, 2011*, 5.

Feka, N. Z., & Ajonina, G. N. (2011). Drivers causing decline of mangrove in West-Central Africa: a review. *International Journal of Biodiversity Science, Ecosystem Services &*

Management, *7*(3), 217–230. https://doi.org/10.1080/21513732.2011.634436

Flores De Santiago, F., Kovacs, J. M., & Lafrance, P. (2013). An object-oriented classification method for mapping mangroves in Guinea, West Africa, using multipolarized ALOS PALSAR L-band data. *International Journal of Remote Sensing*, *34*(2), 563–586. https://doi.org/10.1080/01431161.2012.715773

Fromard, F., Puig, H., Mougin, E., Marty, G., Betoulle, J. L., & Cadamuro, L. (1998). Structure, above-ground biomass and dynamics of mangrove ecosystems: New data from French Guiana. *Oecologia*, *115*(1–2), 39–53. https://doi.org/10.1007/s004420050489

Global Invasive Species Database (GISD). (2015). FULL ACCOUNT FOR: Nypa fruticans Nypa. https://doi.org/10.1017/CBO9781107415324.004

Goessens, A., Satyanarayana, B., Van Der Stocken, T., Zuniga, M. Q., Mohd-Lokman, H., Sulong, I., & Dahdouh-Guebas, F. (2014). Is Matang Mangrove Forest in Malaysia sustainably rejuvenating after more than a century of conservation and harvesting management? *PLoS ONE*, *9*(8). https://doi.org/10.1371/journal.pone.0105069

Green, E. P., Clark, C. D., Mumby, P. J., Edwards, a. J., & Ellis, a. C. (1998). Remote sensing techniques for mangrove mapping. *International Journal of Remote Sensing*, *19*(5), 935–956. https://doi.org/10.1080/014311698215801

Grimsditch, G. (2011). Options for Blue Carbon within the International Climate Change Framework. *Sustainable Development Law and Policy*, *11*(2), 22–24.

Hamdan, O., Khali Aziz, H., & Mohd Hasmadi, I. (2014). L-band ALOS PALSAR for biomass estimation of Matang Mangroves, Malaysia. *Remote Sensing of Environment*, *155*, 69–78. https://doi.org/10.1016/j.rse.2014.04.029

Hawthorne, T. L., Elmore, V., Strong, A., Bennett-Martin, P., Finnie, J., Parkman, J., … Reed, J. (2015). Mapping non-native invasive species and accessibility in an urban forest: A case study of participatory mapping and citizen science in Atlanta, Georgia. *Applied Geography*, *56*, 187–198. https://doi.org/10.1016/j.apgeog.2014.10.005

Henry, M., Bombelli, A., Trotta, C., Alessandrini, A., Birigazzi, L., Sola, G., … Saint-André, L. (2013). GlobAllomeTree: international platform for tree allometric equations to support volume, biomass and carbon assessment. *IForest - Biogeosciences and Forestry*, *6*(5), 326–330. https://doi.org/10.3832/ifor0901-006

Herr, D., & Pidgeon, E. (2011). *Blue Carbon Policy Framework: Based on the first Workshop of teh International Blue Carbon Policy Working Group*.

Heumann, B. W. (2011). Satellite remote sensing of mangrove forests: Recent advances and future opportunities. *Progress in Physical Geography*, *35*(1), 87–108. https://doi.org/10.1177/0309133310385371

Hossain, M., Othman, S., Bujang, J. S., & Kusnan, M. (2008). Net primary productivity of Bruguiera parviflora (Wight & Arn.) dominated mangrove forest at Kuala Selangor, Malaysia. *Forest Ecology and Management*, *255*(1), 179–182. https://doi.org/10.1016/j.foreco.2007.09.011

Hussain, M., Chen, D., Cheng, A., Wei, H., & Stanley, D. (2013). Change detection from remotely sensed images: From pixel-based to object-based approaches. *ISPRS Journal of Photogrammetry and Remote Sensing*, *80*, 91–106. https://doi.org/10.1016/j.isprsjprs.2013.03.006

International Tropical Timber Organization. (2012). Mapping mangroves. *ITTO Tropical Forest Update*, *21*(2), 24.

Invasive Species Compendium. (2011). Datasheet report for Nypa fruticans (nipa palm). https://doi.org/10.1094/PDIS

IPIECA. (2002). Biological impacts of oil pollution: Mangroves. *IPIECA Report Series*, *4*, 28.

Isebor, C. E., Ajayi, T. O., & Anyanwu, A. (2003). *The Incidence of Nypa fruticans (WURMB) and it's Impact on Fisheries Production in the Niger Delta Mangrove Ecosystem*.

IUCN. (2017). Blue Carbon. *Issue Brief*, (November), 21–22. Retrieved from iucn.org/issues-briefs

Jack, J. T. C. B., Akujobi, C. T., Uchechukwu, D. A., & Azubuike, B. O. (2016). Crude Oil Exploration and Underdevelopment in Nigeria: A Resource Curse Analysis. *Technoscience Review*, *7*(November 2016), 31–45.

Jackson, G. (2011). Mangrove Resources Utilization in Nigeria: An Analysis of the Andoni Mangrove Resources Crisis. *Sacha Journal of Environmental Studies*, *1*(1), 49–63.

James, G. K., Adegoke, J. O., Saba, E., Nwilo, P., & Akinyede, J. (2007). Satellite-Based Assessment of the Extent and Changes in the Mangrove Ecosystem of the Niger Delta. *Marine Geodesy*, *30*(3), 249–267. https://doi.org/10.1080/01490410701438224

Jhonnerie, R., Siregar, V. P., Nababan, B., Prasetyo, L. B., & Wouthuyzen, S. (2015). Random Forest Classification for Mangrove Land Cover Mapping Using Landsat 5 TM and Alos Palsar Imageries. *Procedia Environmental Sciences*, *24*, 215–221. https://doi.org/10.1016/j.proenv.2015.03.028

Jones, T., Ratsimba, H., Ravaoarinorotsihoarana, L., Glass, L., Benson, L., Teoh, M., … Roy, P.-F. (2015). The Dynamics, Ecological Variability and Estimated Carbon Stocks of Mangroves in Mahajamba Bay, Madagascar. *Journal of Marine Science and Engineering*, *3*(3), 793–820. https://doi.org/10.3390/jmse3030793

Kairo, J. G., Lang'at, J. K. S., Dahdouh-Guebas, F., Bosire, J., And, & Karachi, M. (2008). Structural development and productivity of replanted mangrove plantations in Kenya. *Forest Ecology and Management*, *255*(7), 2670–2677. https://doi.org/10.1016/j.foreco.2008.01.031

Kauffman, J. B., Heider, C., Cole, T. G., Dwire, K. a., & Donato, D. C. (2011). Ecosystem carbon stocks of micronesian mangrove forests. *Wetlands*, *31*(2), 343–352. https://doi.org/10.1007/s13157-011-0148-9

Kinako, P. D. S. (1977). Conserving the mangrove forest of the Niger Delta. *Biological Conservation*, *11*(1), 35–39. https://doi.org/10.1016/0006-3207(77)90025-8

Komiyama, A., Ong, J. E., & Poungparn, S. (2008). Allometry, biomass, and productivity of mangrove forests: A review. *Aquatic Botany*, *89*(2), 128–137. https://doi.org/10.1016/j.aquabot.2007.12.006

Komiyama, Akira, Poungparn, S., & Kato, S. (2005). Common allometric equations for estimating the tree weight of mangroves. *Journal of Tropical Ecology*, *21*(4), 471–477. https://doi.org/10.1017/S0266467405002476

Langeveld, J. W. A., & Delany, S. (2014). *The impact of oil exploration, extraction and transport on mangrove vegetation and carbon stocks in nigeria*. Amsterdam.

Li, X. W., Guo, H. D., Wang, C. L., Li, Z., & Liao, J. J. (2003). DEM generation in the densely vegetated area of Hotan, north-west China using SIR-C repeat pass polarimetric SAR interferometry. *International Journal of Remote Sensing*, *24*(14), 2997–3003. https://doi.org/10.1080/0143116031000094773

Li, X., Yeh, A., Liu, K., & Wang, S. (2006). Inventory of mangrove wetlands in the Pearl River Estuary of China using remote sensing. *Journal of Geographical Sciences*, *16*(2), 155–

164. https://doi.org/10.1007/s11442-006-0203-2

Lucas, R. M., Mitchell, A. L., Ake, R., Proisy, C., Melius, A. and, & Ticehurst, C. (2007). The potential of L-band SAR for quantifying mangrove characteristics and change: case studies from the tropics. *Aquaric Conservation: Marine and Freshwater Ecosystems*, *19*, 671–675. https://doi.org/10.1002/aqc

Lucas, R., Rebelo, L. M., Fatoyinbo, L., Rosenqvist, A., Itoh, T., Shimada, M., … Hilarides, L. (2014). Contribution of L-band SAR to systematic global mangrove monitoring. *Marine and Freshwater Research*, *65*(7), 589–603. https://doi.org/10.1071/MF13177

Lugo, A. E., & Snedaker, S. C. (1974). The Ecology of Mangroves. *Annual Review of Ecology and Systematics*, *5*(1), 39–64. https://doi.org/10.1146/annurev.es.05.110174.000351

Mcleod, E., & Salm, R. V. (2006). *Managing Mangroves for Resilience to Climate Change*. *Science* (Vol. 64pp). Retrieved from http://www.iucn.org/themes/marine/pubs/pubs.htm

Mitchard, E. T. a., Saatchi, S. S., White, L. J. T., Abernethy, K. a., Jeffery, K. J., Lewis, S. L., … Meir, P. (2012). Mapping tropical forest biomass with radar and spaceborne LiDAR in Lopé National Park, Gabon: overcoming problems of high biomass and persistent cloud. *Biogeosciences*, *9*(1), 179–191. https://doi.org/10.5194/bg-9-179-2012

Mitchard, E. T. a, Saatchi, S. S., Woodhouse, I. H., Nangendo, G., Ribeiro, N. S., Williams, M., … Meir, P. (2009). Using satellite radar backscatter to predict above-ground woody biomass: A consistent relationship across four different African landscapes. *Geophysical Research Letters*, *36*(23), 1–6. https://doi.org/10.1029/2009GL040692

Mmom, P. C., & Arokoyu, S. B. (2010). Mangrove Forest Depletion, Biodiversity Loss and Traditional Resources Management Practices in the Niger Delta, Nigeria. *Research*

Journal of Applied Sciences, Engineering and Technology, *2*(1), 28–34.

Mougin, E., Proisy, C., Marty, G., Fromard, F., Puig, H., Betoulle, J. L., & Rudant, J. P. (1999). Multifrequency and multipolarization radar backscattering from mangrove forests. *IEEE Transactions on Geoscience and Remote Sensing*, *37*(1 PART 1), 94–102. https://doi.org/10.1109/36.739128

Murray, B. C., & Vegh, T. (2012). Incorporating Blue Carbon as a Mitigation Action under the United Nations Framework Convention on Climate Change Technical Issues to Address. *Nicholas Institute Report*, (November).

Myint, S. W., Giri, C. P., Wang, L., Zhu, Z., & Gillette, S. C. (2008). Identifying Mangrove Species and Their Surrounding Land Use and Land Cover Classes Using an Object-Oriented Approach with a Lacunarity Spatial Measure. *GIScience & Remote Sensing*, *45*(2), 188–208. https://doi.org/10.2747/1548-1603.45.2.188

Ndidi, C., Okonkwo, P., Kumar, L., & Taylor, S. (2015). The Niger Delta wetland ecosystem : What threatens it and why should we protect it ? *African Journal of Environmental Science and Technology*, *9*(5), 451–463. https://doi.org/10.5897/AJEST2014.1841

Niphadkar, M., & Nagendra, H. (2016). Remote sensing of invasive plants: incorporating functional traits into the picture. *International Journal of Remote Sensing*, *37*(13), 3074–3085. https://doi.org/10.1080/01431161.2016.1193795

Nwigbo, S. C., Azaka, O. A., Chukwuneke, J. L., & Nwadike, C. E. (2013). Establishing Allometric Relationships Using Crown Diameter for Estimating Above Ground Combustible Fuels in Southern Nigerian Mangrove Vegetations. *International Journal of Multidisciplinary Sciences and Engineering*, *4*(7), 43–52.

Okpiliya F.I. Effiong E.B. and Udida A.A. (2013). Analysis of the Rate of Change of Mangrove

Forest Ecosystem in. *Journal of Environment and Earth Science*, *3*(7), 78–91.

Okugbo, O. T., Usunobun, U., Adegbegi, J. A., & Okiemien, C. O. (2012). A review of Nipa Palm as a renewable energy source in Nigeria. *Research Journal of Applied Sciences, Engineering and Technology*, *4*(15), 2367–2371.

Polidoro, B. a., Carpenter, K. E., Collins, L., Duke, N. C., Ellison, A. M., Ellison, J. C., … Yong, J. W. H. (2010). The loss of species: Mangrove extinction risk and geographic areas of global concern. *PLoS ONE*, *5*(4), e10095. https://doi.org/10.1371/journal.pone.0010095

Proisy, C., Mougin, E., & Fromard, F. (1996). Investigating correlations between radar data and mangrove forests characteristics. *IGARSS '96. 1996 International Geoscience and Remote Sensing Symposium*, *1*, 733–735. https://doi.org/10.1109/IGARSS.1996.516458

Proisy, C., Mougin, E., Fromard, F., & Karam, M. a. (2000). Interpretation of polarimetric radar signatures of mangrove forests. *Remote Sensing of Environment*, *71*(1), 56–66. https://doi.org/10.1016/S0034-4257(99)00064-4

Quiñones, M. J., & Hoekman, D. H. (2004). Exploration of factors limiting biomass estimation by polarimetric radar in tropical forests. *IEEE Transactions on Geoscience and Remote Sensing*, *42*(1), 86–104. https://doi.org/10.1109/TGRS.2003.815402

Rabiatul, K. M. R. and, & Mohd, H. I. (2012). Biomass and Carbon in Mangrove: Measuring and Managing through Remote Sensing Technique. *Malaysia Geospatial Forum*, (March).

Richardson, D. M., Pysek, P., Rejmanek, M., Barbour, M. G., Panetta, F. D., West, J., & Mar, N. (2000). Naturalization and Invasion of Alien Plants : Concepts and Definitions

Naturalization and invasion of alien plants : concepts and definitions, *6*(2), 93–107. https://doi.org/10.1046/j.1472-4642.2000.00083.x

Ross, M. S., Ruiz, P. L., Telesnicki, G. J., & Meeder, J. F. (2001). Aboveground Biomass and Production in Mangrove Communities of Biscayne National Park , Florida (USA), Following Hurricane Andrew. *Environmental Research*, *9*, 27–37.

Ryan, C. M., Williams, M., & Grace, J. (2011). Above- and belowground carbon stocks in a miombo woodland landscape of mozambique. *Biotropica*, *43*(4), 423–432. https://doi.org/10.1111/j.1744-7429.2010.00713.x

Saenger, P., & Bellan, M. F. (1995). The mangrove vegetation of the Atlantic Coast of Africa : a review. *Review Literature And Arts Of The Americas*.

Saenger, P., & Snedaker, S. C. (1993). Pantropical Trends in Mangrove Above-Ground Biomass and Annual Litterfall. *Oecologia*, *96*(3), 293–299.

Sambodo, K. A., & Indriasari, N. (2013). LAND COVER CLASSIFICATION OF ALOS PALSAR DATA USING SUPPORT VECTOR MACHINE. *International Journal of Remote Sensing and Earth Sciences*, *10*(1), 9–18. https://doi.org/10.1128/JB.00758-15

Scavia, D., Field, J. C., Boesch, D. F., Buddemeier, R. W., Burkett, V., Cayan, D. R., … Titus, J. G. (2002). Climate Change Impacts on U . S . Coastal and Marine Ecosystems. *Estuaries*, *25*(2), 149–164. https://doi.org/10.1007/BF02691304

Secretariat of the Convention on Biologival Diversity. (2010). *Global Biodiversity Outlook 3. Journal of the American Podiatric Medical Association* (Vol. 104). https://doi.org/10.7547/0003-0538-104.3.A1

Sessa, R. (2009). Assessment of the status of the development of the standards for the terrestrial essential climate variables: biomass. *GTO System. Rome, Italy. Version*, *10*,

1–18.

Sherman, R. E., Fahey, T. J., & Martinez, P. (2003). Spatial patterns of Biomass and aboveground net primary productivity in a mangrove ecosystem in the Dominican Republic. *Ecosystems*, *6*(4), 384–398. https://doi.org/10.1007/s10021-002-0191-8

Sitoe, A., Mandlate, L., & Guedes, B. (2014). Biomass and Carbon Stocks of Sofala Bay Mangrove Forests. *Forests*, *5*(8), 1967–1981. https://doi.org/10.3390/f5081967

Sunderland, T. C. H., & Morakinyo, T. (2002). Nypa fruticans, a Weed in West Africa. *Palms*, *46*(3), 154–155.

Thomas, N., Lucas, R., Bunting, P., Hardy, A., Rosenqvist, A., & Simard, M. (2017). Distribution and drivers of global mangrove forest change, 1996-2010. *PLoS ONE*, *12*(6), 1–14. https://doi.org/10.1371/journal.pone.0179302

Tian, S., Zhang, X., Tian, J., & Sun, Q. (2016). Random forest classification of wetland landcovers from multi-sensor data in the arid region of Xinjiang, China. *Remote Sensing*, *8*(11), 1–14. https://doi.org/10.3390/rs8110954

Tsuji, K., Sebastian, L. S., Ghazalli, M. N. F., Ariffin, Z., Nordin, M. S., Khaidizar, M. I., & Dulloo, M. E. (2011). Biological and ethnobotanical characteristics of Nipa Palm (Nypa fructicans wurmb.): A review. *Sains Malaysiana*, *40*(12), 1407–1412.

Ukpong, I. E. (1991). The Performance and Distribution of Species along Soil Salinity Gradients of Mangrove Swamps in Southeastern Nigeria. *Vegetatio*, *95*(1), 63–70.

Ukpong, I. E. (1994). Soil-vegetation interrelationships of mangrove swamps as revealed by multivariate analyses. *Geoderma*, *64*(1–2), 167–181. https://doi.org/10.1016/0016-7061(94)90096-5

Ukpong, I. E. (2000a). Ecological classification of Nigerian mangrove using soil nutrient gradient analysis. *Wetland Ecology and Management*, (8), 263–272.

Ukpong, I. E. (2000b). Gradient analysis in mangrove swamp forests. *Tropical Ecology*, *41*(1), 25–32.

Ukpong, I. E. (2015). Nypa Fruticans Invasion and the Integrity of Mangrove Ecosystem Functioning in the Marginal Estuaries of South Eastern Nigeria. In A. Gbadegesin, O. O. I. Orimoogunje, & O. A. Fashae (Eds.), *Frontiers in Environmental Research and Sustainable Environment in the 21st Century* (pp. 1–13). Ibadan University Press Publishing House University of Ibadan Ibadan, Nigeria. ©.

UNEP. (2009). Blue Carbon – the Role of Oceans As Carbon Sinks, 35–43.

Urrego, L. E., Molina, E. C., & Suárez, J. A. (2014). Environmental and anthropogenic influences on the distribution, structure, and floristic composition of mangrove forests of the Gulf of Urabá (Colombian Caribbean). *Aquatic Botany*, *114*, 42–49. https://doi.org/10.1016/j.aquabot.2013.12.006

USAID. (2014). ASSESSMENT OF BIOMASS AND CARBON OF MANGROVES IN WEST AFRICA. *Center for Applied Geographic Information Science, UNC Charlotte*.

Wan Norilani, W. I., Wan Juliana, W. A., Latiff, A., & Salam, M. R. (2014). Community structure at two compartments of a disturbed mangrove forests at pulau langkawi. *AIP Conference Proceedings*, *1614*, 790–794. https://doi.org/10.1063/1.4895303C

Wijaya, A., & Gloaguen, R. (2009). Fusion of ALOS Palsar and Landsat ETM data for land cover classification and biomass modeling using non-linear methods. *Geoscience and Remote Sensing Symposium,2009 IEEE International,IGARSS 2009*, *3*, III-581-III–584. https://doi.org/10.1109/IGARSS.2009.5417824

Yang, X., & Lo, C. P. (2002). Using a time series of satellite imagery to detect land use and land cover changes in the Atlanta, Georgia metropolitan area. *International Journal of Remote Sensing*, *23*(9), 1775–1798. https://doi.org/10.1080/01431160110075802

Chapter 2

Methodology

2.1 Research Questions Overview

My research was carried out in the Niger Delta utilising primary field data and secondary remote sensing data while data analysis involved statistical and spatial tools. Field data collection during my research was divided into two field campaigns: a reconnaissance visit and a main field campaign. Earth observation data was retrieved throughout my thesis using open access sites. Data collection was executed in such a way as to consider the aims and objective of my thesis (**Figure 2.1**). The specific methodology are discussed in the methodology of chapters three to five, but here I layout the summary of techniques used in data collection based on the objective of my thesis.

The relationship between mangrove forests structure and perturbations can be detected using stand and canopy features as proxy. Understanding the natural and anthropogenic trend in mangrove forest structure in the Niger Delta, I assessed basal area, DBH size classes, AGB and LAI within established plots. I compared these parameters to distance to the open ocean, distance from the tidal channel, disturbance regime and distance from the closest settlement. These parameters were chosen due to their connectivity with productivity (AGB, LAI) and stand properties (DBH size class, basal area). I also enumerated the number of nipa stands within each plot to establish a relationship between local disturbance and nipa palm encroachment.

Primary productivity as a major source of biological mass of plants is a function of the energy conversion function of chlorophyll content in leaves. Hence, assessing the relationship between canopy properties and biological mass can form a precursor to monitoring productivity over time. Following from LAI and AGB estimates, I assessed the predictability of biomass from canopy properties. This relationship was also tested using satellite vegetation indices, a proxy for canopy features.

Monitoring forests change over a landscape requires the use of earth observation satellites to detect different land cover types and area. The availability of time series data is the advantage of earth observation satellites in monitoring forest cover change. I used a combination of elevation, optical and radar data in order to classify mangrove forests and nipa palm over the Niger Delta. I used supervised classification involving training and testing regions of interests (ROI). I collected ground control points (GCPs) over the Niger Delta during my field studies as input for ROIs. I tested two different supervised classification methods in order to retrieve the most accurate mangrove and nipa palm cover based on GCPs collected during field surveys. In order to estimate the change in mangrove and nipa area, I applied the LC classification over two years spanning a decade- 2007 and 2017.

Reporting national carbon stock involves assessing the biomass and soil carbon of forest vegetation. Due to the large area covered by forests, regression equations which predict biomass from a relationship between field AGB and radar backscatter provides a basis for estimating mangrove biomass over a landscape. I used the AGB estimated from the field to develop a relationship with radar backscatter. I applied the regression equation to both 2007 and 2017 mangrove radar data which I estimated in the previous research question in order to estimate the change in mangrove forest biomass in the delta.

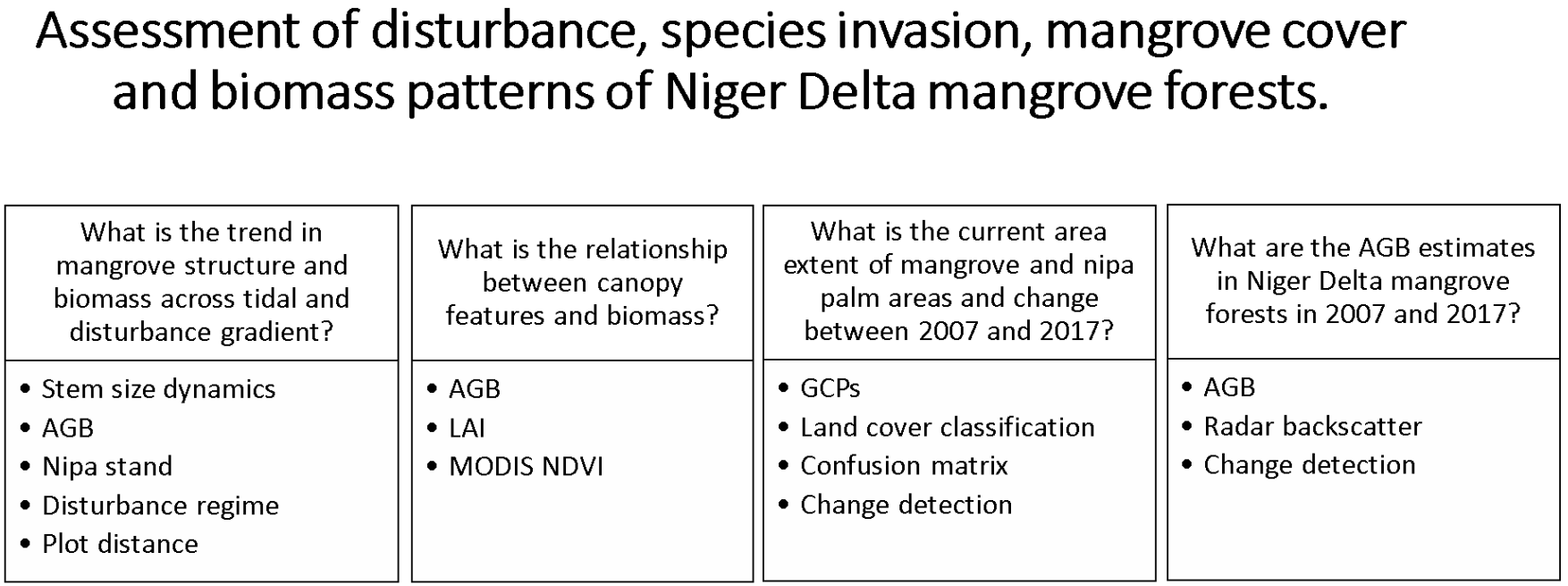

Figure 2.1: *Link of the aim, research questions and parameters measured during my thesis. The top box shows the research questions asked in this thesis. The measured parameters are below the research questions. There is a common theme of continual use of data all across the different research questions.*

2.2 Field Survey

Field data collection formed the basis of my thesis due to paucity of stem diameter inventory over the Niger Delta. In order to carry out a robust stem diameter inventory, I carried out an initial survey of mangrove forest across the Nigerian coastline to designate locations for field plots and feasibility of the field work. Secondly, the recon visit was set up to build a team for the duration of the field work. After a successful recon survey, three locations were picked based on accessibility to mangroves, local contact availability and diverse nature of management.

2.2.1 Reconnaissance Visit

A recon visit was carried out in March, 2016 to give a preliminary assessment of the mangrove ecosystem in the Niger Delta. The aim of this reconnaissance visit was to ascertain the following before the commencing the field study of this thesis:

- Check accessibility to mangrove forests in coastal Nigeria
- Ground-truthing on mangrove characteristics and type
- Relative disturbance of mangrove forests
- Preliminary study in a mangrove stand

Five locations were visited during the visit (**Table 2.1**; **Figure 2.2**), and recorded the GPS of various land cover classes (**Table 2.2**), state of the mangrove forests, economic activities, dominant species, type of mangrove geomorphology and source of stressors. This was done to understand the mangrove ecosystem in Nigeria. Crown cover was estimated using a densiometer. The condition of the mangrove stands during the recon visit was done using visual evidence. The activities and environmental disturbance were determined with communication with local residence and visual observation. However, only the Lagos lagoon location was assessed for AGB and stand characteristics of a pure *Avicennia germinans* stand using DBH and allometric equations generated by Fromard *et al.*, (1998) from a mangrove

study in French Guiana (**Table 2.1**). The plot in the Lagos lagoon was assessed to test the methodologies to be used during the field work. I selected three of these locations (Kono, Ete and Oproama) for plot biomass estimates due to environmental and financial constraints **(Figure 2.2)**.

Table 2.1: Summary of Recon Visit to Coastal Nigeria showing dominant species, forest condition, prevalent activities and stressors.

	Ete Creek	**Oproama**	**Calabar Estuary**	**Kono Creek**	**Lagos Lagoon**
Location	Niger Delta	Niger Delta	Calabar estuary	Niger delta	Barrier Lagoon Coast
GPS	N 4° 32' 36.712'' E 7° 32' 49.127''	N 4°48'11.56'' E 6°50' 23.585''	N 4° 56' 49.693'' E 8° 21' 27.561''	N 4° 34' 30.792'' E 7° 30' 38.213''	N 6° 31' 20.608'' E 3° 23' 54.016''
State	Akwa Ibom	Rivers	Cross River	Rivers	Lagos
Condition	• Degraded • Nipa palm	• Intact • Cleared	• Intact • Cleared • Nipa palm	• Nipa palm • Protected site	• Intact Patches
Activities	• Fishing • Transportation • Farming	• Fishing • farming	• Fishing • Farming	• Fishing • Farming • Construction	• Fishing • Construction
Stressors/ Disturbance	• Invasive species	• Power line	• Dredging • Invasive species	• Invasive species • Clearing for construction	• Domestic Pollution
Type of vegetation	Riverine Forests	Riverine Forests	Fringing/ Riverine Forests	Riverine Forests	Scrub and Dwarf forests
Dominant species	*Nypa fruticans* *Rhizophora* spp.	*Rhizophora* spp. *Laguncularia racemosa* *Avicennia germinans*	*Nypa fruticans* *Rhizophora* spp.	*Nypa fruticans* *Rhizophora* spp.	*Rhizophora* spp. *Avicennia germinans*
Crown cover	-	92.72% 66.72%	-	-	89.6%
DBH range (Mean ± SD	-	-	-	-	6.68cm – 43.9cm (21.03cm±7.76cm)
Biomass estimate (stand density/ basal area)	-	-	-	-	59.897 Mg ha^{-1} (175 ha^{-1}/ 9.18m^2 ha^{-1})

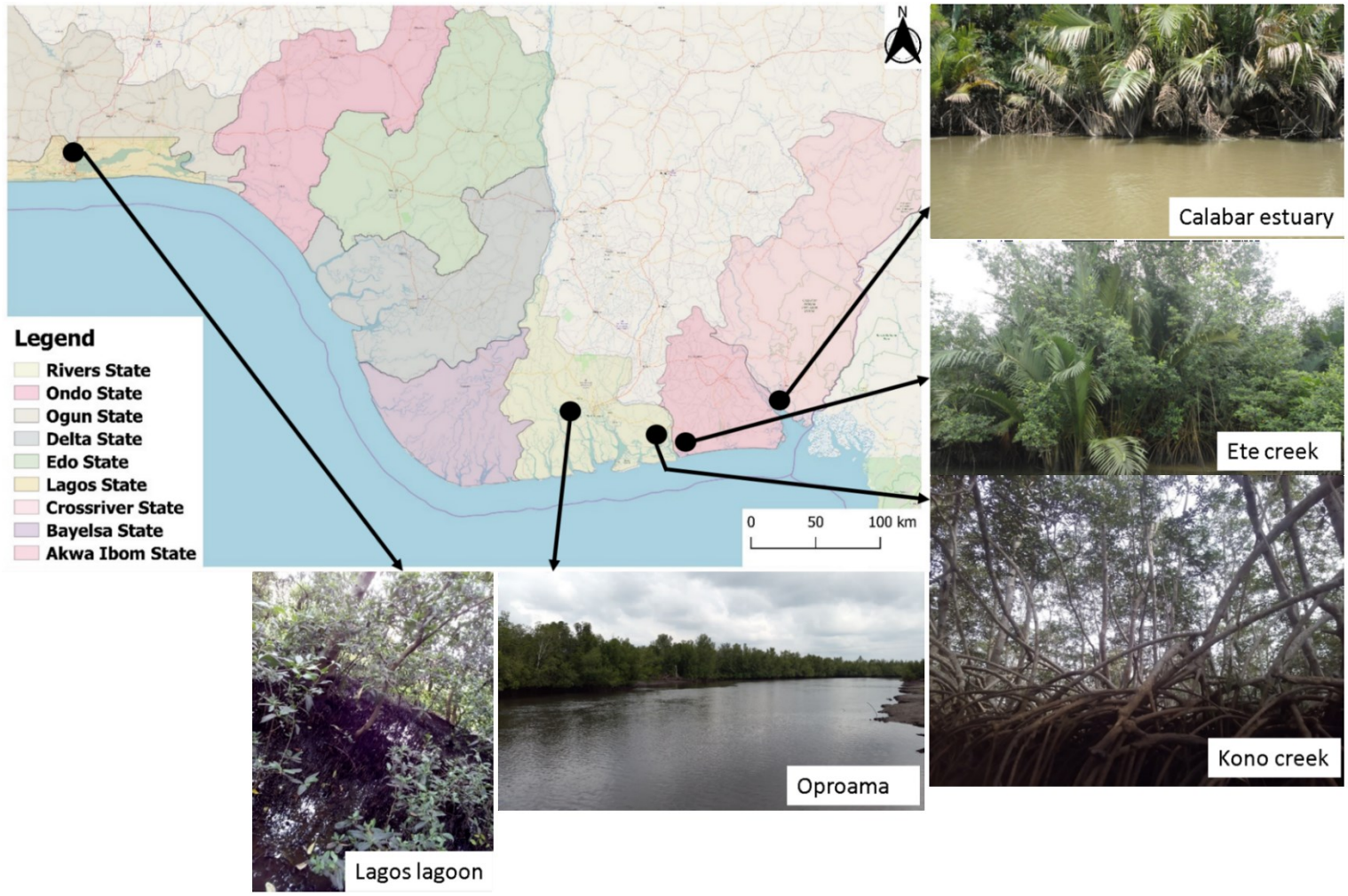

Figure 2.2: Coastal Nigeria with recon visit locations. Black dots show locations visited during the survey. Inset shows pictures of mangrove ecosystem of the location.

2.2.2 Field Sites

Three mangrove study sites were used in this research. The common feature between all sites was their location in the Niger Delta. Beyond this, site selection was based on mangrove extent, accessibility, security and management regime. Limited access to mangrove forests in the Niger Delta is as a result of security issues ranging from kidnapping, oil bunkering and militancy. However, I used the global forest height map (Simard *et al.*, 2011) to randomly select a wide range of biomass within the selected sites. These sites were selected in order to represent the wide range of mangrove community types and ecosystem disturbance experienced by Niger Delta mangroves, evident from the recon visit (**3.2.2**). Field plots were established in the three sites where data collection was done and GCPs established. There has been no report within these sites in terms of mangrove structure, biomass, disturbance and spatial analysis. These three locations are Ete creek, Oproama community and Kono creek (**Table 2.1**, **Figure 2.2**).

Ete creek is located in Ikot Abasi Local Government Area (LGA), Akwa Ibom State (**Figure 2.3**). This creek runs from Ikot Akan and empties into the Imo river estuary at Ikot Abasi. The major economic activity of this region was fishing. However, commercial fishing resulted in a shift to lumbering (**Figure 2.3A**). This shift in economic activity has resulted to a high incident of logging and wood exploitation. There are also two oil wells around the creek and I experienced an oil spill during my field work which was evident from oil film along the creek (**Figure 2.3B**). Ete creek is fringed on either side with mangrove forests which progress into rainforests or farmland. Despite having high logging activity, mangroves in Ete creek are as high as 15m (**Figure 2.3C**). The landward extent of mangrove forests along this creek is dependent on the economic activity of the locals inhabiting the region. The economic activities was primarily farming with minor activities of fishing and sand mining.

Oproama community is located in Asari Toru LGA, Rivers state (**Figure 2.4**). This community is crisscrossed with creeks that empty into Sombreiro river estuary. The mangrove forests around this community is riverine type that gradually changes into a tropical forest ecosystem (**Figure 2.4A**). However, development is gradually reducing the landward extent of the mangrove ecosystems with results in stunted growth inland (**Figure 2.4B**). This is evident from clearance for powerlines and road construction (**Figure 2.4C**). The community believe that illegal cutting can result in annoying a deity. The main economic activity within this region is fisheries and some lumbering in the closest non-mangrove forest.

Kono creek is located in Khana LGA, Rivers state and it empties into Imo river estuary (**Figure 2.5**). There is a protected site along the creek established by the Centre for Environment, Human Rights and Development (CEHRD) where there are dense mangrove forests (**Figure 2.5A**). The communities along the creek are very protective of mangrove forests and foreign activities being carried out within these forests. However, nipa vegetation has long invaded this site due to poor management of replanting activities. The creek is fringed with dense nipa vegetation which makes navigation into mangrove vegetation difficult (**Figure 2.5C**). The main economic activities along this creek are fishing and farming (**Figure 2.5B, E**).

Transects and plots were established and plot-size estimates of LAI, basal area and AGB were recorded (**3.2**). The plots were also categorised into three disturbance regimes and level of nipa invasion (**3.2.7**). Disturbance regime were classified using visual evidence of mangrove wood harvesting (**Figure 3.3**). Level of nipa invasion was divided based on the number of nipa stand within each plot (**3.2.3**).

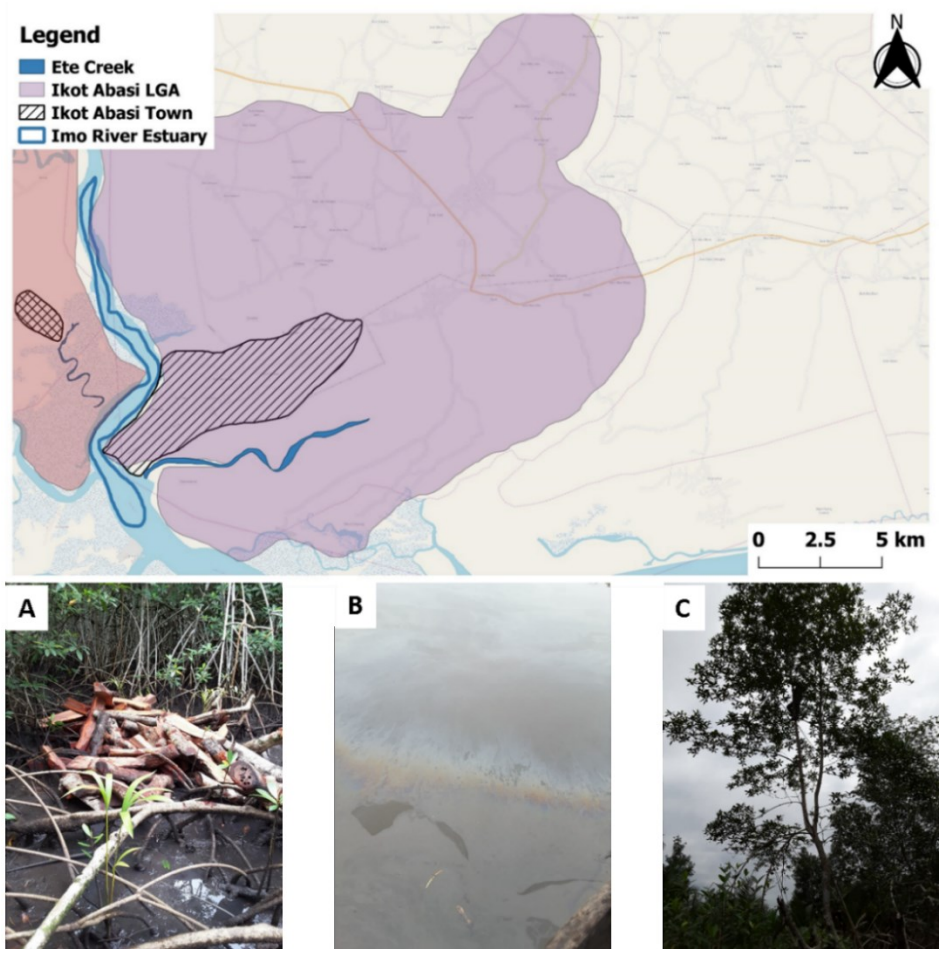

*Figure 2.3: Site Ete Creek with surrounding town and Local Government Area (LGA). Insets show wood exploitation (**A**), oil film on water surface evidence of oil pollution (**B**) and evidence of tall trees measuring above 15m (**C**).*

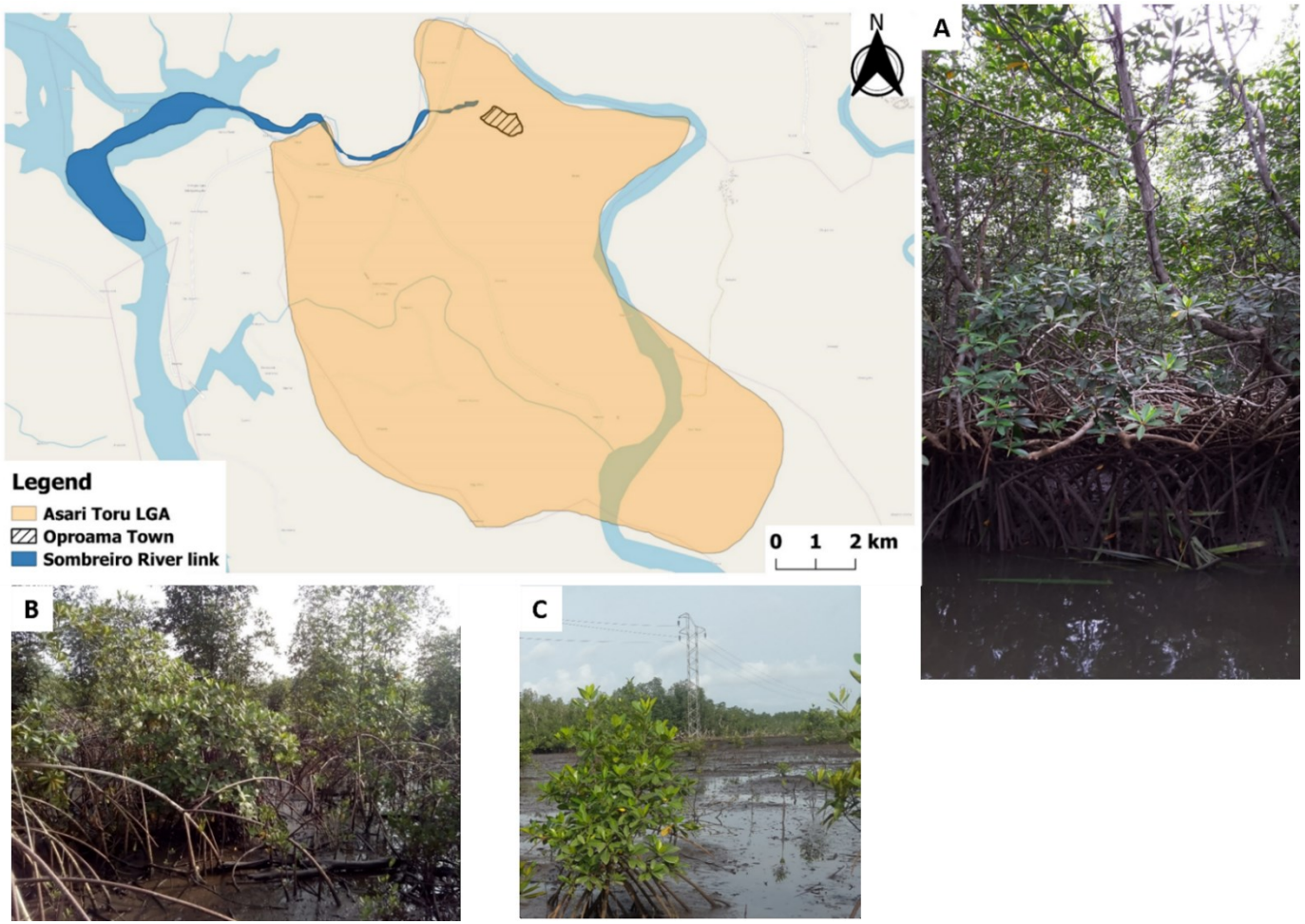

*Figure 2.4: Site Oproama with surrounding town, Local Government Area (LGA) and creek. Insets show mangrove structure at the fringe (**A**), stunted growth of mangrove (**B**) and cleared mangrove area for powerline construction (**C**).*

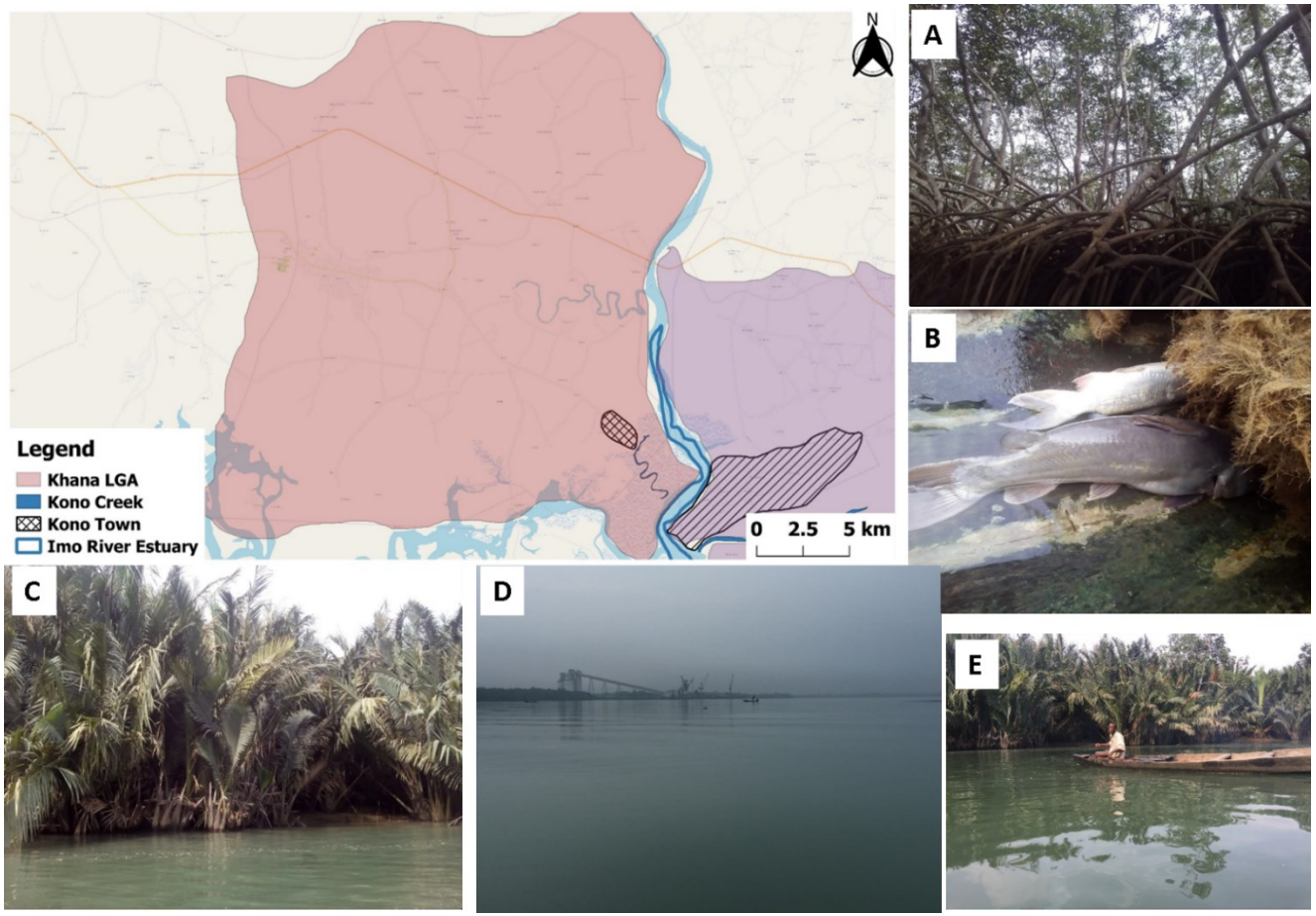

*Figure 2.5: Site Kono Creek with surrounding water body, town and Local Government Area (LGA). Insets show intact dense mangrove stands (**A**), fish catch from local fisherman (**B**) tall nipa fringes along the tidal channel (**C**), Imo River estuary (**D**) and local fisherman with background nipa and mangrove stands (**E**).*

2.2.3 Field-based Data Collection

I assessed structural characteristics of mangrove forests plots, AGB, LAI and disturbance between October, 2016 and September, 2017 across the three locations in the Niger Delta (**3.2**). Mangrove ecosystems are difficult to navigate due to root arrangement, tidal inundation and density of trees. Biomass studies in mangroves are usually done using small plots of about 7m radius but can be modified based on environmental conditions (Kauffman and Donato, 2012). However, in this study, which includes spatial analysis, plots of about 1ha are required in order to correlate pixel size of the remote sensing product in estimating structural properties. Hence, I used sample plot size of 50m by 50m (**Figure 2.6A**) across transects perpendicular to the tidal channel where I carried out forest structural attributes, above ground biomass, LAI and ground truthing activities. I counted and recorded every stand with DBH ≥ 5cm in each plot to account for stem density (**3.2.3**).

2.2.3.1 Assessing mangrove forests structure, disturbance and nipa palm presence

Mangrove forest structure was assessed using DBH as the primary parameter measured in the plot (0.25 ha, **Figure 2.6B**). I recorded DBH of live red mangrove (*Rhizophora* spp) stands with 5cm as the minimum. Trees with branched stem above the breast height (1.37m) were measured as a single stem (**Figure 2.6C**), while the individual stems were measured as single trees if they branched below the breast height (**Figure 2.6D**). Trees with multiple prop roots above the breast height were measured above the highest prop root (**Figure 2.6E**). I divided the measured DBH into stem size classes to determine its relationship to AGB, disturbance gradient and the contributory percentage of each size class to the AGB in each plot (**3.2.3**). The rationale behind this was that the percentage contribution of each size class to plot AGB could be a proxy for forest disturbance. Using DBH, I calculated basal area as a mangrove structural parameter to compare with AGB, LAI, distance and disturbance gradient (**Equation**

3.1). Basal area was also used as a quantitative metric in disturbance regime characterisation (Table 3.1). I randomly estimated the height of three trees within each plot using a clinometer. However, this was not adequate for further analysis (Appendix I).

I estimated stand AGB from the allometric equation (Equation 3.2). I used AGB as a proxy for biomass productivity and related it to LAI, distance and disturbance gradient. I used AGB estimates from a general allometric equation (Komiyama *et al.*, 2005) because of the inclusion of specific density of the tree species and range of DBH (5.1-48.9) used in generating the allometry (3.2.4). The inclusion of SD and DBH range matches the range of DBH (5-42) recorded during this thesis (3.3.1). The allometric equation used had a standard error of 0.085, however, a correction factor had already been applied to the final equation. I also measured mangrove canopy structure using LAI as proxy measured using hemispherical photography (3.2.5). Hemispherical photographs were taken using Nikon D500 fitted with a fish eye lens (Figure 2.6F). The picture was taken north facing with even sky clarity at a height of 1.3m. Forest inventory plots were divided into three different disturbance regimes: heavily exploited, medium exploited and undisturbed using quantitative and qualitative criteria (3.2.7).

2.2.3.2 Retrieving Surface reflectance and Mangrove Productivity

I used LAI as a proxy for productivity. The relationship estimated plot AGB and LAI was also established (3.3.4). I also extracted plot vegetative indices using georeferenced plot outline. (3.2.6). However, due to the 500m resolution of the Moderate Resolution Imaging Spectroradiometer (MODIS) Normalized Difference Vegetation Index (NDVI), I averaged the plots within the same 500m resolution. I then established the relationship between MODIS NDVI and both AGB and LAI.

2.2.3.3 Ground Control Points Selection

During the field survey, GCPs were established by collecting GPS coordinates of 6 land cover types over the Niger Delta (**4.2.6**). GCPs were not limited to the locations of the field plots but over the entire Nigerian coastline. I collected over 500 GCPs and used these as shapefiles for input in land cover classification.

2.2.3.4 GPS Retrieval of Field Plot AGB

Established field plot AGB formed the basis of the relationship between radar backscatter and biomass. However, in order to account for GPS error and backscatter noise, I increased the plot size to 60X60 m when extracting radar backscatter from the satellite imagery in order to reduce speckle (**5.2.3**).

*Figure 2.6: Field data collection in the Niger Delta mangrove forests. **A**). Plot delineation. **B**). DBH measurement. **C**). DBH measurement of branched stand above breast height. **D**). DBH measurement of branched stand below breast height. **E**). DBH measurement above highest prop root. **F**). LAI from hemispherical photography.*

2.3 Earth Observation Data Collection

2.3.1 Reconnaissance Survey

During my recon visit, I collected ROIs of seven land cover types (surface water, agricultural land, forests, mangrove forests, nipa palm, urban regions and sandy beaches; **Figure 2.7**). The GPS locations of each of the training sites were projected onto the image scenes, and the mean values of the radar bands (Horizontal-send Horizontal-receive (HH), Horizontal-send Vertical-receive (HV) and HV HH ratio) extracted for the different land cover types. Detailed pre-processing of earth observation satellite is shown in the individual chapters (**4.2.3**, **5.2.2**). I checked for a difference in radar backscatter between nipa palm invasive vegetation, mangrove ecosystem and other land cover types. The ROIs were not sufficient enough for a complete analysis, however, there was a significant difference in the visual area between mangroves and nipa palm (**Figure 2.8**). The nipa palm was significantly different from mangroves, farm and bush/ forest in the HV and HH bands (**Table 2.2**, **Table 2.3**). None of the vegetative land cover types were significantly different from each other in the HV: HH ratio. However, in the HH band mangroves were significantly different from nipa palm and significantly different from nipa and farm in the HV bands. This difference shows that there seems to be difficulty differentiating mangroves from tropical forests in L-Band SAR data. The bush, farm and mangrove land cover types were not different in the HH and HV scenes however, these would be further separated using Landsat imagery, DEM and tree height. From this preliminary analysis, I predicted that mangrove vegetation can be distinguished from nipa palm vegetation on both bands which can aid in estimating the extent of nipa palm invasion in coastal Nigeria.

The data and analysis I carried out during the reconnaissance survey validated the methodology I used in my thesis. This validation was also accompanied by improvement and considerations in achieving a successful field data collection and remote sensing data.

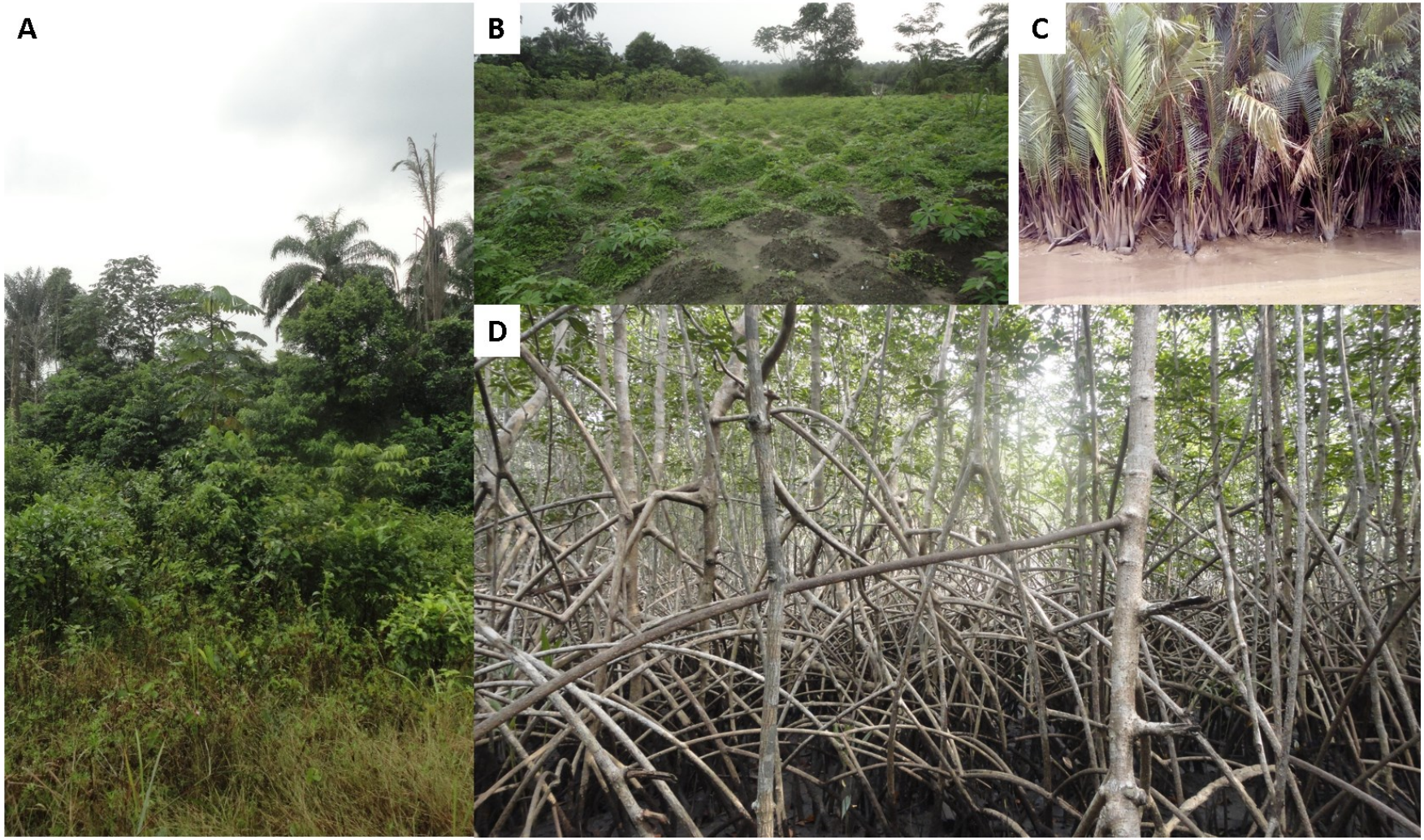

*Figure 2.7: Land cover classes used in land cover classification. **A)** Forest **B)** Agricultural land **C)** Nipa palm **D)** Mangrove forest.*

Figure 2.8: *2015 layer stacked ALOS PALSAR HH-HV-HV/HH Scene showing possible vegetation zonation patterns in relation to the radar backscatter in the Calabar estuary.*

Table 2.2: Mean and SD of ALOS PALSAR 2015 Backscatter for HH, HV and HV/HH for the different predicted land cover types in coastal Nigeria. These Land cover areas were estimated from the recon visit and Google earth imagery in March, 2016 from 4 different states.

Land Cover Type	Frequency	HH mean	HH SD	HV mean	HV SD	HV:HH mean	HVHH SD
Bush/forest	15	-5.39	0.92	-12.11	1.22	0.24	0.07
Farm	12	-7.36	1.29	-13.97	1.34	0.24	0.05
Mangrove	24	-6.10	2.02	-13.47	1.19	0.19	0.07
Nipa palm	22	-9.22	1.10	-16.67	1.54	0.19	0.03
Sandy beach	13	-13.76	3.71	-23.16	5.68	0.15	0.09
Water	13	-0.69	1.48	-14.92	1.40	0.07	0.02
Urban	14	-20.49	2.00	31.63	1.10	0.09	0.05

Table 2.3: Test for significance for ALOS PALSAR 2015 Backscatter for HH, HV and HV/HH between the different predicted land cover types in coastal Nigeria.

Land Cover Type	Frequency	Mangrove			Nipa		
		HH	HV	HV/HH	HH	HV	HV/HH
bush/forest	7	-	-	-	×	×	-
farm	3	-	×	-	×	×	-
mangrove	24	-	-	-	×	×	-
nipa	8	×	×	-	-	-	-

× (significantly different at p< 0.05)/ **-** (not significant)

2.3.2 Remote Sensing Data Collection

The GPS coordinates of the field plots and GCPs were an integral part of the remote sensing on my thesis. Remote sensing data sets used include ALOS PALSAR (2007 and 2017), Shuttle

Radar Topography Mission Digital Elevation Model (SRTM) Digital Elevation Model (DEM) (2000) and Landsat (2007, 2017).

2.3.2.1 Estimating Distance of Field Plots from Coasts, Tidal Channel and Closest Settlement

Distance gradient was measured by collecting the GPS locations of the established plots and closest settlements. The closest settlement was located through communication with the field assistant. I measured the distance between the field plots and settlement from the preferred transportation method (land or water) using Google Earth Pro (GEP) 7.3.2.5776 (March, 2019). The distance between the field plots and the closest oceanic coast was measured using GEP and knowledge of the tidal flow. This was done using the ruler tool in GEP to trace a path between the settlement and the field plots either through a road or the water path. The ruler tool, automatically calculated the distance and this was used for analysis. These distances were measured in order to establish the relationship between mangrove productivity, population pressure and tidal influence (**3.2.2**).

2.3.2.2 MODIS NDVI Retrieval

Vegetation indices were downloaded using Google earth engine (GEE). MODIS was used because of the available daily NDVI record and its accuracy and less time consuming nature. MODIS NDVI for the period of field survey (October 2016 – September 2017) was extracted from the field plots ROIs. MODIS NDVI was then constrained to the growing season in the Niger Delta (March to October). This was done to account for optimum greenness and negative values were excluded due to the influence of tide (**3.2.6**).

2.3.2.3 Processing of Optical and Radar Data for Land Cover Classification and Biomass Map

I retrieved SRTM DEM (30m resolution) tiles over the Niger Delta using the earth explorer site hosted by the USGS (https://earthexplorer.usgs.gov/). These tiles were then mosaicked

in ENVI and projected to Universal Transverse Mercator (UTM) Zone 31 degrees North and World Geodetic System (WGS) 1984 datum. Landsat 7 scene over the Niger Delta was pre-processed using the GEE (Gorelick *et al.*, 2017). Cloud-free composite of USGS Landsat 7 Collection 1 Tier 1 Raw Scenes was created using a customised cloud free composite algorithm.

(https://code.earthengine.google.com/?accept_repo=users/nwobicj/nigerdeltamangrove). The cloud free composite was incorporated into ENVI for processing. The date stamp for the 2007 data ranged between 01-01-2005 and 31-12-2007; while the 2017 scene ranged between 01-01-2015 and 31-12-2017. The extended date stamp was done in order to fill up scenes excluded due to cloud cover. Raw ALOS PALSAR 25m Mosaic files (HH and HV bands) were downloaded from the Japan Aerospace Exploration Agency, Earth Observation Research Centre (http://www.eorc.jaxa.jp/ALOS/en/index.htm) for the years 2007 and 2017. The Individual data tiles were then imported, mosaicked to form a single image file of the Nigerian coastline in both bands and geo-referenced with the projection UTM Zone N31 WGS 1984. The image file of both bands were registered using Landsat band from Hansen *et al.*, (2013) using ground control points. This was then calibrated by converting the digital number (DN) value to decibel (dB) (**Equation 4.1**) based on the coefficients and equations from Shimada *et al.*, (2009). I then enhanced the imagery by reducing the speckle of the imagery using an enhanced Lee filtering process. This filtering system reduces the speckle but also minimizes the loss of information in the image, which gives the best results based on published results (**4.2.3.2.3**). After the calibration and enhancement; the backscatter coefficient (σ^o) is log transformed (P) (**Equation 4.2**) in order to carry out band calculations without being distorted with the negative values of the coefficient. I carried out image texture analysis (data range, mean and variance measures) on the optical and radar bands to add more information for land cover differentiation (**4.2.4**)**.** The DEM, Landsat bands,

ALOS PALSAR bands and texture measures were then layer stacked using ENVI tool and DEM as the base resolution (30m; **4.2.5**). This layer stacked data was now ready for spatial analysis. In order to find the relationship between ALOS PALSAR and field AGB estimates, the inherent 25m resolution was used to create a composite imagery if the HH, HV and HV: HH bands (**5.2**). I also used the shapefiles of the field plots to extract the plot mean values of the bands using GEP, QGIS, ArcGIS and ENVI (ESRI, 2011; QGIS Development Team, 2018; Tuiwawa *et al.*, 2013).

2.4 Data Analysis

All statistical analysis was done using the RStudio version 0.99.491 (RStudio Team, 2015) while spatial analysis was done using ENVI version 5.2 ("Exelis Visual Information Solutions, Boulder, Colorado"), QGIS 3.4 (QGIS Development Team, 2018), GEE (Gorelick *et al.*, 2017), GEP 7.3.2.5776 and ArcGIS 10.4 (ESRI, 2011).

2.4.1 Relationship between Mangrove Structure and Gradient Measures

I used Spearman's correlation to test for the strength and direction of the relationship of plot AGB and the gradient of closest settlement, tidal channel and ocean. I used Analysis of variance (ANOVA) to test for significant difference between disturbance regime with AGB and LAI. I further used a Tukey post hoc test to examine the order of difference amongst the disturbance regime. I also used ANOVA to test for the difference in stem density and size class contribution to AGB amongst disturbance regime. Correlation analysis was done to check for the relationship between plot nipa stand population and distance from sea gradient, basal area, AGB, stem density and LAI. I also used ANOVA to check for significant difference in basal area removed, LAI variance and DBH size class contribution to AGB amongst nipa invasion degree (**3.2.8**).

2.4.2 Relationship between Canopy Features and Biomass

I analysed the relationship between AGB, LAI and MODIS NDVI using spearman's correlation and linear regression model. I did this to check for the predictive power of MODIS NDVI on AGB and LAI; and the predictive power of LAI on AGB (**3.2.8**).

2.4.3 Spatial analysis and Change Detection

Supervised classification was carried on the layer stacked satellite data (**4.2.7**). I used SVM and MLC methods to differentiate 6 land cover types (**4.2.2**). The SVM method was modified based on kernel types to extract the most accurate variant. Confusion matrices were carried out to test for the accuracy of the different classification methods used (**4.2.8**). I estimated the area of mangrove and nipa by multiplying the number of pixels in each class by the spatial resolution in each classification image. I also used the change detection tool to estimate the change in each land cover type from 2007 and 2017 (**4.2.9**).

2.4.4 Relationship between Field AGB Estimates and Radar Backscatter

I used a linear regression model to test the relationship between field AGB and 2017 radar backscatter (**5.3.2**). I applied the best predictive model to the radar mosaic of 2007 and 2017 using the band calculation tool in ENVI (**5.3.3**). I then masked the non-mangrove regions in the mosaic using the mangrove region resulting from the land cover classification from the previous research question (**5.3.3**). I also masked out biomass values below 0 and above 200 Mg ha^{-1} to be conservative with AGB estimates. The mangrove AGB maps generated for both years were then compared for change in mean and total AGB (**5.3.4**).

2.5 References

ESRI. (2011). ArcGIS Desktop: Release 10. Redlands, CA: Environmental Systems Research Institute.

Exelis Visual Information Solutions, Boulder, Colorado. (2010).

Fromard, F., Puig, H., Mougin, E., Marty, G., Betoulle, J. L., & Cadamuro, L. (1998). Structure, above-ground biomass and dynamics of mangrove ecosystems: New data from French Guiana. *Oecologia*, *115*(1–2), 39–53. https://doi.org/10.1007/s004420050489

Gorelick, N., Hancher, M., Dixon, M., Ilyushchenko, S., Thau, D., & Moore, R. (2017). Google Earth Engine: Planetary-scale geospatial analysis for everyone. *Remote Sensing of Environment.*

Hansen, M. C., Potapov, P. V, Moore, R., Hancher, M., Turubanova, S. A., & Tyukavina, A. (2013). High-Resolution Global Maps of 21st-Century Forest Cover Change. *Science*, *342*(6160), 850–853. https://doi.org/10.1126/science.1244693

Kauffman, J., & Donato, D. (2012). Protocols for the measurement, monitoring and reporting of structure, biomass and carbon stocks in mangrove forests. *Center for International Forestry*, *Working pa*, 11. https://doi.org/10.17528/cifor/003749

Komiyama, A., Poungparn, S., & Kato, S. (2005). Common allometric equations for estimating the tree weight of mangroves. *Journal of Tropical Ecology*, *21*(4), 471–477. https://doi.org/10.1017/S0266467405002476

QGIS Development Team. (2018). QGIS Geographic Information System. Retrieved from http://qgis.osgeo.org/

RStudio Team. (2015). RStudio: Integrated Development for R. *[Online] RStudio, Inc.,*

Boston, MA URL Http://Www. Rstudio. Com.

https://doi.org/10.1126/science.aad6351

Shimada, M., Isoguchi, O., Tadono, T., & Isono, K. (2009). PALSAR radiometric and geometric calibration. *IEEE Transactions on Geoscience and Remote Sensing*, *47*(12), 3915–3932. https://doi.org/10.1109/TGRS.2009.2023909

Simard, M., Pinto, N., Fisher, J. B., & Baccini, A. (2011). Mapping forest canopy height globally with spaceborne lidar. *Journal of Geophysical Research: Biogeosciences*, *116*(4), 1–12. https://doi.org/10.1029/2011JG001708

Tuiwawa, M. V., Pene, S., & Tuiwawa, S. H. (2013). *A Rapid Biodiversity Assessment , Socioeconomic Study and Archaeological Survey of the Rewa River Mangroves, Viti Levu, Fiji.*

Chapter 3

Stand, Biomass and Canopy Properties across Disturbance Gradients in Mangrove Forests of the Niger Delta.

C. J. Nwobi[a], M. Williams[a], E.T. A. Mitchard[a]

[a] *School of GeoSciences, University of Edinburgh, Edinburgh, EH9 3JN, UK*

Abstract

Mangrove forests in the Niger Delta are poorly quantified and at risk due to oil pollution, deforestation, and invasive species. Here, I report the most extensive survey yet of mangrove plots for stand, biomass and canopy properties in the Niger Delta, across tidal and disturbance gradients. I established twenty-five geo-referenced 0.25-ha plots across three regions. I estimated aboveground biomass (AGB) from established allometric equations based on stem surveys. Leaf area index (LAI) was recorded using hemispherical photos. I estimated mean AGB of 83.7 Mg ha^{-1} with an order of magnitude range, from 11-241 Mg ha^{-1}. I found significantly higher plot biomass in close proximity to protected site and tidal channel, and the lowest in the sites where urbanisation was actively taking place. The mean LAI was 1.45 and ranged five-fold from 0.46 to 2.41. There was a significant positive correlation between AGB and LAI (R^2= 0.28), supporting a hypothesised link between production and biomass. Satellite observations of NDVI for the growing season correlated positively with in-situ LAI (R^2= 0.63) and AGB (R^2= 0.80). I divided the plots into three disturbance regimes and three nipa palm invasion levels. Lower stem sizes (5-15cm) accounted for 70% of the total biomass in disturbed plots, while undisturbed regimes had a more even contribution of different size classes to AGB. Nipa palm invasion also showed a significant link to larger variations in LAI and proportion of basal area removed within plots. I conclude that forest degradation is removing larger stems (> 15 cm DBH) preferentially from these mangroves and creates an avenue for nipa palm colonisation. This research identifies opportunities to use remote sensing to estimate biomass, based on LAI-AGB-NDVI relationships, and can also serve as a calibration dataset for other remote sensing data, such as radar.

Keywords: *mangrove, aboveground biomass, leaf area index, disturbance, stand structure*.

3.1 Introduction

Mangroves are very productive ecosystems due to their tropical coastal location (Daniel M Alongi, 2009). These ecosystems provide a range of ecosystem services, including provisioning services (such as fisheries and fuelwood), regulatory services (carbon storage, nutrient cycling and shoreline protection), and cultural/aesthetic values (Bouillon *et al.*, 2008; Feka and Ajonina, 2011; Friess, 2016; Kauffman *et al.*, 2011; McLeod and Salm, 2006; Mukherjee *et al.*, 2014). Mangroves act as a valuable carbon sink contributing ~15% to coastal sediment storage of carbon, despite making up about 0.5% of the world coastal area (Daniel M. Alongi, 2014). However, mangrove ecosystems are threatened by deforestation and contribute ~10% of the total global deforestation emissions (Donato *et al.*, 2012). The relevance of carbon storage in mangrove sediments and deforestation rates has made mangrove an essential focus for climate change mitigation through conservation and reforestation projects, for instance under the Reducing Emissions from Deforestation and forest Degradation (REDD+) programme.

Nigeria's coastal zone is made up of lagoons, deltas and estuaries that comprises of mangrove forests and sandy beaches. The mangrove ecosystem in Nigeria is ranked the fifth country with the largest mangrove area globally (Giri *et al.,* 2011; Hutchison *et al.,* 2014; Lucas *et al.,* 2014). The Niger Delta contains about 60% of these mangroves (FAO, 2005; Fatoyinbo and Simard, 2011). Mangrove forests have relatively low diversity in Nigeria, being made up of only three genera which include *Rhizophora* (red mangrove), *Laguncularia* (white mangrove) *and Avicennia* (black mangrove) (Food and Agriculture and Organization, 2007). Intact mangrove forests in Nigeria serve as important sources of seafood including shellfish, finfish and nursery grounds for these organisms (Feka and Ajonina, 2011). These aquatic organisms are also vital indicators of intact mangrove ecosystems in coastal Nigeria (Amadi *et al.*, 2014). Likewise; the presence, absence or abundance of specific floral indicators

related to mangrove species are indicators of mangrove health and perturbation (Mmom and Arokoyu, 2010). However, the increasing population, resultant development and industrial activities are changing this valuable ecosystem. Coastal development, aquaculture expansion and over-harvesting have led to a 30-50% reduction in global mangroves over the past 50 years (J. B. Kauffman *et al.*, 2011). Loss of mangrove regions in the Niger Delta is prominently due to oil spills, land reclamation for housing, road, electricity power lines, port development and dredging points (Feka and Ajonina, 2011). Local communities depend on mangrove cutting for fuelwood and commercially for sale in the Niger Delta. Mangroves also provide wood products to the wood industry in Nigeria. However, this practice is unsustainable and threatens mangrove forests in Nigeria (Kinako, 1977). Unchecked logging of mangrove trees leads to a reduction in mangrove stands and has been linked to the expansion of the invasive *Nypa fruticans* within the Niger Delta (Global Invasive Species Database (GISD), 2015; Okugbo *et al.*, 2012). Information on patterns of mangrove loss is sparse, but vital to support conservation measures. Limited research in mangrove forests in Nigeria is primarily due to social unrest, restricted access and security. These hindrance to mangrove forest research have resulted in non-existent mangrove forest structure data in the Niger Delta, restricting mangrove research to community structure relationship with soil properties, carbon dynamics in litterfall traps, remote sensing of forest area and remediation (Edu *et al.*, 2014; Edu *et al.*, 2014; Fatoyinbo and Simard, 2013; Jackson, 2011; James *et al.,* 2013; James *et al.*, 2007; Ukpong, 1994, 2000b). One viable option for mangrove research in Nigeria include the use of remote sensing due to the challenge of field surveys in the region. However, remote sensing data need ground calibration, and hence field research is still a requirement.

Field estimates of stand structure such basal area (BA) and stem size, canopy properties such as leaf area index (LAI) and aboveground biomass (AGB) can form a baseline to monitor

mangrove forest change and restoration plans, and support calibration of remote sensing data. BA can form the basis for monitoring the removal of mangrove stands from logging activities (Ngoc Le *et al.*, 2016). Both LAI (Clough *et al.*, 1997) and AGB accumulation over time (Daniel M Alongi, 2009) can be used as indicators of net primary productivity. In-situ measurement of ABG and LAI over a forested landscape are vital for integration with satellite imagery forests, both optical and radar data (De Kauwe *et al.*, 2011; McNicol *et al.*, 2017). LAI and AGB can be linked to vegetation indices such as Normalized Difference Vegetation Index (NDVI) and Enhanced Vegetation Index (EVI) in order to investigate long-term trends of forest health (Green *et al.*, 1993; Kovacs *et al.*, 2004). These vegetative indices are retrieved from optical imagery which sometimes faces the problem of cloud cover. Field estimates of biomass can be used to calibrate radar backscatter data for regional assessments of biomass stocks and changes (Mitchard *et al.,* 2009; Ryan *et al.*, 2011). Despite the cloud cover issues over the tropics in analysing optical imagery, a model of vegetative indices, LAI and AGB can form a basis for monitoring mangroves in the Niger Delta. However, in order to monitor local disturbance such as targeted logging or invasive species, a fine scale of observation has to be adopted in mangrove monitoring.

Selective harvesting in natural forests is a subtle activity being carried out by local communities in the Niger Delta. This wood exploitation can result in the change in stand size and canopy structure (Walters, 2005), as a result of targeting particular tree classes in wood harvesting. A target tree size is the most economical range of tree size harvested in order to maximise profit. For mangrove forests located along creeks, target stems are those with maximum harvestable tree sizes that allow efficient water transport to the point of sale. The target size class depend on the type of forest, wood species, the distance of forest from the point of sale, type of harvesting tool, the gender of harvester and transportation means (Allen *et al.*, 2001; Feka and Ajonina, 2011; Walters, 2005). The change in stand size structure

of mangrove forests has a direct effect on stand biomass by altering the relative contribution of different stem sizes to the AGB. Selective harvesting can also result in light gaps which are prominent features of mangrove forests. Forest gaps are established from natural (hurricane or lightning) or anthropogenic (wood exploitation) disturbance. Selective harvesting and the resultant light gaps are detrimental to mangrove forests of the Niger Delta because of the presence of the alien invasive nipa palm. Light gaps created by cutting of tree species create an avenue for either colonisation by invasive species or reestablishment of mangrove species (Harun Rashid *et al.*, 2009; Potin, 2013; Schnitzer *et al.*, 1991). Mangrove and nipa palm shrubs growing together within light gaps formed by logging are common features in the Niger Delta.

This is the first report on mangrove biomass in the Niger Delta that spans two states in Nigeria and covers a wider area from the Niger Delta creeks in Rivers State and the Imo river estuary in Akwa Ibom State. Previous biomass surveys were restricted to one location and small plot size (Numbere and Camilo, 2018; Nwigbo *et al.*, 2013). This is also the first report on mangrove biomass patterns across the Niger Delta in relation to distance from ocean, tidal channel and settlement. Previous reports have studied mangrove distribution in relation to soil patterns but no report on AGB in the delta (Ukpong, 1994, 2000b, 2000a). I also provide a first step to monitor mangrove productivity by establishing a relationship between canopy structures, woody biomass and vegetative indices in the Niger Delta. This analysis can be the basis of modelling mangrove forest productivity in the Niger Delta. The invasion of nipa palm in mangrove forests is a subtle issue in the Delta, slowly replacing the natural mangrove stands as a result of deforestation. Here I report the possible effect of wood exploitation on the colonisation of nipa on mangrove forests. Previous reports have estimated area coverage per state (Isebor *et al.*, 2003) and nipa influence in changing habitat (Ukpong, 2015), but no report has been given on the relationship between nipa invasion and

mangrove forest disturbance. I also report here the first largest stem size survey in the Niger Delta and how local disturbance is altering the contribution of these stands to the biomass of the Niger Delta mangrove forests. The relationship of biomass, disturbance and stand structure in the Niger Delta can inform restoration projects on target stand size and management plan.

The objective in this research is to provide a large survey of the relationships amongst mangrove stand, canopy and biomass patterns in the Niger Delta. I address the following questions: **a)** how does AGB vary with proximity to the ocean, tidal channel and settlement? **b)** What is the relationship between AGB and LAI? **c)** What is the predictive power of surface reflectance to mangrove forest LAI and AGB in the Niger Delta? **d)** What is the effect of local disturbance on the stem size structure of mangrove forests? **e)** Is mangrove cutting a precursor to nipa palm invasion in the Niger Delta? I hypothesise that higher biomass plots will be closer to tidal channel and farther from human settlements. I also hypothesise that vegetative indices and LAI can significantly predict biomass. Lastly, I test the hypothesis that disturbance is removing mangrove stands with higher DBH size and altering their contribution to AGB. I also test the effect of wood exploitation as a precursor to nipa palm invasion in the Niger Delta. The information on the relationship between LAI, AGB and NDVI can provide a basis of mangrove production monitoring in coastal Nigeria. Also, the understanding of local disturbance and nipa palm invasion on mangrove structure can assist in the control of these adverse effects on mangroves.

3.2 Methodology

3.2.1 The Niger Delta

The Niger Delta is the largest coastal delta in Africa and the ninth largest wetland in the world with an estimated area of 19,135 km^2 (Campbell, 2017; Dupont *et al.*, 2000). The Niger Delta (2 M ha) houses the most extensive mangrove in Nigeria making up ~ 60% of the total area in Nigeria. The delta contains all three mangrove species characteristic of the Atlantic coasts. These species are *Rhizophora, Avicennia* and *Laguncularia* species. Temperature ranges from 21°C to 33°C. Mean annual precipitation of 2436 mm (Amechi *et al.*, 2014) ranging between 1500mm to 4000mm (NDDC, 2006). There are two seasons in Nigeria with highest temperatures between February and April; and lowest temperatures during the peak of the rainy season between June and September (NDDC, 2006).

3.2.2 Study Area and Sampling Strategy

The overall approach during the field study was to set up plots to measure stem density, stem size, LAI and AGB across disturbance gradients in the delta. The study was carried out in two states of the Niger Delta - Rivers and Akwa Ibom **(Figure 3.1)**. There were 2 locations in Rivers state and one location in Akwa Ibom state. I picked these locations because of accessibility to mangrove stands, safety within these regions, the presence of local guide within the region, and varying disturbance and distance from the sea and local communities within these locations. Safety and accessibility were the most significant challenges during the field campaign because of social unrest within the Niger Delta. A tree height map (Simard *et al.*, 2011) was also used to identify high biomass regions in the region, however, a proper species representation in the region was not possible as a result of security, time and resources.

I established four transects in Oproama community (**O**- field plot designation), Asari Toru Local Government Area (LGA) in Rivers state. Three transect had three plots each, but on the

fourth I was only able to establish two plots due to local community restrictions. While locals in this community have high aesthetic value for mangroves there is ongoing clearance for the development of roads and power lines. I established one transect with two plots in Kono community (**K**), Khana LGA, Rivers state; due to a high level of nipa invasion at the fringes which made mangrove access difficult. I established five transects in Ete (**E**) Kingdom of Ikot Abasi LGA in Akwa Ibom State; two transects with three plots and three transects with two plots each.

I established transects within each location based on mangrove span from the tidal channel and took into account the variation in mangrove biomass, stand structure and local disturbance. Plots, each 0.25 ha (50 x 50 m), were established within each transect 10 m apart. I chose the plot size to account for the pixel size of remote sensing data which ranged from 25-m for ALOS PALSAR and 30-m for SRTM DEM. The plot sizes were also chosen to maximise sampling time within very dense mangrove forests. The first plot within each transect was established 15 m from the tidal channel **(Figure 3.2)**. Overall, I established twenty-five sample plots (**O- n=11, K- n= 2, E- n= 12)** from October 2016 to September 2017. During the field survey, I observed that *Rhizophora* species dominated these plots with no *Avicennia* or *Languncularia* species identified within the plots. I collected global positioning system (GPS) points of the field plots and closest settlement during the field survey using Garmin eTrex 20x. I also measured the distance between field plots and distance from the ocean, tidal channel and closest settlement from GPS locations using Google earth Pro.

3.2.3 Forest Inventory

I counted, measured, and recorded all trees with a diameter at breast height (DBH)>5 cm within the sample plot. I measured DBH at 1.3 m above the ground, and if the tree branched below 1.3 m, individual stems were measured and counted as one tree. However, there were unusual cases where I used modified DBH measurement due to the structural complexities

of *Rhizophora* spp (Dahdouh-Guebas and Koedam, 2006; Hossain *et al.*, 2017). I divided the measured DBH into four size classes: 5cm – 10cm, 10cm – 15cm, 15cm – 20cm and >20cm; to account for the DBH range, stand density and to analyse stand size structure. Basal area was also calculated by summing over all (n) trees per plot, using the equation **(Equation 3.1)** using DBH in cm (***DBH***), described by Cintron and Novelli, (1984), and reported in metres per hectare (m^2 ha^{-1}) by normalising using plot area (***A***) in ha. I also measure height of three stands within in each plot using a Suunto clinometer PM- 5. Within each plot, I enumerated nipa palm and calculated the ratio between nipa stand to mangrove stand. I classified the plots into three invasion classes: no invasion (**NI-** 0%), moderate invasion (**MI-** 0-10%) and heavy invasion (**HI-** >10%) based on the number of nipa stands within each plot. This division was used to check for the incident of mangrove cutting as a precursor for nipa invasion.

$$\textbf{Basal area} = \left(\sum_{i=1}^{n} \boldsymbol{\pi} \left(\frac{\boldsymbol{DBH_i}}{\boldsymbol{200}}\right)^{\boldsymbol{2}}\right) \div \boldsymbol{A} \qquad \textbf{(Equation 3.1)}$$

3.2.4 Aboveground Biomass

I calculated aboveground biomass (AGB, B_{above}) using a common allometric model (**Equation 3.2**) for mangrove developed by Komiyama *et al.*, (2005):

$$\boldsymbol{B_{above}} = 0.251 \times \boldsymbol{\rho} \times \boldsymbol{DBH}^{2.46} \qquad \textbf{(Equation 3.2)}$$

Where ρ = average wood density (0.8998 g cm^{-3}) of the 3 indigenous *Rhizophora* species *R. racemosa*= 0.9330 g cm^{-3}, *R. harrisonii*= 0.86 g/cm^3, *R. mangle*= 0.9064 g/cm^3 [Wood Density database Website] and *DBH* is the diameter at breast height in cm. The wood density used is same as reported by a local study in Nigeria (Adedeji *et al.*, 2013). I used the general

mangrove allometric equation developed by Komiyama *et al.*, (2005) due to the absence of a site specific allometry. This was the preferred allometric equation over two other allometric equations developed in Cameroun (Ajonina, 2008) and an inventory data from the Niger Delta (Nwigbo *et al.*, 2013). These other allometric equations couldn't be followed up due to incomplete information and non-communication from the authors. The general allometric equation was developed from 104 trees of 10 mangrove species with dbh range 5 to 48.9 cm. The dbh range from this study ranged from 5 to 42 cm falling within the range of the allometric equation used. The inclusion of wood density in the general allometric equation could account for site variation in species and is important in estimating the different parts of the biomass (Komiyama *et al.*, 2005).

I investigated how variations in AGB related to differences in stand structure, disturbance regime and the distribution of stem sizes. I calculated the proportional contribution of each DBH size class to the total measured AGB within each plot. Also, I established the relation of AGB to LAI and NDVI.

3.2.5 Leaf Area Index

I estimated canopy cover and LAI from hemispherical photographs taken at 3 points within each plot **(Figure 3.2);** using a Nikon D500 camera fitted with a Sigma EX DC HSM (4.5mm; 1:2.8) circular fisheye lens and Jessop's ultraviolet filter. In order to attain even sky illumination, I took fish eye photos between 9 am and 3 pm at the peak of exposure and conditions of even skylight (Bequet *et al.,* 2011). I waited for even cloudy cover when sky conditions were not too sunny nor too dark. Adequate periods of canopy properties, dusk and dawn, were not possible as a result of accessibility to field plots. I also waited for minimal wind movement to obtain adequate shutter speed to freeze any foliage movement at small ISO settings. I set the aperture at f-9, and the camera was set to auto exposure so that shutter speed would auto-compensate for changes in ISO. I analysed hemispherical photographs

using the Gap Light Analyser (GLA) imaging software used to extract forest canopy structure and gap light transmission indices (Frazer, Canham, and Lertzman, 1999). Default threshold levels used in defining leaf and sky features during image analysis were adjusted manually in order to reduce the contribution of sunlight and cloud cover shades to canopy features.

3.2.6 Vegetation Indices

I extracted plot-wise 16-day composite Moderate-Resolution Imaging Spectroradiometer (MODIS) NDVI data from Google Earth Engine (GEE) (Gorelick *et al.,* 2017) from the dates October 2016 to September 2017 using plot GPS. MODIS NDVI was preferred over Landsat calculation as a result cloud cover affecting the validity of the data. I extracted data for the mangrove growing season from March to October (Odenkunle, 2004) to account for the optimum greenness of the region and optimum relationship between NDVI and LAI during the study. As a result of the 500m resolution of the MODIS product, I averaged the plot-wise NDVI over a 500m transect from the image collection to examine the relationship between AGB, LAI and VI data. This reduced the twenty-five plot inventory to six. Establishing a relationship between vegetative indices and LAI can form a baseline to model mangrove forest productivity.

3.2.7 Disturbance characterization

I classified the plots into three disturbance regimes as follows: heavily exploited (HE), moderately exploited (ME) and undisturbed (Und) (**Table 3.1**). I based the classification on a quantitative and qualitative criteria (**Table 3.1**). I based the qualitative criteria for disturbance characterisations on visual evidence of disturbance, undergrowth and indicator species- mudskippers; while the basal area was the only quantitative criteria (Ajonina, 2008). I used the basal area because it is a more direct metric on the state of the system (Cox *et al.*, 2016; Ngoc Le *et al.,* 2016). I compared the basal area of each plot in the exploited regime to the mean basal area of the plots of the undisturbed plots within each of the three study

locations. I made this comparison to obtain a quantitative measurement of disturbance. The undisturbed plots were given the status of the maximum basal area a plot could hold. I then estimated the proportion of basal area removed from other plots within respective regions. I used this quantitative criterion to estimate how much of the vegetation was removed within disturbed plots per study region based on the basal area of the undisturbed plots.

The process of classifying plots into different disturbance regimes is complicated as various factors could contribute to the measured and observed criteria for characterisation. For example, the presence of nipa was only prominent in two (Kono and Ete) of the three locations. The second complication is the mode of exploitation of different plots depending on location. Mode of exploitation ranged from logging for fuelwood (Ete), total clearance for construction activities (Oproama) and passage for boat transport (all locations). The first criteria for classifying plots into disturbance categories were (**Figure 3.3**): 1) the observed wood exploitation in the region – i.e. logging, forest gaps or clearance; and 2) presence or absence of undergrowth within forest gaps. Plots were considered disturbed if they met these two criteria. The next criteria were based on the quantitative criteria of proportion of BA removed and presence of indicator species. To obtain a disturbance pattern, the BA of each plot were compared to the mean basal area of the undisturbed plot in each zone (plot with highest BA). This established the disturbance scale based on the proportion of basal area removed for all twenty five plots in all three regimes of exploitation.

3.2.8 Data Analysis

Linear regression models were used to establish the correlation between biomass (AGB), canopy characteristics (LAI) and vegetation indices (NDVI). Spearman's correlation followed by a Tukey HSD post-ad hoc tests were used to test for the significant relationship among

plot level stand parameters, AGB and canopy properties amongst plots of broadly similar disturbance regimes. I carried out analysis of variance (ANOVA) to assess significant differences in stand, AGB and canopy properties between disturbance regime, DBH size classes and nipa invasion. All data analyses were performed using RStudio version 0.99.491 (RStudio Team, 2015).

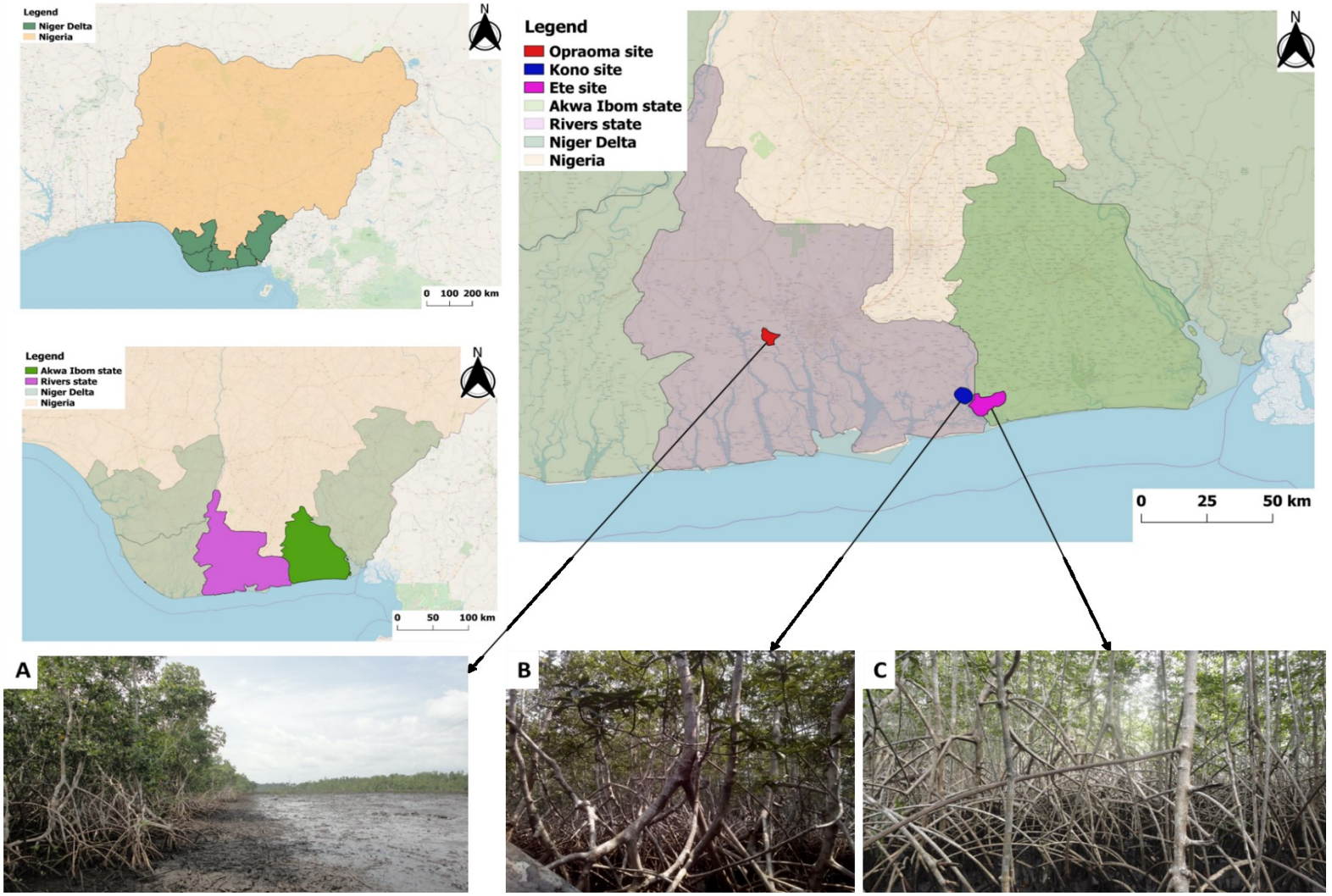

Figure 3.1: Location of the Niger Delta, sample states and field sites with inset pictures of the sites A- Oproama, B- Kono and C- Ete.

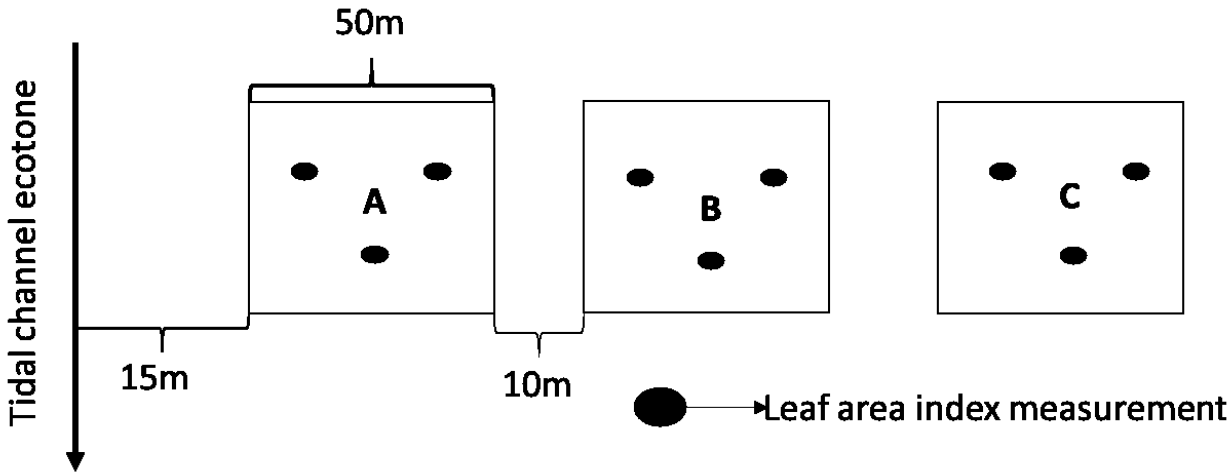

*Figure 3.2: Schematic of the plot layout for mangroves sampled. Letters A-C identify distance from tidal channel in all plot identifiers with **A** closest to the tidal channel. Plot identifier: **A1B** (**A**: location, **1**: transect number, **B**: plot distance from tidal channel)*

Table 3.1: Factors used to classify disturbance regimes in mangrove sites of the Niger Delta (Ajonina, 2008). Qualitative criteria were based on the visual state of the plots including the presence or absence of key species while quantitative characteristics were based on the basal area.

Criteria	Characteristics	Sub-Criteria	Instrument/ Method	Perturbation Regimes		
				Heavily Exploited (HE)	**Moderately Exploited (ME)**	**Undisturbed/ Unexploited (UND)**
Qualitative	**Evidence of cutting with forest gaps**		Visual observation	Present	Present	Absent
	Undergrowth	Density	Visual observation	Present in light gaps	Low	Absent
	Key indicator species	Mud skippers (*Periophthalmus nigrodigitatus*)	Visual observation	Absent	Present	Present
Quantitative	**Basal area (m^2ha^{-1})**	Ete		<8	8-15	⩾14
		Kono		-	-	⩾15
		Oproama		<4	4-7.5	⩾7.5
	Proportion removed	Ete		⩾0.7	0.4-7.0	<0.7
		Kono		-	-	<0.25
		Oproama		⩾0.5	0.3-0.5	<0.25

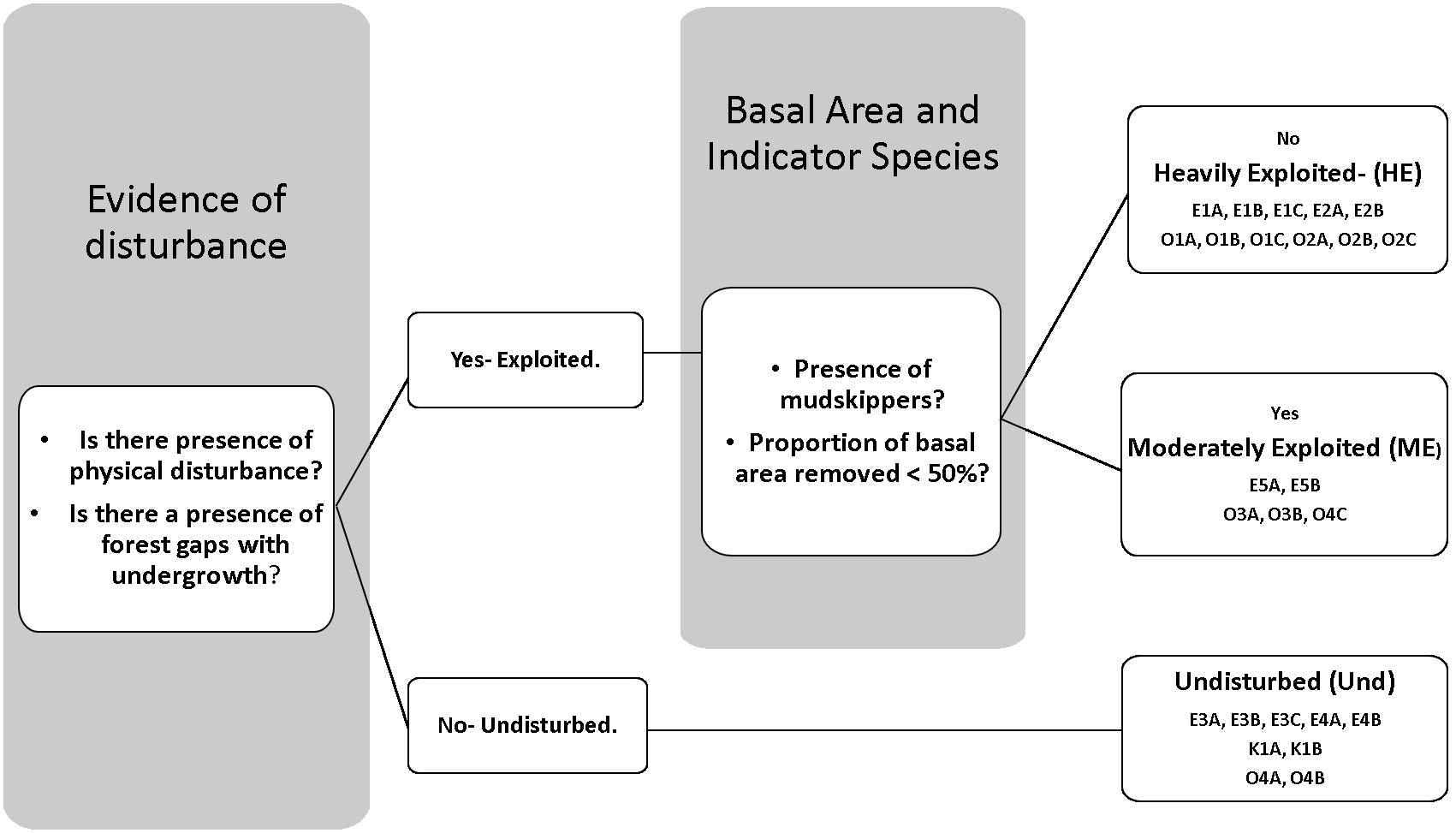

Figure 3.3: Hierarchal order for disturbance regime classification of study plots in the Niger Delta. Initial grouping of undisturbed plots was done using physical evidence of disturbance while basal area and indicative species were used to separate heavily from moderately exploited plots.

3.3 Results

3.3.1 Forest Inventory

I enumerated and measured a total of 5 729 trees across the 6.3 ha surveyed in the region. Mean stem density was 903 stems ha^{-1} and mean DBH was 9.9 cm (median= 9cm). DBH distribution was skewed and unimodal (**Figure 3.4**). I recorded the highest stem density (4,037stems ha^{-1}) in E3A and the lowest in O1C (204 stems ha^{-1}). I recorded the highest plot mean DBH (13.9 cm) in Kono (plot K1B) and the lowest (7.5 cm) in Ete (plot E4A). I recorded a mean plot basal area of 8.9 m^2 ha^{-1} and a median of 6.34 m^2 ha^{-1} (**Figure 3.5**). I also recorded the highest basal area (27.24 m^2 ha^{-1}) in Ete (E3A) and the lowest basal area (1.36 m^2 ha^{-1}) in Oproama (O1C) **(Appendix I)**.

Total stem measurements were stratified by stem size classes as follows; Class 1 (5-10cm) n= 3 709, Class 2 (10-15cm) n= 1 509, Class 3 (15-20cm) n= 360 and Class 4 (> 20cm) n= 151. The lowest size classes accounted for a majority (65%) of the stem density (**Table 3.2**). However, the DBH size class 4 (> 20cm) make up 22% of the total AGB of the region. I also discovered that stem size 15-20cm accounted for the lowest contribution (19%) to AGB in the study area, while the 10-15cm strata accounted for the highest biomass contribution (32%). I recorded the highest percentage (9.7 %) of stems > 20cm in Kono (K1B) while there was no record of stems > 20 cm in Oproama plots (O1C, O2B, O2C, O3B).

3.3.2 Aboveground Biomass

I estimated a mean plot AGB of 83.7 Mg ha^{-1} ranging from 11.1 to 241.2 Mg ha^{-1} **(Appendix II)**. Plot AGB for the study region was bimodal and skewed to the low AGB values (**Figure 3.5**). Plots with the highest biomass (>150 Mg ha^{-1}) were found in the community protected site in Ete and Kono, located close to the mouth of the Imo estuary. The lowest biomass (< 50 Mg ha^{-1}) was observed in the more inland creek (Oproama) sites where shrub mangroves were dominant and urbanisation actively taking place **(Appendix II)**. The highest AGB (241

Mg ha^{-1}) in the study was observed in the undisturbed plot in Ete (E3A) where the mangroves were protected from logging. In contrast, the lowest AGB (11 Mg ha^{-1}) was found in the disturbed plot in Oproama (O1C) community where a power line was constructed to convey electricity to the community. I observed significant difference in AGB amongst the three locations (Ete, Kono and Oproama) of the study area ($p < 0.001$) but Oproama alone showed significant lower AGB when compared to Kono and Ete locations ($p < 0.01$).

Stem density had a strong positive correlation with AGB (p-value = <0.00001, Spearman's rho (r_s) = 0.88), thus the higher the stem density, the higher the AGB in the plots. There was significant weak positive relationship (p-value < 0.05, r_s = 0.47) between AGB and distance from closest settlement. The farther the plots were from the settlement, the higher the AGB in the region. There was a weak negative correlation between AGB and distance from the sea (p-value < 0.05, r_s = -0.41) and tidal channel (p-value < 0.05, r_s = -0.50).

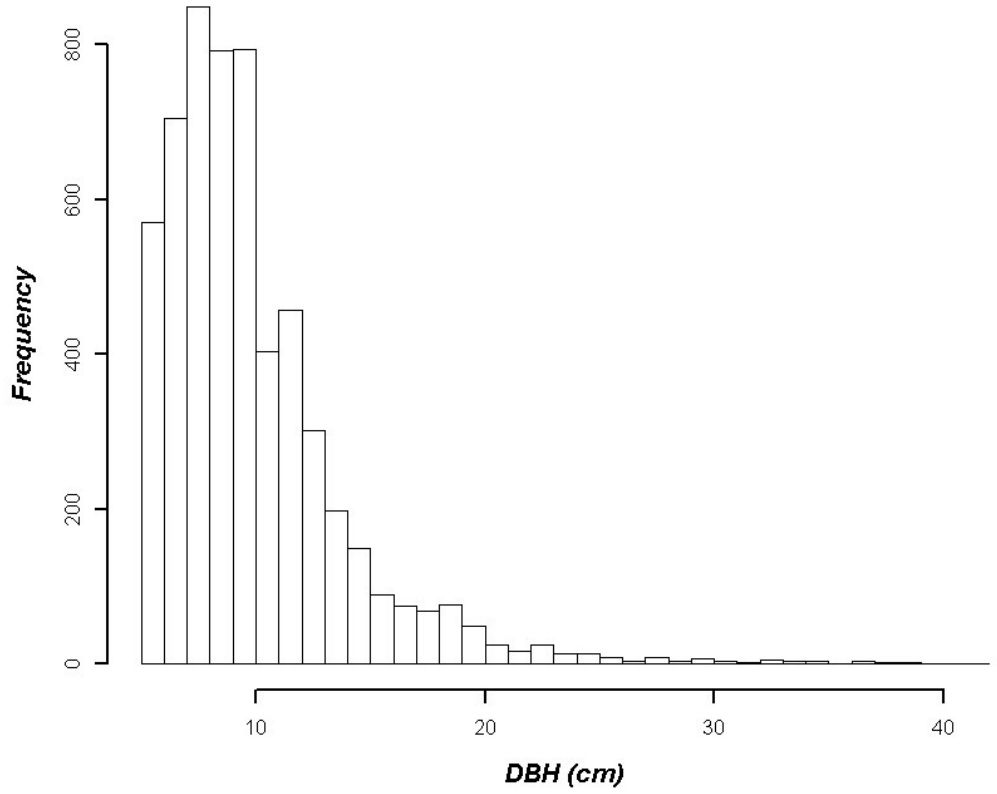

Figure 3.4: Spread of DBH measured at stand scale. The skewed DBH distribution to the left is indicative of normal J-tree distribution.

Table 3.2: Structural characteristics of DBH size class the study plots. Proportional contribution of DBH size classes to structural characteristics of the entire study region.

Class	DBH range (cm)	Stem Density (trees ha^{-1})	Percentage contribution of stem density (%)	Basal Area (m^2 ha^{-1})	Basal area Percentage contribution (%)	Aboveground Biomass (t ha^{-1})	AGB Percentage contribution (%)
1	**5.0 - <10.0**	588	65.0	2.82	34.4	21.2	27.0
2	**10.0- <15.0**	239	26.0	2.74	33.5	25.0	32.0
3	**15.0- <20.0**	57	6.0	1.35	16.5	14.5	19.0
4	**≥20**	24	3.0	1.27	15.6	16.8	22.0

3.3.3 Leaf Area Index

The LAI skewed more to the higher range of values **(Figure 3.5)**. LAI across the study ranged from 0.08 to 2.78, with a mean of 1.45. I recorded the highest plot mean LAI (2.41) in E1C at Ete which is a heavily exploited site with the modified site now gradually colonised by nipa palm. I recorded the lowest plot mean (0.42) in O1C at Oproama another heavily exploited site with less dense vegetation. I observed significant difference in LAI amongst the three locations (Ete, Kono and Oproama) of the study area ($p < 0.01$) but only the more landward Oproama showed significant lower LAI when compared to Ete located closer to the ocean ($p < 0.01$). I also analysed the variance of the LAI measurements within each plot to determine the spread of data. I found the highest variation (1.17) in E1A at Ete a heavily exploited site which can account for intermittent open and closed canopies. I found the lowest variation (0.01) in the protected sites Kono.

3.3.4 Leaf Area Index, Stand Structure and Aboveground Biomass

There was a significant positive correlation between LAI and AGB (p-value < 0.01, r_s = 0.62), stem density (p-value < 0.001, r_s = 0.63) and basal area (p-value < 0.01, r_s = 0.60) at plot scale (n=25). Linear regression models indicated that 28% of LAI accounted for plot AGB (r^2= 0.28, p-value< 0.001) **(**Figure 3.6**)**. The model was improved with log-transformed AGB resulting in 36% of LAI accounting for plot AGB (r^2= 0.36, p-value< 0.001). Standard error (SE) from the regression model was 0.52 while root mean square error (RMSE) was 50 Mg ha^{-1} from predicted AGB (range= 28.5-137.5 Mg ha^{-1}).

3.3.5 Leaf Area Index, Aboveground Biomass and Vegetation Indices

MODIS NDVI ranged from -0.072 to 1 over the survey plots during the growing season (March to October). I constrained NDVI data from the growing season to 0.15, eliminating negative values and very low values in order to account for tidal influence and cloud cover on mangrove forests reflectance. I also averaged NDVI values for all plots within a 500m transect to account for MODIS spatial resolution. This resulted in six data points in analysing the relationship between NDVI and LAI and AGB. I observed significant strong positive correlation of NDVI with AGB (p-value < 0.05, r_s = 0.89) but the strong positive correlation with LAI and basal area were both insignificant (p-value > 0.05, r_s = 0.77). Linear regression models indicated that 63% of LAI (R^2= 0.63, p-value < 0.05), 80% of AGB (R^2= 0.80, p-value < 0.05) and 69% of basal area (R^2= 0.69, p-value < 0.01) could be explained by NDVI (Figure 3.7). I applied the regression model to the plot NDVI values and determined the RMSE between NDVI-predicted values of plot LAI (0.55) and AGB (46 Mg ha^{-1}) against observed values. These RMSE are high due to the reduced sample size of the analysis.

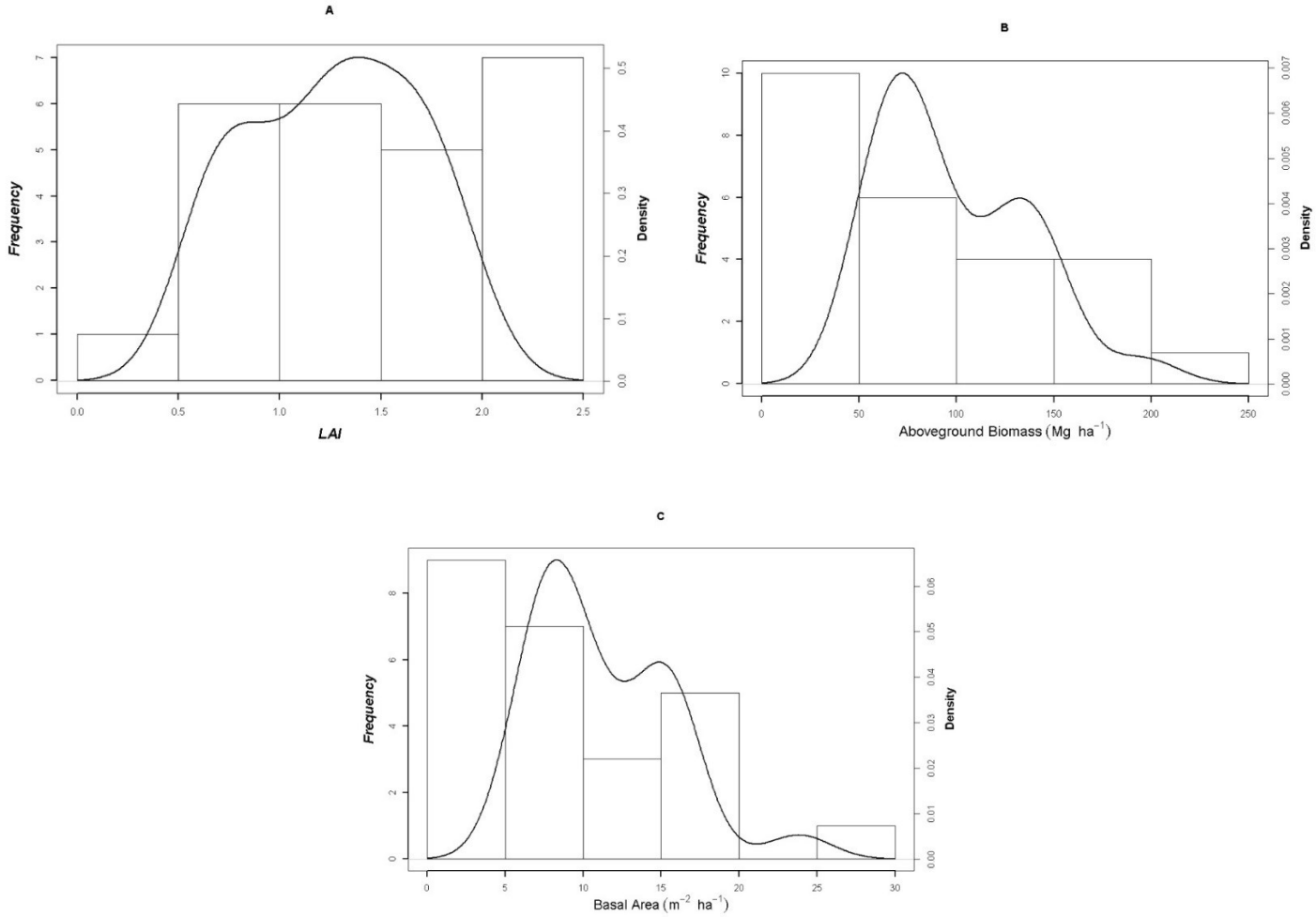

*Figure 3.5: Distribution of LAI (**A**), AGB (**B**) and basal area (**C**) at plot scale (**N=25**) for the entire study region. AGB and BA skewed to the lower range of values. LAI skewed to the right but had a peak close to the mean value (1.45). The lines indicate the distribution of the data in terms of density.*

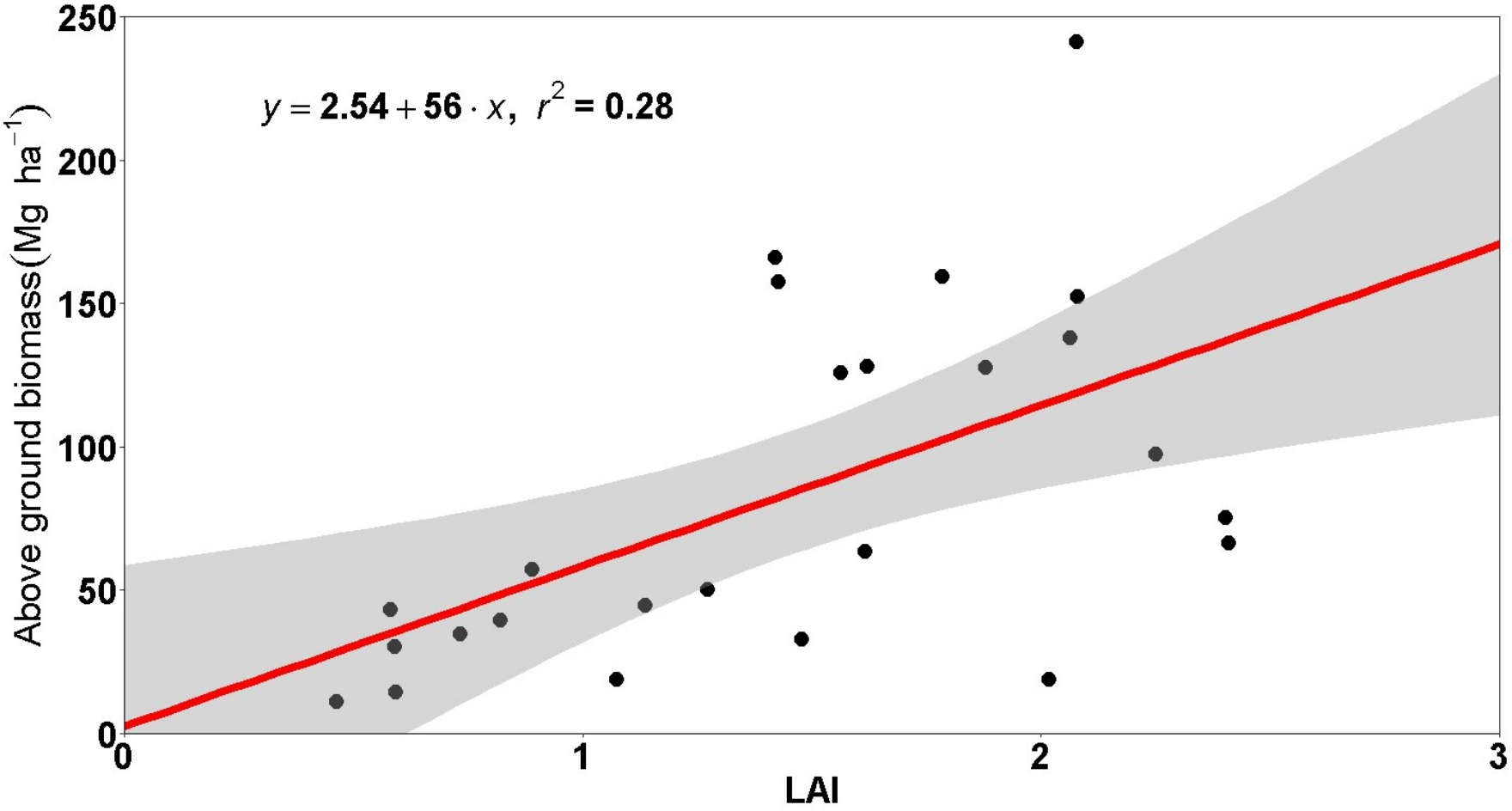

*Figure 3.6: Fitted linear regression of plot of LAI and AGB (**N=25**). Each point represents the plot during the field survey.*

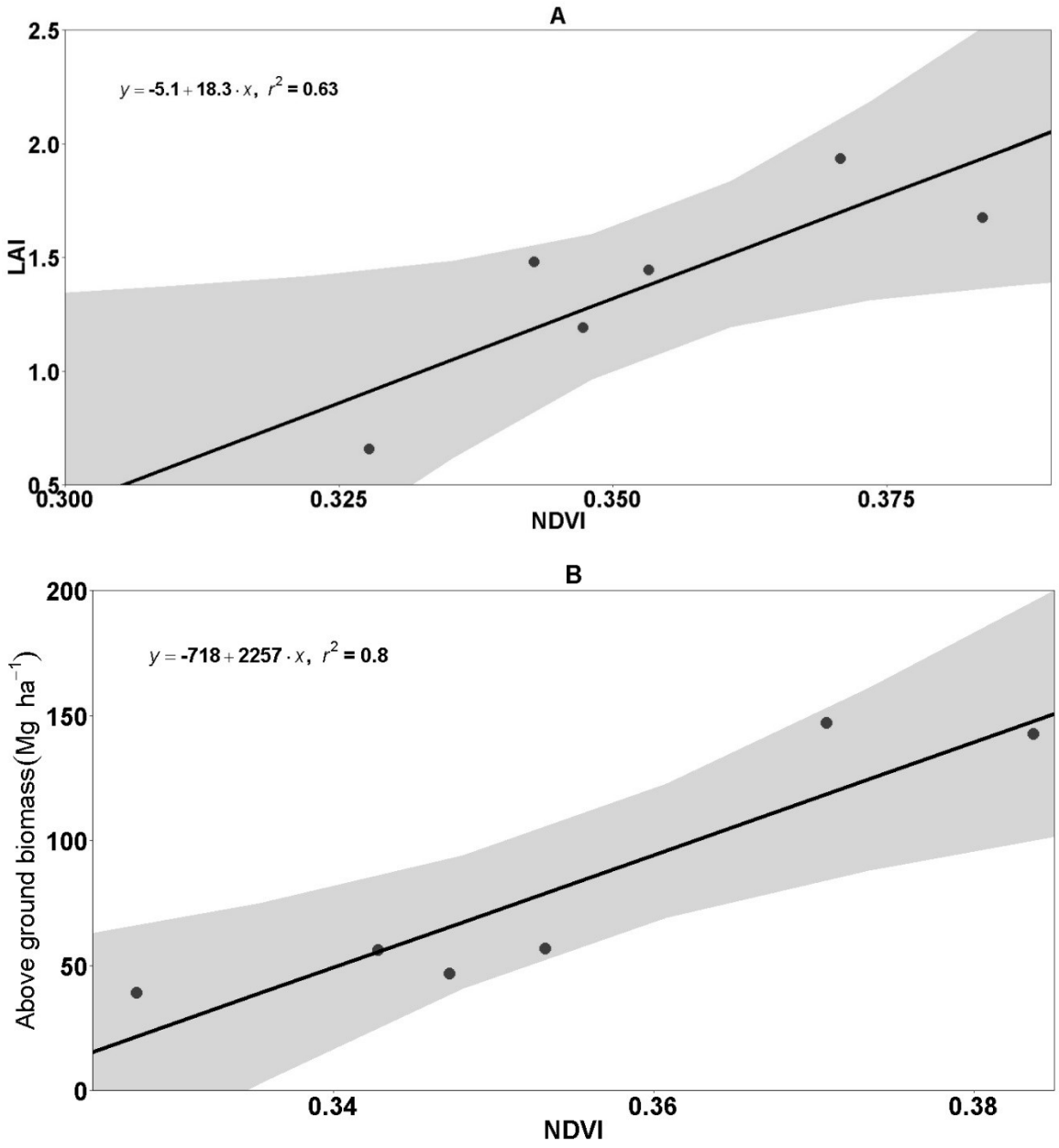

*Figure 3.7: Fitted linear regression lines of in-situ LAI (**A**) and AGB (**B**) measurements against MODIS $NDVI_{1.5}$. Each point represents averaged plot NDVI, LAI and AGB within the spatial resolution of 500m.*

3.3.6 Disturbance Regime

I recorded five HE, two ME and five Und plots in Ete (**Figure 3.3**). Exploited plots in the Ete site were primarily affected by cutting for fuel which is the primary source of income in the region. These plots are now gradually being invaded by nipa palm (**Figure 3.8A**). I observed six HE, three ME and two Und plots in Oproama. The resulting HE category of the Oproama site was primarily due to a historical disturbance. About 6 ha of mangrove forest was cleared in 2013 to create a path for the construction of powerlines (**Figure 3.8B**). The high level of shell fishing was also a major observation in these plots where mangrove was cleared in order to make more waterways to the mangrove interiors hence reducing travel time. The plots in Kono are located adjacent to a protected mangrove site. However, I discovered that Kono was the most affected site during the study with nipa invasion (**Figure 3.8C**). The Kono plots are culturally protected by the locals manually removing nipa seedlings from the mangrove forest floor. I observed numerous nipa seedlings on the forest floor of this site (**Figure 3.8D**).

3.3.6.1 Disturbance Regime, Aboveground Biomass and Leaf Area Index

I observed significant difference in plot AGB amongst disturbance regime ($F(2, 22) = 16.43$, $p < 0.0001$). However, following a Tukey post hoc test, only Und plots had a significantly higher AGB than HE plots (mean difference= 104.6 Mg ha^{-1}, $p < 0.0001$) and ME plots (mean difference= 59.4 Mg ha^{-1}, $p < 0.05$). I observed a significant difference in plot LAI against disturbance regime ($F(2, 22) = 11.43$, $p < 0.0001$). However, only Und plots had a significantly higher LAI than HE plots (mean difference= 0.7, $p < 0.001$) and ME plots (mean difference= 0.9, $p < 0.001$).

I analysed the variability in LAI measurements within each plot and disturbance regime **(Appendix I, Table 3.3)**. Variance in LAI measurement was not significant amongst

disturbance regime (F (2, 22) = 2.465, p > 0.05). However, I observed higher variation in LAI measured in heavily exploited (0.7) plots compared to undisturbed plots (0.2). HE plots in Ete recorded the highest variation of about 1.4.

3.3.6.2 Disturbance Regime and Stand Structure

I observed significantly different plot stem density amongst disturbance regime (F (2, 22) = 7.58, p < 0.01) however, only Und plots had a significantly higher plot density when compared to HE plots (mean difference= 195.5 stem ha^{-1}, p < 0.01). DBH size class 3 (range 15-20 cm) showed significantly lower contribution to stem density (mean difference= 7 stem ha^{-1}, p < 0.05), basal area (mean difference= 11.3 m^2 ha^{-1}, p < 0.05) and AGB (mean difference= 11.7 Mg ha^{-1}, p < 0.05) in HE plots compared to Und plots.

In the undisturbed regime, the highest DBH size class (> 20cm) made up about 3% of the mean plot stem density, but contributed 24% of the AGB. The percentage contribution of each DBH size class to the AGB in the undisturbed regime were more evenly distributed (20-30%) compared to the HE and ME regimes, where the lowest two DBH size classes (1 and 2) make up about 70% of the AGB **(Figure 3.9, Table 3.3)**.

3.3.7 Nipa Stand Patterns

I recorded a total of 179 (0 – 33) nipa palm stands during the survey with a mean of 7 stands per plot. I observed no nipa palm colonisation in the more inland Oproama location while sea ward Ete and Kono were heavily invaded by the mangrove palm. This observation was evident from the strong negative correlation of nipa stand population to distance from sea (p < 0.00001; r_s = - 0.86). I recorded 5 plots with high nipa invasion (**HI**), 7 plots with moderate invasion (**MI**) and 13 plots with no nipa (**NI**) stand during the field study. Analysis of plot nipa population showed no correlation with basal area, AGB, stem density and LAI. However, I discovered that nipa population had a significant weak positive correlation with plot LAI

variation ($p < 0.05$; $r_s = 0.43$) and proportion of basal removed ($p < 0.05$; $r_s = 0.43$). I also observed that nipa stand population showed a weak negative correlation to the contribution of DBH size class 2 (10- 15 cm) to basal area ($p < 0.05$; $r_s = -0.45$) and AGB ($p < 0.05$; $r_s = -0.45$). I also observed that there was no significant relationship between nipa stands and disturbance regime. ANOVA amongst the level of nipa invasion showed that LAI variance, proportion of basal area removed and the contribution of the size class 3 (15-20cm) to AGB were significantly different. HI plots showed a significantly higher LAI variation ($p <0.01$, mean difference= 0.6) and proportion of BA removed ($p <0.01$, mean difference= 0.4) to MI and NI (**Figure 3.10**). NI plots also showed significantly higher contribution of DBH size class 3 (15-20cm) to AGB than MI and HI plots.

*Figure 3.8: Visual representation of disturbance in the Niger Delta. **A**) Cleared plots in Ete showing nipa palm encroachment. **B**) Fragmented mangrove landscape in Oproama due to power line construction. **C**) Nipa palm fringes along Kono creek. **D**) Nipa palm seedlings littered around Kono location.*

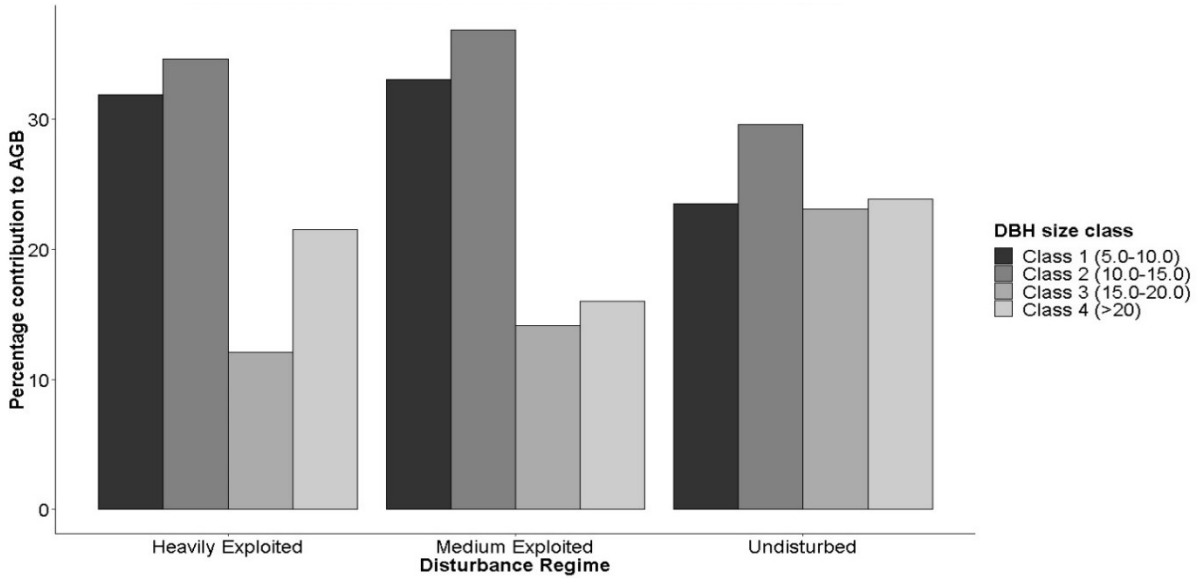

Figure 3.9: Percentage contribution of size classes to within plots of the same disturbance group. Each bar represents the average contribution of plots within each disturbance group.

Table 3.3: Proportion of DBH size classes contributing to stand density, basal area and AGB in different disturbance regime.

Disturbance Regime	DBH size class (cm)	Stand population	Stand density (stem ha^{-1})	Stand density Proportion (%)	Basal Area (m^2 ha^{-1})	Basal Area Proportion (%)	AGB (t ha^{-1})	AGB Proportion (%)	LAI mean (variance)
Heavily exploited (2.75 ha)	**Class 1 (5.0-10.0)**	865	279	66.3	1.4	38.9	10.7	31.8	1.2 (0.7)
	Class 2 (10.0-15.0)	358	116	27.5	1.3	35.5	11.6	34.6	
	Class 3 (15.0-20.0)	49	16	3.8	0.4	10.4	4.0	12.1	
	Class 4 (>20)	32	10	2.5	0.5	15.2	7.2	21.5	
Moderately exploited (1.25 ha)	**Class 1 (5.0-10.0)**	972	823	66.9	4.0	39.9	30.3	33.0	1.0 (0.4)
	Class 2 (10.0-15.0)	399	338	27.4	3.7	37.2	33.8	36.9	
	Class 3 (15.0-20.0)	61	52	4.2	1.2	12.0	13.0	14.1	
	Class 4 (>20)	22	19	1.5	1.1	10.9	14.7	16.0	
Undisturbed (2.25 ha)	**Class 1 (5.0-10.0)**	1872	922	63.0	4.3	30.4	32.1	23.5	1.9 (0.2)
	Class 2 (10.0-15.0)	752	371	25.3	4.4	31.2	40.3	29.6	
	Class 3 (15.0-20.0)	250	123	8.4	2.9	20.8	31.5	23.1	
	Class 4 (>20)	97	48	3.3	2.5	17.6	32.6	23.9	

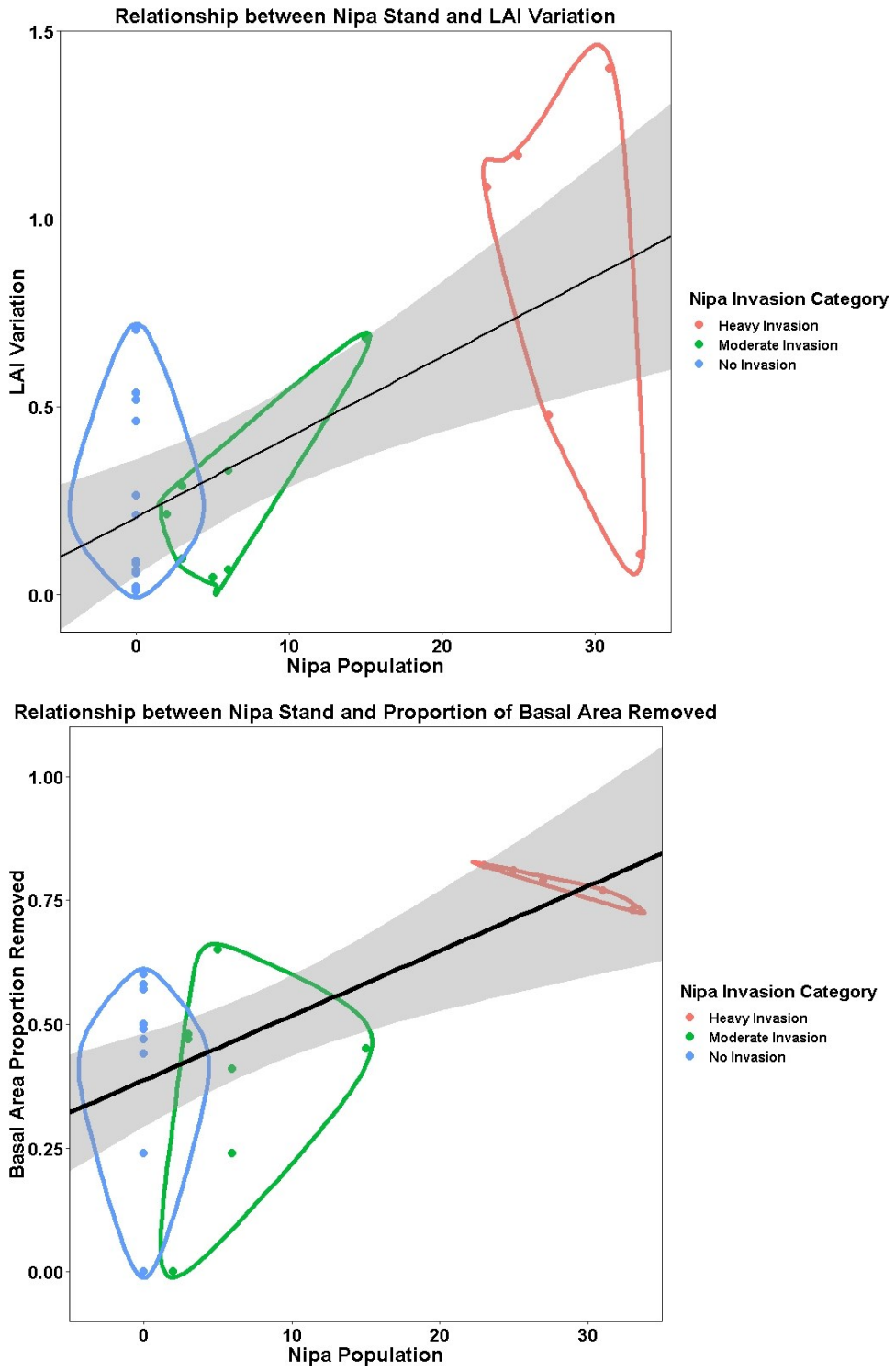

Figure 3.10: *Relationship between nipa population and LAI variation (top) and proportion of basal area removed (bottom) Points represent nipa stand population in each plots (**N=25).** Circles represent the nipa palm invasion groups (**HI-** heavy invasion, **MI-** moderate invasion and **NI**- no invasion). Plots with HI had a significant higher LAI variation and BA proportion removed compared to Moderate and no invasion plots.*

3.4 Discussion

I have created the largest mangrove stem, biomass and canopy structure survey in Nigeria which introduces the potential to monitor mangrove productivity through vegetation indices. I showed a general pattern of AGB across gradients from sea, tidal channel and closest settlement. I also showed weak influence of possible wood exploitation effect on AGB in the region due to the relationship between AGB and distance of the plots from the closest settlement. The predictive power of AGB from LAI and NDVI can be the first step in creating a baseline for upscaling mangrove productivity and monitoring regional deforestation in the Niger Delta. I also address the subtle effect of local disturbance on stem size distribution, the possible target mangrove size class by locals and the resultant encroachment of nipa palm in mangrove forests of the Niger Delta. I also gave evidence of the cause and effect relationship of mangrove clearing and the encroachment of nipa palm.

3.4.1 Aboveground Biomass Patterns in the Niger Delta

Forest productivity has a direct influence from nutrient availability and external influence from disturbance. Here I report the zonation of mangrove forests in terms of productivity. I observed that higher AGB and BA were located in plots with closer proximity to the ocean and tidal channel. This could be as a result of the mixing effect of tide which assist in nutrient mixing in mangrove forests. Castaneda, (2010) reported that mangrove productivity in South Florida mangrove forests may be limited by phosphorus fertility which showed a negative gradient with distance from the ocean (Castaneda, 2010). He also gave evidence that tidal inundation duration and frequency influences the fertility of mangrove soils, hence productivity. The significant difference in mangrove forest structure and biomass across the tidal channel during the study may be linked to this influence. Further affecting the biomass pattern of mangrove forests in the Niger Delta could be the proximity to settlements which may alter the nutrient loading of mangrove forests. Flooding which maybe as a result of

heavy rainfall may contribute to the phosphorus balance of mangrove forests (Chen and Twilley, 1999). This study showed that AGB were lower at plots closer to settlements which could be as a result of either nutrient limitation, pollution, flooding or a consequence of perturbation through logging and fishing. The study creates a baseline for investigating the influence of soil nutrients on the productivity of mangrove forests in the Niger Delta.

3.4.2 Biomass Prediction from Canopy Properties

Monitoring landscape productivity is a vital means of assessing productivity patterns and deforestation rates in mangrove forests. LAI is a strong proxy for primary production through its relation to photosynthetic capacity of the canopy (Araujo *et al.*, 1997; Pool, 1973; Williams *et al.,* 1997). Productivity capacity of mangrove forests is influenced by important environmental and structural parameters including LAI, nutrient dynamics and litterfall (Rodríguez, 2008). I showed a significant positive correlation (r_s = 0.63) and a regression equation (R^2= 0.28) between LAI and AGB indicating the potential for LAI to be used as a proxy for mangrove productivity in the Niger Delta. This study was the first within the region that establishes a relationship between these parameters. Compared to other regions (**Table 3.4**), I recorded low LAI (< 3). This record could be as a result of the stage of the mangrove forests, disturbance and methodology. I employed the indirect method for estimating LAI in this study using hemispherical photography which has been seldom employed in the estimation of LAI in mangrove forests. This method has been known to underestimate LAI and could explain the high difference in LAI from comparative studies using direct methods (Ishil and Tateda, 2004). A study by Pool (1973), showed that mangrove forests in early succession have reduced LAI while higher LAI can be characteristic of later succession especially in mixed stands (Pool, 1973). This relationship was evident in this study where I recorded the lowest LAI in a site that had been cleared out in 2013. This resultant low LAI in some of the plots could be as a result of the sites being in early succession as a result of a

previous disturbance (Pool, 1973). Another reason for the low values of LAI in this study could be as a result of the monospecific *Rhizophora* nature of the sample plots. Clough *et al.,* (1997) characterised *Rhizophora* spp as canopy shy because of the numerous light gaps between trees which could increase the area of light penetration within plots (Clough *et al.,* 1997). The established correlation between LAI and AGB is the first step in monitoring the productivity of mangroves in Nigeria.

3.4.3 Vegetative Indices Relationship with Leaf Area Index and Aboveground Biomass

The ability of optical sensors to detect the greenness of a forest can aid in monitoring the productivity of mangrove forests through its relationship with canopy structures. Previous researchers have observed significant relationships between vegetation indices, LAI and AGB in forested landscapes (Baloloy *et al.,* 2018; Heiskanen, 2006; Ishil and Tateda, 2004; Wong and Fung, 2013). This study shows that while there was some relationship various characteristics of the mangrove forests resulted in low R^2 values (< 0.5). This could be as a result of mixed reflectance of canopy cover and tidal influence in mangrove forests. Also, this effect of flooding in mangrove forests can be increased in areas of deforestation where more forest floor is exposed. Relationship of LAI and VI can be beneficial in estimating LAI when canopy features are closed and uniform (Gigante *et al.*, 2009; Heiskanen, 2006). Secondly, the improved NDVI-LAI model was as a result of adjusting the NDVI values, hence, eliminating background noise. This indicated adjusted NDVI predicting LAI especially in mixed pixels (Brown, 2001). AGB also had a higher correlation with VI than LAI. This could be as a result of undergrowth reflectance present in most plots during this study. More than 50 % of the plots had undergrowth due to recruitment from previous disturbance and involves the dual recruitment of mangroves and nipa palm. NDVI also saturate in areas of high vegetation leaf area especially LAI (0 – 3) (Gigante *et al.,* 2009). This was evident from plot NDVI not varying

much across the landscape within study locations. This study has shown the potential in estimating productivity of mangrove forests in the Niger Delta over spatial and temporal scale stemming from the link between canopy features and wood productivity.

3.4.4 Local Disturbance Effect on Biomass, Stand Structure and Canopy Properties

Stand structure in forest landscape provides a means to monitor local scale wood exploitation in mangrove forests. Natural sources of perturbation such as hurricane and anthropogenic sources such as wood harvesting can modify the stand structure of the ecosystem thereby affecting the accumulated productivity of mangrove forests (Wan Norilani *et al.*, 2014). In this study, I observed that DBH size class contribution to AGB had a significant difference between disturbance regimes with heavily exploited plots having an uneven contribution to AGB. Norilani *et al.,* (2014) reported that there was a uniform distribution of stem size classes in a naturally disturbed area compared with a harvested region at Kisap Forest Reserve, Malaysia(Norilani *et al.,* 2014). This uniformity was also reflected in this research where the contributory proportion of each stem size class to the AGB in the undisturbed regime was more even (20-30%) than with the other groups where the lowest two classes (5-10 cm and 10-15 cm) made up about 70% of the AGB.

The stem size class 3 (15-20cm) having the lowest contributory proportion to AGB in all disturbance groups has an effect on the target stem size for harvest (**Table 3.3**). This stem size class could be the target tree size within the region. The target tree size is the most convenient tree size to harvest in order to maximise the effort of loggers by reducing the cost of logging and transportation in order to increase profit. Another possible reason for the targeted DBH size class is the location of the larger stem size class close to the tidal channel would have resulted in cut logs falling into the creek. The effect of target harvesting of mangrove stands results in the change in stand structure and light gap creation within

mangrove stands (Amir and Duke, 2009; Clarke and Kerrigan, 2000; Duke, 2001; Mohamed *et al.*, 2009). The incident of cutting mangroves in the Niger Delta could be as a result of a shift in economy. There was a historical reason for the cutting of mangroves as a source of income due to a shift from fishing primarily as a result of bad fishing practice (Personal communication, 2017). The use of Gamallin-20 (a paralysing fish chemical) and small net mesh sizes resulted in depleting fish stock in the region (Olaoye and Ojebiyi, 2018).

The change in stand structure of mangrove forests as a result of wood exploitation also has an effect on canopy properties. Disturbance can also play an important role in modifying LAI (Araujo *et al.,* 1997). Disturbance within the study region resulted in LAI variation where heavily exploited plots had a higher variation in LAI than undisturbed plots. These light gap in mangrove forests are naturally created from dead mangrove trunks (Amir and Duke, 2009), but these can also be created by small-scale disturbance (Duke, 2001). Irregular harvesting, as seen in heavily exploited plots in the study resulted in the open ground within these plots. These light gaps have an implication on regeneration and recruitment on juvenile mangrove trees (Duke, 2001; Mohamed *et al.,* 2009); these were also evident from disturbed plots. However, due to the invasion of nipa palm, the regeneration of mangrove stands in light gaps within the study region is significantly affected. Juvenile mangrove and nipa stands are found growing in the competition. This is a common feature along the Imo estuary (Ete and Kono plots). The effect of selective harvesting can have a negative influence in the natural growth of a mangrove ecosystem especially the presence of an invasive species to colonise available cleared mangrove area in the Niger Delta.

3.4.5 Pattern of Nipa Palm Invasion

There is a growing interest of invasion ecology globally due to its influence on ecosystem function and economic impacts. Elaborate studies have been done by Ukpong, (2015) on nipa zonation and soil conditions in Niger Delta mangrove forests (Ukpong, 2015). I reported

here a possible nipa palm (*Nypa fruticans*) colonisation in mangrove forest of the Niger Delta. Reports have shown the close link between mangrove deforestation and non-native species colonisation (Harun Rashid *et al.,* 2009). Harun Rashid *et al.,* (2009) gave evidence that the colonisation of non-native invasive species in Bangladesh can be as a result of forest gaps formed from catastrophic events affecting mangrove forests (Harun Rashid *et al.,* 2009). This trend was reported in this study. Higher LAI variance and proportion of BA removed were significantly higher in plots classified as high nipa invasion (**HI**) compared to moderate (**MI**) and no invaded plots (**NI**). This relationship is an indication that nipa seedlings penetrate mangrove stands and colonise cleared out forest spaces. Ukpong, (2015) also argued that the slow development process of red mangrove (*Rhizophora*) regeneration and its inability to regenerate after being cut also aids in nipa outcompeting these native species (Ukpong, 2015). Further research can investigate the impact of nipa invasion on soil properties especially with climate change likely to intensify these stressors on coastal ecosystems.

3.4.6 Limitations

Allometric equation used in estimating AGB was from a general allometric equation which includes DBH and specific density as determining parameters. These AGB may not be very representative of the specific region. However, comparison with an unverified allometric equation (Ajonina, 2008) showed a RMSE of 8.6 Mg ha^{-1} and significant correlation of 99.5%. Secondly, LAI was acquired from three points in a plot and may not be a complete representation of the plot canopy cover. Due to mangrove mobility difficulty, more points couldn't be taken. Vegetation indices used in finding the relationship of canopy and productivity were averaged over the region resulting in 6 data points and this may not be enough to extrapolate over the study region. As a result of the small sample size used in regression analysis between surface reflectance, AGB and LAI. Care should be taken when extrapolating over a wider region.

Table 3.4: LAI study comparisons based on methodology and location.

	Location	**LAI**	**AGB (**t ha^{-1})	**R^2 NDVI**	**Method**
this study	Niger Delta	1.45 (0.08-2.78)	83.7 (11.1 -241.2)	LAI= 0.20 AGB= 0.34	Hemispherical photo
Kovacs *et al.,* 2004	Mexico	1.8; 1.9	-	LAI = 0.7 -0.73	LAI- 2000
Ishii and Tateda, 2004	Thailand	4.1-5.5	-	Not reported	LAI- 2000 and total leaf count
Wong and Fung, 2013	Hong Kong	1.75 – 2.45	-	LAI = 0.02	Hemispherical photo (WinSCANOPY)
Rodriguez, 2008	Puerto Rico	1.69-7.43	-	LAI = 0.72 (IKONOS)	AccuPAR
Green *et al.,* 1993	Caicos Island	0.8- 7.0	-	LAI = 0.74 (SPOT)	Radiometer
Winarso *et al.,* 2017(Winarso *et al.,* 2017)	Indonesia	-		AGB = 0.43	
Clough *et al.,* 1997	Malaysia	2.20-7.40			LiCOR
Clough *et al.,* 1997	Malaysia	4.90-5.10			Light flux density instrument
Clough *et al.,* 1997	Malaysia	4.4			Direct beam
Pool 1973	Florida	0.80-5.10			Plum line
Araujo 1997	Florida	0-10			LiCor quantum sensor

3.5 Conclusion

Mangrove productivity is dependent on both the natural properties of the region and the level of disturbance evident in the difference in AGB and stand structure of plots within the same site and the entire region; despite being monospecific stands. The use of LAI in the estimation of mangrove production and its relationship to NDVI is the first step in using map-based data in estimating landscape mangrove productivity in the Niger Delta. The relationship between LAI and vegetative indices such as NDVI can be utilised as a baseline in the estimation of biomass loss over time due to logging and oil pollution in local and regional scales. These estimates, however, can only be applied with an updated mangrove area and biomass mass with the inclusion of more plot data and control points in order to cover a diverse and large mangrove area in Nigeria.

Secondly, the formulation of a management plan for the exploitation of mangrove wood can be a first step in monitoring mangrove loss from fuelwood harvesting. The local dependence on surrounding forests by local communities for livelihood and cooking reduces the chances of a total ban on mangrove wood harvests. A mangrove protected which was initially formed by an NGO in River State is being encroached by nipa palm, indicating the need for a management option of protected regions. Hence, we need more research in understanding local effects of both wood exploitation and oil exploration in the Niger Delta on mangrove forests to inform the various stakeholders on how to manage the effects of their activities on this delicate blue forests.

3.6 References

Adedeji, G. A., Ogunsanwo, O. Y., & John, J. (2013). DENSITY VARIATIONS IN RED MANGROVE (Rhizophora racemosa GFW Meyer) IN ONNE, RIVER STATE, NIGERIA. *International Journal of Science and Nature*, *4*(1), 165–168. Retrieved from http://www.scienceandnature.org/IJSN_Vol4(1)M2013/IJSN-VOL4(1)13-29.pdf

Ajonina, G. N. (2008). Inventory and Modelling Mangrove Forest Stand Dynamics Following Different Levels of Wood Exploitation Pressures in the Douala-Edea Atlantic Coast of Cameroon, Central Africa, 215. Retrieved from http://www.freidok.uni-freiburg.de/volltexte/6132/pdf/Gordon_N._Ajonina_Thesis.pdf

Allen, J. A., Ewel, K. C., & Jack, J. (2001). Patterns of natural and anthropogenic disturbance of the mangroves on the Pacific Island of Kosrae. *Wetlands Ecology and Management*, *9*(3), 291–301. https://doi.org/10.1016/S0964-5691(02)00051-0

Alongi, D. M. (2009). *The energetics of mangrove forests*. *The Energetics of Mangrove Forests*. https://doi.org/10.1007/978-1-4020-4271-3

Alongi, D. M. (2014). Carbon Cycling and Storage in Mangrove Forests. *Annual Review of Marine Science*, *6*(1), 195–219. https://doi.org/10.1146/annurev-marine-010213-135020

Amadi, J.E. Adebola, M.O. and Eze, C. S. (2014). A Survey of the Mangrove Vegetation in the Niger Delta Region of Nigeria. *International Journal of Research (IJR)*, *1*(8), 1129–1138.

Amechi, H., Maureen, N., & Akudo, N. (2014). Analysis of Rainfall Variations in the Niger Delta Region of Nigeria, *8*(1), 25–30. https://doi.org/10.9790/2402-08162530

Amir, A., & Duke, N. (2009). A forever young ecosystem: light gap creation and turnover of subtropical mangrove forests in Moreton Bay, Southeast Queensland, Australia. *11th*

Pacific Science Inter-Congress in Conjunction with the 2nd Symposium on French Research in the Pacific, 1–5.

Araujo, R. J., Jaramillo, J. C., & Snedaker, S. C. (1997). Lai and Leaf Size Differences in Two. *Bulletin of Marine Science*, *60*(3), 643–647.

Baloloy, B. A., Blanco, C. A., Candido, G. C., Argamosa, R. J. L., Dumalag, J. B. L. C., Dimapilis, L. L. C., & Paringit, E. C. (2018). ESTIMATION of MANGROVE FOREST ABOVEGROUND BIOMASS USING MULTISPECTRAL BANDS, VEGETATION INDICES and BIOPHYSICAL VARIABLES DERIVED from OPTICAL SATELLITE IMAGERIES: RAPIDEYE, PLANETSCOPE and SENTINEL-2. *ISPRS Annals of the Photogrammetry, Remote Sensing and Spatial Information Sciences*, *4*(3), 29–36. https://doi.org/10.5194/isprs-annals-IV-3-29-2018

Bequet, R., Campioli, M., Kint, V., Vansteenkiste, D., Muys, B., & Ceulemans, R. (2011). Leaf area index development in temperate oak and beech forests is driven by stand characteristics and weather conditions. *Trees - Structure and Function*, *25*(5), 935–946. https://doi.org/10.1007/s00468-011-0568-4

Bouillon, S., Borges, A. V., Castañeda-Moya, E., Diele, K., Dittmar, T., Duke, N. C., … Twilley, R. R. (2008). Mangrove production and carbon sinks: A revision of global budget estimates. *Global Biogeochemical Cycles*, *22*(2), 12. https://doi.org/10.1029/2007GB003052

Brown, D. G. (2001). A Spectral Unmixing Approach to Leaf Area Index (LAI) Estimation at the Alpine Treeline Ecotone. *GIS and Remote Sensing Applications in Biogeography and Ecology*, 7–21. https://doi.org/10.1007/978-1-4615-1523-4_2

Campbell, D. C. (2017). Glacial Landforms and Features - The shape of the land, Forces and changes, Spotlight on famous forms, For More Information. *Science Clarified*.

Retrieved from http://www.scienceclarified.com/landforms/Faults-to-Mountains/Glacial-Landforms-and-Features.html

Castaneda, E. (2010). Landscape patterns of community structure, biomass and net primary productivity of mangrove forests in the Florida Coastal Everglades as a function of resources, regulators, hydroperiod, and hurricane disturbance. *Oceanography and Coastal Sciences*, *Ph.D.*(August), 171.

Chen, R., & Twilley, R. R. (1999). A simulation model of organic matter and nutrient accumulation in mangrove wetland soils. *Biogeochemistry*, *44*(1), 93–118. https://doi.org/10.1023/A:1006076405557

Cintron G. A.; Novelli Y. S. (1984). Methods for studying mangrove structure. *The Mangrove Ecosystem: Research Methods*, 91–113.

Clarke, P. J., & Kerrigan, R. A. (2000). Do forest gaps influence the population structure and species composition of mangrove stands in northern Australia? *Biotropica*, *32*(4), 642–652. https://doi.org/10.1111/j.1744-7429.2000.tb00511.x

Clough, B. F., Ong, J. E., & Gong, G. W. (1997). Estimating leaf area index and photosynthetic production in mangrove forest canopies. *Marine Ecology Progress Series*, *159*, 285–292. https://doi.org/10.3354/meps159285

Cox, L. E., Hart, J. L., Dey, D. C., & Schweitzer, C. J. (2016). Composition, structure, and intra-stand spatial patterns along a disturbance severity gradient in a Quercus stand. *Forest Ecology and Management*, *381*, 305–317. https://doi.org/10.1016/j.foreco.2016.09.040

Dahdouh-Guebas, F., & Koedam, N. (2006). Empirical estimate of the reliability of the use of the Point-Centred Quarter Method (PCQM): Solutions to ambiguous field situations

and description of the PCQM+ protocol. *Forest Ecology and Management*, *228*(1–3), 1–18. https://doi.org/10.1016/j.foreco.2005.10.076

De Kauwe, M. G., Disney, M. I., Quaife, T., Lewis, P., Williams, M., & A. (2011). An assessment of the MODIS collection 5 leaf area index product for a region of mixed coniferous forest. *Remote Sensing of Environment*, *115*(2), 767–780. https://doi.org/10.1016/j.rse.2010.11.004

Donato, D. C., Kauffman, J. B., Mackenzie, R. a., Ainsworth, a., & Pfleeger, a. Z. (2012). Whole-island carbon stocks in the tropical Pacific: Implications for mangrove conservation and upland restoration. *Journal of Environmental Management*, *97*(1), 89–96. https://doi.org/10.1016/j.jenvman.2011.12.004

Duke, N. C. (2001). Gap creation and regenerative processes driving diversity and structure of mangrove ecosystems. *Wetlands Ecology and Management*, *9*, 257–269. https://doi.org/10.1023/A:1011121109886

Dupont, L. M., Jahns, S., Marret, F., & Ning, S. (2000). Vegetation change in equatorial West Africa: Time-slices for the last 150 ka. *Palaeogeography, Palaeoclimatology, Palaeoecology*, *155*(1–2), 95–122. https://doi.org/10.1016/S0031-0182(99)00095-4

Edu, E. A. B., Nsirim, L. E. W. and, & Martins, O. O. (2014). Monitoring and Assessment of Leaf Litter Dynamics in a Mixed Mangal Forest of the Cross River Estuary, Nigeria. *International Journal of Environmental Monitoring and Analysis*, *2*(3), 163. https://doi.org/10.11648/j.ijema.20140203.16

Edu, E. A., Edwin-Wosu, N. L., Ononyume, M. O., & Nkang, a. E. (2014). Carbon credits assessment in a mixed mangrove forest vegetation of. *Asian Journal of Plant Science and Research*, *4*(4), 1–12.

FAO. (2005). *Global Forest Resources Assessment 2005: Thematic Study on Mangroves. Nigeria Country Profile*. *Forest Resources Development Service Forest Resources Division Forestry, Forestry Department FAO, Rome (Italy)*.

Fatoyinbo, T. E., & Simard, M. (2013). Height and biomass of mangroves in Africa from ICESat/GLAS and SRTM. *International Journal of Remote Sensing*, *34*(2), 668–681. https://doi.org/10.1080/01431161.2012.712224

Fatoyinbo, T., & Simard, M. (2011). Remote Sensing of Mangrove Structure and Biomass. *Workshop on Tropical Wetland Ecosystems on Indonesia: Science Needs to Address Climate Change Adaption and Mitigation. Sanur Beach Hotel, Bali 11-14th April, 2011*, 5.

Feka, N. Z., & Ajonina, G. N. (2011). Drivers causing decline of mangrove in West-Central Africa: a review. *International Journal of Biodiversity Science, Ecosystem Services & Management*, *7*(3), 217–230. https://doi.org/10.1080/21513732.2011.634436

Food and Agriculture and Organization. (2007). The world's mangrove 1980-2005. *FAO Forestry Paper*, *153*, 89.

Frazer, G. W., Canham, C. D., & Lertzman, K. P. (1999). *Gap Light Analyzer (GLA), Version 2.0: Imaging Fisheye, software to extract canopy structure and gap light transmission indices from true-colour Photographs, users manual and program documentation. Simon Fraser University Burnaby, British Columbia, and the Institute of Ecosystem Studies, Millbrook, New York.*

Friess, D. A. (2016). Ecosystem services and disservices of mangrove forests: Insights from historical colonial observations. *Forests*, *7*(9). https://doi.org/10.3390/f7090183

Gigante, V., Iacobellis, V., Manfreda, S., Milella, P., & Portoghese, I. (2009). Influences of

leaf area index estimations on water balance modeling in a mediterranean semi-arid basin. *Natural Hazards and Earth System Science*, *9*(3), 979–991. https://doi.org/10.5194/nhess-9-979-2009

Giri, C., Ochieng, E., Tieszen, L. L., Zhu, Z., Singh, A., Loveland, T., … Duke, N. (2011). Status and distribution of mangrove forests of the world using earth observation satellite data. *Global Ecology and Biogeography*, *20*(1), 154–159. https://doi.org/10.1111/j.1466-8238.2010.00584.x

Global Invasive Species Database (GISD). (2015). FULL ACCOUNT FOR: Nypa fruticans Nypa. https://doi.org/10.1017/CBO9781107415324.004

Gorelick, N., Hancher, M., Dixon, M., Ilyushchenko, S., Thau, D., & Moore, R. (2017). Google Earth Engine: Planetary-scale geospatial analysis for everyone. *Remote Sensing of Environment.*

Green, E. P., Mumby, P. J., Edwards, A. J., Clark, C. D., & Ellis, A. C. (1993). Estimating leaf area index from satellite data. *Geoscience and Remote Sensing, IEEE Transactions On*, *31*(3), 727–734. https://doi.org/10.1109/36.225538

Harun Rashid, S., Biswas, S. R., Böcker, R., & Kruse, M. (2009). Mangrove community recovery potential after catastrophic disturbances in Bangladesh. *Forest Ecology and Management*, *257*(3), 923–930. https://doi.org/10.1016/j.foreco.2008.10.028

Heiskanen, J. (2006). Estimating aboveground tree biomass and leaf area index in a mountain birch forest using ASTER satellite data. *International Journal of Remote Sensing*, *27*(6), 1135–1158. https://doi.org/10.1080/01431160500353858

Hossain, M., Raqibul, M., & Siddique, H. (2017). *MANUAL FOR BUILDING TREE VOLUME AND BIOMASS ALLOMETRIC MANUAL FOR BUILDING TREE VOLUME AND BIO- MASS*

ALLOMETRIC EQUATION.

Hutchison, J., Manica, A., Swetnam, R., Balmford, A., & Spalding, M. (2014). Predicting global patterns in mangrove forest biomass. *Conservation Letters*, *7*(3), 233–240. https://doi.org/10.1111/conl.12060

Isebor, C. E., Ajayi, T. O., & Anyanwu, A. (2003). *The Incidence of Nypa fruticans (WURMB) and it's Impact on Fisheries Production in the Niger Delta Mangrove Ecosystem*.

Ishil, T., & Tateda, Y. (2004). Leaf area index and biomass estimation for mangrove plantation in Thailand. *IGARSS 2004. 2004 IEEE International Geoscience and Remote Sensing Symposium*, *4*(c), 2323–2326. https://doi.org/10.1109/IGARSS.2004.1369751

Jackson, G. (2011). Mangrove Resources Utilization in Nigeria: An Analysis of the Andoni Mangrove Resources Crisis. *Sacha Journal of Environmental Studies*, *1*(1), 49–63.

James, G. K., Adegoke, J. O., Osagie, S., Ekechukwu, S., Nwilo, P., & Akinyede, J. (2013). Social valuation of mangroves in the Niger Delta region of Nigeria. *International Journal of Biodiversity Science, Ecosystem Services & Management*, *9*(4), 311–323. https://doi.org/10.1080/21513732.2013.842611

James, G. K., Adegoke, J. O., Saba, E., Nwilo, P., & Akinyede, J. (2007). Satellite-Based Assessment of the Extent and Changes in the Mangrove Ecosystem of the Niger Delta. *Marine Geodesy*, *30*(3), 249–267. https://doi.org/10.1080/01490410701438224

Kauffman, J. B., Heider, C., Cole, T. G., Dwire, K. a., & Donato, D. C. (2011). Ecosystem carbon stocks of micronesian mangrove forests. *Wetlands*, *31*(2), 343–352. https://doi.org/10.1007/s13157-011-0148-9

Kinako, P. D. S. (1977). Conserving the mangrove forest of the Niger Delta. *Biological Conservation*, *11*(1), 35–39. https://doi.org/10.1016/0006-3207(77)90025-8

Komiyama, A., Poungparn, S., & Kato, S. (2005). Common allometric equations for estimating the tree weight of mangroves. *Journal of Tropical Ecology*, *21*(4), 471–477. https://doi.org/10.1017/S0266467405002476

Kovacs, J. M., Flores-Verdugo, F., Wang, J., & Aspden, L. P. (2004). Estimating leaf area index of a degraded mangrove forest using high spatial resolution satellite data. *Aquatic Botany*, *80*(1), 13–22. https://doi.org/10.1016/j.aquabot.2004.06.001

Lucas, R., Rebelo, L. M., Fatoyinbo, L., Rosenqvist, A., Itoh, T., Shimada, M., … Hilarides, L. (2014). Contribution of L-band SAR to systematic global mangrove monitoring. *Marine and Freshwater Research*, *65*(7), 589–603. https://doi.org/10.1071/MF13177

McLeod, E., & Salm, R. (2006). *Managing mangroves for resilience to climate change*. Retrieved from http://mangroverestoration.com/pdfs/McCleod and Salm 2006 resilience.pdf

McNicol, I. M., Ryan, C. M., Dexter, K. G., Ball, S. M. J., & Williams, M. (2017). Aboveground Carbon Storage and Its Links to Stand Structure, Tree Diversity and Floristic Composition in South-Eastern Tanzania. *Ecosystems*. https://doi.org/10.1007/s10021-017-0180-6

Mitchard, E. T. a, Saatchi, S. S., Woodhouse, I. H., Nangendo, G., Ribeiro, N. S., Williams, M., … Meir, P. (2009). Using satellite radar backscatter to predict above-ground woody biomass: A consistent relationship across four different African landscapes. *Geophysical Research Letters*, *36*(23), 1–6. https://doi.org/10.1029/2009GL040692

Mmom, P. C., & Arokoyu, S. B. (2010). Mangrove forest depletion, biodiversity loss and traditional resources management practices in the Niger Delta, Nigeria. *Research Journal of Applied Sciences, Engineering and Technology*, *2*(1), 28–34.

Mohamed, M. O. S., Neukermans, G., Kairo, J. G., Dahdouh-Guebas, F., & Koedam, N. (2009). Mangrove forests in a peri-urban setting: The case of Mombasa (Kenya). *Wetlands Ecology and Management*, *17*(3), 243–255. https://doi.org/10.1007/s11273-008-9104-8

Mukherjee, N., Sutherland, W. J., Dicks, L., Hugé, J., Koedam, N., & Dahdouh-Guebas, F. (2014). Ecosystem service valuations of mangrove ecosystems to inform decision making and future valuation exercises. *PLoS ONE*, *9*(9), 1–9. https://doi.org/10.1371/journal.pone.0107706

NDDC. (2006). Niger Delta Region Land and People. In *Niger Delta Regional Development Masterplan* (pp. 48–99). Printing Development Company Limited, Port Harcourt, Rivers State. Retrieved from http://www.nddc.gov.ng/NDRMP Chapter 1.pdf

Ngoc Le, D. T., Van Thinh, N., The Dung, N., & Mitlöhner, R. (2016). Effect of Disturbance Regimes on Spatial Patterns of Tree Species in Three Sites in a Tropical Evergreen Forest in Vietnam. *International Journal of Forestry Research*, *2016*. https://doi.org/10.1155/2016/4903749

Numbere, A. O., & Camilo, G. R. (2018). Structural characteristics, above-ground biomass and productivity of mangrove forest situated in areas with different levels of pollution in the Niger Delta, Nigeria. *African Journal of Ecology*, (March), 1–11. https://doi.org/10.1111/aje.12519

Nwigbo, S. C., Azaka, O. A., Chukwuneke, J. L., & Nwadike, C. E. (2013). Establishing Allometric Relationships Using Crown Diameter for Estimating Above Ground Combustible Fuels in Southern Nigerian Mangrove Vegetations. *International Journal of Multidisciplinary Sciences and Engineering*, *4*(7), 43–52.

Odenkunle, T. O. (2004). Rainfall and the length of the growing season in Nigeria. *International Journal of Climatology*, *24*(4), 467–479. https://doi.org/10.1002/joc.1012

Okugbo, O. T., Usunobun, U., Adegbegi, J. A., & Okiemien, C. O. (2012). A review of Nipa Palm as a renewable energy source in Nigeria. *Research Journal of Applied Sciences, Engineering and Technology*, *4*(15), 2367–2371.

Olaoye, O. J., & Ojebiyi, W. G. (2018). Marine Fisheries in Nigeria: A Review. *IntechOpen*, *i*(Marine Ecology-Biotic and Abiotic Interactions), 155–173. https://doi.org/http://dx.doi.org/10.5772/57353

Pool, D. J. (1973). *The Role of Mangrove Ecosystems: Mangrove leaf area indices*.

Potin, P. (2013). ESA Sentinel 1 handbook. *European Space Agency Technical Note*, 1–80. https://doi.org/10.1017/CBO9781107415324.004

Rodríguez, M. V. (2008). *Estimating Primary Productivity of Red Mangroves in Southwestern Puerto Rico from Remote Sensing and Field Measurements*.

RStudio Team. (2015). RStudio: Integrated Development for R. *[Online] RStudio, Inc., Boston, MA URL Http://Www. Rstudio. Com*. https://doi.org/10.1126/science.aad6351

Ryan, C. M., Williams, M., & Grace, J. (2011). Above- and belowground carbon stocks in a Miombo wooodland landscape of Mozambique. *Biotropica*, *43*(4), 423–432. https://doi.org/10.1111.j.1744-7429.2010.00713.x

Schnitzer, S. a, Mascaro, J., & Carson, W. P. (1991). Treefall Gaps and the Maintenance of Plant Species Diversity in Tropical Forests. *Ecology*, *82*(1947), 913–919. Retrieved from http://wolfweb.unr.edu/~ldyer/classes/396/schnitzer.pdf

Simard, M., Pinto, N., Fisher, J. B., & Baccini, A. (2011). Mapping forest canopy height globally with spaceborne lidar. *Journal of Geophysical Research: Biogeosciences*, *116*(4), 1–12. https://doi.org/10.1029/2011JG001708

Ukpong, I. E. (1994). Soil-vegetation interrelationships of mangrove swamps as revealed by multivariate analyses. *Geoderma*, *64*(1–2), 167–181. https://doi.org/10.1016/0016-7061(94)90096-5

Ukpong, I. E. (2000a). Ecological classification of Nigerian mangrove using soil nutrient gradient analysis. *Wetland Ecology and Management*, (8), 263–272.

Ukpong, I. E. (2000b). Gradient analysis in mangrove swamp forests. *Tropical Ecology*, *41*(1), 25–32.

Ukpong, I. E. (2015). Nypa Fruticans Invasion and the Integrity of Mangrove Ecosystem Functioning in the Marginal Estuaries of South Eastern Nigeria. In A. Gbadegesin, O. O. I. Orimoogunje, & O. A. Fashae (Eds.), *Frontiers in Environmental Research and Sustainable Environment in the 21st Century* (pp. 1–13). Ibadan University Press Publishing House University of Ibadan Ibadan, Nigeria. ©.

Walters, B. B. (2005). Patterns of Local Wood use and Cutting of Philippine Mangrove Forests. *Economic Botany*, *59*(1), 66–76. https://doi.org/10.1663/0013-0001(2005)059[0066:POLWUA]2.0.CO;2

Wan Norilani, W. I., Wan Juliana, W. A., Latiff, A., & Salam, M. R. (2014). Community structure at two compartments of a disturbed mangrove forests at pulau langkawi. *AIP Conference Proceedings*, *1614*, 790–794. https://doi.org/10.1063/1.4895303C

Williams, M., Rastetter, E. B., Fernandes, D. N., Goulden, M. L., Shaver, G. R., & Johnson, L. C. (1997). Predicting gross primary productivity in terrestrial ecosystems. *Ecological*

Applications [Ecol. Appl.], *7*(3), 882–894. https://doi.org/10.1890/1051-0761(1997)007[0882:PGPPIT]2.0.CO;2

Winarso, G., Vetrita, Y., Purwanto, A. D., Anggraini, N., Darmawan, S., & Yuwono, D. M. (2017). Mangrove Above Ground Biomass Estimation Using Combination of Landsat 8 and Alos Palsar Data. *International Journal of Remote Sensing and Earth Sciences (IJReSES)*, *12*(2), 85. https://doi.org/10.30536/j.ijreses.2015.v12.a2687

Wong, F. K. K., & Fung, T. (2013). Combining Hyperspectral and Radar Imagery for Mangrove Leaf Area Index Modeling. *Photogrammetric Engineering & Remote Sensing*, *79*(5), 479–490. https://doi.org/10.14358/PERS.79.5.479

Chapter 4

Rapid Loss of Mangroves and 7-fold Expansion in the Area of Nipa Palm (Nypa fruticans) in the Niger Delta over 10 years.

C. J. Nwobi[a], M. Williams[a], E.T. A. Mitchard[a]

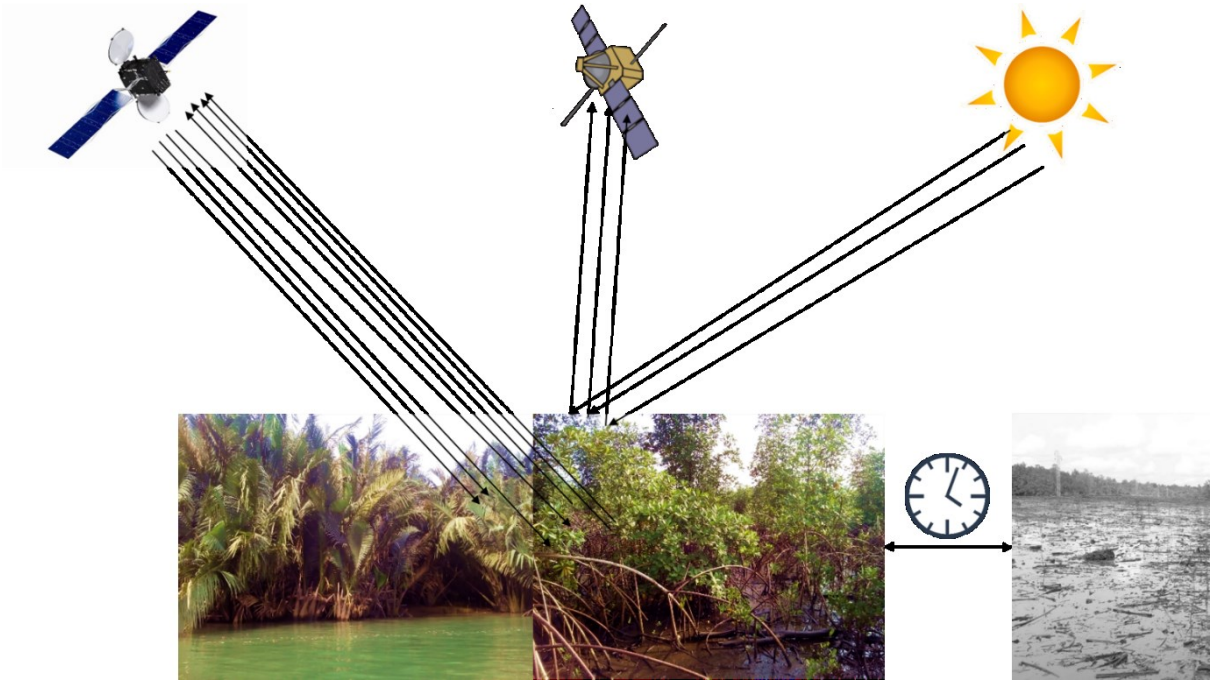

[a] ***School of GeoSciences, University of Edinburgh, Edinburgh, EH9 3JN, UK***

Abstract

Mangrove forests in the Niger Delta are important in providing ecosystem services such as fisheries, coastal protection and aesthetic values. However, they are under threat from urbanisation, logging and oil pollution. A further threat to mangroves is the proliferation of nipa palm. Nipa palm (Nypa fruticans) is an exotic species introduced to the area from South-East Asia in 1906. However, there is no data on the current area extent of mangrove forest in the Niger Delta, its rate of loss, or the rate of nipa palm colonisation. Here, I use an extensive field dataset collected during three field campaigns in 2016-17, Synthetic Aperture Radar (SAR), optical satellite data and elevation data to estimate the area of nipa palm and mangrove forests in the Niger Delta in 2017, and for 2007 to obtain change information. Using a collection of 567 ground control points and a combination of three earth observation satellites: Advanced Land Observatory Satellite Phased Array L-band SAR (ALOS PALSAR), Landsat ETM+ and the Shuttle Radar Topography Mission Digital Elevation Model 2000 (SRTM DEM) data; I performed supervised classifications using Maximum Likelihood (ML) and Support Vector machine (SVM) classifiers. The classification results showed SVM (overall accuracy 85 %) performed better than ML across the Niger Delta. Producers accuracy (PA) and Users accuracy (UA) for the best SVM classification were above 80 % for most classes, however these were considerably lower for mangrove (PA- 87 %, UA- 62 %) and nipa palm (PA- 16 %, UA- 88 %). I estimated a current mangrove area of 801 774 ha and nipa extent of 11 447 ha. The results indicate a 12% decrease in mangrove area and 694 % increase in nipa palm between 2007 and 2017. It is clear from these results that mapping efforts should continue for policy targeting and monitoring. It is also clear that the mangroves of the Niger Delta are at risk, from rapid clearance as well as from the invasive species nipa palm. This is of great concern given the dense carbon stocks and the value of these mangroves to local communities for generating fish stocks and protection from the sea.

Keywords: *mangrove, nipa, disturbance, classification, non-native invasive species, Landsat, alos*.

4.1 Introduction

The ecosystem services provided by mangrove forests are under threat from natural and anthropogenic factors. In Nigeria, mangroves provide erosion control, climate change regulation, wood for fuel and construction, sacred sites and fisheries (Akanni *et al.*, 2017). However, the super-imposition of high coastal population density and mangrove distribution within the same area increases the risk of mangrove deterioration. In Nigeria; oil pollution, urbanisation, and over-exploitation for fuelwood are the significant causes of mangrove loss (Mmom and Arokoyu, 2010). Fuelwood exploitation by poor coastal communities of mangrove stands results in a change of the forest stand structure or canopy structure (**Chapter 3**). These changes can result in loss of large tree stems and forest gap formation creating an opportunity nipa palm invasion. Non-native species can proliferate in areas where they were not intended to through introduction, naturalisation and invasion (Biswas *et al.*, 2007; Richardson *et al.*, 2000). The colonisation of invasive species can lead to a change in community structure and biodiversity by altering the function of the ecosystem (Hawthorne *et al.*, 2015). The Secretariat of the Convention on Biological Diversity (Secretariat of the Convention on Biologival Diversity, 2010) has stated that the threat of invasive alien species to biodiversity is a continuing and growing threat.

Nypa fruticans is a mangrove palm, native in the Indian Ocean coasts but was introduced in the Calabar estuary-eastern coast of Nigeria in 1906 to control erosion. The proliferation of nipa palm in the Niger Delta is known to be occurring in the Niger Delta due to local logging activities, dredging and oil pollution (Okugbo *et al.*, 2012; UNEP, 2011). Nipa palm spread is further compounded by the lack of use of this palm as a resource, as it is in Asia and Oceania for juice, dessert and palm fronds for roof construction (Isebor *et al.*, 2003). This mangrove palm was initially intended to serve as a plantation in eastern Niger Delta to check beach erosion along the cross-river estuary (Ukpong, 2015). However, the colonisation of nipa palm

has gradually replaced mangrove forests in the Niger Delta, especially in areas of high exploitation (Langeveld and Delany, 2014). Various attempts have been made to use the Nipa palm's potential products, which include its sap (which is sugar rich), its tannins, its potential for bioenergy, and its palm leaves as a building material (Hossain, 2015; Okugbo *et al.*, 2012; Tsuji *et al.*, 2011). However, the location of the nipa palm along the tidal channels places it at an unfavourable location for transportation of the resource generated. Cultural management of nipa spread is done by removal of nipa seedlings in some parts of the Niger Delta, but there is no report of a large-scale management plan of nipa invasion in the Niger Delta. Monitoring vegetation over space and time is essential for successful management of invasive species, as well as other threats to the mangroves of the Niger Delta. From the experience in the field, management of nipa spread is performed by some communities in some parts of the Niger Delta, through the removal of nipa seedlings, but there is no formal or large scale management plan for nipa invasion in the Niger Delta. Monitoring the extent of native species and spread of invasive species can provide the key to control the alien species and manage the conservation of native species (Myint *et al.*, 2008). Monitoring of mangrove forests is important in identifying areas of mangrove loss, to track causes of deforestation and create a baseline for restoration and remediation plans.

Field-based methods of monitoring are very useful as they can accurately assess species presence and their size/cover/biomass, and assess the localised cause of degradation and environmental conditions resulting from this disturbance. However, difficulties with working within the complex structure of mangroves makes this method challenging, and regular monitoring of a dense plot network in mangroves would be very difficult: remote sensing is essential for scaling field measurements up. (**Figure 4.1**). Mangrove root structure, tidal cycles and muddy sediments are some of the hindrances to field work in this ecosystem. Furthermore, the vast global extent of mangroves (> 14 million hectares) and their

importance as a carbon store, requires the use of spatial analysis to monitor them consistently, and assess the spread of degradation/deforestation, conduct vulnerability assessments and regional analysis of secondary factors which contribute to mangrove loss.

Satellite remote sensing is the most appropriate method of mapping land cover (LC) and land cover change. Optical remote sensors such as the Landsat ETM+ record the reflectance characteristics of the land surface, while active sensors such as Synthetic Aperture Radar (SAR) record the surface structures (Fatoyinbo and Simard, 2011; Li *et al.*, 2006; Lucas *et al.*, 2007). Although these two sensor types can be used separately, more recent studies have fused the two to achieve higher accuracy in classification due to their combined individual strengths (Bunting *et al.*, 2018; Green*et al*, 1998; Joshi *et al.*, 2016; Li *et al.*, 2006). Optical sensors freely available and with high resolution are Sentinel 2, launched in 2014, and Landsat products, available since the 1970s. Although, these products are mostly cloudy over mangrove regions, they can be improved by creating cloud free composites by combining images over time. Synthetic Aperture Radar (SAR) is a cloud free active sensors but these are typically expensive and hard to process. However, a real difference has been made from the free PALSAR mosaics which are available for 2007-10 and 2015-17. The availability of these sensors has made forest spatial analysis using satellite imagery cost effective and less time consuming compared to field analysis.

Figure 4.1: Mangrove forest structure in the Niger Delta hindering field survey.

There are various factors involved in accurately defining land cover types in classification. However, different classification types can improve the discrimination between LC classes surrounding mangrove forests. LC classification can be done using unsupervised or supervised methods. Unsupervised classification predicts different classes based on statistics from the spectral characteristic of the satellite products; while supervised methods predict LC types using ground control points as training data (Ajay *et al.*, 2004). A simple and common supervised classification used is the Maximum Likelihood Classifier (MLC); a parametric method that assumes a normal distribution of the multispectral data (Deilmai *et al.*, 2014; Jean *et al.*, 2017). The Support Vector Machine (SVM) classifier, contrary to MLC, is non-parametric assuming the data distribution is not defined by a set of known parameters. SVM identifies the optimum boundary between classes utilising the edge of the class distribution (Heumann, 2011; Huang *et al.*, 2002). The accuracy of SVM has been shown to be better than MLC, Artificial Neural Networks (ANN) and decision tree (David and Ballado, 2015; Heumann, 2011; Jean *et al.*, 2017); however the use of SVM and MLC in detecting fringe invasive species is largely unstudied. Mapped results are validated for accuracy by comparing with other mapped products, using accuracy assessments or field verification (Bradley, 2009). The accuracy of the mapped result would depend on the goal of the LC classification. Accuracy improvements in classification and change detection can be achieved using variations of datasets and methodology comparison.

Here, I estimate mangrove forest and nipa palm cover in the Niger Delta of two years a decade apart, as well as the area of other inland land cover classes, needed to train the classifier to correctly identify my two focal classes. I also compare the accuracy of MLC and SVM in estimating coastal vegetation. Mangrove extent in the Niger Delta has been estimated by James *et al.* (2007) and Fatoyinbo and Simard (2013) using an unsupervised classification ISODATA method to estimate mangrove area from Landsat ETM+. These

studies show the ability of remote sensing options in estimating mangrove area; however, the use of fused SAR and optical data, with ground control points, has not yet been explored in the estimation and change detection of coastal vegetation in the Niger Delta. My study compares two methods of supervised classification and provides a new regional estimate of mangrove and nipa palm area in the Niger Delta. Specifically, I aimed to **(1) compare the two different types of classification in estimating mangrove area, (2) estimate current area extent of mangrove and nipa palm; and (3) carry out a change detection of mangrove area over a decade from 2007 and 2017**. From my knowledge of the literature, I hypothesise that SVM will have a better accuracy than MLC in predicting LC classes using fused data. I also predict from my knowledge of the region that mangrove area will have reduced in the delta due to deforestation and nipa palm extent increased over the study period.

4.2 Methodology

4.2.1 Study Area

The Niger Delta study region (**Figure 4.2**) spans from the Benin River estuary in the west to the Calabar river estuary in the east. Economic activity is primarily farming within these regions while fuelwood and fisheries account for minor sources of income (Ndidi *et al.*, 2015). Increased urbanisation is occurring within this region including road construction, port establishment and building structures (Langeveld and Delany, 2014). Mangroves in this region are riverine and estuarine, while species zonation is influenced by soil and saline conditions (Ukpong, 1994, 2000b, 2000a). However, *Nypa fruticans* interrupts this zonation along mangrove fringe and inland sections where wood exploitation has taken place (Ukpong, 2015).

4.2.2 Field Data and Sampling Strategy

I adopted a multiclass method consisting of 6 broad classes from spectral representation (**Figure 2.8**), knowledge of the region and field work (**Table 4.1**). These classes were chosen to give a general overview of other landcover types in the region; while focused on mangrove and nipa palm. The other classes During three field campaigns in March 2016, between October 2016 to January 2017; and June 2017 to September 2017, I collected 567 GCPs across the East-West Highway (which connects the entire coastal state); during surveys on a boat, and during sample collection. Areas of interest during GCP selection were Islands off the Calabar estuary and along the Imo river estuary where a clear transition of nipa palm, to mangrove species, then to agricultural lands or rainforests were present. Another essential region were creeklets in Rivers State where settlements were surrounded by a transition of mangrove forests and rainforests. I selected points with distinct spectral characteristics in order to improve accuracy and validation of the classification output.

Table 4.1: Land cover classes, training and test pixels for 2007 and 2017.

No	Class name	Description	Training Pixels (2017)	Testing pixels (2017)	Training Pixels (2007)	Testing pixels (2007)
1	Mangrove Forests	Mangrove forests located in intertidal regions strictly vegetated with red (*Rhizophora* spp), black (*Avicennia germinans*) or white (*Laguncularia racemosa*) mangrove species.	25522	399	31956	37
2	Nipa palm	*Nypa fruticans* stands within mangrove forests or along the fringes.	751	298	103	50
3	Inland forests	All other forested vegetation, palm plantations and evergreen forests	257398	478	252798	36
4	Surface water	All areas with open water including coastal waters.	249912	393	249983	43
5	Built up regions	Developed land with constructed structures including industries, residential area, roads	2931	318	52341	53
6	Agricultural land	Cultivated land, pastures, other herbaceous vegetation, parks	2864	305	68329	40

Despite not having GCPs in 2007, I used Google Earth Pro software to locate the GCPs collected during my field campaign and estimated the land cover classes they were in 2007. GCPs obstructed by cloud cover in 2007 imagery were removed in 2007 land cover classification. I used 417 GCPs in supervised classification for 2007 data. The GCPs over the entire region were uneven as a result of the proportion cover of the entire Niger Delta. Hence, more training pixels were needed for classes with more coverage in order to effectively classify the land classes. The GCPs were divided in the 70: 30 ratio. 70% for training the classification algorithm and 30% for testing. However, due to the uneven number of pixels for the different land classes. The test pixels were further split to make a more even distribution for accuracy assessment with mangrove pixels (~20%) being the main focus of this study.

4.2.3 Image Processing

Spatial data analysis was done using ENVI version 5.1 (Exelis Visual Information Solutions, Boulder, Colorado), QGIS 3.4 (QGIS Development Team, 2018), Google Earth Engine (Gorelick *et al.*, 2017), Google Earth Pro (GEP) 7.3.2.5776 and ArcGIS 10.4 (ESRI, 2011). Three datasets were used for LC classification: Shuttle Radar Topography Mission (SRTM) Digital Elevation Model (DEM), ALOS PALSAR and Landsat 7 ETM+ (**Figure 4.3**).

4.2.3.1 Digital Elevation Model

The SRTM made use of two SAR in C and X bands designed for single-pass operation interferometry (Farr *et al.*, 2007). This design was to make up for difficulties in repeat-pass operations such as atmospheric changes between passes and satellite orbit uncertainties. The SRTM DEM 1 arc sec (30 m) version was as it filled gaps and void with elevation data primarily from the Terra Advanced Space borne Thermal Emission and Reflection Radiometer (ASTER) Global Digital Elevation Model Version 2.0 (GDEM2) and secondarily from the USGS GMTED2010 elevation model or the USGS National Elevation Dataset (NED) (SRTM, 2015). I used the SRTM DEM in order to aid the LC classification of the Niger Delta because I know that such sea-influenced vegetation will change with elevation above sea level (USGS, 2004). Mangrove and nipa vegetation occur at the intertidal zones of the coast. Hence, this will significantly aid in differentiating coastal vegetation from other vegetation types. I downloaded SRTM DEM 2000 data for twelve tiles covering the Niger Delta using Earth Explorer at a 30m resolution. Mosaicking and registration was performed using Landsat bands from Hansen (2013) using 10 GCPs with a root mean square error of 0.06 (Hansen *et al.*, 2013).

4.2.3.2 Synthetic Aperture Radar Data

Japanese Aerospace Exploration Agency (JAXA) has successfully launched land observation missions in order to monitor disaster, cultivated land, increase data archives and tropical rainforests (JAXA, 1997). These missions are the Advanced Land Observing Satellite 1 and 2 (ALOS PALSAR and ALOS-2 PALSAR-2). ALOS-2 is was sequel to ALOS "DIACHI", which was launched in May 2014 with a lifetime of 5 years. ALOS is made up of three sensors for elevation, land surface monitoring and land observation (Rosenqvist *et al.*, 2004). The ALOS 2 uses the Phased Array type L-band Synthetic Aperture Radar (PALSAR-2) capable of night and day all weather observations. ALOS-2 PALSAR-2 emits L-band wave that penetrates clouds, vegetation and reaches the ground. Hence it is not, affected by weather and can retrieve vegetation structure which can become a problem when the ground is moist, increasing the backscatter information. PALSAR-2 also retrieves information in 3 modes- spotlight, strip map and ScanSAR. Raw ALOS PALSAR 25m Mosaic files (HH and HV bands) were downloaded from the Japan Aerospace Exploration Agency, Earth Observation Research Centre (http://www.eorc.jaxa.jp/ALOS/en/index.htm) for the years 2007 and 2017. The data tiles were N07 E002, N07 E003, N07 E004, N07 E005, N07 E006, N07 E007, N07 E008, N06 E004, N06 E005, N06 E006, N06 E007, N06 E008, N05 E005, N05 E006, N05 E007 and N05 E008.

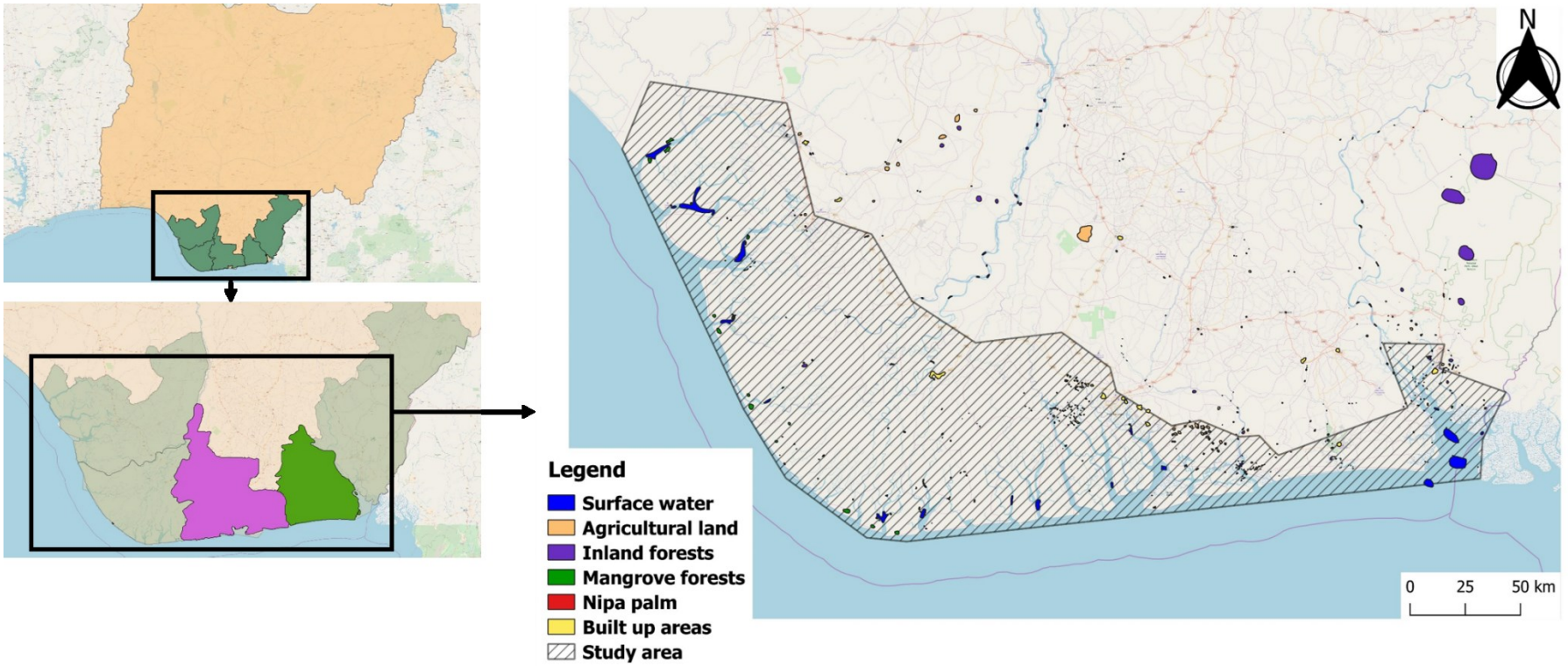

Figure 4.2: Location of the Niger Delta, study area and ground control points (GCP) established during the field survey.

Source: Open street map

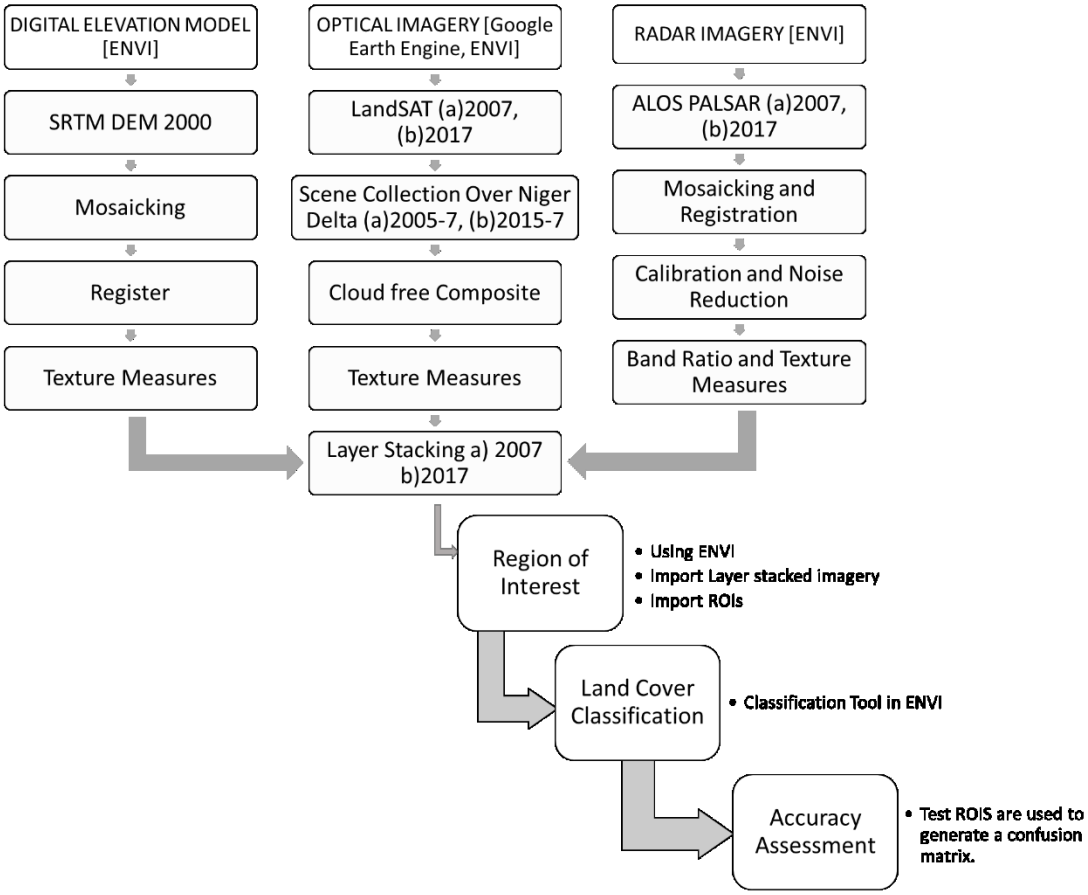

Figure 4.3: Image processing steps prior to LC classification. DEM, ALOS PALSAR and Landsat were pre-processed separately before they were stacked together with the SRTM DEM 30m resolution. Landsat and ALOS PALSAR data were collected for 2007 and 2017 periods.

4.2.3.2.1 Mosaicking and Registration

The individual data tiles were then mosaicked to form a single image file of the Nigerian coastline in both bands and geo-referenced with the projection Universal Transverse Mercator (UTM) Zone 31 North and World Geodetic System (WGS) 1984 datum. The image file of both bands was registered using Landsat bands from Hansen (2013) using 41 GCPs with a root mean square error of 0.27 (Hansen *et al.*, 2013).

4.2.3.2.2 Calibration

Calibration of ALOS PALSAR backscatter was through two stages, the first step is to convert the digital number (DN) value on the original image so that brightness value of the units in the converted image in the form of decibel (dB) (Equation 4.1) based on the coefficients and equations from (Shimada *et al.*, 2009).

Conversion of DN to σ^o (dB) $= \mathbf{10} \times \left(\mathbf{log_{10}}\left(\boldsymbol{DN^2}\right)\right) - \mathbf{83}$ **(Equation 4.1)**

4.2.3.2.3 Noise Reduction (speckle)

Speckle associated with Synthetic Aperture Radar (SAR) data reduces the efficiency of class characterisation by affecting the radiometric and textural qualities. However, filtering processes can reduce the noise associated with SAR data. These filtering techniques can reduce or eliminate the information contained in the image, in particular resulting in a smoothing out of the (real) hard boundary between two land cover types (Dewantoro and Farda, 2012; Lopes *et al.*, 1990). Adaptive filters have been developed to attempt to reduce this problem: and thus I used the Enhanced Lee Filter to reduce the speckle. Adaptive filtering makes a choice about how to average a pixel based on its neighbourhood. The Enhanced Lee Filter determines the grey level for each pixel by computing the weighted sum of the centre pixel value, the mean value, and the variance calculated in a square kernel surrounding the pixel. This filter is used primarily to suppress speckle by smoothening image data without removing edges or sharp features in the images while minimising the loss of radiometric and textural information (PCI Geomatics, 2016).

I carried out the filtering process in this study used a 7x7 window on both HH and HV bands to minimise the loss of information in the image, which gives the best results based on published results (Lee, 1980; PCI Geomatics, 2016).

4.2.3.2.4 Band Ratio

In order to carry out band calculations without being distorted with the log nature of the sigma (σ^o) backscatter coefficient, I transformed the enhanced bands into power space. (**Equation 4.2**). The ratio of the HV and HH bands were then calculated. This resulted in three bands **HH, HV and HV: HH**.

Conversion of σ^o to power $= \mathbf{10}^{(\sigma^\circ/\mathbf{10})}$ (**Equation 4.2**)

4.2.3.3 Optical Data

Landsat ETM+ 7 Collection 1 Tier 1 Digital Number values was pre-processed and downloaded using the Google Earth Engine (GEE) (Gorelick *et al.*, 2017). In order to assess two different time periods, I created a composite of Tof of the Atmosphere (TOA) data from 2005 and 2007; and from 2015 and 2017. A cloud-free composite was created using the ee.Algorithms.Landsat.simpleComposite() method that converts the subset of the scene at each location to TOA reflectance . The median of the least cloudy pixel is then taken after a cloud score is applied. I also calculate the cloud score of the scenes in the Landsat collection used in the creation of a cloud free composite. The GEE code can be assessed here: https://code.earthengine.google.com/?accept_repo=users/nwobicj/nigerdeltamangrove or assess through GIT repository git clone https://earthengine.googlesource.com/users/nwobicj/nigerdeltamangrove

I calculated a range in cloud score for the 2005-07 range 0-100 was with a mean 48% and mean of 50% (range: 0-100) for the 2015-17 dataset. However, after applying a cloud free composite algorithm (removing the cloud pixels), 1.5 % of the Landsat data used in LC classification was affected by cloud removal in 2017 and 1.6 % in the 2007 data.

4.2.4 Texture Measures

I performed occurrence statistics on DEM, ALOS PALSAR and Landsat 7 ETM+ bands. I applied a 7×7 window size for all image texture analysis. This window size has the advantage of capturing the heterogeneity of pixel values over small extents. Texture measures were selected based on their established ability to characterise vegetation structure. I calculated three first order texture measures (data range, mean and variance) using the ALOS PALSAR and Landsat 7 bands.

4.2.5 Layer Stacking

I stacked all remote sensing layers for both time periods (2007 and 2017) using a 30m scale including:

i. SRTM DEM 2000

ii. ALOS PALSAR 2017 HH, HV and ratio

iii. Landsat 7 ETM+ bands 1 (blue), 2 (green), 3 (red), 4 (Near Infrared), 5 (Short-wave Infrared 1) and 7 (Short-wave Infrared 2).

iv. Texture Measures

   a. ALOS PALSAR 2017 HH, HV and ratio (data range, mean and variance)

   b. Landsat 7 ETM+ bands used (data range, mean).

4.2.6 Geographic Extraction of Ground Control Points

I registered the training and testing sites recorded during the field campaign on Google Earth Pro (Google Earth, 2018) extracted them as kml files. I converted the kml files to shapefile format using QGIS (QGIS Development Team, 2018). I also projected and dissolved the shapefiles into their respective classes using ArcGIS 10.0 (ESRI, 2011) for land cover classification. GPS had an error of 10m.

4.2.7 Supervised Classification

I implemented MLC and SVM to classify the layer stacked data for 2007 and 2017 into six classes: built up areas, agricultural land, mangrove, nipa palm, surface water and forest. I masked the bands where there were no data values in the MLC to avoid error during statistics computation. The kernel function in SVM involves a better representation of the data to be used for classification by mapping them into a higher dimensional space (Nanda *et al.*, 2018). This dimensional space could be radial basis function, sigmoid and polynomial. Penalty parameter (C) is the degree of how much error given in the classification. A higher C will result in error minimal error (Karatzoglou *et al.*, 2006). Gamma is a function of how the distance between training data affect the similarity of those points. This only applies to non-linear kernel and I used the default value (inverse of the number of bands used in the classification- 31 bands). Pyramid levels determines what resolution the classification will be performed on to reduce time. Here, it was set at 0 so as to classify the image at it resolution. Setting the pyramid level > 0 increases processing time but could affect the quality of the classification. I tested two types of kernel type for SVM classification based on results of Yang, (2011) who tested various parameters of SVM in a LC classification.

i. Linear Kernel type, Penalty Parameter (100.00), Pyramid levels (0).
ii. Linear Kernel type, Penalty Parameter (50.00), Pyramid levels (0).
iii. Radial Basis Function (RBF) Kernel Type, Gamma in Kernel Function (0.032), Penalty Parameter (100.00), and Pyramid levels (0).
iv. Polynomial Kernel Type, Gamma in Kernel Function (0.032), Penalty Parameter (100.00), and Pyramid levels (0).

In order to carry out a change detection analysis, I classified the same set of data for the year 2007 and 2017.

4.2.8 Accuracy Assessment

I assessed the performance of the models by carrying out post classification confusion matrices and overall accuracies using testing pixel (Table 4.1) independent of the training pixels. I used identical training and testing pixels for the different types of classifiers to minimise bias separately for both years. I placed particular interests in the following confusion matrix variables:

i. Overall accuracy (gives a measure of how accurate the total classes were classified)
ii. Kappa coefficient (the degree of agreement between the classified image and test pixels)
iii. Producer's accuracy (the probability of how accurate each of the classes were classified)
iv. User's accuracy (the probability that a certain class prediction belongs to that class)

I used prior knowledge of the study site from both field work and communication with the locals, as well as Google earth Pro timeline images. Areas of focus for the visual search included roads, smaller developed areas embedded within larger homogenous forest classes, and developed areas along rocky and sandy coastlines which possess spectral similarities. I also reported the individual confusion matrices of the different land cover classes.

4.2.9 Change detection

I performed change detection analysis of the resultant LC types the change detection statistics tool in ENVI. This tool analyses the change from a base initial image for each class. It does this by evaluating the number and percentage of pixels change in classes between the initial and final images. The time intervals investigated in this study were 2007 (initial) to

2017 (final). I particularly assessed the change in nipa palm and mangrove forests over the decade.

4.3 Results

4.3.1 Accuracy Assessment

I had improved overall accuracy from the SVM classification (86 %) when I compared to the MLC method (81%).The overall accuracy (84-86 %) did not differ amongst the kernel types in the SVM method (**Table 4.2**). I discovered that surface water, urban regions and agricultural lands were easily detected by the SVM with producer's accuracy above 80% for all classifiers (**Appendix III**, **Appendix IV**). The results of the SVM classification of the 2007 data over the Niger Delta resulted in an overall classification of 78 % for both RBF and polynomial kernel type (**Table 4.2**).

I discovered that the mangrove class had the lowest producer's accuracy (53 %) in the MLC but had the best classification accuracy (90 %) using the SVM method under the linear kernel type (**Table 4.2**). I also discovered that while the highest producer's accuracy (90%) on the nipa invasive species was in the MLC method (due to overestimation), it also had a very low user's accuracy (63 %) (**Table 4.2**). The best classification result I estimated was the SVM method under the Radial Basis Function kernel type which had the highest classification and user's accuracy for mangrove (87%, 62%) and nipa (16 %, 88 %). I also discovered that both SVM polynomial and RBF kernel classifiers in 2007 had similar classification results (**Appendix V**). However, I chose the RBF because it had a higher producer's accuracy for nipa palm (42 %) (**Table 4.2**). There was high confusion of nipa palm with both surface water and mangrove forests as a result of the land cover class transition between the classes.

I also visually compared the different classification results (**Figure 4.5**). Across three regions: Calabar estuary (**Figure 4.5a**), Oproama community (**Figure 4.5b**) and Imo River Estuary (**Figure 4.5c**); MLC overestimated nipa palm vegetation especially in areas where they are non-existent. SVM classifiers performed better in estimating nipa from mangrove and other

LC classes. I also observed that there was no difference amongst the SVM kernel types (linear, radial and polynomial) across the three regions.

4.3.2 Classification Results

I generated a LC map of the Niger Delta for both 2017 (Figure 4.4) and 2007 sets; and estimated mangrove and nipa areas of the region. I estimated mangrove area of **801 774 ha** and a nipa area of **11 447 ha** in 2017 and **911 548 ha** mangrove area and **1 441 ha** nipa area in 2007 (Table 4.3). My analysis shows that mangrove forests in the Niger Delta make up about 1% of the total land surface area of Nigeria. In 2017, I estimated the lowest nipa (**514 ha**) and mangrove (**24 478 ha**) area in Cross river state while I estimated the highest mangrove cover (**239 881 ha**) in Bayelsa state and largest nipa (**3 746 ha**) influence in Rivers state (Table 4.4). In 2007, while Cross river had the lowest mangrove area (**28 154 ha**) and Delta state had the highest mangrove area (**290 797 ha**), I estimated lowest nipa area in Rivers state (**86 ha**) and highest nipa area in Akwa Ibom (**429 ha**). I also estimated mangrove area based on the coastal division of Nigeria by Hughes and Hughes, (1992) (Hughes and Hughes, 1992) (Table 4.5**)**. In 2017, I estimated a mangrove area of **722 321 ha** in the Niger Delta basin and **48 680 ha** in the Cross River Estuary while I estimated nipa palm area of **8 256 ha** in the Niger Delta basin and **2 911 ha** in the Cross River estuary. In 2007, I estimated a mangrove area of **844 187 ha** in the Niger Delta basin and **52 866 ha** in the Cross River Estuary while I estimated nipa palm area of **634 ha** in the Niger Delta basin and **669 ha** in the Cross River estuary.

I observed that mangrove forests extended about 60 km in western Niger Delta basin (Delta state- Figure 4.4a), 40 km in central Niger Delta basin (Bayelsa State- Figure 4.4b), 60 km inland around the eastern Niger Delta basin (Rivers state- Figure 4.4c), 20 km in Imo River (Akwa Ibom state- Figure 4.4d) and about 3 km along the Cross River estuary (Figure 4.4e). I observed from the classification maps that agricultural lands were around settlements and

rain forests close to river water shed (**Figure 4.4f**). Along the coast I observed nipa palm fringes followed by a longer strip of mangrove forests before transitioning to tropical forests. I observed most of the nipa fringes along Imo river estuaries especially in Kono creek and Ete creek. These nipa fringes were also associated with urban settlements such as Opobo, Rivers State and Ikot Abasi, Akwa Ibom State (**Figure 4.6**).

4.3.3 Change detection of Mangrove and Nipa Area

I used the SVM RBF kernel classification results for the change detection analysis. I observed a 12 % decrease in forest over the entire delta and an increase in agricultural land (11 %) and urban regions (50 %). I compared the change in mangrove and nipa palm area over the two periods (**Table 4.3**). Over the decade, I observed a 12 % decrease in mangrove area and over 600 % increase in nipa palm extent in the Niger Delta. I observed that ~50% of nipa area was colonized from mangrove forests (**Appendix VI**) and ~6% of mangroves were converted to farmlands or urban regions. The largest decrease in mangrove area was observed in Delta state (18 %) and I observed the lowest decrease in Rivers state (6 %) (**Table 4.4**). Nipa palm increase was observed to be highest in Rivers state. Based on the coastal division by Hughes and Hughes, (1992); I observed an 8% loss of mangrove area at the Cross River estuary and 14 % loss in the Niger Delta basin (**Table 4.5**).

I also analysed the loss of mangrove and nipa spread over some local regions notably Benin River, Imo River and Calabar estuary (**Figure 4.6**). I observed a 15% reduction in mangrove area and over fivefold increase of nipa palm area in the Benin River estuary. Imo river estuary had a 40% decrease in mangrove area with over 50% of nipa colonisation from these regions. I recorded a reduction of 9% in mangrove area in the third region along the Calabar estuary.

4.3.4 Comparison with Global Mangrove Datasets

I compared my regional map to global maps (**Figure 4.7**) generated by Giri *et al.*, 2010, Spalding *et al.*, 2010 and the Global Mangrove Watch (Bunting *et al.*, 2018; Dahdouh-Guebas,

2011; Giri *et al.*, 2011; Spalding *et al.*, 2010). Data for comparison were acquired using the UN Ocean Data Viewer (Schlitzer, 2018). It is important to note that these maps were from different time periods (**Table 4.6**). I classified a dataset spanning 2007 to 2017. However, the GMW is a 2010 map, while the Giri *et al.*, 2011 and Spalding *et al.*, 2010 are 2000s maps. I recorded a higher mangrove area for 2017 than those reported by other maps. I recorded about 10% higher mangrove in the 2017 estimates than reported by the GMW over the Niger Delta in 2010, 25% more than recorded by Giri *et al.*, 2010 and about 10% recorded by Spalding *et al.*, 2010. I compared two regions along the Niger Delta, Opraoma creek (**Figure 4.7a**) and Benin River estuary (**Figure 4.7b**) in my study and the maps generated by the GMW showing similarity in mangrove forests in the Niger Delta. This similarity could be possibly as a result of similar datasets used. However, there were some underestimation in some regions from the GMW which may have resulted in under estimation of mangrove cover due to unavailability of ground control points and I used an independent supervised classification from my datasets. I also showed a trend in nipa invasion in the Calabar estuary (**Figure 4.7c**) by comparing the global maps from different time periods.

Table 4.2: *LC classification accuracy (%) of two classifiers.*

Year	Classification type	Kernel type	Penalty parameter	Overall Accuracy (%)	Kappa Coefficient		surface water	agricultural land	rain forest	mangrove forest	nipa palm	built up areas
2017	**Maximum Likelihood**	**–**	**–**	**80.5%**	**0.77**	**Producer's Accuracy**	99	100	72	53	90	76
						User's Accuracy	100	72	97	62	63	99
	Support vector Machine	**Linear**	**100**	**84.1%**	**0.81**	**Producer's Accuracy**	100	99	99	90	5	100
						User's Accuracy	85	99	98	58	94	98
			50	**84.0%**	**0.81**	**Producer's Accuracy**	100	99	99	90	4	100
						User's Accuracy	85	99	98	58	92	98
		Radial basis function	**100**	**85.4%**	**0.82**	**Producer's Accuracy**	100	99	100	**87**	**16**	100
						User's Accuracy	83	100	97	**62**	**88**	99
		Polynomial	**100**	**85.4%**	**0.82**	**Producer's Accuracy**	100	99	100	**88**	**16**	100
						User's Accuracy	82	100	97	**62**	**89**	99
2007	**Support vector Machine**	**Radial basis function**	**100**	**77.6%**	**0.73**	**Producer's Accuracy**	70	98	97	**72**	**42**	95
						User's Accuracy	62	89	85	**63**	**85**	83
		Polynomial	**100**	**76.5%**	**0.72**	**Producer's Accuracy**	70	98	97	**72**	**38**	93
						User's Accuracy	55	89	85	**62**	**87**	86

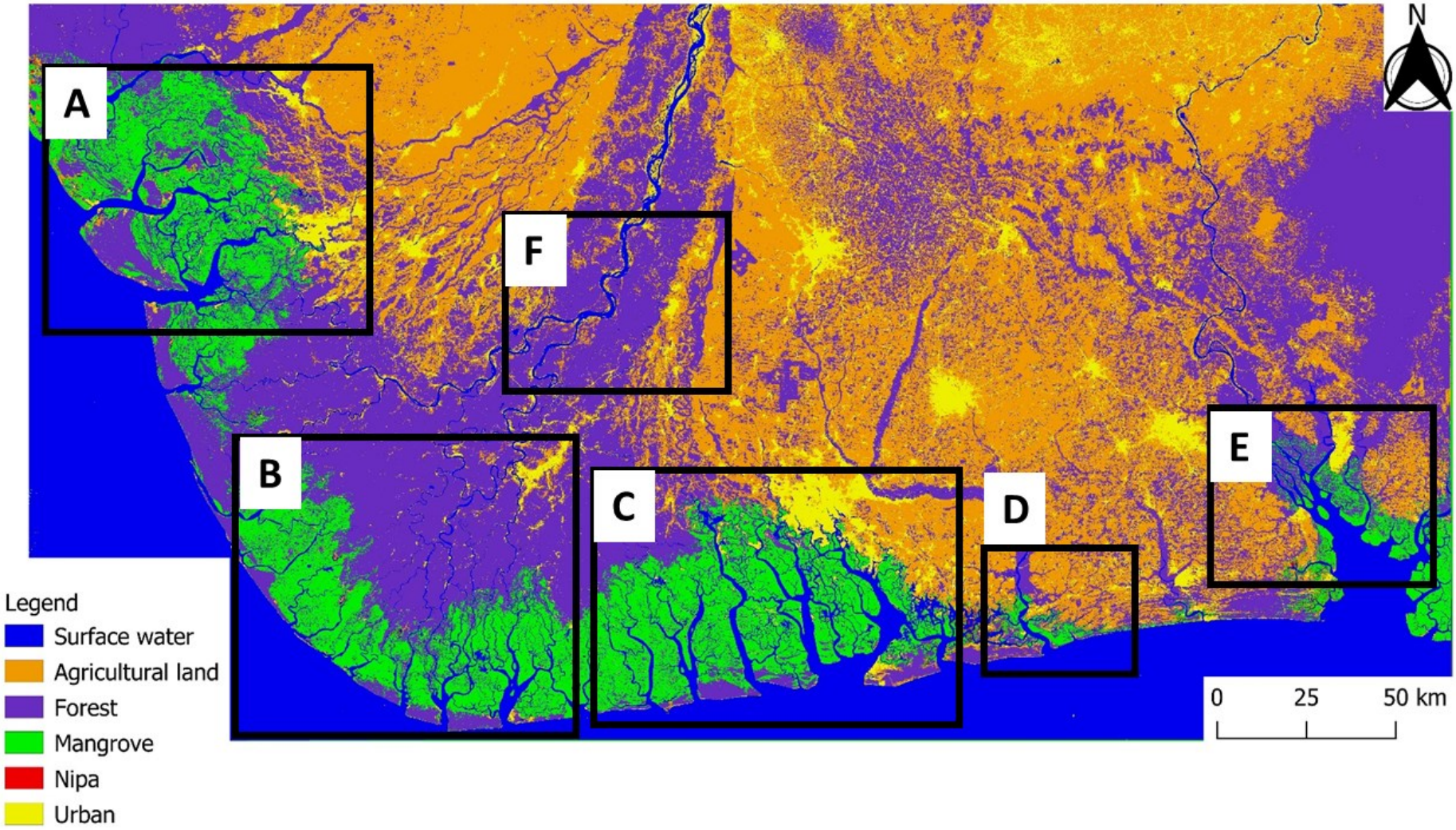
A
F
B
C
D
E
N
Legend
Surface water
Agricultural land
Forest
Mangrove
Nipa
Urban
0
25
50 km

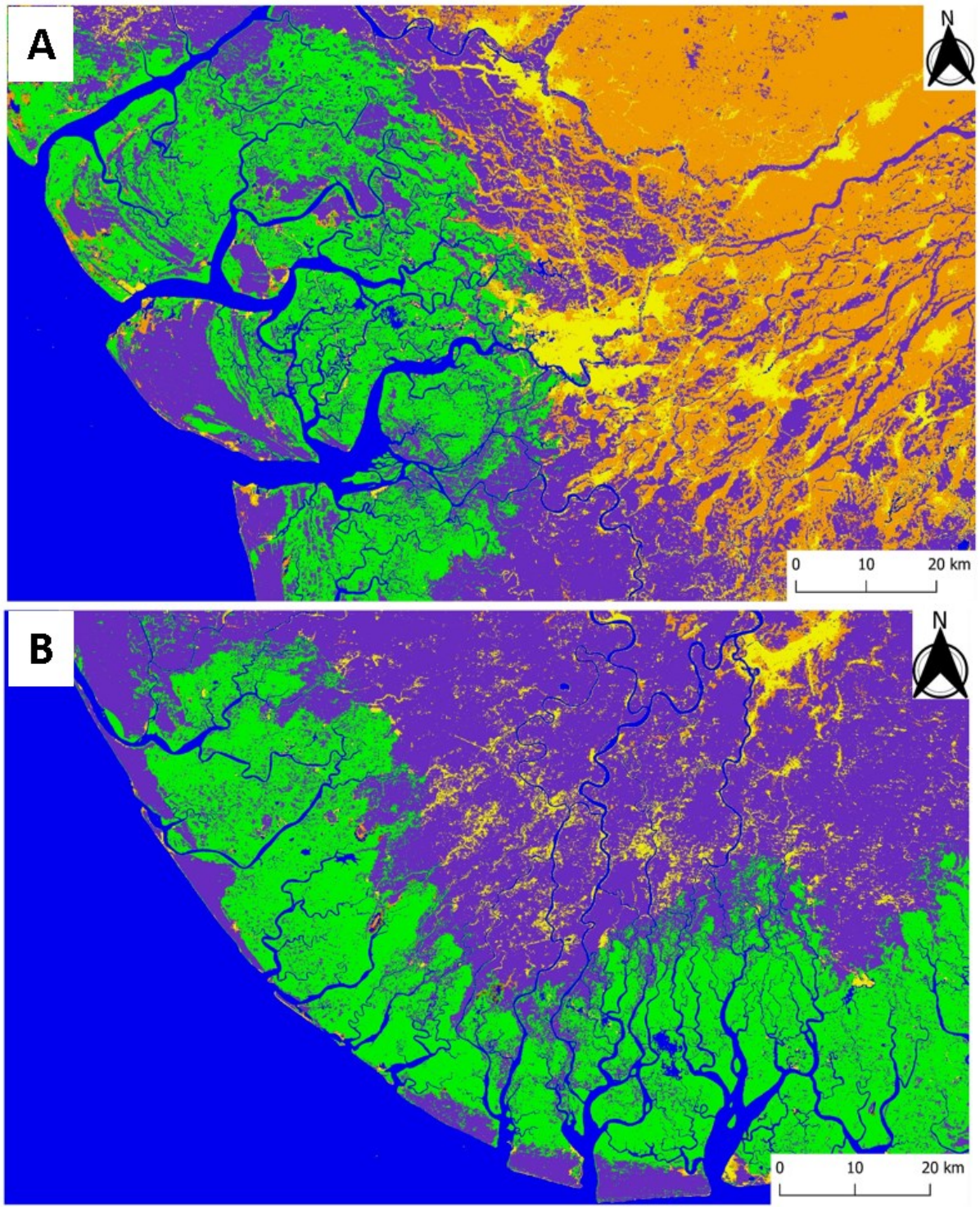
A
N
0
10
20 km
B
N
0
10
20 km

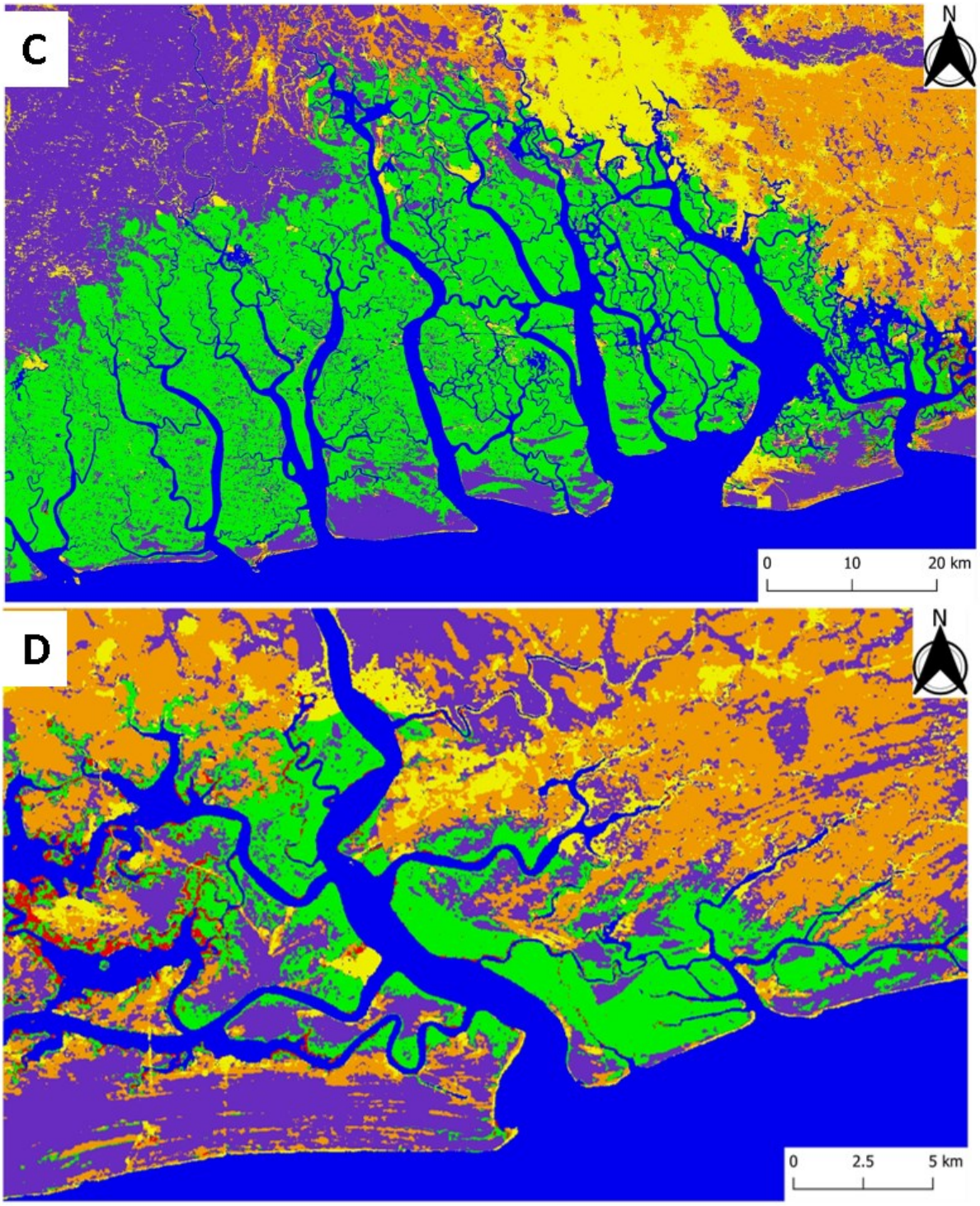
C
N
0
10
20 km
D
N
0
2.5
5 km

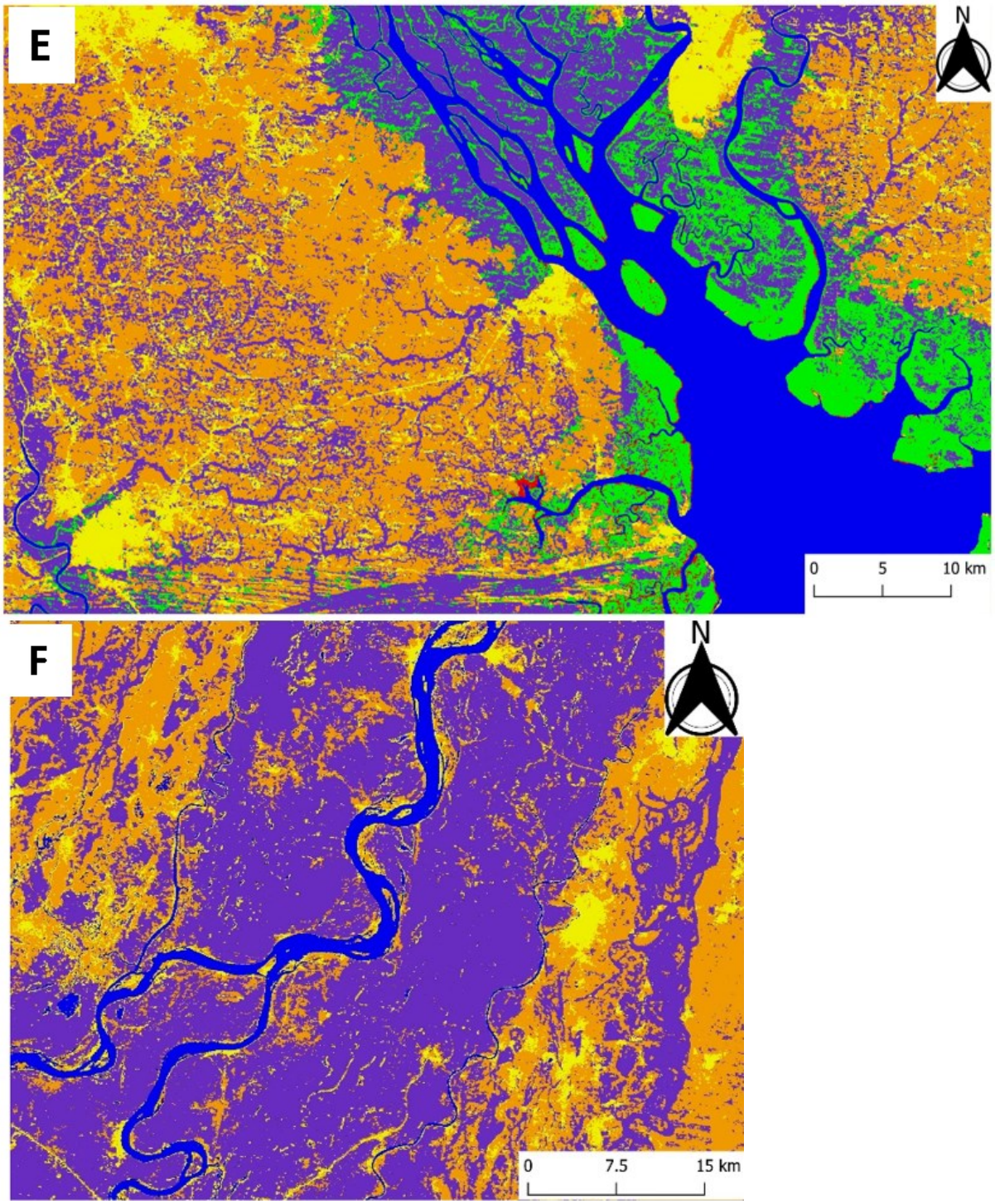

*Figure 4.4: 2017 Thematic map derived from the classification of layer stacked SRTM DEM, ALOS PALSAR and Landsat 7 of the Niger Delta using SVM with Radial Basis Function Kernel. Inset shows the inland extent of mangrove forests in **A)** western Niger Delta **B)** central Niger Delta **C)** eastern Niger Delta **D)** Imo River estuary **E)** Calabar estuary; and **F)** the River Niger Basin bifurcation and the spread of surface water proximity to rain forests and agricultural land surrounding urban settlements.*

Table 4.3: Change Detection analysis Using SVM- RBF kernel for each Land cover between 2007 and 2017 over the Study Area.

Land Cover Classes	2017		2007		2017-2007	
	Area (ha)	Area (%)	Area (ha)	Area (%)	Change (ha)	Change (%)
Agricultural land	2,417,929	37.9	2,173,317	34.10	-244,213	11
Tropical Forest	2,549,919	40	2,889,083	45.35	339,164	-12
Mangrove forest	801,774	12.6	911,548	14.31	109,774	-12
Nipa palm	11,444	0.18	1,441	0.02	-10,003	694
Built up areas	593,759	9.31	394,985	6.20	-198,774	50

Table 4.4: Area of Mangrove and Nipa palm in Niger Delta States and Change in Land Cover Classes from 2007 and 2017 over the region.

Nigerian State	Mangrove area (ha)			Nipa Area (ha)		
	2017	2007	Change (%)	2017	2007	Change (%)
Akwa Ibom	27 853	31 888	-4 034 (**13**)	2 414	429	1 986 (463)
Bayelsa	239 881	284 840	-44 960 (**16**)	1 225	167	1 059 (635)
Cross River	24 478	28 154	-3 676 (**13**)	514	269	245 (91)
Delta	238 697	290 797	-52 100 (**18**)	2 930	322	2 608 (809)
Rivers	236 234	252 468	-16 234 (**6**)	3 746	86	3 660 (4263)

Table 4.5: Mangrove and Nipa palm Extent across Coastal Divisions of Coastal Nigeria

Coastal Division	Mangrove area (ha)			Nipa Area (ha)		
	2017	2007	Change (%)	2017	2007	Change (%)
Cross River Estuary	48 680	52 866	-4 187 (-8)	2 911	669	2 242 (335)
Niger Delta basin	722 321	844 187	-121 867 (-14)	8 256	634	7 622 (1203)

Table 4.6: Comparison of Mangrove Area estimated by Global Datasets

	This study	GMW 2010	Giri *et al.*	Spalding *et al.*
Mangrove Area (ha)	801,774	695,800	622,373	713,000

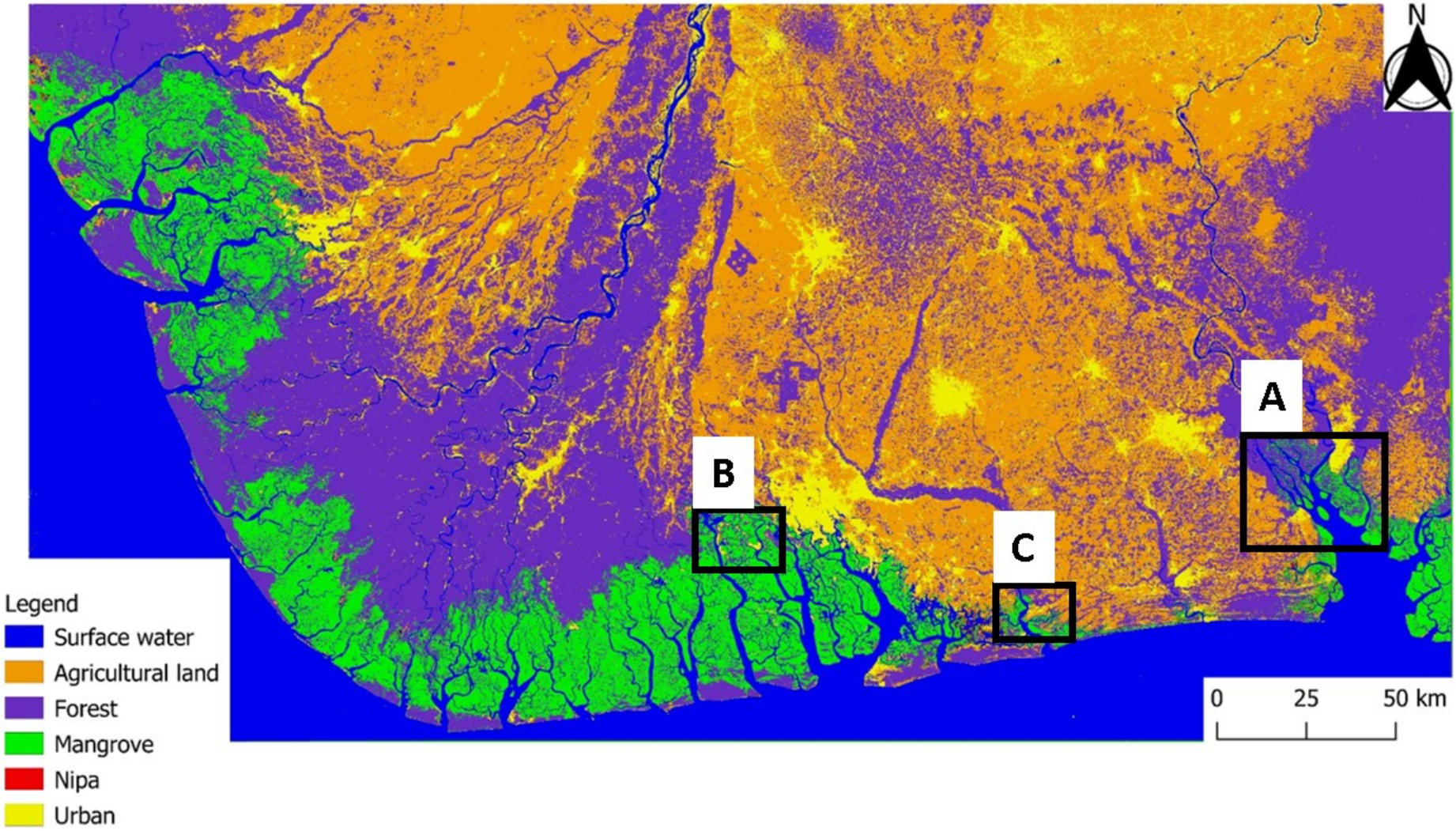
N
A
B
C
Legend
Surface water
Agricultural land
Forest
Mangrove
Nipa
Urban
0
25
50 km

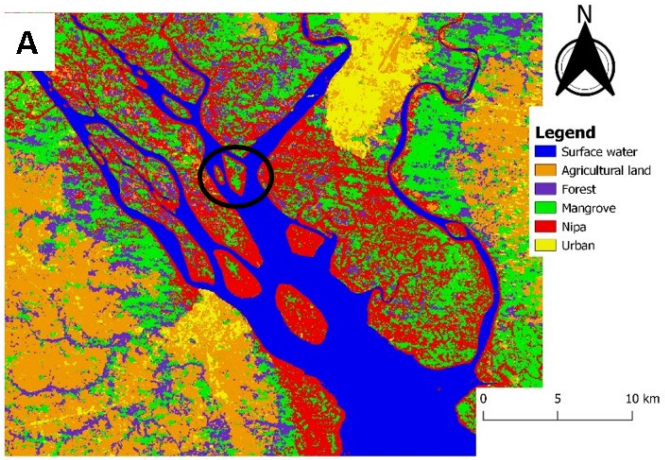

Maximum Likelihood Classifier

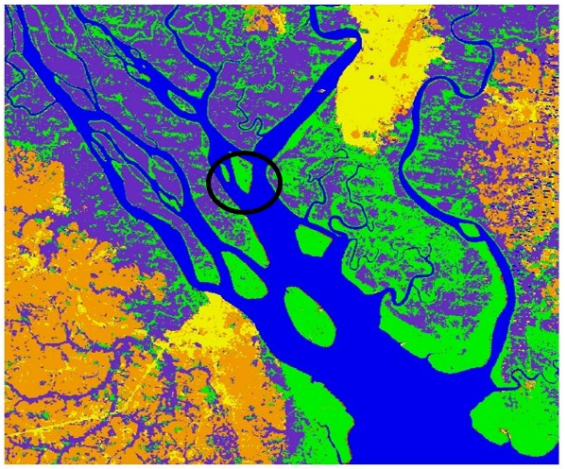

Linear Support Vector Machine

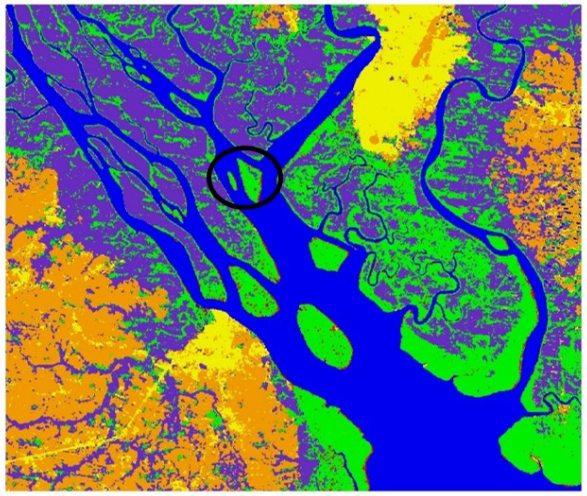

Polynomial Support Vector Machine

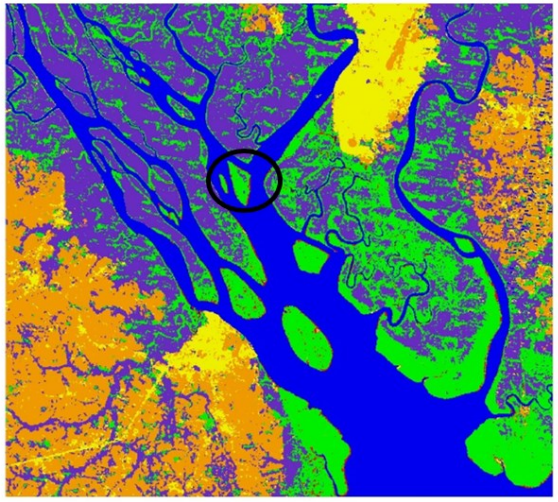

Radial Support Vector Machine

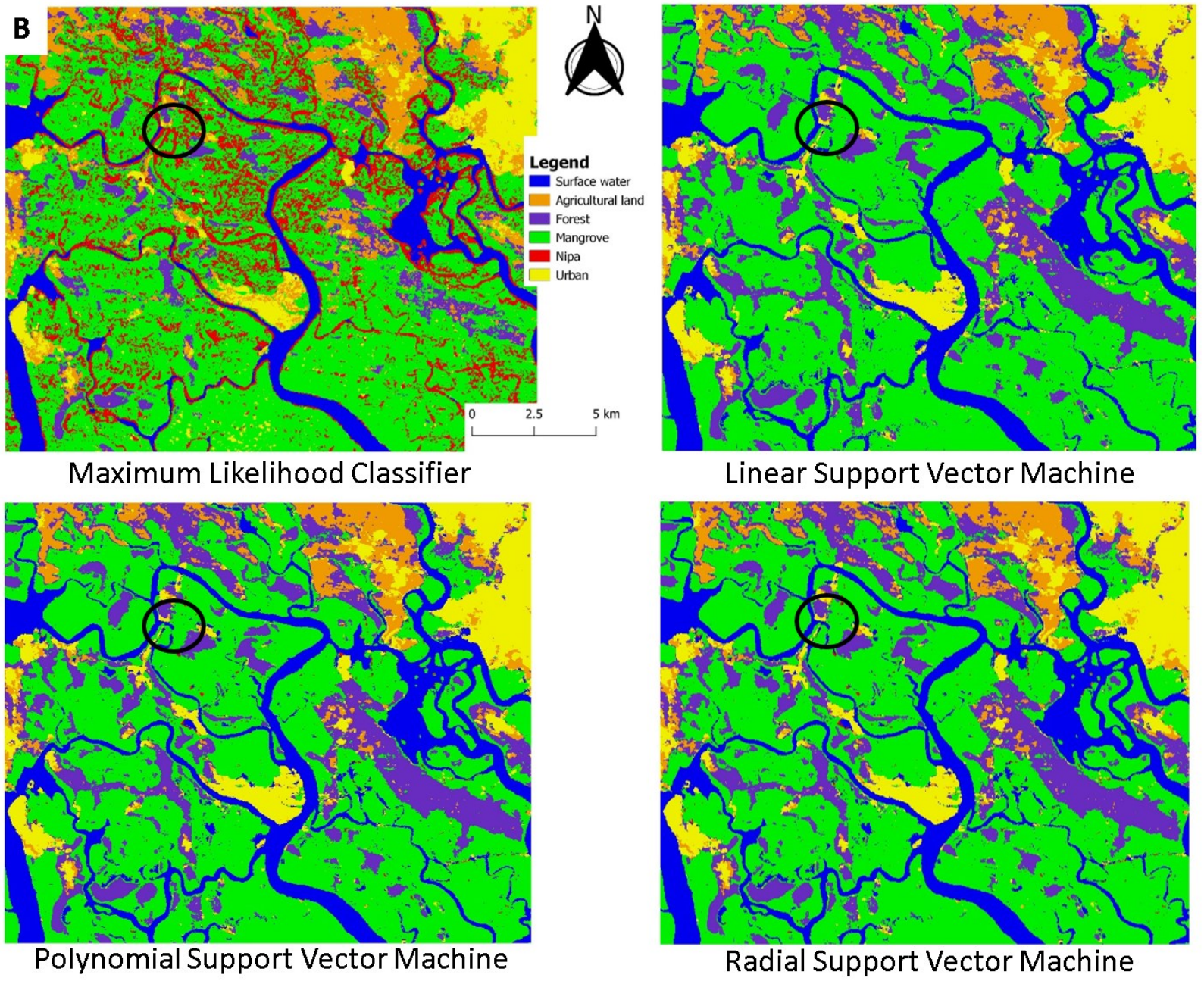
B
N
Legend
Surface water
Agricultural land
Forest
Mangrove
Nipa
Urban
0
2.5
5 km
Maximum Likelihood Classifier
Linear Support Vector Machine
Polynomial Support Vector Machine
Radial Support Vector Machine

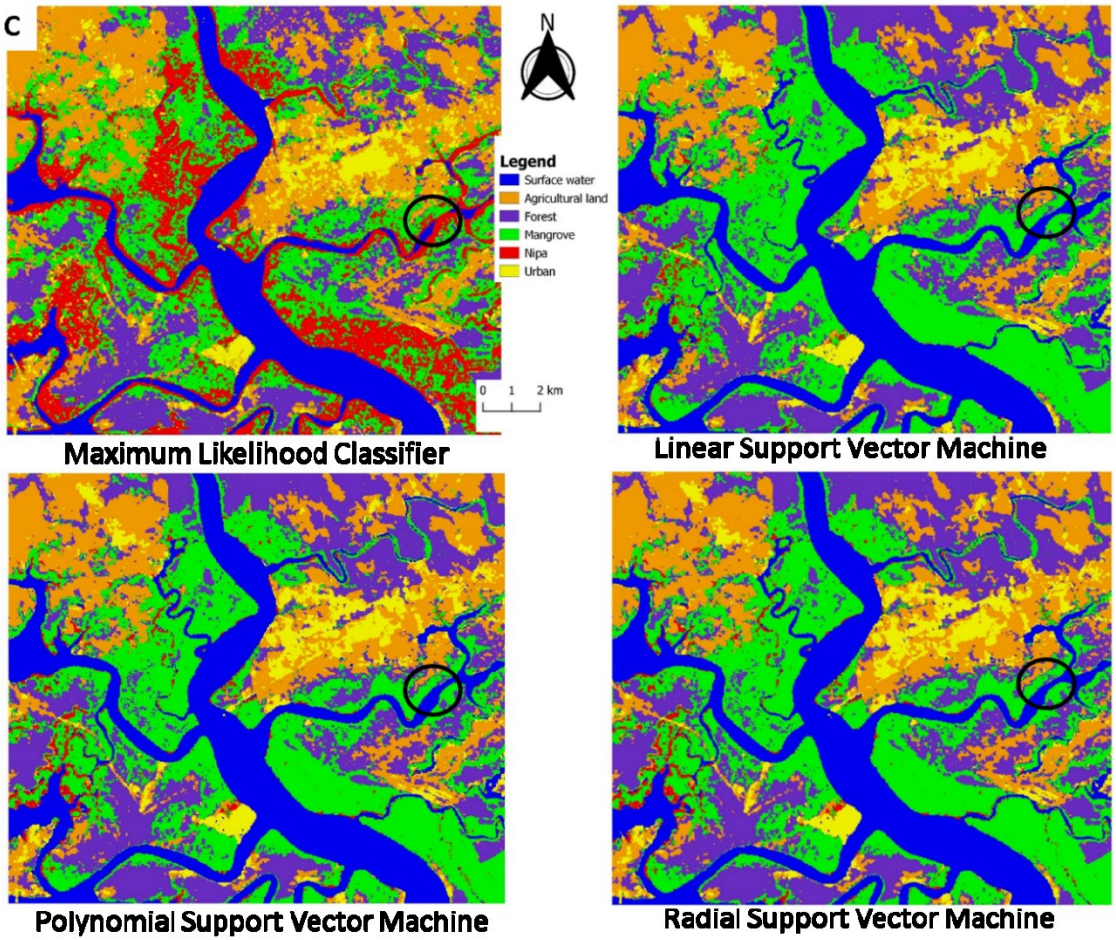

Figure 4.5: Detailed analysis of the thematic maps produced by the different classifiers (Maximum Likelihood, Support Vector machine: Linear, Polynomial and Radial Basis Function kernel types) in three regions of the Niger Delta: ***A)*** *Calabar Estuary,* ***B)*** *Oproama Community and* ***C)*** *Imo River Estuary. Note that circles indicate some problematic areas for class identification.*

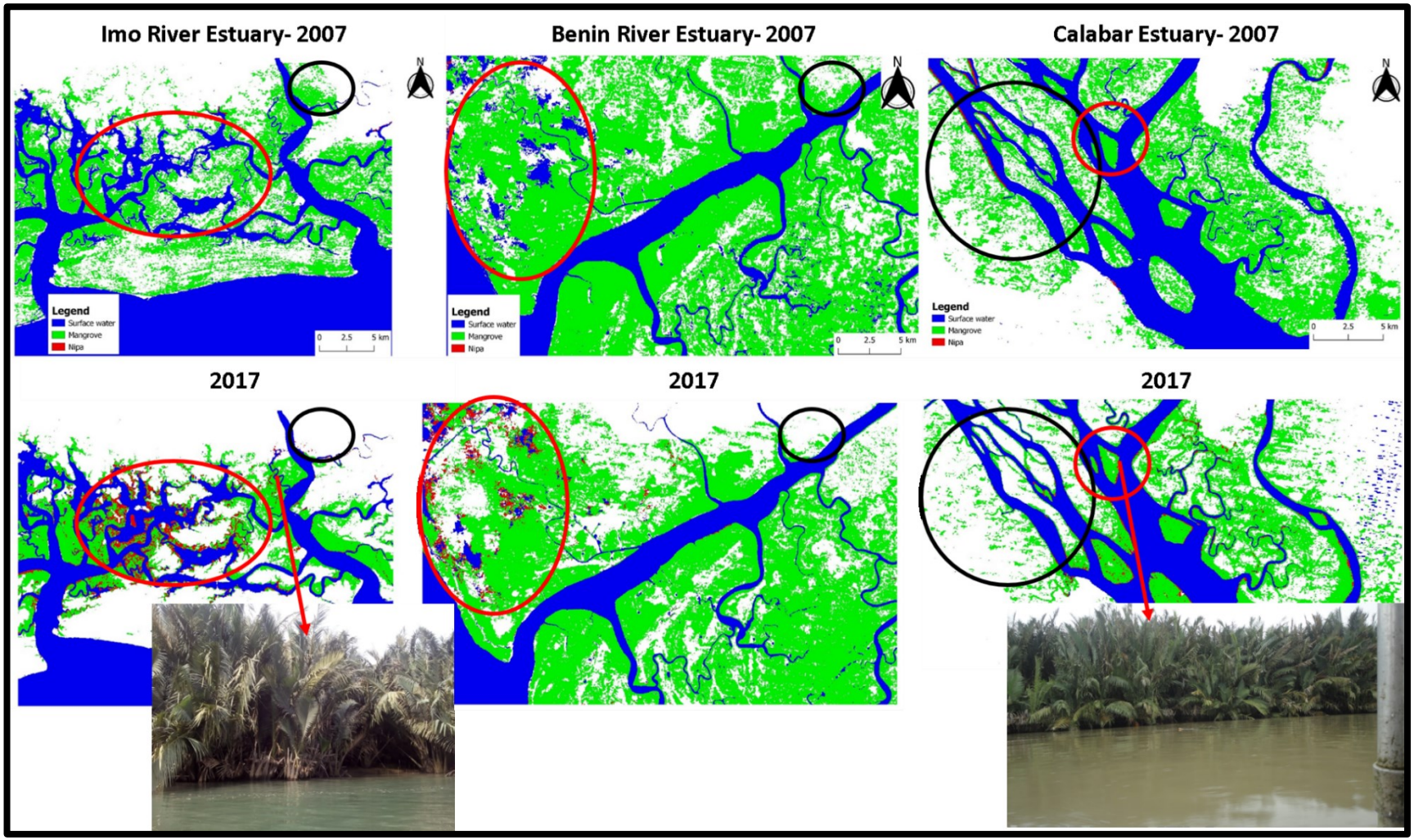

Figure 4.6: Mangrove loss and nipa colonisation in some regions of three regions of the Niger Delta. Black circles represent mangrove loss while red circles represent nipa colonisation. Inset pictures of study sites during GCP selection.

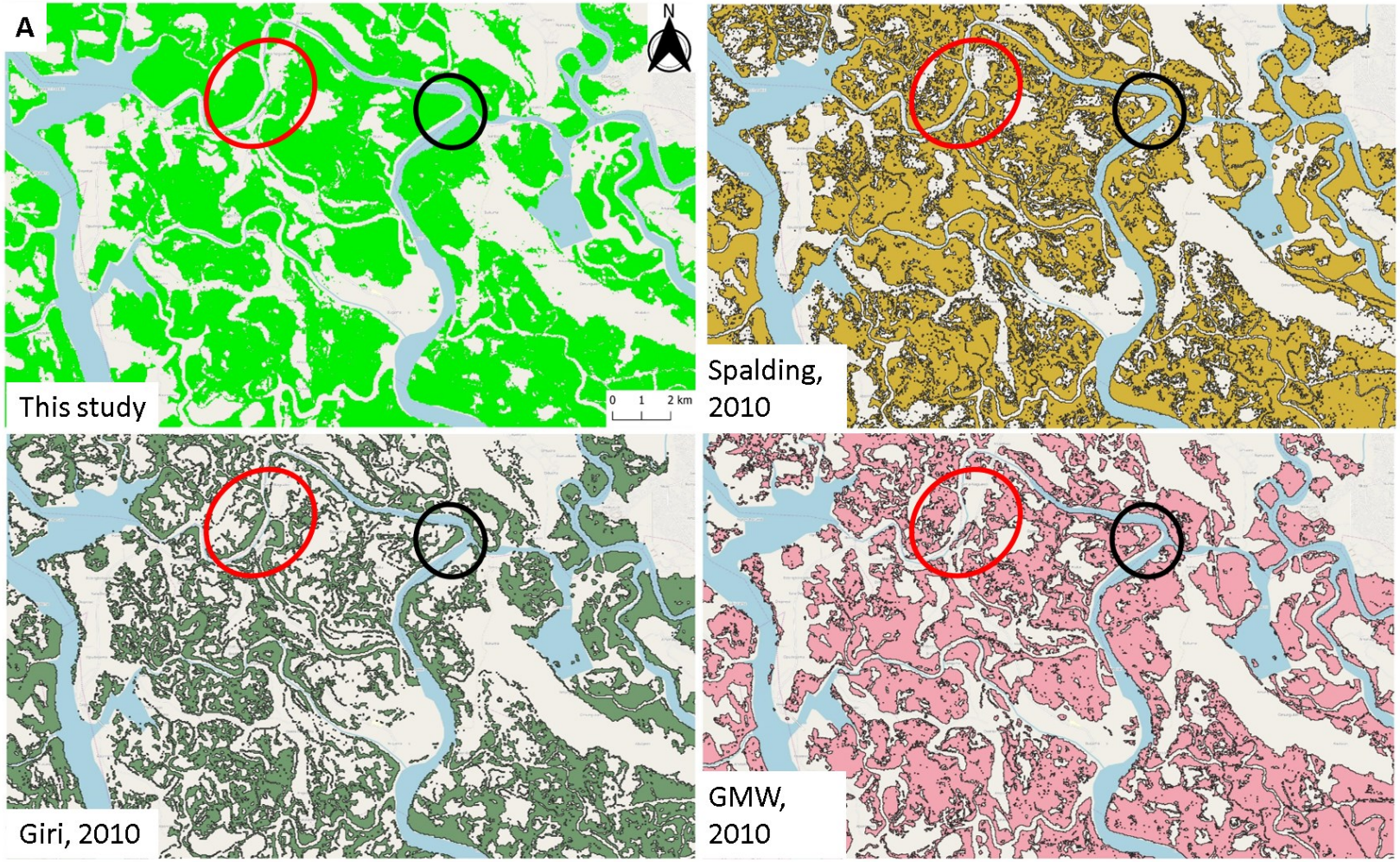
A
N
This study
0 1 2 km
Spalding, 2010
Giri, 2010
GMW, 2010

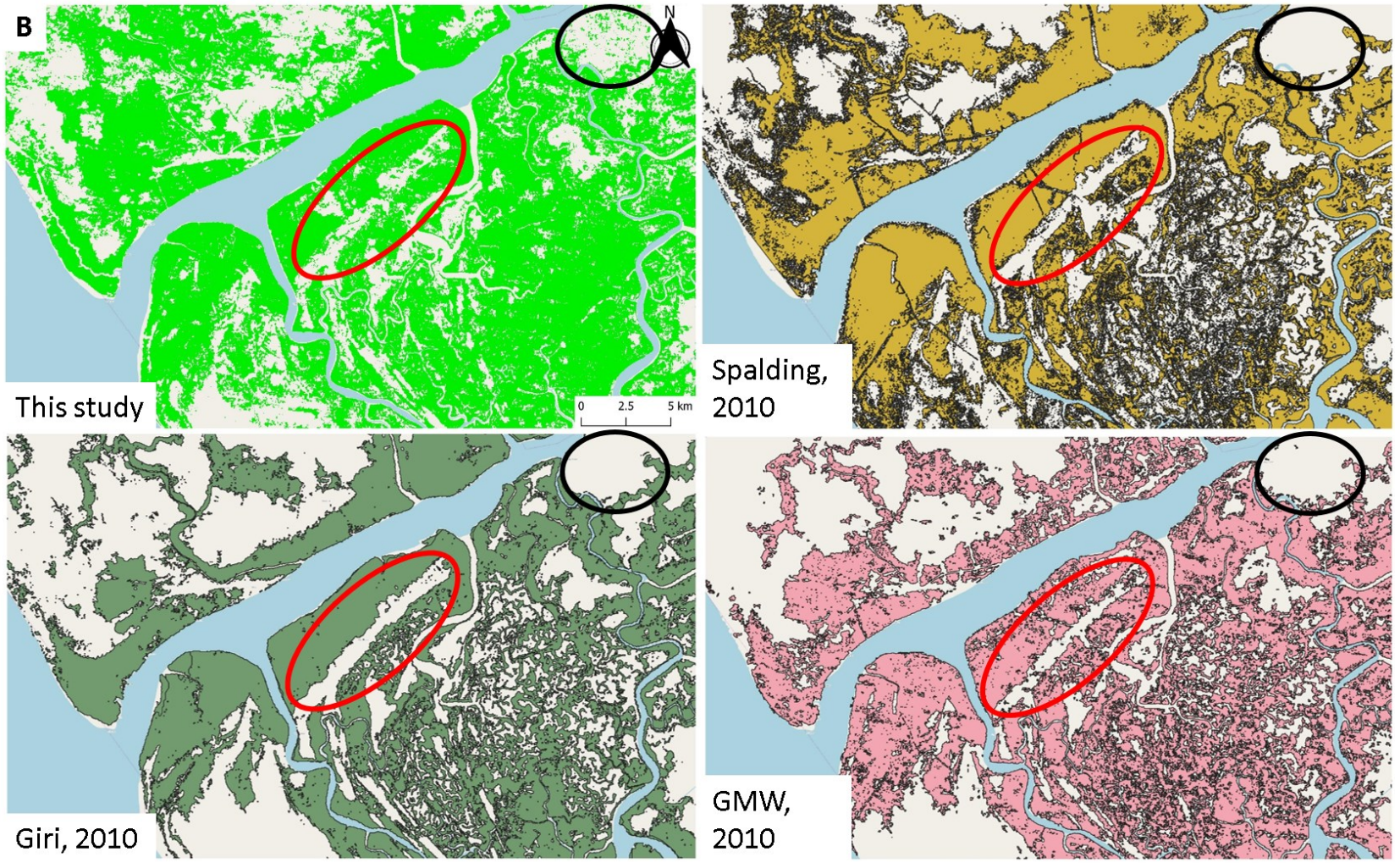
B
N
0 2.5 5 km
This study
Spalding, 2010
Giri, 2010
GMW, 2010

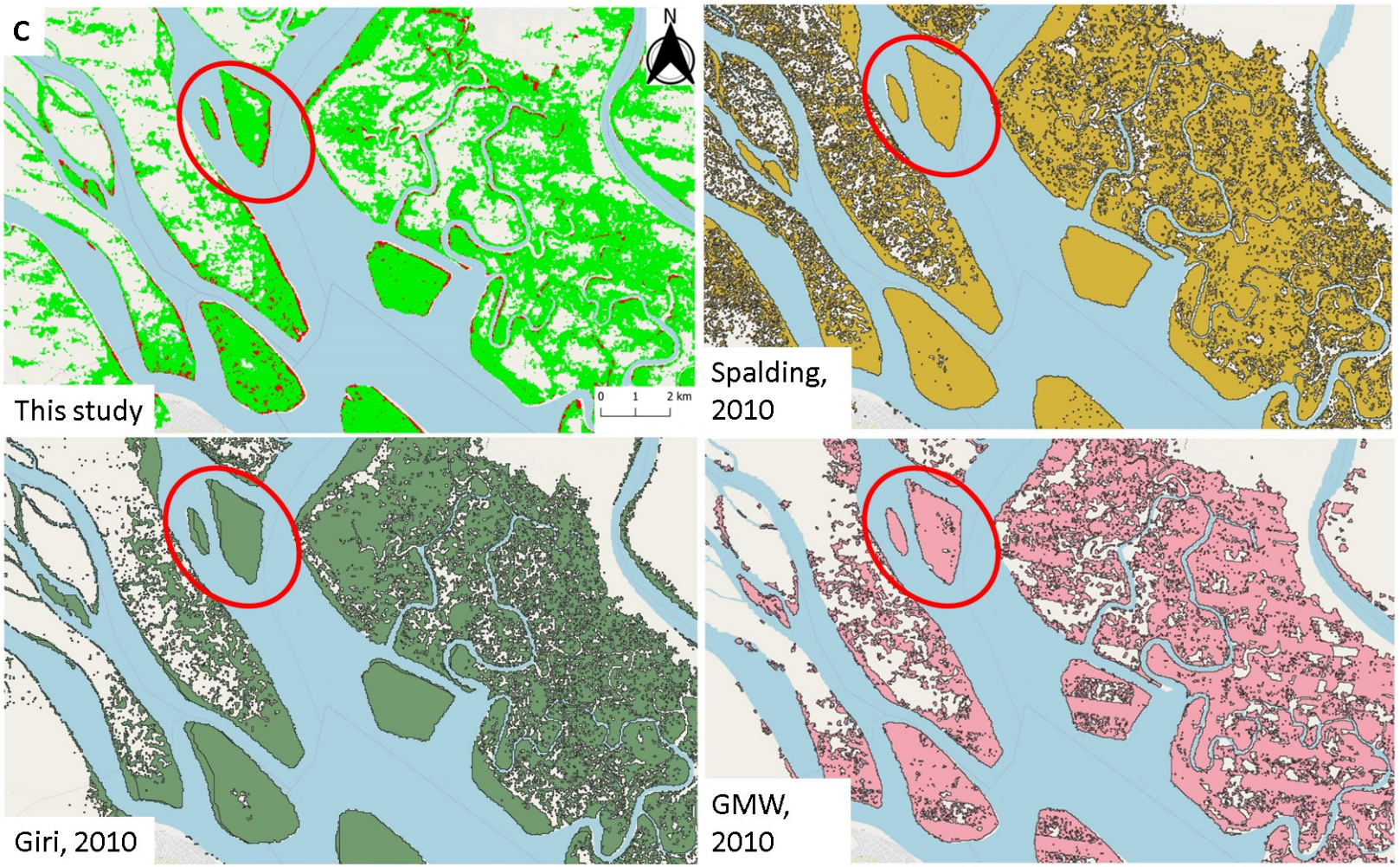

Figure 4.7: Comparison of different mangrove maps with red circles showing similarities and black circles showing underestimation. ***A)*** *Opraoma creek;* ***B)*** *Benin river estuary; and* ***C)*** *Calabar estuary showing nipa cover on Alligator Island compared with global maps.*

4.4 Discussion

I produced the first LC classification of the Niger Delta based on comprehensive ground data. I used both radar and optical imagery to produce the most accurate possible result (Joshi *et al.*, 2016) and compared the accuracy of different types of classification algorithms in effectively classifying these LC classes. The results of this analysis show that the Niger Delta has nearly a million hectares of mangroves, itself more than any other country in Africa (Hamilton and Casey, 2016), and previous global studies may have underestimated mangrove forests in Nigeria. However, I also found rapid changes are occurring, with a decrease in mangrove area and increase in the invasive nipa palm from 2007 to 2017.

4.4.1 Comparison of Classification Performance

The classification results showed the SVM has a better ability to accurately classify LC in this region using these datasets. This is not surprising, as the SVM classifier has been known to outperform MLC (Kavzoglu and Colkesen, 2009) in other areas because it allows a more complex separation plane between classes (Huang *et al.*, 2002). SVM creates a multi-dimensional plane which allows for a separation boundary to be established amongst classes (Nanda *et al.*, 2018). This optimum boundary can also be referred to as the Optimum Separation Hyperplane (OSH), and the training samples at the class distribution edge can be referred to as the support vectors (Ajay *et al.*, 2004; Szuster, Chen, and Borger, 2011).Huang (2002) reported that SVM had a more stable overall accuracy over MLC, Neural Network Classifiers (NNC) and Decision Tree Classifiers (DTC). I observed similar trend where MLC had the lower classification accuracy overall and for the individual classes (**Table 4.2**). SVM has been effectively used to classify mangrove forests (Chance *et al.*, 2016) and invasive species(Wang, 2008).

The urban area and water classes had uniformly high accuracy. This easy detection could be due to spectral nature of the classes (quite different to the vegetation classes of the rest of

the images), and the inclusion of DEM which takes into account the height of these classes above sea level. I found the lowest accuracy was the nipa palm which again is not surprising. Nipa palm is spectrally quite similar to forest and mangrove, but further occurs as a thin fringes along mangrove forests and hence its spectral qualities are mixed with those of mangroves (**Figure 4.4**). Field surveys showed mature mixed stands of mangrove and nipa, causing even more difficulties for the classifier. As there is no clear hard border between nipa and mangroves, trying to produce a binary classification into two classes will always cause errors. Secondly, the fringe nature of nipa palm created a large percentage of confusion with surface water. This confusion is as a result of the tidal nature of coastal vegetation which can interfere with both optical and radar satellite data. In order to improve my classification accuracy, I applied texture measures on my radar and optical data, theorising that the uniform height and composition of dense nipa stands compared to mangrove forests would have smoother textural characteristics than mangroves. This did improve the classification accuracy, but significant errors still remain.

A further issue peculiar to coastal regions is the tide: changing water levels can cause misclassification of nipa, mangrove and surface waters as the water level differs at the time of remote sensing data acquisition. Ideally all imagery would have been collected at a particular point in the tide cycle (e.g. low tide), but the lack of data (both radar and cloud-free optical) made this selection impossible: I had to use what was available.

4.4.2 Current Mangrove and Nipa Palm Extent

Mangrove and nipa area from this study are comparable to past studies. My estimates of mangroves area in the Niger Delta (794 561 ha) is ~ 14% higher than those reported by Bunting *et al.*, (2018). The relatively large variation in reports of mangrove area regionally and globally are a result of the methodology used in land cover classification (**Table 4.6**). The various reports of mangrove area regionally and globally will naturally contain errors in this

area as they are based on global algorithms and ground data. I believe the differences in area is particularly caused by the landward extent of mangrove forests from the coast, which is high in Nigeria, possibly higher than average: this is an important threshold in mangrove classification that varies regionally. I therefore conclude that mangrove area in Nigeria (and also the rate of Nigeria's mangrove area loss) has been underestimated by global datasets.

The pattern of mangrove extent in the Niger Delta was encouragingly mirrored by the global mangrove maps (**Figure 4.7**). I observed that more than 90% of the mangrove area lie within the core Niger Delta states of Delta, Bayelsa and Rivers states. This coverage was also reported by Fatoyinbo and Simard, (2013) reporting about 80 % of mangroves lie within the Niger Delta swamps. The ability of regional maps to estimate the presence of mangrove patches could also be a reason of differences in area. The utilisation of > 500 GCPs during my study aided in the identification of mangrove patches which may have been undetected due to generalization. Secondly, the landward extent of mangrove forests is an important threshold in mangrove classification as they vary regionally; GCPs are likely important in fixing this boundary.

4.4.3 Change Detection of Mangrove and Nipa

Urbanisation, oil pollution and unsustainable exploitation of wood products are a major cause of mangrove deforestation in Nigeria. I recorded a 12% loss of mangrove and tropical forests over the decade which could have been as a result of population dependent factors such as pollution, urbanization, agricultural expansion and nipa palm invasion. This conversion rate shows the influence of population growth on forest resources in the Niger Delta, with pressure on land areas and food resources increasing. The Niger Delta region had a population density of 290 people km^{-2} in 2005 but this is projected to almost double with estimated population of about 25 million in 2020 (NDDC, 2006). Hence, there will be increasing the demand for available land for urbanisation and cultivation. The increasing

urbanisation in the Delta could have possible effects on mangrove productivity. The replacement of mangrove regions in the Niger Delta could also be as a result of hydrographic modifications in the Niger delta due to urbanisation. This cuts off sea water supply to the regions and hence, cuts of the estuarine properties in which mangrove forests thrive.

I reported a 10-fold increase in nipa palm from 1 441 ha in 2007 to 11 444 ha in 2017. Nipa proliferation was greater in mangrove cleared areas. The significant increase in nipa palm was majorly as a result of mangrove loss; ~ 50% of the nipa palm area in my analysis was from the loss of mangrove cover in the region especially in Akwa Ibom state. This non-native invasive species colonise structurally matured native species through disturbance or a pattern of penetrating these stands (**Figure 4.6**).

4.4.4 Caveats and Limitations

I encountered two major problems in my land cover classification. Cloud cover is a limitation in using Landsat imagery for land cover analysis. Cloudiness had an effect on the clarity of optical data which is visible in my classification results over the Niger Delta (**Figure 4.8**), with scan lines from the Landsat equipment movement affecting some of my regions during my classification (Bunting *et al.*, 2018). Over the mangrove forests estimated in both years, there was no cloud influence in 2007 and 1.8% in 2017. Future regional classification of mangrove forests can make use of air-borne instruments on air planes while nipa palm differentiation can make use of drones. These instruments will be able to account for the optical characteristics of coastal vegetation which is an important criteria for accuracy.

I also encountered the problem of creating training classes for nipa palm classification, because nipa palm occurs in a strip along mangrove fringes which only go some metres inland. However, the fine resolution of the sensors (30 m) assisted as this could account for a larger coverage especially in areas of heavy colonisation. Future research can take into account finer scale remote sensing products.

My results also show low accuracy in classifying nipa palm evident from the low Producer's and User's accuracies (**Table 4.2**). Care should be taken when interpreting these results.

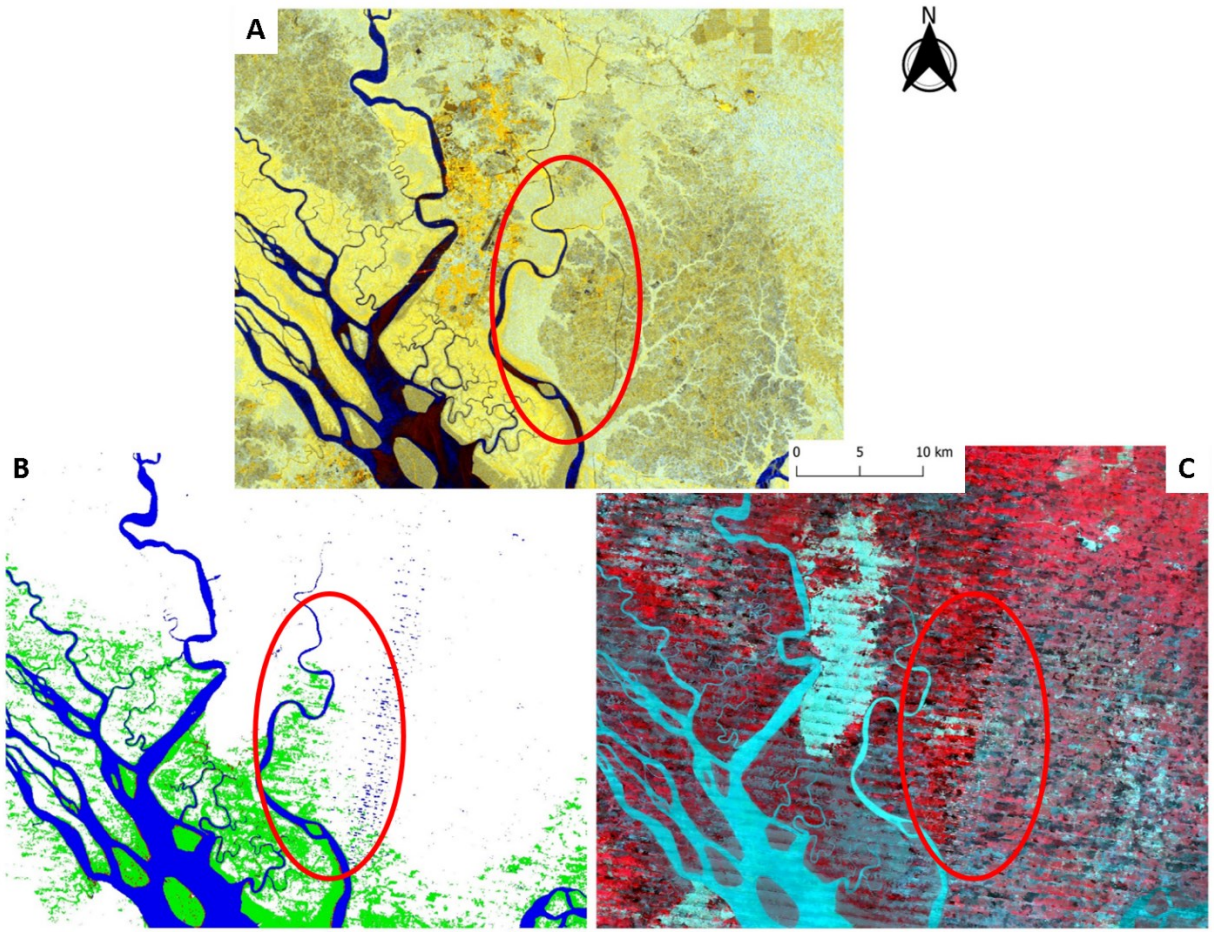

Figure 4.8: Cloud cover limitation of Optical data over Kwa Ibo river south eastern Nigeria. ***A)*** *ALOS PALSAR radar scene* ***B)*** *Classification imagery* ***C)*** *Infrared scene.*

4.5 Conclusion

Combination of optical and radar sensors with inclusion of texture measures which can account for both canopy and woody structure variation can better distinguish different forest types. Difficulty in cloud cover in optical data and misclassification of nipa fringes can be remedied by the use of finer scale remote sensing products or local optical data. However, a classification map is only as good as the training data, hence, more accurate training region of interests will improve the map output for effective management planning. I also discovered more evidence of the vast mangrove area in Nigeria. The results have shown opportunities for conservation of mangrove forests in the Niger Delta. However, the effect of urbanisation, industrialization and wood exploitation are rendering mangrove forests vulnerable. I observed a gradual reduction in mangrove area and a rapid increase in nipa palm colonisation in the Niger Delta. Nipa palm in the Niger Delta is a non-resourceful invasive species which if not checked will eradicate the valuable mangroves. Improved mapping precision can target areas with high incidence of logging, population growth and economic activity in order to generate a mangrove vulnerability map in the Niger Delta. This can be a pioneer path to restoring mangrove forests in Nigeria, Africa and globally.

4.6 References

Ajay, M., Foody, G. M., & Mathur, A. (2004). Land Cover Classification by Support Vector Machine : Towards Efficient Training. *Geoscience and Remote Sensing Symposium, 2004.IGARSS '04.Proceedings.2004 IEEE International*, *00*(C), 742–744.

Akanni, A., Onwuteaka, J., Uwagbae, M., Mulwa, R., & Elegbede, I. O. (2017). *The Values of Mangrove Ecosystem Services in the Niger Delta Region of Nigeria*. *The Political Ecology of Oil and Gas Activities in the Nigerian Aquatic Ecosystem* (Vol. 1980). Elsevier Inc. https://doi.org/10.1016/B978-0-12-809399-3.00025-2

Biswas, S. R., Choudhury, J. K., Nishat, A., & Rahman, M. M. (2007). Do invasive plants threaten the Sundarbans mangrove forest of Bangladesh? *Forest Ecology and Management*, *245*(1–3), 1–9. https://doi.org/10.1016/j.foreco.2007.02.011

Bradley, B. A. (2009). Accuracy assessment of mixed land cover using a GIS-designed sampling scheme. *International Journal of Remote Sensing*, *30*(13), 3515–3529. https://doi.org/10.1080/01431160802562263

Bunting, P., Rosenqvist, A., Lucas, R. M., Rebelo, L.-M., Hilarides, L., Thomas, N., … Finlayson, C. M. (2018). The Global Mangrove Watch-A New 2010 Global Baseline of Mangrove Extent, *10*, 1669. https://doi.org/10.3390/rs10101669

Chance, C. M., Coops, N. C., Plowright, A. A., Tooke, T. R., Christen, A., & Aven, N. (2016). Invasive Shrub Mapping in an Urban Environment from Hyperspectral and LiDAR-Derived Attributes. *Frontiers in Plant Science*, *07*(October), 1–19. https://doi.org/10.3389/fpls.2016.01528

Dahdouh-Guebas, F. (2011). World Atlas of Mangroves. *Human Ecology*. https://doi.org/10.1080/00207233.2012.671593

David, L. C. G., & Ballado, A. H. (2015). Mapping Mangrove Forest from LiDAR Data Using Object-Based Image Analysis and Support Vector Machine : The Case of Calatagan , Batangas. *8th IEEE International Conference Humanoid, Nanotechnology, Information Technology Communication and Control, Environment and Management (HNICEM) The Institute of Electrical and Electronics Engineers Inc. (IEEE) – Philippine Section 9-12 December 2015 Wat*, (December).

Deilmai, B. R., Ahmad, B. Bin, & Zabihi, H. (2014). Comparison of two Classification methods (MLC and SVM) to extract land use and land cover in Johor Malaysia. *IOP Conference Series: Earth and Environmental Science*, *20*(1). https://doi.org/10.1088/1755-1315/20/1/012052

Dewantoro, M. D. R., & Farda, N. M. (2012). ALOS PALSAR Image for Landcover Classification Using Pulse Coupled Neural Network (PCNN). *International Journal of Advanced Research in Computer and Engineering*, *1*(5), 289–294.

ESRI. (2011). ArcGIS Desktop: Release 10. Redlands, CA: Environmental Systems Research Institute.

Farid Hossain, M. (2015). Utilization of Mangrove Forest Plant: Nipa Palm (Nypa fruticans Wurmb.). *American Journal of Agriculture and Forestry*, *3*(4), 156. https://doi.org/10.11648/j.ajaf.20150304.16

Farr, T. G., Rosen, P. A., Caro, E., Crippen, R., Duren, R., Hensley, S., … Alsdorf, D. E. (2007). The shuttle radar topography mission. *Reviews of Geophysics*, *45*(2). https://doi.org/10.1029/2005RG000183

Fatoyinbo, T. E., & Simard, M. (2013). Height and biomass of mangroves in Africa from ICESat/GLAS and SRTM. *International Journal of Remote Sensing*, *34*(2), 668–681.

https://doi.org/10.1080/01431161.2012.712224

Fatoyinbo, T., & Simard, M. (2011). Remote Sensing of Mangrove Structure and Biomass. *Workshop on Tropical Wetland Ecosystems on Indonesia: Science Needs to Address Climate Change Adaption and Mitigation. Sanur Beach Hotel, Bali 11-14th April, 2011*, 5.

Giri, C., Ochieng, E., Tieszen, L. L., Zhu, Z., Singh, A., Loveland, T., … Duke, N. (2011). Status and distribution of mangrove forests of the world using earth observation satellite data. *Global Ecology and Biogeography*, *20*(1), 154–159. https://doi.org/10.1111/j.1466-8238.2010.00584.x

Google Earth. (2018). Google Earth. Retrieved from https://www.google.com/earth/download/ge/

Gorelick, N., Hancher, M., Dixon, M., Ilyushchenko, S., Thau, D., & Moore, R. (2017). Google Earth Engine: Planetary-scale geospatial analysis for everyone. *Remote Sensing of Environment.*

Green, E. P., Clark, C. D., Mumby, P. J., Edwards, a. J., & Ellis, a. C. (1998). Remote sensing techniques for mangrove mapping. *International Journal of Remote Sensing*, *19*(5), 935–956. https://doi.org/10.1080/014311698215801

Hamilton, S. E., & Casey, D. (2016). Creation of a high spatio-temporal resolution global database of continuous mangrove forest cover for the 21st century (CGMFC-21). *Global Ecology and Biogeography*, *25*(6), 729–738. https://doi.org/10.1111/geb.12449

Hansen, M. C., Potapov, P. V, Moore, R., Hancher, M., Turubanova, S. A., & Tyukavina, A. (2013). High-Resolution Global Maps of 21st-Century Forest Cover Change. *Science*,

342(6160), 850–853. https://doi.org/10.1126/science.1244693

Hawthorne, T. L., Elmore, V., Strong, A., Bennett-Martin, P., Finnie, J., Parkman, J., … Reed, J. (2015). Mapping non-native invasive species and accessibility in an urban forest: A case study of participatory mapping and citizen science in Atlanta, Georgia. *Applied Geography*, *56*, 187–198. https://doi.org/10.1016/j.apgeog.2014.10.005

Heumann, B. W. (2011). Satellite remote sensing of mangrove forests: Recent advances and future opportunities. *Progress in Physical Geography*, *35*(1), 87–108. https://doi.org/10.1177/0309133310385371

Heumann, Benjamin W. (2011). An object-based classification of mangroves using a hybrid decision tree-support vector machine approach. *Remote Sensing*, *3*(11), 2440–2460. https://doi.org/10.3390/rs3112440

Huang, C., Davis, L. S., & Townshend, J. R. G. (2002). An assessment of support vector machines for land cover classification. *International Journal of Remote Sensing*, *23*(4), 725–749. https://doi.org/10.1080/01431160110040323

Hughes, R. H., & Hughes, J. S. (1992). *A Directory of African Wetlands* (34th ed.). IUCN, Gland Switzerland and Cambridge, UK; UNEP, Nairobi, Kenya and WCMC, Cambridge, UK.

Isebor, C. E., Ajayi, T. O., & Anyanwu, A. (2003). *The Incidence of Nypa fruticans (WURMB) and it's Impact on Fisheries Production in the Niger Delta Mangrove Ecosystem*.

JAXA. (1997). ALOS-2 Overview.

Jean, C., Madanguit, G., Paul, J., Oñez, L., Tan, H. G., Villanueva, M. D., … Novero, A. U. (2017). Application of Support Vector Machine (SVM) and Quick Unbiased Efficient Statistical Tree (QUEST) Algorithms on Mangrove and Agricultural Resource Mapping

using LiDAR Data Sets. *International Journal of Applied Environmental Sciences ISSN*, *12*(10), 973–6077. Retrieved from http://www.ripublication.com

Joshi, N., Baumann, M., Ehammer, A., Fensholt, R., Grogan, K., Hostert, P., … Waske, B. (2016). A Review of the Application of Optical and Radar Remote Sensing Data Fusion to Land Use Mapping and Monitoring. *Proceedings, Annual Convention - Gas Processors Association*, *8*(70), 1–23. https://doi.org/10.3390/rs8010070

Karatzoglou, A., Meyer, D., & Hornik, K. (2006). Support Vector Algorithm in R. *Journal of Statistical Software*, *15*(9), 1–28.

Kavzoglu, T., & Colkesen, I. (2009). A kernel functions analysis for support vector machines for land cover classification. *International Journal of Applied Earth Observation and Geoinformation*, *11*(5), 352–359. https://doi.org/10.1016/j.jag.2009.06.002

Langeveld, J. W. A., & Delany, S. (2014). *The impact of oil exploration, extraction and transport on mangrove vegetation and carbon stocks in nigeria*. Amsterdam.

Lee, J. S. (1980). Digital image enhancement and noise filtering by use of local statistics. *IEEE Transactions on Pattern Analysis and Machine Intelligence*, *2*(2), 165–168. https://doi.org/10.1109/TPAMI.1980.4766994

Li, X., Yeh, A., Liu, K., & Wang, S. (2006). Inventory of mangrove wetlands in the Pearl River Estuary of China using remote sensing. *Journal of Geographical Sciences*, *16*(2), 155–164. https://doi.org/10.1007/s11442-006-0203-2

Lopes, A., Touzi, R., & Nezry, E. (1990). Adaptive Speckle Filters and Scene Heterogeneity. *IEEE Transactions on Geoscience and Remote Sensing*, *28*(6), 992–1000. https://doi.org/10.1109/36.62623

Lucas, R. M., Mitchell, A. L., Ake, R., Proisy, C., Melius, A. and, & Ticehurst, C. (2007). The

potential of L-band SAR for quantifying mangrove characteristics and change: case studies from the tropics. *Aquaric Conservation: Marine and Freshwater Ecosystems*, *19*, 671–675. https://doi.org/10.1002/aqc

Mmom, P. C., & Arokoyu, S. B. (2010). Mangrove forest depletion, biodiversity loss and traditional resources management practices in the Niger Delta, Nigeria. *Research Journal of Applied Sciences, Engineering and Technology*, *2*(1), 28–34.

Myint, S. W., Giri, C. P., Wang, L., Zhu, Z., & Gillette, S. C. (2008). Identifying Mangrove Species and Their Surrounding Land Use and Land Cover Classes Using an Object-Oriented Approach with a Lacunarity Spatial Measure. *GIScience & Remote Sensing*, *45*(2), 188–208. https://doi.org/10.2747/1548-1603.45.2.188

Nanda, M. A., Seminar, K. B., Nandika, D., & Maddu, A. (2018). A comparison study of kernel functions in the support vector machine and its application for termite detection. *Information (Switzerland)*, *9*(1). https://doi.org/10.3390/info9010005

NDDC. (2006). Niger Delta Region Land and People. In *Niger Delta Regional Development Masterplan* (pp. 48–99). Printing Development Company Limited, Port Harcourt, Rivers State. Retrieved from http://www.nddc.gov.ng/NDRMP Chapter 1.pdf

Ndidi, C., Okonkwo, P., Kumar, L., & Taylor, S. (2015). The Niger Delta wetland ecosystem : What threatens it and why should we protect it ? *African Journal of Environmental Science and Technology*, *9*(5), 451–463. https://doi.org/10.5897/AJEST2014.1841

Okugbo, O. T., Usunobun, U., Adegbegi, J. A., & Okiemien, C. O. (2012). A review of Nipa Palm as a renewable energy source in Nigeria. *Research Journal of Applied Sciences, Engineering and Technology*, *4*(15), 2367–2371.

PCI Geomatics. (2016). Radar Enhanced Lee Filter. Retrieved May 22, 2016, from

http://www.pcigeomatics.com/geomatica-help/concepts/orthoengine_c/chapter_825.html

QGIS Development Team. (2018). QGIS Geographic Information System. Retrieved from http://qgis.osgeo.org/

Richardson, D. M., Pysek, P., Rejmanek, M., Barbour, M. G., Panetta, F. D., West, J., & Mar, N. (2000). Naturalization and Invasion of Alien Plants : Concepts and Definitions Naturalization and invasion of alien plants : concepts and definitions, *6*(2), 93–107. https://doi.org/10.1046/j.1472-4642.2000.00083.x

Rosenqvist, A., Shimada, M., & Watanabe, M. (2004). ALOS PALSAR: Technical outline and mission concepts. *Proceedings of the International Symposium on Retrieval of Bio- and Geophysical Parameters from SAR Data for Land Applications*, *1*(7), 1–7. https://doi.org/10.1186/1471-2377-6-11

Schlitzer, R. (2018). Ocean Data View.

Secretariat of the Convention on Biologival Diversity. (2010). *Global Biodiversity Outlook 3. Journal of the American Podiatric Medical Association* (Vol. 104). https://doi.org/10.7547/0003-0538-104.3.A1

Shimada, M., Isoguchi, O., Tadono, T., & Isono, K. (2009). PALSAR radiometric and geometric calibration. *IEEE Transactions on Geoscience and Remote Sensing*, *47*(12), 3915–3932. https://doi.org/10.1109/TGRS.2009.2023909

Spalding, M., Kainuma, M., & Collins, L. (2010). Book review: World atlas of mangroves. *Wetlands*. https://doi.org/10.1007/s13157-011-0224-1

SRTM. (2015). The Shuttle Radar Topography Mission (SRTM) Collection User Guide.

Szuster, B. W., Chen, Q., & Borger, M. (2011). A comparison of classification techniques to support land cover and land use analysis in tropical coastal zones. *Applied Geography*, *31*(2), 525–532. https://doi.org/10.1016/j.apgeog.2010.11.007

Tsuji, K., Sebastian, L. S., Ghazalli, M. N. F., Ariffin, Z., Nordin, M. S., Khaidizar, M. I., & Dulloo, M. E. (2011). Biological and ethnobotanical characteristics of Nipa Palm (Nypa fructicans wurmb.): A review. *Sains Malaysiana*, *40*(12), 1407–1412.

Ukpong, I. E. (1994). Soil-vegetation interrelationships of mangrove swamps as revealed by multivariate analyses. *Geoderma*, *64*(1–2), 167–181. https://doi.org/10.1016/0016-7061(94)90096-5

Ukpong, I. E. (2000a). Ecological classification of Nigerian mangrove using soil nutrient gradient analysis. *Wetland Ecology and Management*, (8), 263–272.

Ukpong, I. E. (2000b). Gradient analysis in mangrove swamp forests. *Tropical Ecology*, *41*(1), 25–32.

Ukpong, I. E. (2015). Nypa Fruticans Invasion and the Integrity of Mangrove Ecosystem Functioning in the Marginal Estuaries of South Eastern Nigeria. In A. Gbadegesin, O. O. I. Orimoogunje, & O. A. Fashae (Eds.), *Frontiers in Environmental Research and Sustainable Environment in the 21st Century* (pp. 1–13). Ibadan University Press Publishing House University of Ibadan Ibadan, Nigeria. ©.

UNEP. (2011). *Environmental Assessment of Ogoniland*. https://doi.org/10.3370/lca.2.73

USGS. (2004). Shuttle Radar Topography Mission, 1 Arc Second. *Global Land Cover Facility, University of Maryland, College Park, Maryland, February 2000.*, *Scenes: n0*.

Wang, L. (2008). Invasive Species Spread Mapping Using Multi-Resolution Remote Sensing Data. *The International Archives of the Photogrammetry, Remote Sensing and Spatial*

Information Sciences, *37*, 135–142.

Yang, X. (2011). Parameterizing Support Vector Machines for Land Cover Classification. *Photogrammetric Engineering and Remote Sensing*, *77*(1). https://doi.org/10.14358/PERS.77.1.27

Chapter 5

Mapping Aboveground Biomass and Decadal Biomass Change of Mangrove Forests in the Niger Delta

C. J. Nwobi[a], M. Williams[a], E.T. A. Mitchard[a]

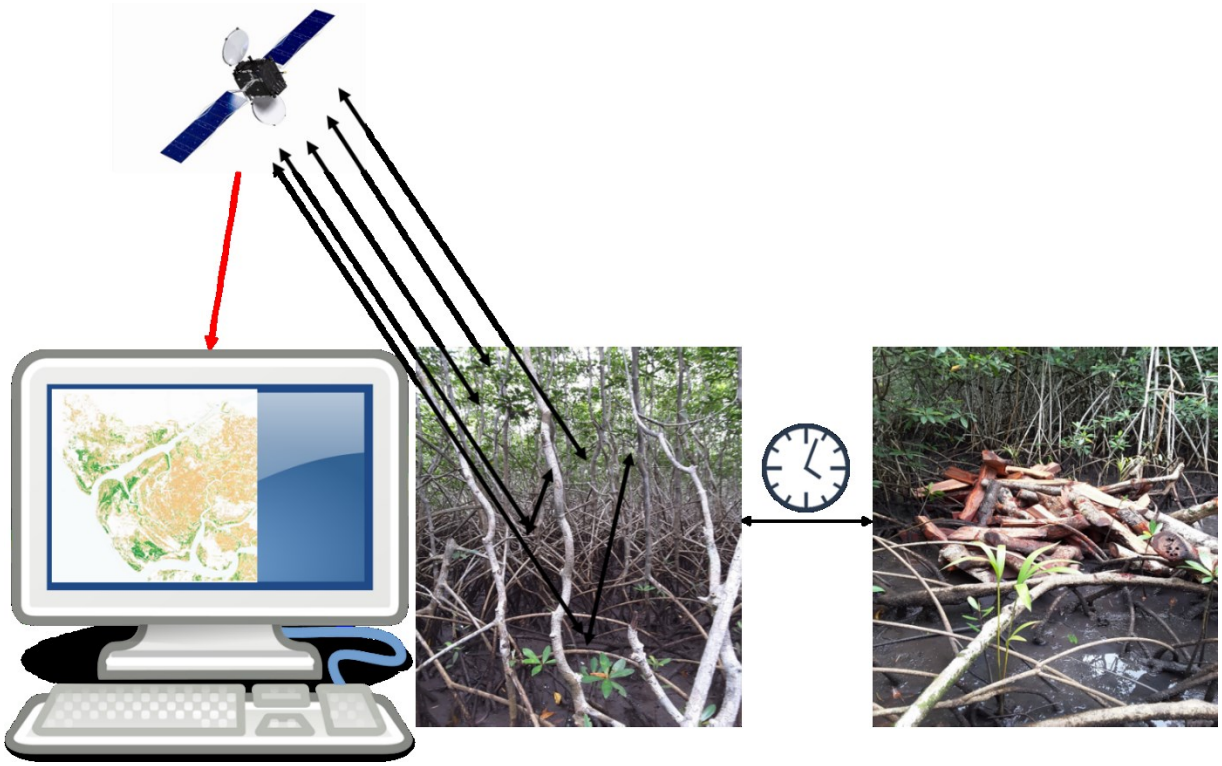

[a] *School of GeoSciences, University of Edinburgh, Edinburgh, EH9 3JN, UK*

Abstract

The conservation and sustainability of mangrove forests is a globally important topic due to their large stocks of biomass and other natural capital. Niger Delta mangroves are threatened from urbanisation, oil pollution and wood exploitation. While there are global mangrove biomass baselines, there is no local, high resolution biomass map for this region based on local field data. Here, I generate the first mangrove biomass map for the region, for 2007 and 2017. I determined aboveground biomass (AGB) using inventory data from 25 plots in the Delta, recording mean (range) AGB of 83.7 (11 - 241) Mg ha^{-1}. I established a relationship between field estimates of AGB and Advanced Land Observatory Satellite (ALOS) L-band radar backscatter. The strongest relationship between radar backscatter and field estimates of AGB was from the combination of HV/HH ratio and HV bands together (R^2= 0.62, $p < 0.001$). Using this relationship, I estimated a mean and total AGB of 90.5 Mg ha^{-1} and 82 X 10^6 Mg in 2007, and 83.4 Mg ha^{-1} and 65 X 10^6 Mg in 2017, representing a 21% reduction. Deforestation accounted for 69% of AGB loss and degradation accounted for 28%. These AGB values are considerably lower than those from other global tropical and mangrove biomass maps, even though the extent of mangrove mapped is larger. I conclude that radar sensors can provide effective monitoring of mangrove forest carbon stocks, deforestation, degradation and regrowth. Assessing carbon stocks of mangrove forests in the Niger Delta can create a baseline for regional conservation and regeneration plans. These plans can create opportunities for generating funding for conservation under international programs such as reducing emissions from deforestation and forest degradation (REDD+), and monitoring their success.

Keywords: *mangrove, aboveground biomass, radar backscatter, biomass map*.

5.1 Introduction

Mangrove ecosystems are intertidal regions at the land-sea, fresh-salt water interface; hence they have characteristics of both zones. Mangrove systems also have peculiar properties such as anaerobism, salinity fluctuation and tidal influence (Lugo and Medina, 2014). Due to the transitional nature of mangroves, they are breeding, nursery and migratory sites for various life forms including vertebrate and invertebrate marine life, mammals and birds (Alongi, 2011; Alongi, 2009; Kathiresan, 2006; Kathiresan and Bingham, 2001; Salem and Mercer, 2012). Beyond this though, the carbon storage of mangroves has made them increasingly seen as important for climate mitigation (Herri *et al.,* 2011; Karmaker, 2006). Mangroves can store similar amounts of woody carbon per hectare as tropical rainforests (Alongi, 2009), but with a much higher quantity of carbon in their sediments than could ever be stored in the soil of tropical forests (Donato *et al.*, 2011).

The superimposition of mangroves with the high population density of coastal communities has resulted in rapid and increasing deforestation (Karmaker, 2006). Mangrove clearance by local communities for fuelwood and fisheries are compounded by urbanisation in coastal regions. This results in increasing loss of the carbon stored in this ecosystem to the atmosphere and oceans. Mangrove carbon stocks potential has triggered the international community under the Paris Agreement to consider carbon stored in coastal ecosystems including mangroves as a mitigation strategy in future Intended Nationally Determined Contributions (INDCs) and ratified National Determined Contributions (NDCs) in coastal countries (Herr and Landis, 2016). Monitoring carbon emissions and gains from deforestation and restoration activities are essential for planning and implementing conservation and climate change avoidance measures (Lucas *et al.,* 2010; Lucas *et al.,* 2015; Mitchard *et al.,* 2012, 2009). Mapping mangrove forest biomass across space and time can help provide information on the progress of restoration programs and detect areas of high mangrove

deterioration, enabling conservation targeting and policy implementation (Karmaker, 2006). However, this mapping is sparse and existing data have limited reliability due to the difficulty and cost of accessing mangrove forests for validation as a result of their tidal nature and intricate root system (Hamdan, Khali Aziz, and Mohd Hasmadi, 2014). Political unrest in the Niger Delta further complicates safe field access. While remote sensing can overcome these problems, some ground data is required to calibrate satellite signals.

Remote sensing provides the means for retrieving and monitoring AGB of forest over a larger scale, in time and space (Ni *et al.,* 2013), and for generating continuous spatial estimates and consistent updates through time. The vast extent of forests requires methodologies that span the entire landscape. The most robust techniques require field estimates of aboveground biomass. These are then used to create algorithms that generate biomass maps from remote sensing data (Ni *et al.,* 2013). Remote sensing data splits broadly into two types: passive or active (Lucas *et al.,* 2015). Passive instruments use reflected solar radiation to monitor the observed region, while active sensors emit signals that interact with surface or sub-surface features (Fatoyinbo and Armstrong, 2010). Passive sensors are sensitive to the greenness of an ecosystem, while active sensors have the penetrative power to retrieve forest structure including the woody biomass. Optical sensors are very beneficial in monitoring productivity and the degree of canopy cover. However, optical data is often corrupted by cloud cover, which is always a problem in coastal tropical regions (Karmaker, 2006).

Synthetic aperture radar (SAR) sensors send a signal that is received after being scattered by surface structures. Radar can penetrate clouds which makes them suitable for detecting forest biophysical structures, i.e. stems and branches (Fatoyinbo and Armstrong, 2010). L-band SAR has been shown to be sensitive to growth stages and biophysical parameters of

forests (Lucas *et al.*, 2009). The backscatter signal is affected by the type of forest reflecting the signal. The environmental conditions of the forest also affect the return signal strength (Mermoz *et al.*, 2014). While most SAR data is collected at only a single wavelength, compared to many for optical data, SAR sensors can also collect data at different combinations of sending and receiving polarisations, which can offer different information on the target structures and environment. These polarisation are the geometric positioning of the wave emitted and received by the SAR sensor. For example, Horizontal-send Vertical-receive (HV) is less sensitive to soil moisture than Horizontal-send Horizontal-receive (HH) backscatter from L band SAR (Carreiras *et al.*, 2012; Mitchard *et al.*, 2009). There are two problems with using SAR for estimating AGB of forests (Quiñones and Hoekman, 2004). The radar signals will become less sensitive, and eventually saturated, as biomass increases (Richard Lucas *et al.*, 2010). This saturation varies for different bands and forest type. Several studies have recorded higher saturation values for L- band as 150 and 200 Mg ha^{-1} (Mitchard *et al.*, 2009) and P- band as 300 Mg ha^{-1} (Ho Tong Minh *et al.*, 2014). The second hindrance is the sensitivity of the backscatter to ground moisture (Hamdan *et al.,* 2014) which is of particular interest because mangrove forests are intertidal ecosystems with intermittent flooding. Radar signals could be intensified depending on the tidal state of the mangrove during radar collection.

The Niger Delta is located on the coast of Nigeria and is influenced by the Gulf of Guinea. The Delta is a hub of the economy in Nigeria because the oil industry of the country is largely based in the Delta. Further, the Delta is also a significant fisheries resource in the country. It is therefore known for its incidence of oil spills, urbanisation and deforestation rates with little information of the documentation of the effects of these activities on the carbon stock in these mangrove forests (Langeveld and Delany, 2014). The Niger Delta supports commercial fisheries and timber products (Adekola and Mitchell, 2011; Ndidi *et al.*, 2015).

Niger Delta mangroves are also associated with an alien invasive mangrove palm, *Nypa fruticans*. This mangrove palm was introduced for beautification and beach erosion control, but the poor management of the palm has resulted in the proliferation of this species. The spread of nipa palm is also aided by the unsustainable logging of mangrove species (**Chapter 3**). Studies have reported area extent of mangroves (James *et al.*, , 2007) but I reported a new mangrove area from 2017 earth observation data (**Chapter 4**). However, the only mangrove biomass map in Nigeria was reported by Fatoyinbo and Simard (2013) using a global mangrove height-biomass relationship produced by Saenger and Snedaker, (1993). Fatoyinbo and Simard, (2013) estimated mangrove height from 2008 GLA14 elevation products to estimate mean biomass of 111 Mg ha^{-1} and total biomass of 94.8 X 10^6 Mg in Nigeria. However, there is no report of mangrove biomass based on local mangrove forest plots and remote sensing data. There are, perhaps more critically, no existing maps or estimates of how the carbon stocks of these mangroves are changing with time.

The development of a spatiotemporal map of mangrove area and biomass can form a baseline for mangrove conservation and restoration in Nigeria (Carreiras *et al.,* 2012). This study aims to generate, for the first time, a locally calibrated biomass map of mangrove forests in the Niger Delta using ALOS PALSAR and ALOS-2 PALSAR-2 data to produce estimates of decadal changes in biomass stocks. I aimed to (1) establish an empirical relationship between AGB and SAR data in mangrove forests of the Niger Delta; (2) generate woody biomass map of mangrove forests in the Niger Delta and; (3) detect and report the change of mangrove biomass from 2007 to 2017. I hypothesise that plot AGB will have a significant relationship with HV backscatter based on reported relationship between mangrove biomass and radar backscatter.

5.2 Methodology

5.2.1 Study Strategy and Field Data Collection

I carried out field work (**Figure 5.1**) between October 2016 to January 2017; and June 2017 to September 2017 across the Niger Delta. I established plots in three locations, chosen largely because they avoided security risks and had local access granted by communities (**Figure 5.2**).

I established 25 square plots of 0.25 ha. I chose the plot size to account for the pixel size of remote sensing data which ranged from 25-m for ALOS PALSAR and 30-m for SRTM DEM. The plot sizes were also chosen to maximise sampling time within very dense mangrove forests – these were the largest size that was practical. The first plot within each transect was established 15 m from the tidal channel. I measured and enumerated mangrove stems ≥ 5cm dbh. I measured DBH at 1.3 m height above the ground, and if the tree branched below 1.3 m, individual stems were measured and counted as one tree (**Chapter 3**). AGB was also estimated using allometric equation developed by Komiyama *et al.,* (2005) (i).

$$\boldsymbol{W_{top}} = 0.251 \times \rho \times D^{2.46} \qquad \textbf{(i)}$$

Where **D**= diameter at breast height, $\mathbf{W_{top}}$ = Aboveground biomass, **ρ** = average wood density of the 3 indigenous *Rhizophora* species *R. racemosa*= 0.9330 g/cm3, *R. harrisonii*= 0.86 g/cm3, *R. mangle*= 0.9064 g/cm3 [Wood Density database Website]. I collected global positioning system (GPS) points of the field plots and closest settlement during the field survey using Garmin eTrex 20x. I also measured the distance between field plots and distance from the ocean, tidal channel and closest settlement from GPS locations using Google earth Pro (**2.3.2.1**).

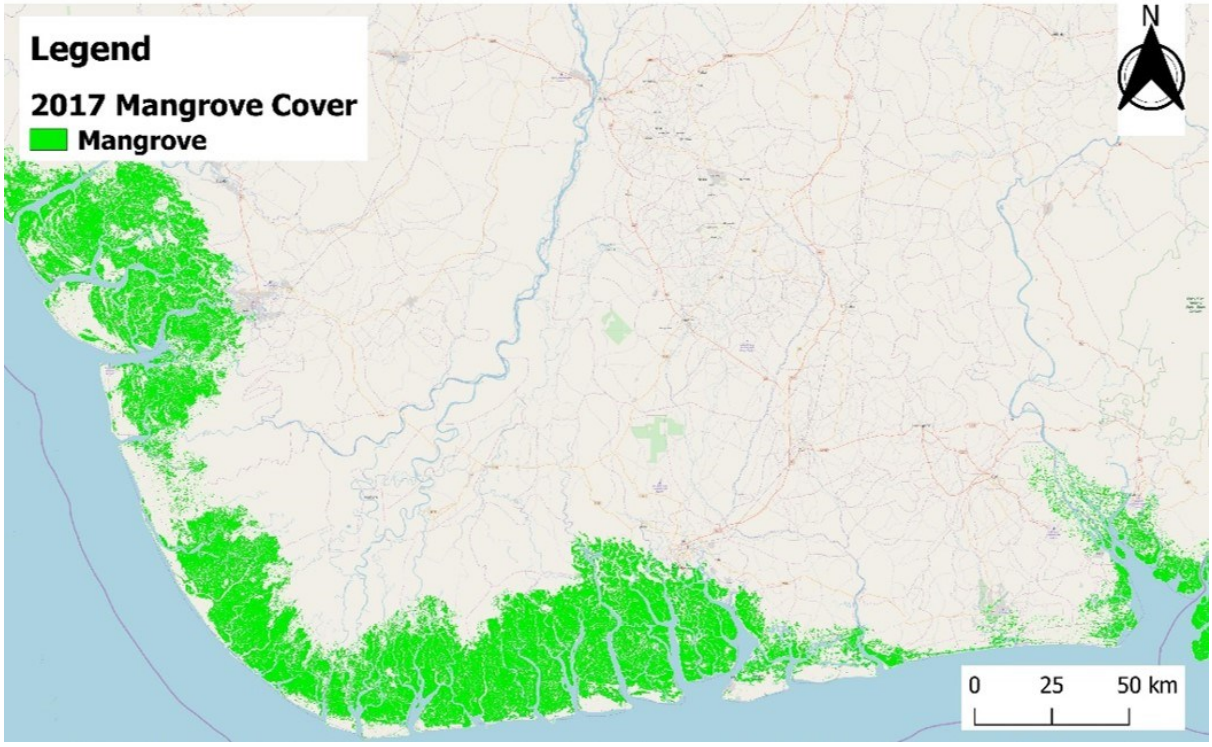

Figure 5.1: 2017 mangrove map of the Niger Delta from Chapter 4.

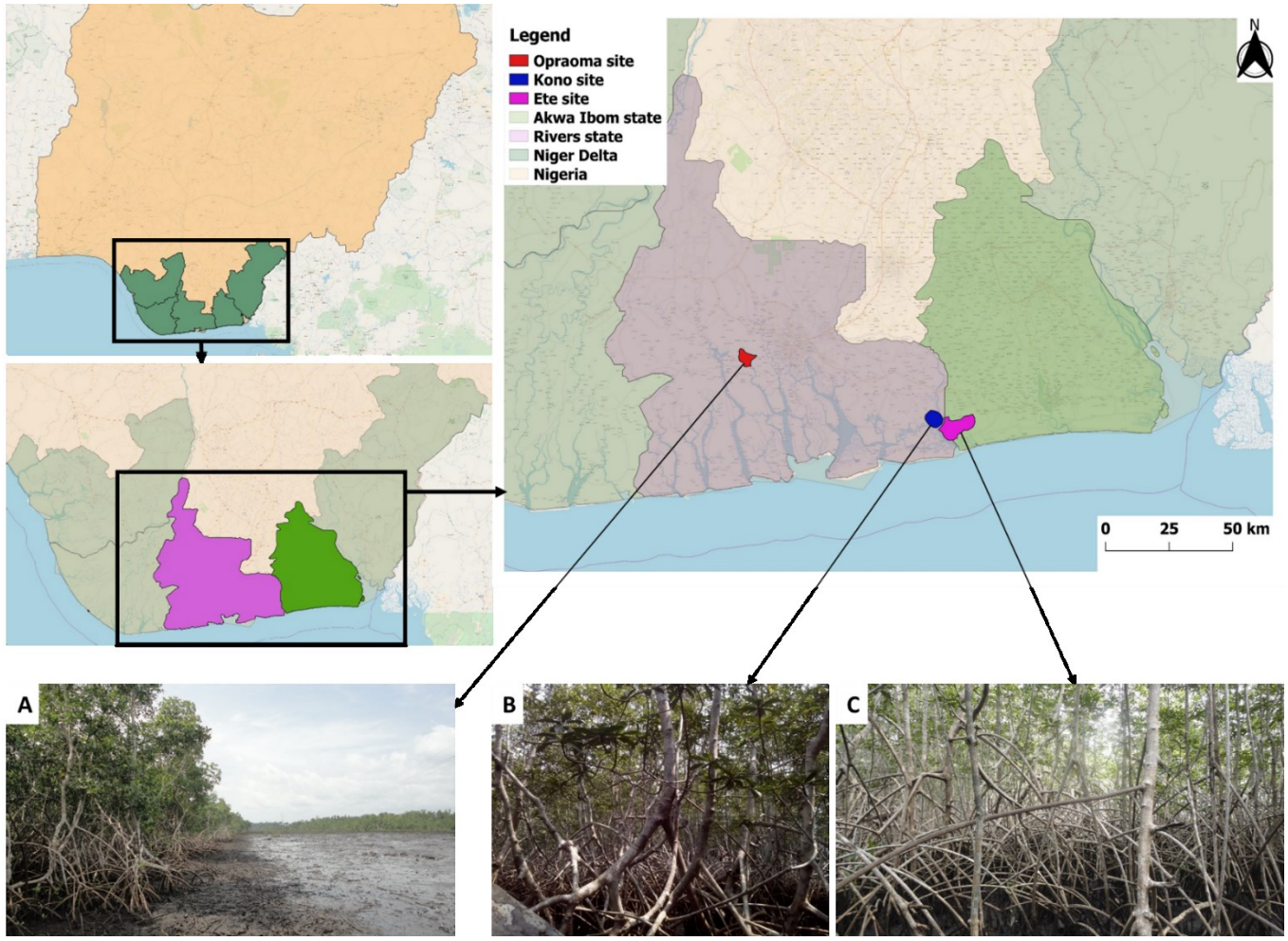

*Figure 5.2: Location of field sample site in coastal Nigeria and pictorial representation of plots. **A**- Oproama community (inland mangrove forests), **B**- Kono and **C**- Ete (fringing mangrove forests).*

5.2.2 Satellite Data Processing

I made use of the Advanced Land Observing Satellite 1 and 2 (ALOS, ALOS-2), launched by the Japan Aerospace Exploration Agency (JAXA). ALOS was launched in 2006, and ALOS-2 was launched in May 2014, with near-identical L-band SAR sensors, both with a lifetime of 5 years (JAXA, 2003). SAR data acquired globally from the ALOS PASAR sensor during 2007 and 2010 and ALOS PALSAR-2 during 2015 till present were obtained through the Earth Observation Research Centre, Japan Aerospace Exploration Agency website. These L-band SAR scene were acquired in Fine Beam Dual (FBD) polarisation mode with off-nadir angle 34.3° for ALOS PALSAR and off-nadir angle 7.3-58.8° for ALOS PALSAR-2 and pixel size of 0.8 arc sec (~ 25m). The DEM used in preparation of the 25m resolution product Global Mosaic were SRTM 3 (ALOS PALSAR) and SRTM 1 (ALOS PALSAR-2) both subset of the mission. The algorithm used in preparing the SAR backscattering coefficient layers was the JAXA Sigma-SAR processor, which involved calibration (radiometric and geometric), ortho-rectification, slope correction, co-registration, and intensity tuning of neighbouring strip data (Shimada and Ohtaki, 2010). Pre-processing steps were done using ENVI in the following steps (**Figure 5.3**). ALOS PALSAR data tiles from JAXA were taken at different times during the year and mosaicked.

5.2.2.1 Import, Mosaicking and Registration

Pre-processing SAR data is difficult – there are many steps involved in georectifying and terrain correcting the raw satellite data. In order to increase the usability of the data, JAXA have produced pre-processed mosaics where they have performed these steps in advance. I downloaded such ALOS PALSAR and ALOS-2 PALSAR-2 25m Mosaic files (HH and HV bands) from the Japan Aerospace Exploration Agency, Earth Observation Research Centre (http://www.eorc.jaxa.jp/ALOS/en/index.htm) for the years 2007 and 2017.

The individual data tiles (non-overlapping) were then mosaicked, using the georeferenced tool, to form a single image file of the Nigerian coastline in both bands and geo-referenced

with the projection Universal Transverse Mercator (UTM) Zone 31 North and World Geodetic System (WGS) 1984 datum. The image file of both bands was registered using the image to image ground control points with Landsat band from Hansen *et al.,* (2013) as the base image.

5.2.2.2 Calibration of ALOS PALSAR image Back Scattering

Calibration of ALOS PALSAR backscattering on the image through two stages. I first converted the digital number (DN) value on the original image to decibel (dB) (**equation ii**) based on the coefficients and equations from Shimada *et al.*, (2009). The average 2016 and 2017 mosaic were used to reduce the noise.

$$\text{Conversion of DN to } \sigma^{o} \text{ (dB)} = 10 \times (\log_{10}(DN^2)) - 83 \quad \text{..... (ii)}$$

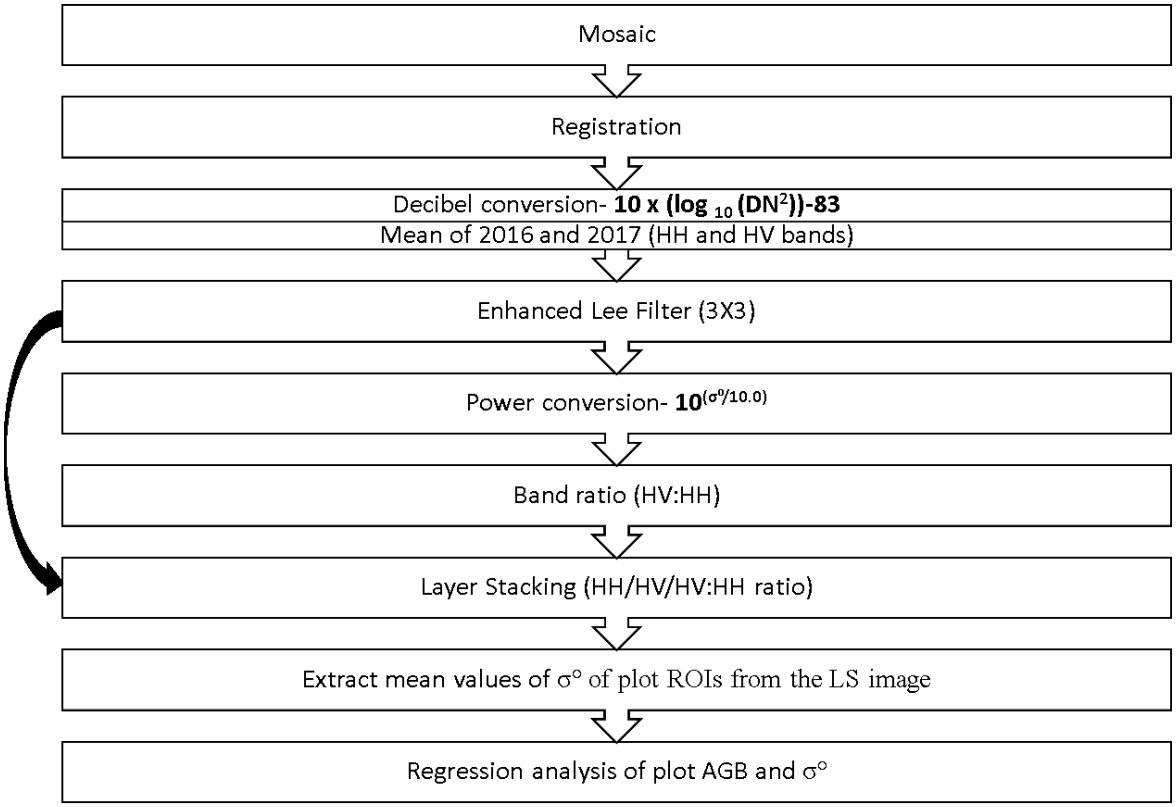

Figure 5.3: ALOS PALSAR processing steps.

5.2.2.3 Noise Reduction (speckle)

Speckle associated with SAR reduces the efficiency of class characterisation by affecting the radiometric and textural qualities, but filtering processes can reduce interference with the radar image and soften the image. However, these filtering techniques in some cases can reduce or eliminate the information contained in the image due to the sensitivity of the adaptive filter (Dewantoro and Farda, 2012; Lopes *et al.*, , 1990). In this case, the Enhanced Lee Filter, a type of adaptive filtering, was used to reduce the speckle.

Adaptive filtering creates a new pixel value from the standard deviation of the pixels within a grid surrounding each pixel. Hence, adaptive filtering replaces the original pixel value and preserves image sharpness and detail while suppressing noise (Harris Geospatial Solutions, 2016). The Enhanced Lee Filter determines the grey level for each pixel by computing the weighted sum of the centre pixel value, the mean value, and the variance calculated in a square kernel surrounding the pixel. The Enhanced Lee filter is used primarily to suppress speckle by smoothening image data but preserves the edges or sharp features and radiometric and textural information (PCI Geomatics, 2016). Filtering process in this study used a 3x3 window to minimise the loss of information in the image, which gives the best results based on published results (Lee, 1980; PCI Geomatics, 2016).

5.2.2.4 Conversion between sigma0 (log) and power domains

After the conversion of digital value to the backscatter coefficient (σ^o) and speckle reduction performed, the ratio of the bands were calculated by log transformation (P) (**equation iii**) without being distorted with the negative values of the coefficient. This was the make the arithmetic, not geometric ratios were used.

Conversion of σ^o to power (**P**) = $10^{(\sigma^o/10.0)}$ …….. (**iii**)

5.2.2.5 Layer Stacking

The Enhanced HH and HV bands were then layer stacked with the ratio band in order to generate an RGB composite image (Figure 5.4).

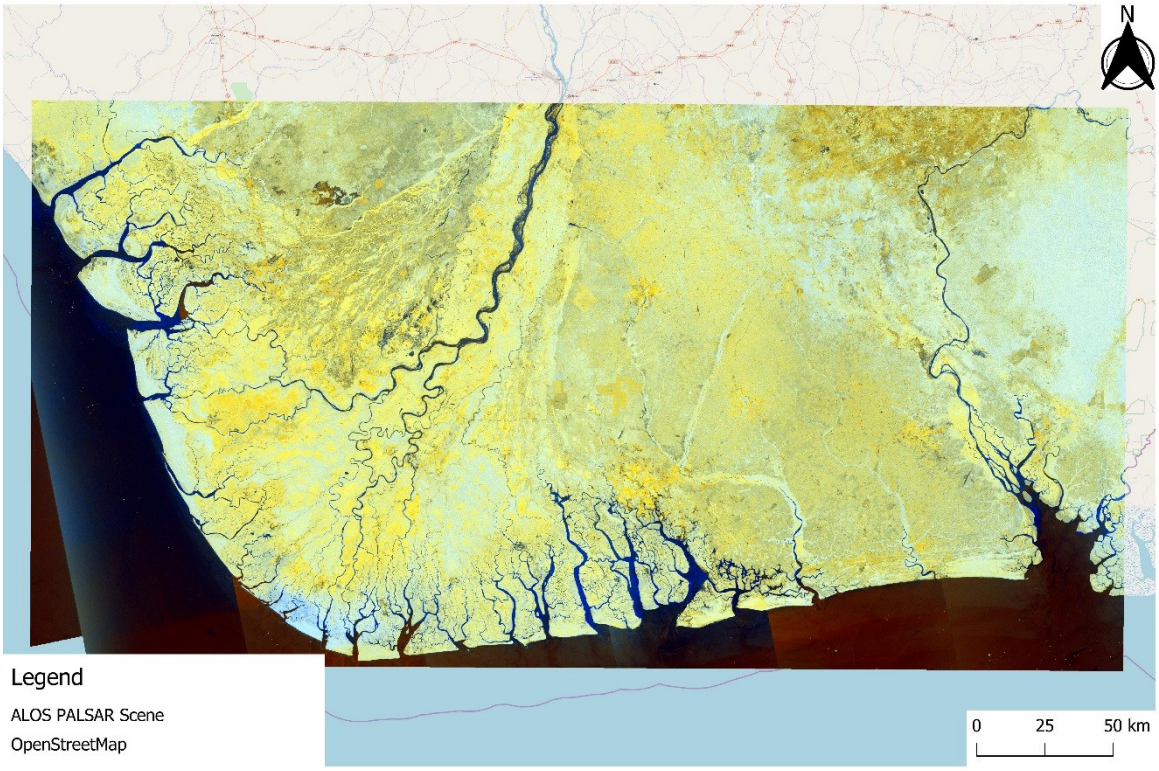

Figure 5.4: ALOS PALSAR (HH, HV, HV: HH composite) scene (2016-2017 mean) of the Niger Delta.

5.2.3 ALOS PALSAR Data Extraction of Field Plots.

The coordinates of the plots were collected with the Global Positioning System (GPS) and to reduce the noise in ALOS PALSAR values, the field plot areas were increased to a 60 by 60 m area (Carreiras *et al.,* 2012). The extra 5m buffer in each square edge were carefully selected to include only homogenous mangrove zones. I extracted the mean of the HH, HV and HV: HH bands backscatter values for each of the 25 field plots and used to establish a relationship with plot-based AGB.

5.2.4 Modelling and Relationship of field AGB and Satellite Data.

I then established the relationship between plot estimates of AGB and 2017 ALOS PALSAR backscatter using regression models in order to generate the best-fit equation to estimate AGB in the Niger Delta. I used the R statistical software version 2.15.0 (R Development Core Team, 2012) to carry out the analysis. I also derived the uncertainty of the regression model used in the AGB estimate.

5.2.5 AGB estimates and Difference.

I applied the best-fit equation to the SAR data to generate an AGB map of the Niger Delta. I then excluded non-mangrove areas from the ALOS PALSAR scene using the mangrove raster file derived from the land cover classification of the Niger Delta using ALOS PALSAR and Landsat images of the same region (**Chapter 4**). I extracted the mean and total AGB from the mangrove AGB map of the Niger Delta over both years (2007 and 2017). I also divided the study region into political zones in order to estimate regional AGB dynamics of the Delta. I divided the maps into high biomass (>100 Mg ha^{-1}), medium biomass (50-100 Mg ha^{-1}) and low biomass mangrove forests (< 50 Mg ha^{-1}) based on field data obtained in **Chapter 3**. These divisions were made in order to estimate how AGB change was affecting mangrove forests in the Niger Delta. The change in AGB between both years was estimated. Deforestation was classified as pixels with biomass loss > 80% from 2007 values while degradation was classified with biomass change between 20-80%. This was decided comparing the mean percentage difference between exploited and undisturbed plots in **Chapter 3** and studies by McNicol *et al.*, (2018) in southern African woodlands. Mangrove biomass gain was estimated from increase in biomass within each pixels. However, I excluded mangrove forests without biomass values in 2007 within these estimates in order to account for just increase in AGB and not re-vegetation. This excluded the estimation of

non-mangrove forest biomass change, including landward area expansion. I also limited biomass increase over the decade to 75 Mg ha^{-1} based on mean annual AGB growth in pure *Rhizophora* mangrove stands in Cameroun-7.35 Mg ha^{-1} yr^{-1} (Ajonina, 2008) and Mexico- 7.72 Mg ha^{-1} yr^{-1} (Day *et al.*, 1987). Another category was classified as minor changes representing biomass change between 20% loss and 20% gain, which are probably below the sensitivity of the method to differentiate from each other, or from no change.

5.3 Results

5.3.1 Summary of field AGB plots.

I estimated a mean plot AGB of 83.7 Mg ha^{-1}, with plots ranging in biomass from 11.1 to 241.2 Mg ha^{-1}. AGB for the study region was bimodal and skewed to the lower end of the mean (Table 5.1, Figure 3.5). Plots with the highest biomass (>150 Mg ha^{-1}) were found in the community protected site plots in Ete site, and Kono located close to the mouth of the Imo estuary. The lowest biomass (< 50 Mg ha^{-1}) was observed in the more inland creek (Oproama) sites where shrub mangroves were dominant and urbanisation actively taking place. The highest AGB (241 Mg ha^{-1}) in the study was observed in the undisturbed plot in Ete (E3A) where the mangroves were protected from logging activities. In contrast, the lowest AGB (11 Mg ha^{-1}) was found in the disturbed plot in Oproama (O1C) community where a power line was constructed to conduct electricity to the community. I observed significant difference in AGB amongst the three locations (Ete, Kono and Oproama) of the study area ($p < 0.001$) but Oproama alone showed significant lower AGB when compared to Kono and Ete locations ($p < 0.01$). Stem density had a strong positive correlation with AGB ($p = <0.00001$, Spearman's rho (r_s) = 0.88), thus the higher the stem density, the higher the AGB in the plots (3.3.2).

5.3.2 Regression models of radar backscatter.

Correlation analysis showed that plot level AGB were not significantly correlated with either the raw HH (Figure 5.5A) or HV data (Figure 5.5B) (though a weak relationship appeared visible), however the ratio of HV: HH showed a significant positive correlation (Figure 5.5C) with plot level AGB ($p = <0.00001$, Spearman's rho (r_s) = 0.76). This HV: HH ratio explained about 44% of the variance in AGB. However, log transformed AGB showed a stronger relationship with the HV: HH ratio band (R^2= 0.55; Table 5.2). The best relationship with plot AGB was from a combination of HV: HH ratio and the HV band (R^2= 0.62, Table 5.2).

In assessing the ability of these equations to map AGB, I calculated the Root Mean Squared Error (RMSE) and correlation analysis between the observed and predicted AGB. This had a value of 52 Mg ha^{-1} for the HV: HH ratio relationship alone (p= <0.000001, r_s = 0.76) and 50 Mg ha^{-1} for the combination of **HV:HH** and **HV** relationship (p= <0.000001, r_s = 0.78, **Figure 5.6**).

Table 5.1: Structural characteristics of the field plots and mean ALOS PALSAR back scatter coefficient.

Plot ID	Location	Aboveground Biomass (Mg ha^{-1})	Mean Stem dbh (cm)	Stem Density ha^{-1} (dbh ≥ 5cm)	Basal Area (m^2 ha^{-1})	HH backscatter mean	HV backscatter mean	HV HH ratio
O1C	Oproama	11.1	9	204	1.36	-9.21	-16.05	0.21
O2C	Oproama	14.2	8.5	299	1.78	-6.08	-13.28	0.19
O1B	Oproama	18.7	10.1	234	2.07	-8.44	-15.49	0.2
O1A	Oproama	19	10.4	218	2.06	-9.84	-16.92	0.2
O2B	Oproama	30.2	8.9	555	3.67	-7.53	-13.64	0.25
O2A	Oproama	33	9.3	516	3.82	-10.57	-17.01	0.23
O3A	Oproama	34.6	9.4	530	4	-8.63	-15.14	0.22
O4C	Oproama	39.3	9.6	559	4.45	-6.24	-12.98	0.21
O3B	Oproama	43.2	9.5	663	5.04	-5.88	-12.99	0.19
E1A	Ete	44.6	9.1	739	5.21	-7.26	-13.92	0.22
E2A	Ete	50.2	10.7	430	4.83	-6.26	-12.86	0.22
E1B	Ete	57.2	10.6	547	5.77	-6.97	-13.39	0.23
E2B	Ete	63.2	10.1	650	6.34	-6.49	-12.22	0.27
E1C	Ete	66.3	9.7	899	7.44	-6.62	-13.29	0.22
E4A	Ete	75.3	7.5	1988	9.58	-10.51	-16.27	0.27
O4B	Oproama	97.5	11.7	822	9.95	-7.78	-13.81	0.25
K1B	Kono	125.8	13.9	698	11.93	-9.05	-15.59	0.23
E4B	Ete	127.8	9	1938	14.35	-7.42	-13	0.28
E5B	Ete	128	9.1	2122	15.05	-8.49	-13.6	0.31
E3B	Ete	137.9	9.7	1571	14.16	-7.67	-13.11	0.29
E3C	Ete	152.2	10.9	1380	15.3	-7.33	-12.97	0.27
O4A	Oproama	157.6	12.2	1187	15.65	-10.51	-16.27	0.27
K1A	Kono	159.3	12.3	1089	15.24	-8.86	-14.03	0.3
E5A	Ete	166	10.6	1439	15.98	-7.67	-13.7	0.25
E3A	Ete	241.2	8.7	4037	27.24	-6.84	-13.07	0.24

Table 5.2: Fitted parameters for each backscatter-AGB model.

Explanatory Variable	a (intercept)	b (coefficients)	R^2	*P* value	*Root Mean Square Error (rmse)* ($Mg\ ha^{-1}$)
HH	4.13	0.00	2×10^{-6}	0.99	64
HV	6.85	0.19	0.10	0.11	62
HV:HH	-0.32	18.51	0.55	<0.0001	53
HV+ HV: HH	1.33	HV- 0.1 HV:HH- 17.59	0.58	<0.0001	53
(HV:HH):HV	14.74	HV:HH- 40.10 HV- 1.06 (HV:HH):HV- 4.13	0.62	<0.001	50

5.3.3 Application of regression equation and exclusion of non-mangrove areas.

I applied the best regression equation to the 2007 and 2017 ALOS PALSAR mosaic of the study region (**Figure 5.4**) and excluded non-mangrove regions using a mangrove ask developed in **Chapter 4**. I constrained AGB calculations to 200 Mg ha^{-1} in order to reduce over-estimating mangrove forest AGB in the region. This was done because of the low number of plots (n=25) used for the analysis, hence a way to reduced error due to overestimation of AGB in the region. Mean and total AGB was calculated from the AGB map generated for both years. I estimated a mean and total AGB of 83.4 Mg ha^{-1} and 65 X 10^6 Mg in 2017; 90.5 Mg ha^{-1} and AGB of 82 X 10^6 Mg in 2007.

5.3.4 Biomass map generation and change detection.

I generated a biomass map for the mangrove regions in 2007(**Figure 5.7A**) and 2017 (**Figure 5.7B**). I observed a similar trend from chapter 3 where model derived AGB of the field plots were negatively correlated to distance from sea (p-value < 0.05, r_s = -0.4) and positively correlated to distance from settlement (p-value < 0.05, r_s = 0.48). Although there was no significant relationship with distance from tidal ecotone (p-value > 0.05, r_s = -0.29), the

generated map showed a trend of higher biomass closer to the tidal channel and reduced inland (**Figure 5.8**).

I assessed a georeferenced disturbed region in Opraoma community in Rivers state where some hectares of mangrove were cleared in 2013 for power line construction (**Figure 5.9**). This area was analysed for change in biomass (**Table 5.3**). I observed a net change of loss of 86 tonnes of AGB from a 5 ha loss of mangrove area (**Figure 5.10**).

I also generated a change map of the AGB between the two periods (**Figure 5.7C**). Mean AGB of mangrove forests in the Niger Delta showed an 8% reduction and total AGB a 21% loss over 10 years. There was a net AGB change of -27 X 10^6 Mg over the decade with mangrove AGB gain of 7.6 X 10^6 Mg (2.2 ± 1.9 Mg ha^{-1} yr^{-1}, median ± SD) from 31% of the mangrove region and mangrove loss of 35 X 10^6 Mg from 60% of the mangrove region. Mangrove deforestation contributed to 69% (24 X 10^6 Mg; 9.3 ± 6 Mg ha^{-1} yr^{-1}) of AGB loss (**Figure 5.11**). Degradation made up 28% (10 X 10^6 Mg; 13.4 ± 3.8 Mg ha^{-1} yr^{-1}) of mangrove loss while the rest were minor changes. Biomass range 100-150 Mg ha^{-1} and 150-200 Mg ha^{-1} had a higher net loss of 31% and 37% over the decade. AGB range 50-100 Mg ha^{-1} had a net gain of 7% across the Niger Delta over the decade (**Appendix VII**).

I also estimated mean and total AGB from the 5 states making up the Niger Delta and estimated the change in mean and total biomass of the region. Bayelsa had the highest mean AGB (92.6 Mg ha^{-1}) while I recorded the lowest in Akwa Ibom (60.3 Mg ha^{-1}) in 2017. All five states in the Niger Delta showed a net loss in AGB over the decade (**Table 5.3**). However, Akwa Ibom had the highest biomass loss rate of 5.6 Mg ha^{-1} yr^{-1} while the lowest loss rate was recorded in Rivers state 2.6 Mg ha^{-1} yr^{-1}. All states showed deforestation as the higher contributor of AGB loss (>60%) (**Appendix VIII**).

Mangrove stands (> 100 Mg ha^{-1}) made up 36% of mangrove forest area in 2007 but showed a 35% reduction accounting for 27% of the mangrove area in 2017 (**Appendix IX**). I

discovered that mangrove forests (> 100 Mg ha^{-1}) recorded the highest AGB loss (29.2 X 10^6 Mg) recording a 58% loss from 2007 AGB values and 71% of total AGB loss. Mangrove forests (< 50 Mg ha^{-1}) made up about 28% of mangrove forest area in 2007 and also had a 15% loss in mangrove coverage but still accounted for about 27% in 2017 (**Appendix IX**). Mangrove forests (< 50 Mg ha^{-1}) recorded the highest gain (3.9 X 10^6 Mg) accounting for 51% of AGB gain and a 53% increase from 2007 AGB values. However, mangrove forests (50-100 Mg ha^{-1}) stands had a 7% increase in mangrove area from 333 000 ha in 2007 to 358 000 ha in 2017 (**Appendix IX** Mangrove stands (50-100 Mg ha^{-1} and > 100 Mg ha^{-1}) had a net loss of biomass while mangrove stands (< 50 Mg ha^{-1}) had a net gain in AGB. Percentage contribution of mangrove stands (> 100 Mg ha^{-1}) to AGB in the Niger Delta reduced from 61% in 2007 to 50% in 2017; mangrove forests (50-100 Mg ha^{-1}) increased from 30% to 41% over the decade while mangrove stands (< 50 Mg ha^{-1}) percentage contribution to Niger Delta AGB remained the same (9%) (**Appendix IX**).

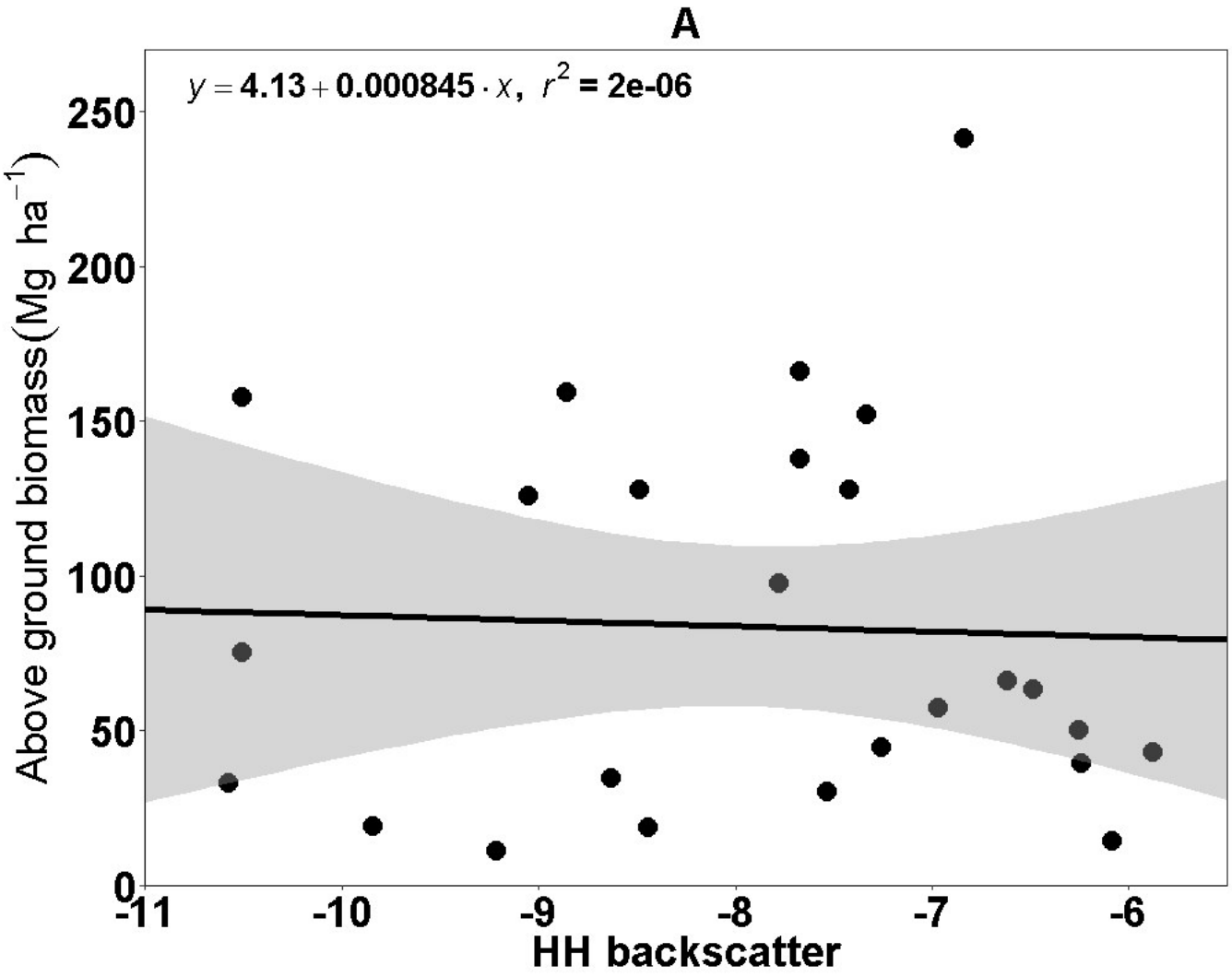
A
$y = 4.13 + 0.000845 \cdot x$, r^2 = 2e-06
Above ground biomass(Mg ha^{-1})
250
200
150
100
50
0
-11
-10
-9
-8
-7
-6
HH backscatter

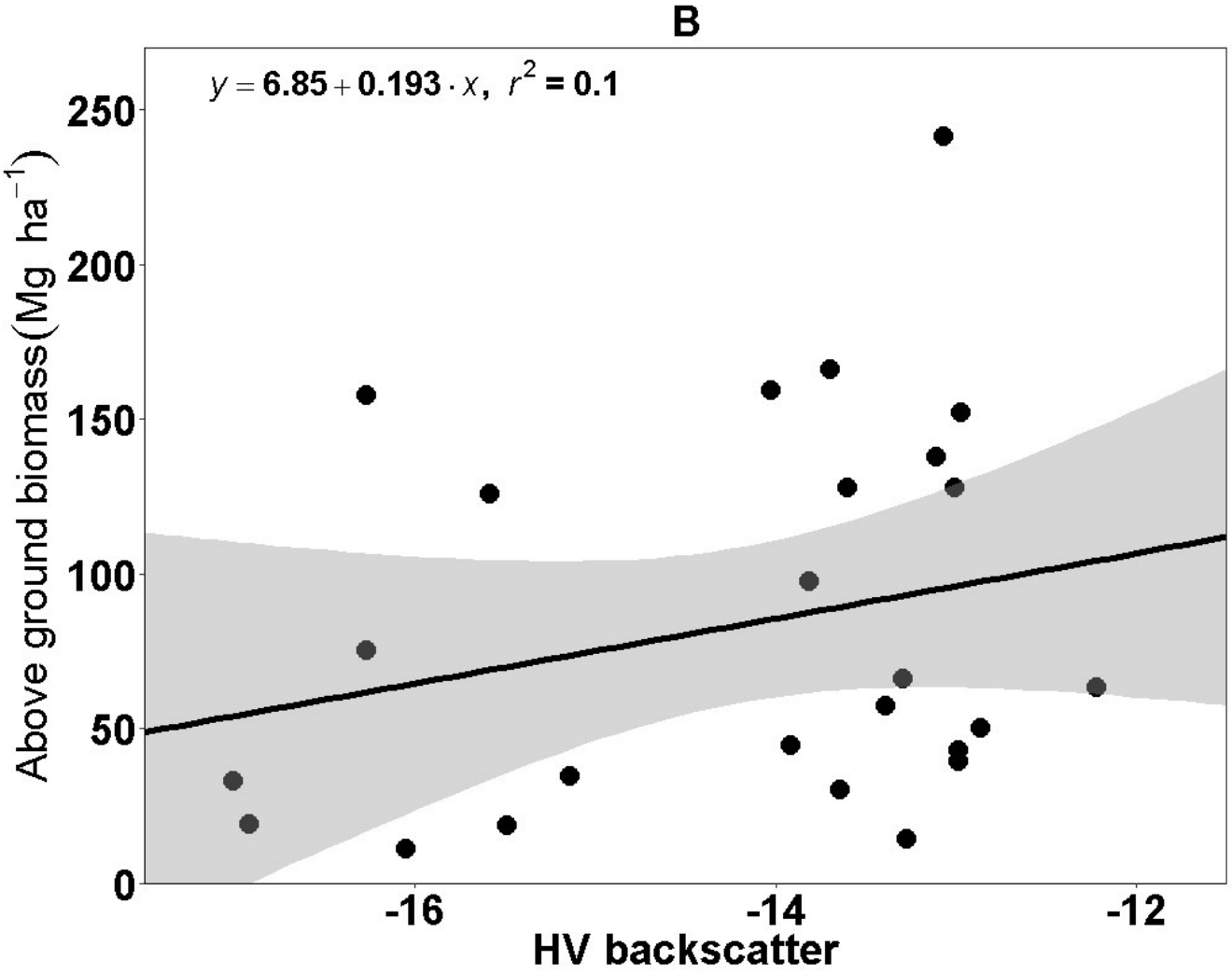
B
$y = 6.85 + 0.193 \cdot x$, $r^2 = 0.1$
Above ground biomass(Mg ha^{-1})
250
200
150
100
50
0
-16
-14
-12
HV backscatter

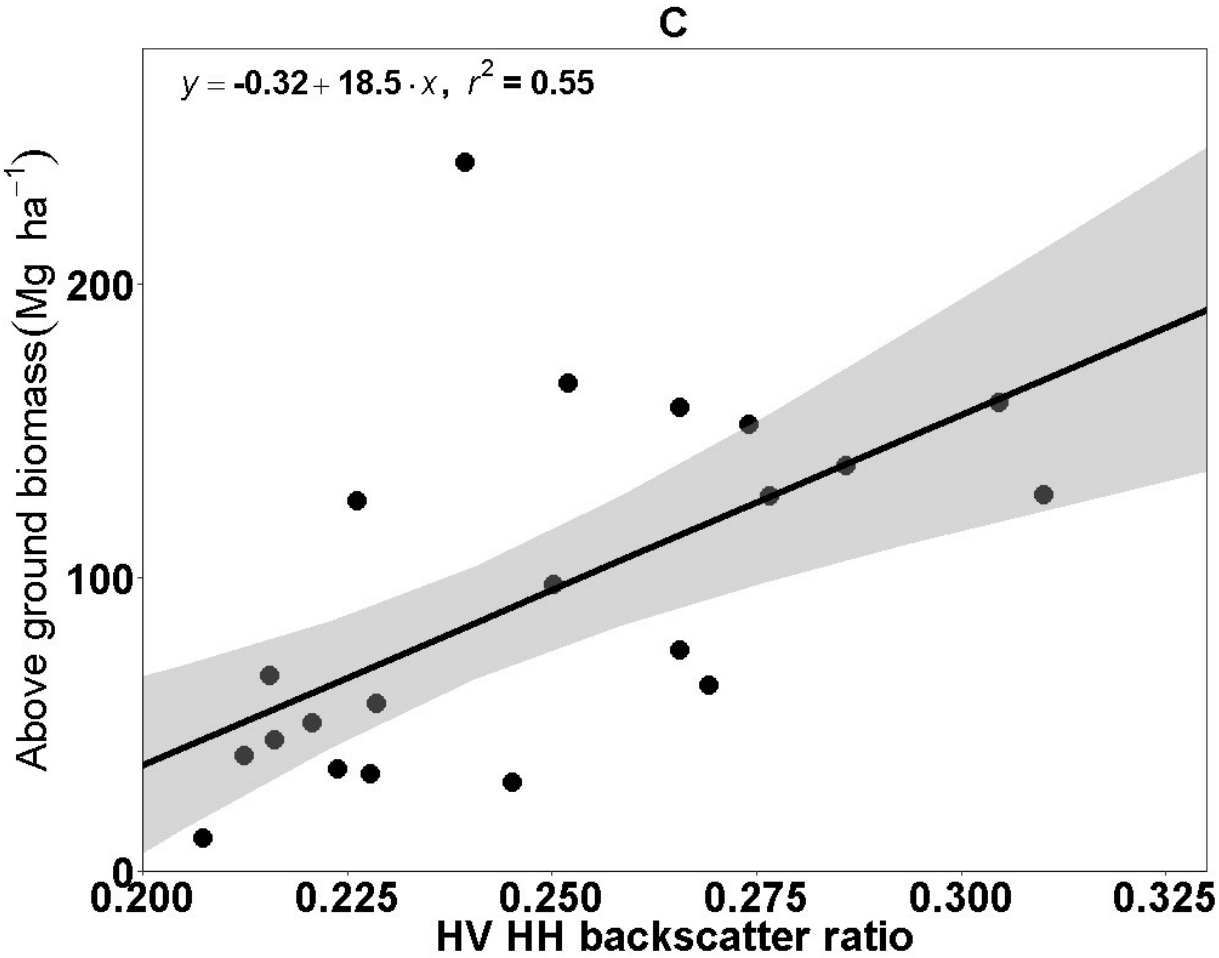

*Figure 5.5: Relationship between L-band HH backscatter (**A**), HV backscatter (**B**), HV: HH backscatter ratio (**C**) and field-based plot AGB estimates. The solid black line represents the line of best fit while the shaded region is the 95% confidence interval of the best-fit line.*

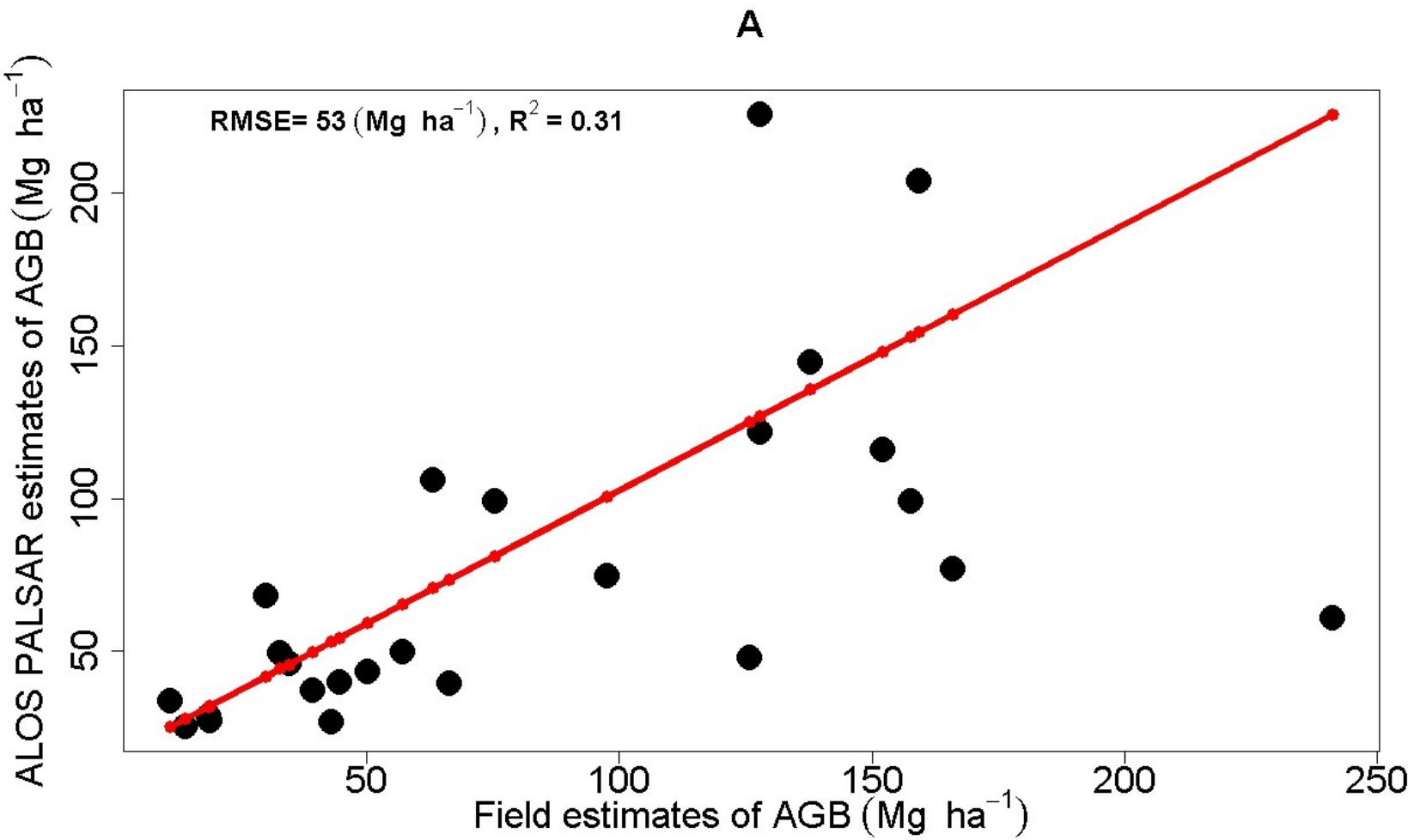
A
RMSE= 53 (Mg ha^{-1}), R^2 = 0.31
ALOS PALSAR estimates of AGB (Mg ha^{-1})
Field estimates of AGB (Mg ha^{-1})
50
100
150
200
250

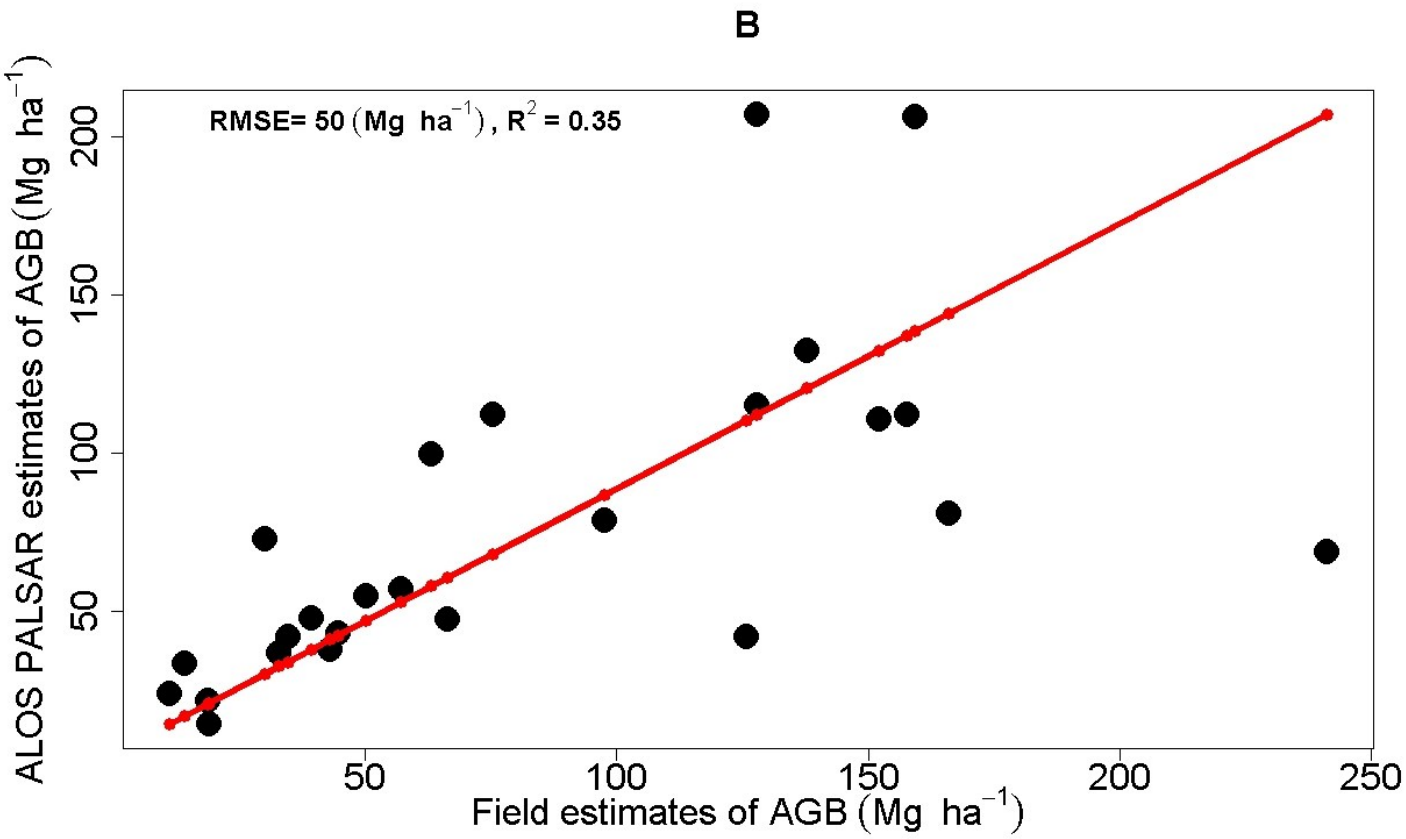

*Figure 5.6: Correlation between field-based plot AGB estimates against model derived AGB from L-band HV: HH ratio backscatter (**A**) and combination of HV: HH ratio and HV backscatter (**B**). The solid red line represents a 1:1 perfect agreement relationship while black points represent the data points of field and model derived AGB estimates (root mean square error and coefficient of determination are shown)*

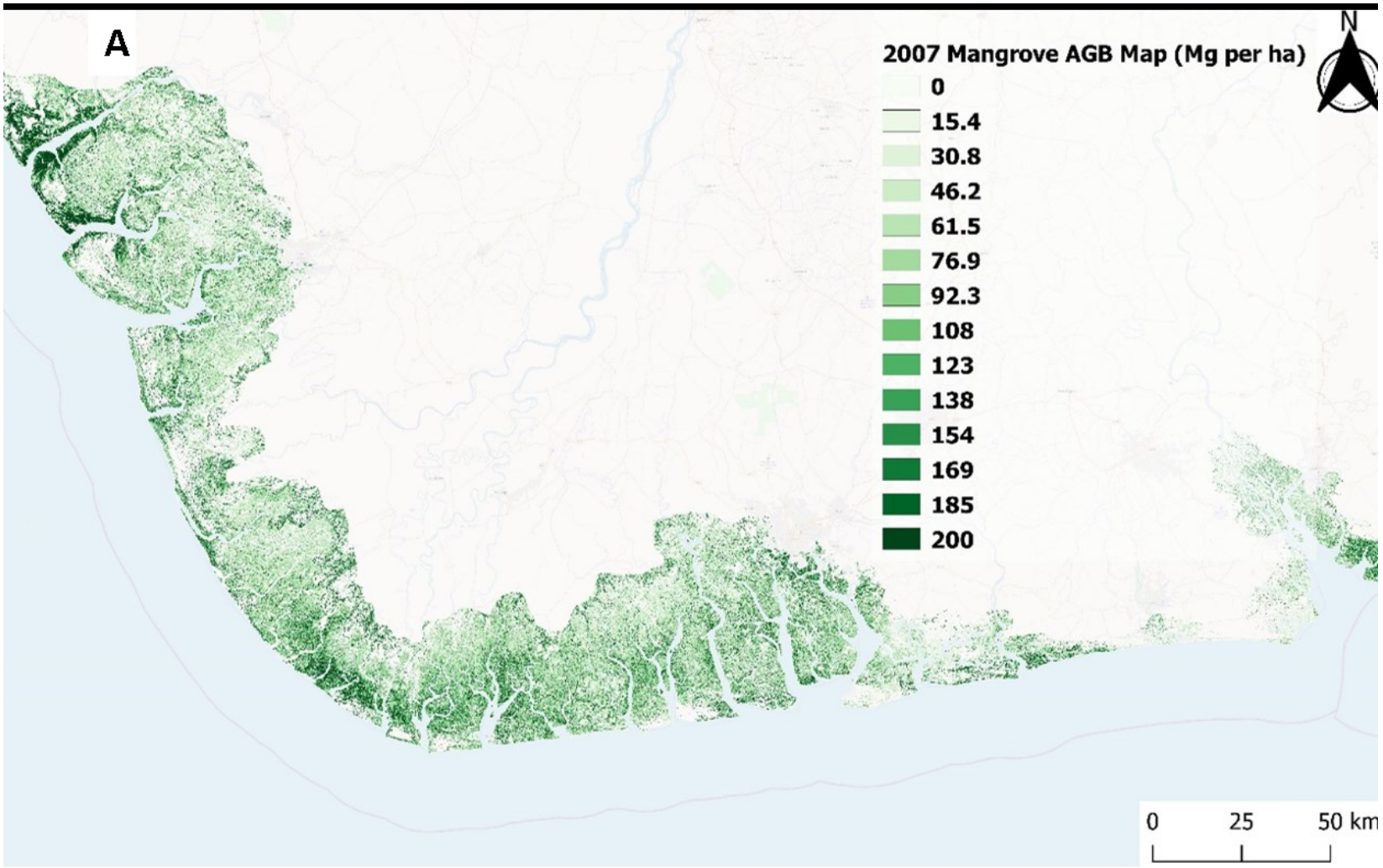
A
2007 Mangrove AGB Map (Mg per ha)
0
15.4
30.8
46.2
61.5
76.9
92.3
108
123
138
154
169
185
200
N
0
25
50 km

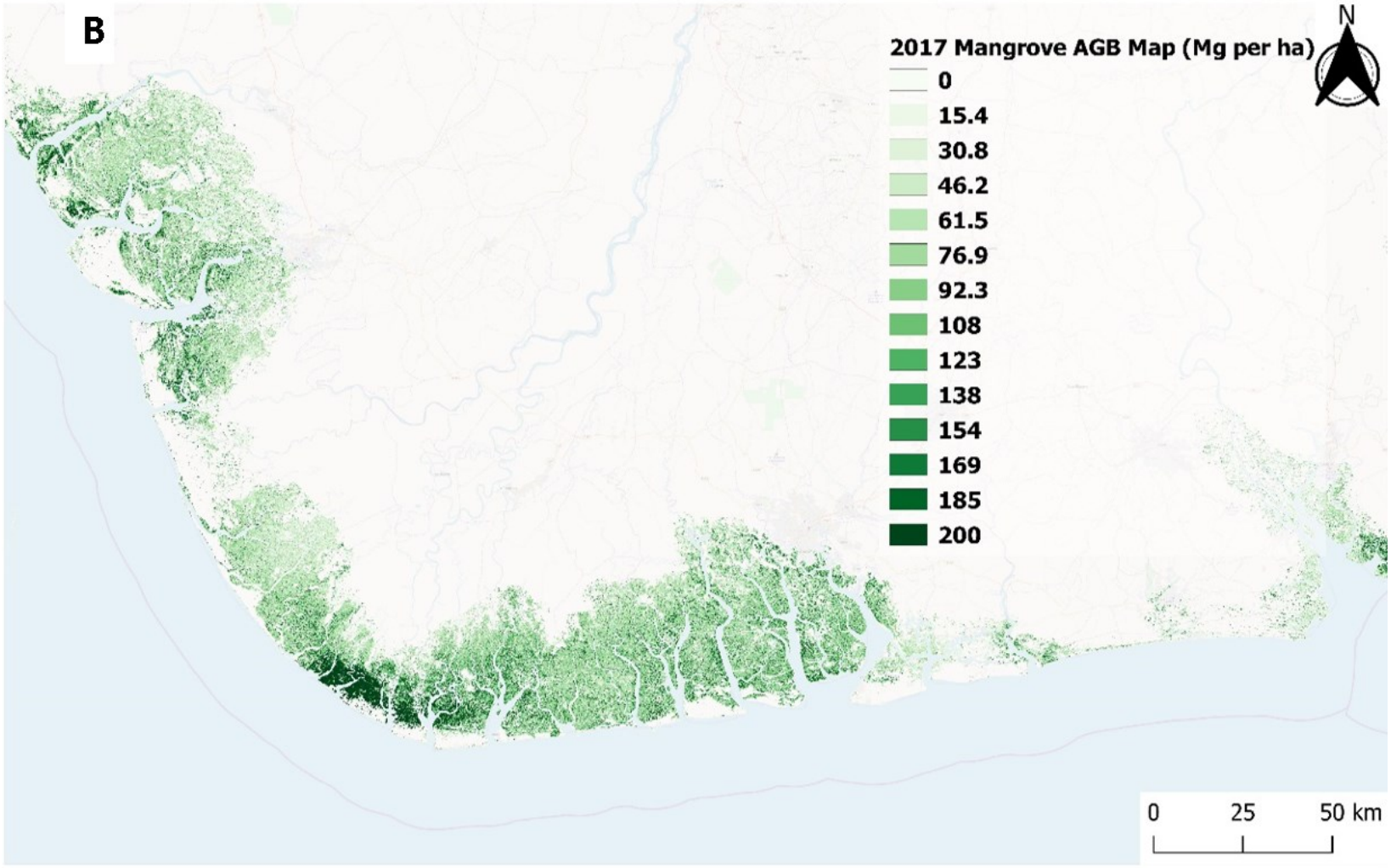
B
2017 Mangrove AGB Map (Mg per ha)
0
15.4
30.8
46.2
61.5
76.9
92.3
108
123
138
154
169
185
200
N
0
25
50 km

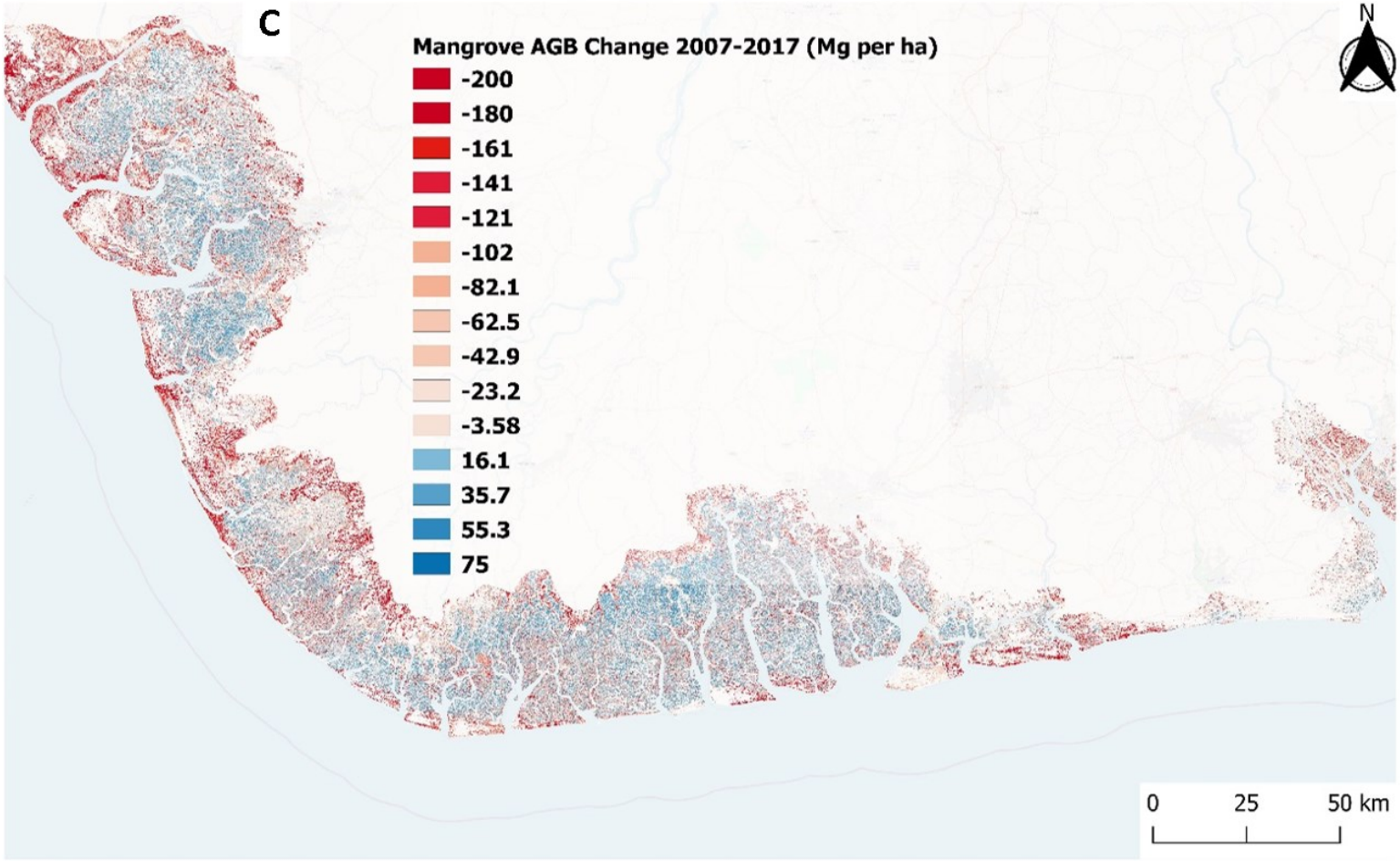

Figure 5.7: 2017 ALOS PALSAR generated AGB (Mg ha^{-1}) map of the Niger Delta using regression model developed in Figure 5.5b for 2007 (A), 2017 (B) and change difference map of the two time periods (C).

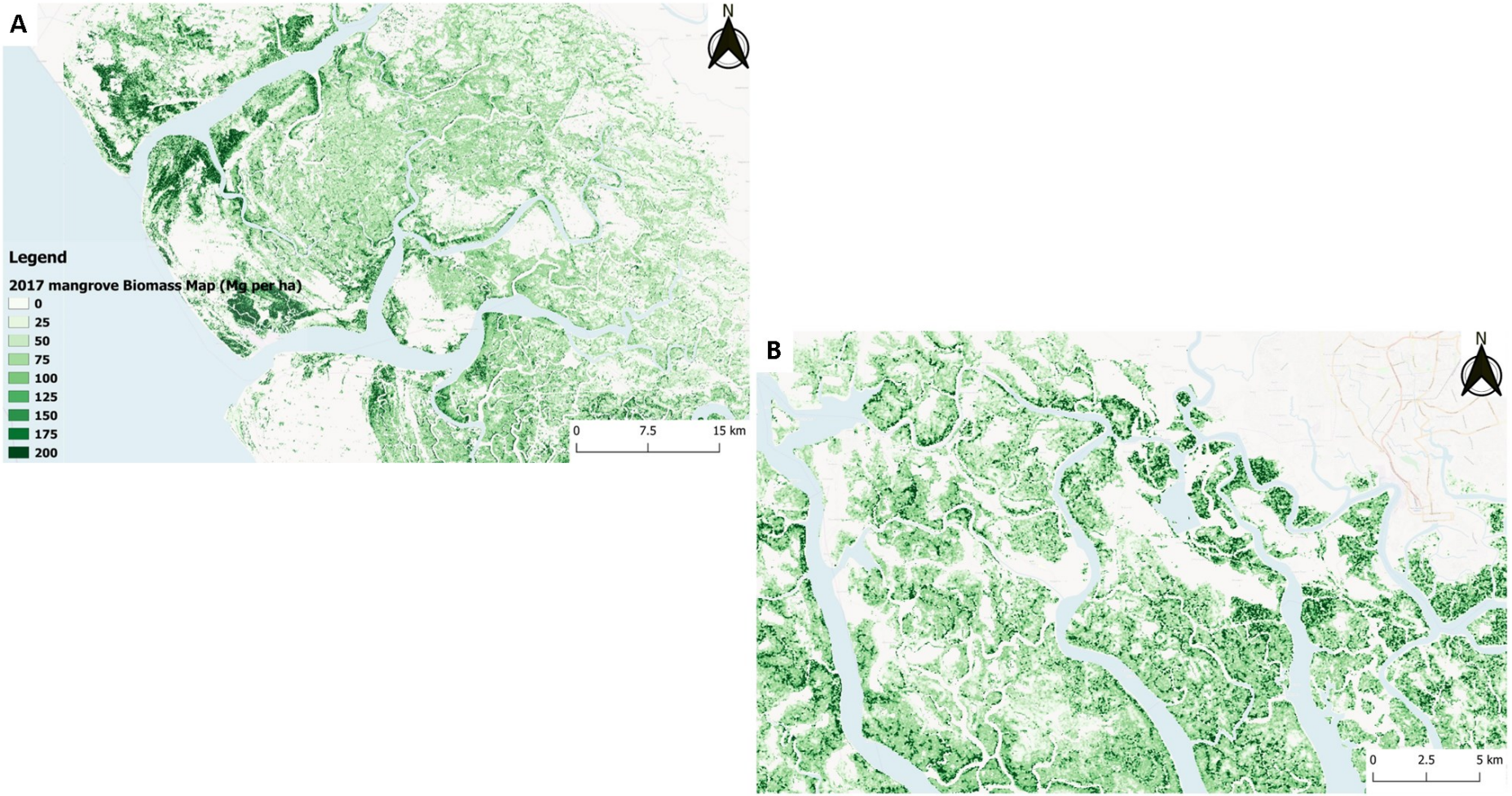

Figure 5.8: AGB map of Benin River estuary (A), Niger Delta Creeks (B) and Imo River estuary (C). Higher biomass along creeklets which reduce inland.

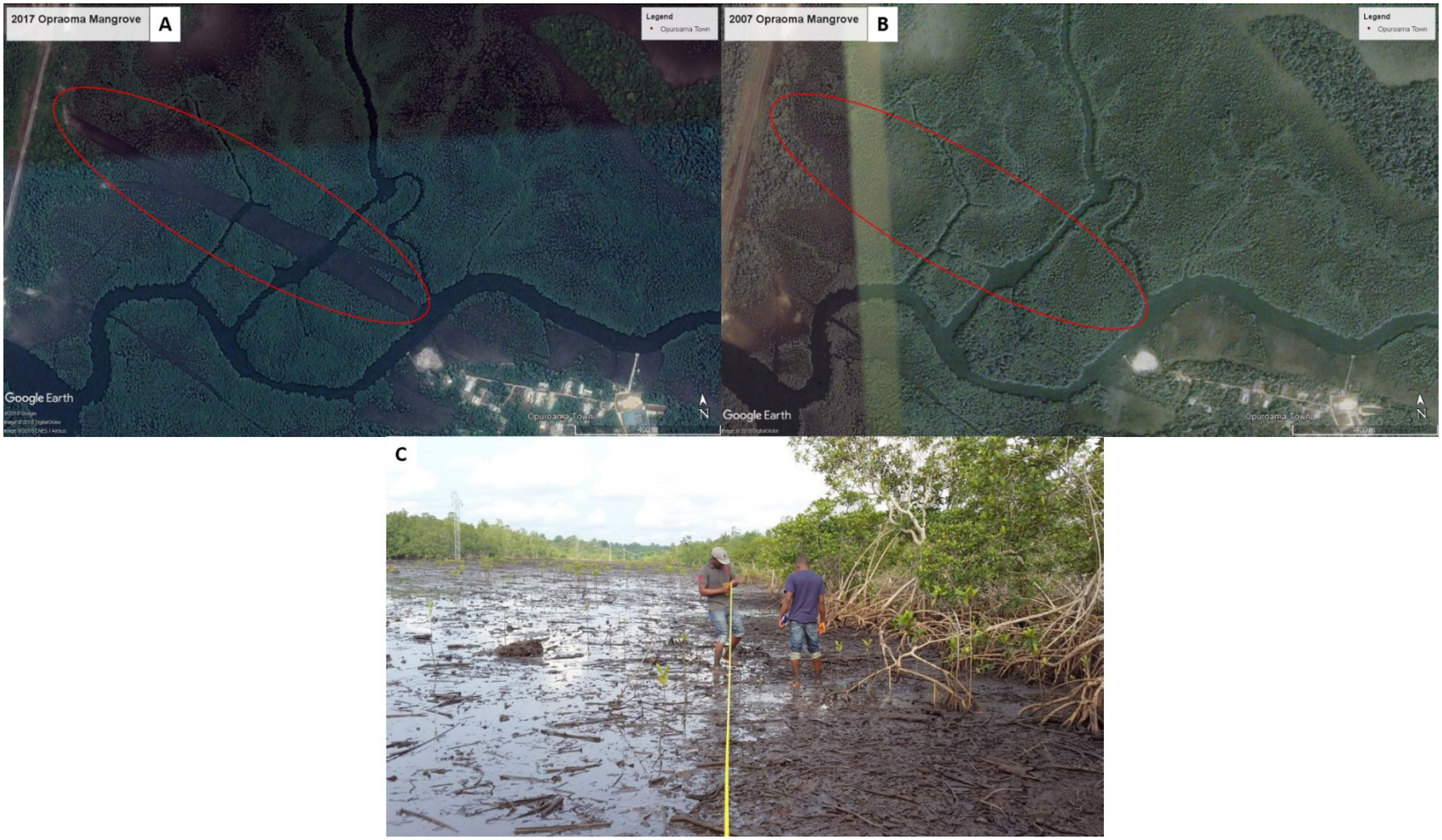

Figure 5.9: Cleared mangrove forest in Opraoma community, rivers state. Google imagery of 2017 (A), 2007 (B) and pictorial representation of the site (C).

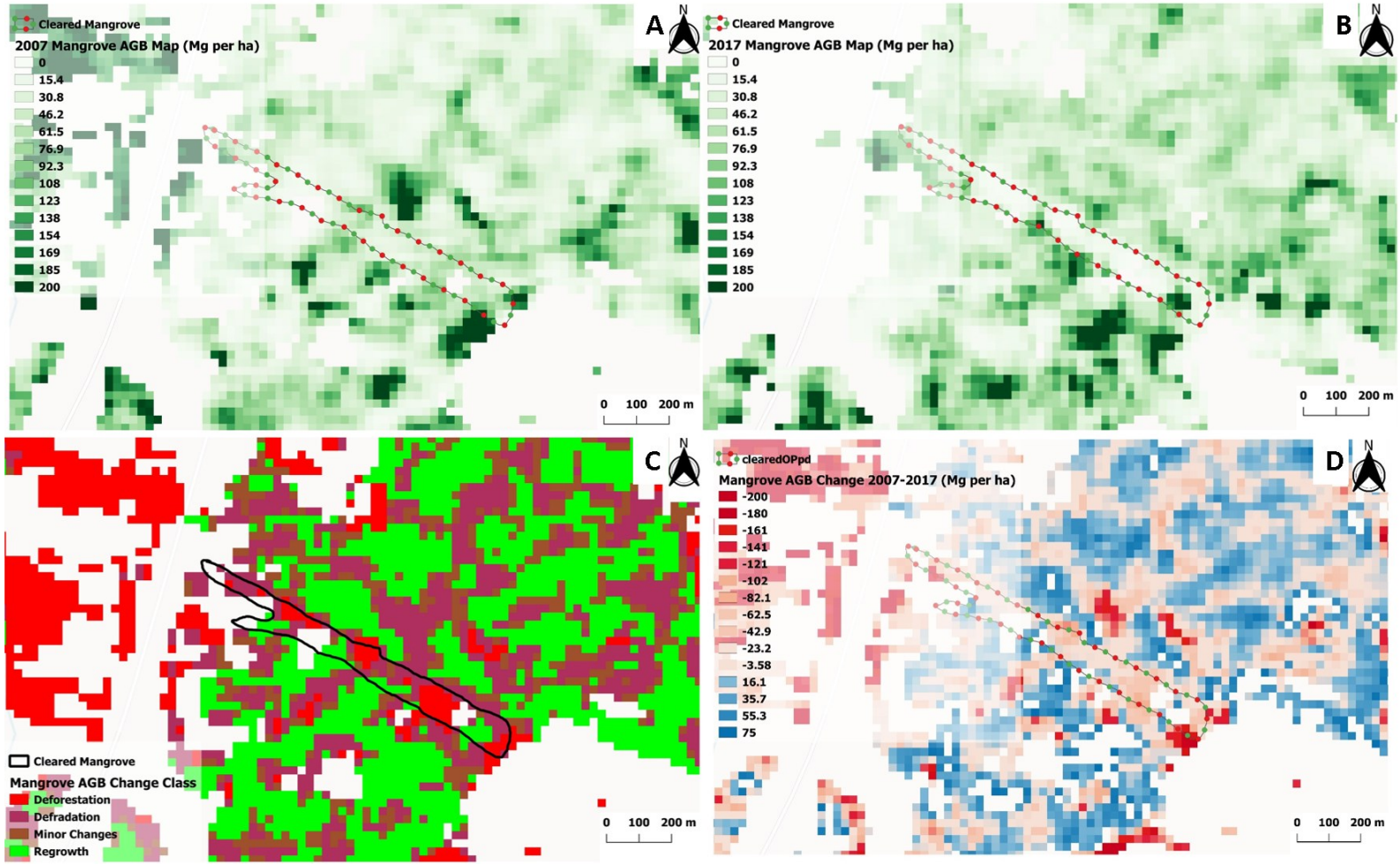

*Figure 5.10: AGB map of a cleared mangrove forest in Opraoma community in 2007 (**A**), 2017 (**B**), AGB change classes (**C**) and AGB difference map of both years (**D**).*

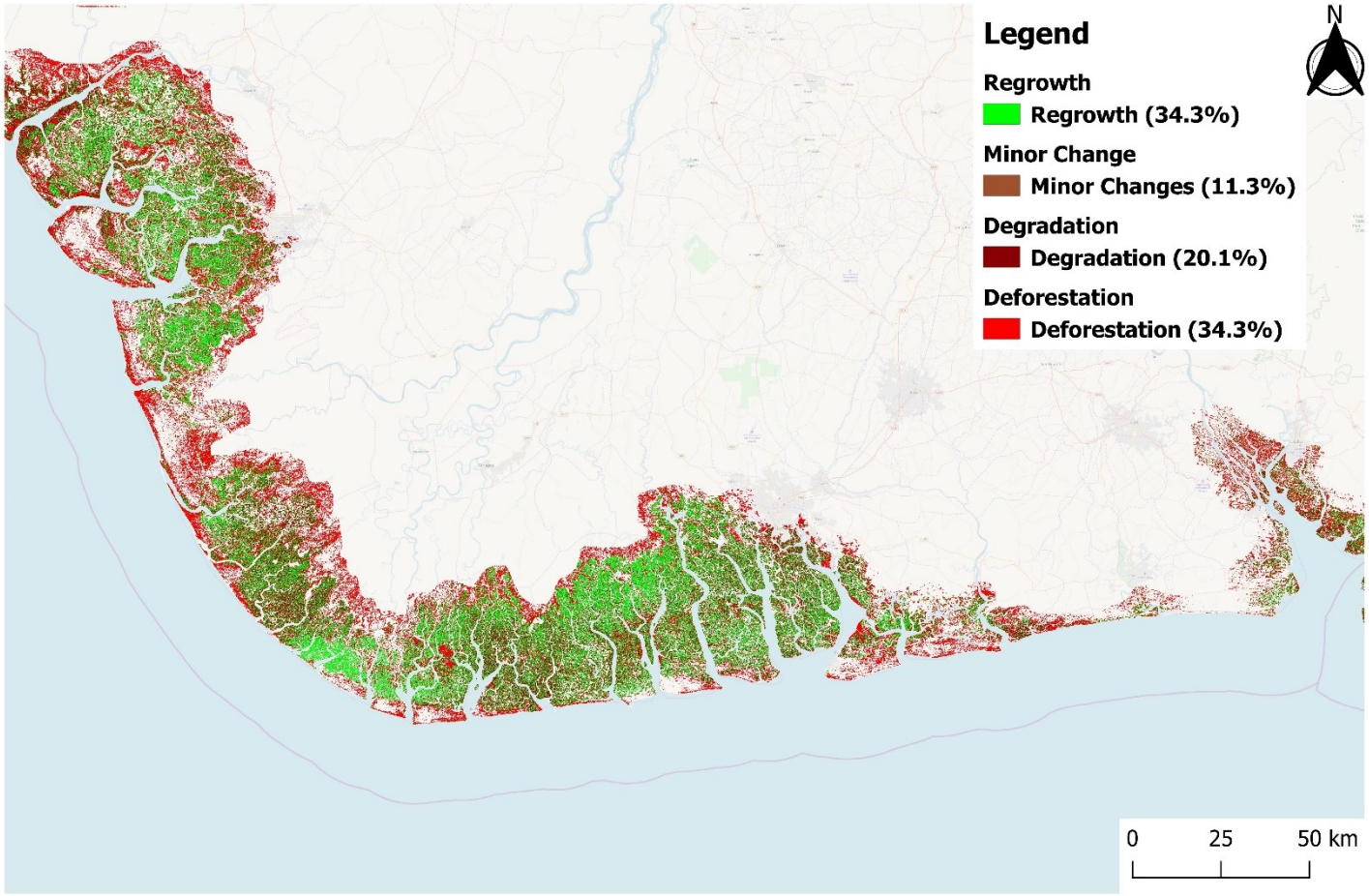

Figure 5.11: Mangrove AGB change classes in the Niger Delta showing the biomass dynamics between 2007 and 2017. Deforestation and regrowth showed equal area of change. However mean biomass change over the same classes showed a higher loss of AGB (90 Mg ha^{-1}) in deforested areas than regrowth (29 Mg ha^{-1}).

Table 5.3: Aboveground Biomass change between 2007 and 2017 in the Niger Delta and Sub-divisions

Region	2007			2017		
	Mean AGB (Mg ha^{-1})	**Total AGB (Mg)**	**Area (ha)**	**Mean AGB (Mg ha^{-1})**	**Total AGB (Mg)**	**Area (ha)**
Niger Delta	90.5	82 387 000	911,548	83.4	65 058 000	801,774
Akwa Ibom	77.3	2 464 000	31 888	60.3	1 661 000	27 853
Bayelsa	96.8	27 499 000	284 840	92.6	22 005 000	239 881
Cross River	100.0	2 822 000	28 154	82.4	2 002 000	24 478
Delta	88.5	25 668 000	290 797	75.7	17 878 000	238 697
Rivers	83.5	21 048 000	252 468	82.4	19 376 000	236 234
Disturbed Mangrove forest (Figure 5.9, 5.10)	46.4	510		35.2	425	

5.4 Discussion

This study represents the first attempt to produce high resolution maps of the AGB of mangrove forests of the Niger Delta. Further, I also generate maps of two years a decade apart, allowing change detection to be performed. I generated a regression equation based on field data collected over the same period as recent satellite radar data. The results showed that the annual AGB loss was 6.4 Mg ha^{-1} yr^{-1} and this was partly from a 12% loss of mangrove area and partly from an 8% reduction in mean AGB between 2007 and 2017. The mangrove loss over the decade accounted for 69% of the total AGB loss while 28% was as a result of degradation. I also recorded regional and local reduction in AGB from observed in-situ analysis. This study represent only the aboveground portion of biomass, excluding belowground roots, and much more significant substrate-bound organic carbon in this campaign. Alongi, (2014) reported that mean global mangrove ecosystem carbon stock of 956 t C ha^{-1} of which soils make up 75%, meaning that carbon stocks in the Niger Delta likely represent 10 times the numbers from my findings. Mangroves are probably Nigeria's most carbon dense ecosystem, and have been a very major source of carbon emissions since 2007.

5.4.1 Relationship between Aboveground Biomass and Radar backscatter

Synthetic aperture Radar (SAR) offers an effective method in retrieving forest biomass. The ability of the emitted signals to penetrate cloud and canopy features makes them efficient in biomass analysis of forests with different structural forms (Lucas *et al.*, 2004). The various mechanisms which SAR backscatter is related to different vegetation types have been previously reported (Moghaddam *et al.*, 1995; Ranson *et al.*, 1997). The polarimetry of SAR provides information of forest structure based on these backscatter mechanisms: surface scattering, double bounce scattering and volume scattering. These mechanisms include ground, branch layer, trunk-ground double bounce and branch-ground double bounce (Moghaddam *et al.*, 1995; Ningthoujam *et al.*, 2017). HH polarisation is related to double

bounce scattering between the vegetation and the ground surface due to its strong reflectivity at the surface, while volume scattering is associated with HV polarisation due to weaker interaction of V polarisation to the surface, hence, multiple crown interactions (Proisy *et al.*, 2000). Mangrove forests are characterised by complex root system, large trunks and dense canopy cover which make them easily detectable in SAR analysis.

The relationship between forest structure and SAR backscatter forms the basis of predicting AGB in forested landscapes. The relationship between field-based AGB and radar backscatter relationship was peculiar in my study, as there was no significant relationship with either HV or HH bands in isolation, whereas other studies have found significant relationships using the same L-band sensor. The insignificant HH backscatter could be as a result of the attenuation effect of a complex root structure in mangrove forests. Despite having dense stems which would increase the HH scatter, the double bounce effect would have been cancelled out by the root structures and a dense canopy. HV band has been shown to provide a stronger significant relationship to forest biomass (Carreiras *et al.,* 2012; Hamdan *et al.,* 2014; Mitchard *et al.,* 2009). Despite some studies showing HV band being more sensitive to AGB in mangrove forests, Cohen (2014) observed the best relationship with Kenyan mangrove forests in the HH band (R^2 =0.45), in a negative direction. In this study, the insignificance of HV polarisation could be as a result of the varied complex structure within my field plots which could have affected the backscatter signal of the canopies (Lucas *et al.*, 2007). Although they did not analyse the significance of their ratio, Hamdan *et al.,* (2014) showed a higher relationship between mangrove AGB and HH (R^2 =0.16) and HV (R^2 =0.42) bands. Their results however, showed no significance in the ratio of HV HH band. My results showed that despite having low significance in both HV and HH bands, there was a stronger significant relationship between HV HH ratio (R^2 = 0.55) and plot AGB. Proisy *et al.*, (2000) have stated the importance of polarisation ratios in detecting mangrove forest structures.

There are several factors that may have contributed to the differences in the relationship between AGB and radar data. The 25 plots in this study ranged from plots without disturbance, disturbed plots with forest gaps and low biomass plots. These varied forest structure and degrees of canopy openness could have contributed to the relationship with radar backscatter and AGB we saw here: it is very different to the more intact mangroves studied for example by Cohen (2014) in Kenya.

Mangrove forests have a regional characteristics based on tidal influence, species diversity, mangrove forests type and zonation. Mangrove forest measured in the Niger Delta is of semi-diurnal nature, hence more intermittently inundated by tidal water compared to other regions. The flooding condition and topography of the mangrove forests affect the backscatter potential of mangrove forests (Darmawan *et al.*, 2015). Darmawan *et al.,* (2015) gave evidence of the unique characteristics of HV and HH bands when received from open and flooded mangrove forests. This flooding effect could be one of the reasons for a reduced predictive power of both bands during this study. Secondly, the plots measured during this study were monospecific consisting of only *Rhizophora* species. Radar backscatter have been shown to be affected by the stage of mangrove forests homogenous pioneers to heterogeneous mature stands (Proisy *et al.*, 2003). Generally, mangrove forests of the Atlantic have a lower species diversity compared to other regions such as the Indian Ocean. Proisy *et al.,* (2003) gave evidence of change in radar signatures from changing forest structures from a pioneer to a mature stand. The monospecific nature of field plots compounded with recovery from past disturbance may have contributed to the difference in radar signal compared to other studies. Despite the possible influence of tide, topography, forest stage and species diversity from field data, the significant relationship between the HV HH ratio band and field plot data shows the potential for robust results from combined

strengths of individual L-bands. The collection of more plots and over larger plot sizes with less disturbance could further improve AGB predictive power of radar backscatter.

5.4.2 Radar-Aboveground Biomass Estimates

Estimating AGB over forested landscape can provide a baseline for monitoring biomass change and hence planning conservation and restoration plans for REDD+ programs. The 2017 estimates of mean AGB (83.4 Mg ha^{-1}) were lower compared with those estimated by other studies (**Table 5.4**). I recorded 31% lower total AGB than those recorded by Fatoyinbo and Simard, (2013) and 57% lower than those reported by Hutchison *et al.,* (2014). Methodology used in estimating AGB may have been a contributory factor, while Fatoyinbo and Simard (2013) estimated global mangrove biomass using a height relationship to AGB, Hutchison *et al.,* (2014) used a climate model in estimating global mangrove biomass (Fatoyinbo and Simard, 2013; Hutchison *et al.*, 2014). However, the estimates in this study are more reliable owing to the established relationship between measured 25 0.25 ha mangrove forest plots and radar backscatter (**Chapter 3**). Despite estimating a higher mangrove area than Fatoyinbo and Simard, (2013), I estimated lower mean and total AGB. I constrained predicted AGB to 200 Mg ha^{-1} in order to avoid overestimation which may have reduced the total AGB as it is possible some areas do exceed this considerably.

Mangrove forest degradation will have also contributed to the lower AGB estimates in this study. Ongoing mangrove degradation in the Niger Delta from oil pollution and wood exploitation may have contributed to reduced biomass by removing larger stems which contribute a greater percentage to AGB (McNicol *et al.*, 2017). Despite having a predictive power of 62%, the best model had a RMSE of 50 Mg ha^{-1} which gives an indication of the uncertainty in biomass estimate from radar imagery. This uncertainty could be as a result of various factors including error from ground-based AGB estimates, tidal influence and forest structure (Cohen, 2014). In order to investigate similarities or peculiarity in AGB estimates of

mangrove forest using radar sensors, the regional relationship of AGB to these sensors could better explain the uncertainties encountered in these estimates.

Table 5.4: Comparison with Global Mangrove Biomass Estimates. Note that both comparisons are for the whole of Nigeria.

	Region	Mangrove area	Mean AGB (t ha^{-1})	Total AGB (t)
This study (2017)	Niger Delta	794,561	83.4	65 X 10^6
Fatoyinbo and Simard, 2013	Nigeria	857,300	111	94.8 X 10^6
Hutchison *et al.*, 2014	Nigeria	778,944	195	152 X 10^6

5.4.3 Mangrove Biomass Change

Carbon stored in woody biomass and soil over a long period of time are released to the atmosphere due to deforestation from various effects. Mangrove forest loss and degradation is an ongoing discussion because of the impact on climate change (Gilman *et al.,* 2006; Hamilton and Friess, 2018; Kauffman *et al.*, 2014). I recorded a 21% reduction in total AGB between 2007 and 2017 over the study region, and a reduction of 8% in the mean AGB of the remaining mangroves (**Appendix VIII**). Loss of biomass could be as a complete removal of mangrove stands in terms of land use change or a change in mangrove structure resulting in the reduction of stand contribution to AGB. In Chapter 4, we estimated a 12% reduction of mangrove area between 2007 and 2017. Hence, showing a means of combining field surveys and earth observation in monitoring mangrove forest degradation. Loss of mangrove area have been reported in the Niger Delta due to oil pollution, land reclamation and logging (James *et al.*, 2007). This study also showed evidence of the effect of land clearance on AGB reduction. My analysis of a cleared mangrove forest in Rivers state resulted in about 14% of the standing biomass due to the development.

However, mangrove biomass loss could be considerably more if there was not a concurrent increase in biomass in some regions. Being a natural forest, abandoned mangrove forests are likely to get reforested by natural means. The mean AGB gain was lower than reported

by other studies. Ajonina (2008) estimated a mean AGB growth of 7.35 Mg ha^{-1} yr^{-1} while Day *et al.*, (1996) estimated 7.72 Mg ha^{-1} yr^{-1}. Mangrove regrowth from disturbance could be slower than the biomass increment from undisturbed stands (Proffitt and Devlin, 2005). This slowed regrowth could be as environmental conditions. Mangrove biomass have been reported to be increasing in biomass due to increased CO_2 concentrations in the atmosphere (Wang *et al.*, 2017). Delayed response of mangrove biomass to these effects could be another reason for rapid biomass loss within the region. The Niger delta is known for its incidence of oil spills, forest fires and drainage hindrance. Thomas *et al.,* (2017) gave evidence on the effects of past negative effects on mangrove forests when investigating mangrove loss drivers between 1996 and 2010 (Thomas *et al.,* 2017). According to Shell, there was a total of 301 oil spill incidents in swamp areas of the Niger Delta from 2013 to 2018. These effects can have an immediate effect on mangrove forests, however, lag effects on biomass can affect biomass accumulation over time. This may include clogging lenticels in mangrove structures needed for gaseous exchange and heavy metal pollution (International Petroleum Industry Environmental Conservation Association (IPIECA), 1993). Mangrove forests in the Niger delta can therefore take many months or years for complete dieback from past disturbance.

Mangrove loss showed a landward origin, possibly from population density and growth, agricultural expansion and urban regions at the landward extent and within creeklets. The link between coastal urbanisation and mangrove deforestation has always existed (Giri *et al.*, 2011). Migration to coastal communities in order to benefit from coastal development has is a threat to mangroves of the Eastern African coastline (Hoberg, 2009). There was also a noticeable loss of mangrove biomass along the coastline (**Figure 5.7**). This could be as a result of oil spills, sea level rise and beach encroachment. Urban expansion and population increase is also reflected in coastal areas of the Niger Delta. The need for regional mangrove biomass

maps for use in assessing trend of mangrove loss from various adverse effects and also strengthen areas on positive gain of biomass due to conservation plans.

5.4.4 Limitations

Mangrove forest biomass estimates from satellite imagery are not without limitations. I used 25 0.25 ha plots with to develop a model using ALOS PALSAR. These plots, despite having a significant relationship with radar backscatter may have been insufficient for the mangrove area in the Niger Delta. The study plots were also of one genus (*Rhizophora*) which is a third of the three genera found in the Niger Delta (*Laguncularia racemosa*, *Avicennia* spp). This limitation was a result of the challenge of field work in the Niger Delta. Disturbance in the Niger Delta could also have affected the relationship between mangrove biomass and radar backscatter. In order to estimate the AGB in 2007 using the radar-AGB model, I used the ALOS PALSAR 2007 dataset which may have some variation in radar backscatter due to the different ALOS missions or moisture conditions at the time of data collection. The ALOS PALSAR data were taken at different times in the year, hence we didn't account for the temporal variability of the tiles used in the analysis. It is important to note that the regression model generated in this chapter had a RMSE of 50 Mg ha^{-1}. Hence it should be used with careful consideration with other regions without calibration datasets. I also used two data products, a decade apart, hence activities within mangrove forests between these dates cannot be accounted for.

5.5 Conclusion

Our study has shown the potential to map biomass of mangrove forests in the Niger delta using radar backscatter. I reported an annual biomass loss of 3.5 X 10^6 Mg (0.4%) between 2007 and 2017 over the Niger delta. I have also been able to show the possibility to monitor mangrove forest degradation over the landscape. I have also given evidence of the possible limitations when using this methodology in estimating AGB. The Niger Delta is a globally important region in the world owing to oil production, population growth, social unrest and ecosystem diversity in the region. Various attempts have been made to conserve and restore disturbed forests in this delta. However, very little scientific data is available to support landscape restoration and conservation of mangrove forests. Availability of remote sensing products from various agencies have provided a means to monitor the change of mangrove forest biomass over time.

Mangrove forest in Nigeria is ranked about the top 10 in the world in terms of area and biomass but this may be rapidly changing due to adverse effects from development, logging and sea level rise. Utilisation of remote sensing products which can provide a baseline too in spatial and temporal analysis can be the first step in a national mangrove forests monitoring plan. These plans can be beneficial under the Payment for Ecosystem Services (PES) and REDD+ programs which entails recording carbon loss from ecosystems and greenhouse gas emissions. The combination of field work, remote sensing and modelling can help in reporting spatial and temporal mangrove forest productivity.

5.6 References

Adekola, O., & Mitchell, G. (2011). The Niger Delta wetlands: Threats to ecosystem services, their importance to dependent communities and possible management measures. *International Journal of Biodiversity Science, Ecosystem Services and Management*, *7*(1), 50–68. https://doi.org/10.1080/21513732.2011.603138

Ajonina, G. N. (2008). Inventory and Modelling Mangrove Forest Stand Dynamics Following Different Levels of Wood Exploitation Pressures in the Douala-Edea Atlantic Coast of Cameroon, Central Africa, 215. Retrieved from http://www.freidok.uni-freiburg.de/volltexte/6132/pdf/Gordon_N._Ajonina_Thesis.pdf

Alongi, D M. (2011). Mangroves, 393–404. https://doi.org/10.1111/j.1365-2664.2012.02198.x.Roca

Alongi, Daniel M. (2014). Carbon Cycling and Storage in Mangrove Forests. *Annual Review of Marine Science*, *6*(1), 195–219. https://doi.org/10.1146/annurev-marine-010213-135020

Alongi, Daniel M. (2009). *The energetics of mangrove forests*. *The Energetics of Mangrove Forests*. https://doi.org/10.1007/978-1-4020-4271-3

Carreiras, J. M. B., Vasconcelos, M. J., & Lucas, R. M. (2012). Understanding the relationship between aboveground biomass and ALOS PALSAR data in the forests of Guinea-Bissau (West Africa). *Remote Sensing of Environment*, *121*, 426–442. https://doi.org/10.1016/j.rse.2012.02.012

Cohen, R. (2014). Estimating the above-ground biomass of mangrove forests in Kenya. *Ph.D. Thesis*, 122.

Darmawan, S., Takeuchi, W., Vetrita, Y., Wikantika, K., & Sari, D. K. (2015). Impact of tidal

height on characteristics of ALOS PALSAR measurements to estimate above ground biomass of mangrove forest in Indonesia. *Journal of Sensor*, *2015*. https://doi.org/http://dx.doi.org/10.1155/2015/641798

Day, J. W., Conner, W., Ley-Lou, F., Day, R., And, & Navarro, A. (1987). The productivity and composition of mangrove forests, Laguna de Términos, Mexico. *Aquatic Botany*, *27*, 267–284. https://doi.org/10.1016/0304-3770(87)90046-5

Dewantoro, M. D. R., & Farda, N. M. (2012). ALOS PALSAR Image for Landcover Classification Using Pulse Coupled Neural Network (PCNN). *International Journal of Advanced Research in Computer and Engineering*, *1*(5), 289–294.

Donato, D. C., Kauffman, J. B., Murdiyarso, D., Kurnianto, S., Stidham, M., & Kanninen, M. (2011). Mangroves among the most carbon-rich forests in the tropics. *Nature Geoscience*, *4*(5), 293–297. https://doi.org/10.1038/ngeo1123

Fatoyinbo, T. E., & Armstrong, A. H. (2010). Remote Characterization of Biomass Measurements: Case Study of Mangrove Forests. In M. N. B. Momba (Ed.), *Biomass* (1st ed., pp. 65–78). Retrieved from http://www.intechopen.com/books/biomass/remote-characterization-of-biomass-measurements-case-study-of- mangrove-forests

Fatoyinbo, T. E., & Simard, M. (2013). Height and biomass of mangroves in Africa from ICESat/GLAS and SRTM. *International Journal of Remote Sensing*, *34*(2), 668–681. https://doi.org/10.1080/01431161.2012.712224

Gilman, E. L., Ellison, J., Jungblut, V., Van Lavieren, H., Wilson, L., Areki, F., … Yuknavage, K. (2006). Adapting to Pacific Island mangrove responses to sea level rise and climate change. *Climate Research*, *32*(3), 161–176. https://doi.org/10.3354/cr032161

Giri, C., Ochieng, E., Tieszen, L. L., Zhu, Z., Singh, A., Loveland, T., … Duke, N. (2011). Status and distribution of mangrove forests of the world using earth observation satellite data. *Global Ecology and Biogeography*, *20*(1), 154–159. https://doi.org/10.1111/j.1466-8238.2010.00584.x

Hamdan, O., Khali Aziz, H., & Mohd Hasmadi, I. (2014). L-band ALOS PALSAR for biomass estimation of Matang Mangroves, Malaysia. *Remote Sensing of Environment*, *155*, 69–78. https://doi.org/10.1016/j.rse.2014.04.029

Hamilton, S. E., & Friess, D. A. (2018). Global carbon stocks and potential emissions due to mangrove deforestation from 2000 to 2012. *Nature Climate Change*, *8*(3), 240–244. https://doi.org/10.1038/s41558-018-0090-4

Hansen, M. C., Potapov, P. V, Moore, R., Hancher, M., Turubanova, S. A., & Tyukavina, A. (2013). High-Resolution Global Maps of 21st-Century Forest Cover Change. *Science*, *342*(6160), 850–853. https://doi.org/10.1126/science.1244693

Harris Geospatial Solutions. (2016). Adaptive Filters. Retrieved May 22, 2016, from http://www.exelisvis.com/docs/BroadbandGreenness.html#Visible

Herr, D., & Landis, E. (2016). *Coastal blue carbon ecosystems. Opportunities for Nationally Determined Contributions. Policy Brief*. Gland, Switzerland. https://doi.org/http://dx.doi.org/10.2305/IUCN.CH.2015.10.en

Herr, D., Pidgeon, E., & Laffoley, D. (2011). *Blue carbon policy framework*.

Ho Tong Minh, D., Le Toan, T., Rocca, F., Tebaldini, S., D'Alessandro, M. M., & Villard, L. (2014). Relating P-band synthetic aperture radar tomography to tropical forest biomass. *IEEE Transactions on Geoscience and Remote Sensing*, *52*(2), 967–979. https://doi.org/10.1109/TGRS.2013.2246170

Hoberg, J. (2009). *Economic Analysis of Mangrove Forests: A case study in Gazi Bay*. *Journal of Sustainable Forestry* (Vol. 28).

Hutchison, J., Manica, A., Swetnam, R., Balmford, A., & Spalding, M. (2014). Predicting global patterns in mangrove forest biomass. *Conservation Letters*, *7*(3), 233–240. https://doi.org/10.1111/conl.12060

International Petroleum Industry Environmental Conservation Association (IPIECA). (1993). Biological impacts of oil pollution: Mangroves. *IPIECA Series Report*, *4*, 1–24. Retrieved from file:///C:/Lit Database/International Petroleum Industry Environmental Conservation Association/1992/Unknown/International Petroleum Industry Environmental Conservation Association_1992_Biological impacts of oil pollution Mangroves.pdf

James, G. K., Adegoke, J. O., Saba, E., Nwilo, P., & Akinyede, J. (2007). Satellite-Based Assessment of the Extent and Changes in the Mangrove Ecosystem of the Niger Delta. *Marine Geodesy*, *30*(3), 249–267. https://doi.org/10.1080/01490410701438224

JAXA. (2003). JAXA | Advanced Land Observing Satellite-2 (ALOS-2). Retrieved from http://www.jaxa.jp/projects/sat/alos2/index_e.html

Karmaker, S. (2006). Study of Mangrove Biomass, Net Primary Production & Species Distribution using Optical & Microwave Remote Sensing Data.

Kathiresan, K. (2006). 3.5. Importance of Mangrove Ecosystem. *Centre of Advanced Study in Marine Biology, Annamalai University*, 2–500.

Kathiresan, K., & Bingham, B. L. (2001). Biology of mangroves and mangrove Ecosystems, *2881*(October), 81–251. https://doi.org/10.1016/S0065-2881(01)40003-4

Kauffman, J. B., Heider, C., Norfolk, J., & Payton, F. (2014). Carbon stocks of intact

mangroves and carbon emissions arising from their conversion in the Dominican Republic. *Ecological Applications*, *24*(3), 518–527. https://doi.org/10.1890/13-0640.1

Langeveld, J. W. A., & Delany, S. (2014). *The impact of oil exploration, extraction and transport on mangrove vegetation and carbon stocks in nigeria*. Amsterdam.

Lee, J. S. (1980). Digital image enhancement and noise filtering by use of local statistics. *IEEE Transactions on Pattern Analysis and Machine Intelligence*, *2*(2), 165–168. https://doi.org/10.1109/TPAMI.1980.4766994

Lopes, A., Touzi, R., & Nezry, E. (1990). Adaptive Speckle Filters and Scene Heterogeneity. *IEEE Transactions on Geoscience and Remote Sensing*, *28*(6), 992–1000. https://doi.org/10.1109/36.62623

Lucas, R. M., Mitchell, A. L., Ake, R., Proisy, C., Melius, A. and, & Ticehurst, C. (2007). The potential of L-band SAR for quantifying mangrove characteristics and change: case studies from the tropics. *Aquaric Conservation: Marine and Freshwater Ecosystems*, *19*, 671–675. https://doi.org/10.1002/aqc

Lucas, R. M., Mitchell, A. L., & Armston, J. (2015). Measurement of forest above ground biomass using active and passive remote sensing at large (country and continental) scales. *Forestry Reports (in Review)*, 162–177. https://doi.org/10.1007/s40725-015-0021-9

Lucas, R. M., Moghaddam, M., Member, S., & Cronin, N. (2004). Microwave Scattering From Mixed-Species. *October*, *42*(10), 2142–2159.

Lucas, Richard, Bunting, P., Clewley, D., Armston, J., Fairfax, R., Fensham, R., … Shimada, M. (2010). An Evaluation of the ALOS PALSAR L-Band Backscatter—Above Ground Biomass Relationship Queensland, Australia: Impacts of Surface Moisture Condition

and Vegetation Structure. *IEEE Journal of Selected Topics in Applied Earth Observations and Remote Sensing*, *3*(4), 576–593. https://doi.org/10.1109/JSTARS.2010.2086436

Lucas, Rm, Bunting, P., Clewley, D., & Proisy, C. (2009). Characterisation and Monitoring of Mangroves Using ALOS PALSAR Data. *Eorc.Jaxa.Jp*. Retrieved from http://www.eorc.jaxa.jp/ALOS/en/kyoto/phase_1/KC-Phase1-report_Lucas_WT.pdf

Lugo, A. E. and, & Medina, E. (2014). Mangrove Forests. *Encyclopedia of Natural Resources*, (January 2015), 343–352. https://doi.org/10.1081/E-ENRL-120047500

McNicol, I. M., Ryan, C. M., Dexter, K. G., Ball, S. M. J., & Williams, M. (2017). Aboveground Carbon Storage and Its Links to Stand Structure, Tree Diversity and Floristic Composition in South-Eastern Tanzania. *Ecosystems*. https://doi.org/10.1007/s10021-017-0180-6

McNicol, I. M., Ryan, C. M., & Mitchard, E. T. A. (2018). Carbon losses from deforestation and widespread degradation offset by extensive growth in African woodlands. *Nature Communications*, *9*(1). https://doi.org/10.1038/s41467-018-05386-z

Mermoz, S., Le Toan, T., Villard, L., Rejou-Mechain, M., & Seifert-Granzin, J. (2014). Biomass assessment in the Cameroon savanna using ALOS PALSAR data. *Remote Sensing of Environment*, *155*, 109–119. https://doi.org/10.1016/j.rse.2014.01.029

Mitchard, E. T. a., Saatchi, S. S., White, L. J. T., Abernethy, K. a., Jeffery, K. J., Lewis, S. L., … Meir, P. (2012). Mapping tropical forest biomass with radar and spaceborne LiDAR in Lopé National Park, Gabon: overcoming problems of high biomass and persistent cloud. *Biogeosciences*, *9*(1), 179–191. https://doi.org/10.5194/bg-9-179-2012

Mitchard, E. T. a, Saatchi, S. S., Woodhouse, I. H., Nangendo, G., Ribeiro, N. S., Williams, M.,

… Meir, P. (2009). Using satellite radar backscatter to predict above-ground woody biomass: A consistent relationship across four different African landscapes. *Geophysical Research Letters*, *36*(23), 1–6. https://doi.org/10.1029/2009GL040692

Moghaddam, M., Saatchi, S., & Collection, A. A. D. (1995). Analysis of Scattering Mechanisms in SAR Imagery over Boreal Forest.pdf. *IEEE Transactions on Geoscience and Remote Sensing*, *33*(5), 1290–1926.

Ndidi, C., Okonkwo, P., Kumar, L., & Taylor, S. (2015). The Niger Delta wetland ecosystem : What threatens it and why should we protect it ? *African Journal of Environmental Science and Technology*, *9*(5), 451–463. https://doi.org/10.5897/AJEST2014.1841

Ni, W., Sun, G., Guo, Z., Zhang, Z., He, Y., & Huang, W. (2013). Retrieval of forest biomass from ALOS PALSAR data using a lookup table method. *IEEE Journal of Selected Topics in Applied Earth Observations and Remote Sensing*, *6*(2), 875–886. https://doi.org/10.1109/JSTARS.2012.2212701

Ningthoujam, R. K., Balzter, H., Tansey, K., Feldpausch, T. R., Mitchard, E. T. A., Wani, A. A., & Joshi, P. K. (2017). Relationships of S-band radar backscatter and forest aboveground biomass in different forest types. *Remote Sensing*, *9*(11), 1–17. https://doi.org/10.3390/rs9111116

Nwobi, C. J., Williams, M., & Mitchard, E. (2019). Stand, Biomass and Canopy Patterns across Disturbance Gradients in Mangrove Forests of the Niger Delta.

PCI Geomatics. (2016). Radar Enhanced Lee Filter. Retrieved May 22, 2016, from http://www.pcigeomatics.com/geomatica-help/concepts/orthoengine_c/chapter_825.html

Proffitt, C. E., & Devlin, D. J. (2005). Long-term growth and succession in restored and

natural mangrove forests in southwestern Florida. *Wetlands Ecology and Management*, *13*(5), 531–551. https://doi.org/10.1007/s11273-004-2411-9

Proisy, C., Mougin, E., Fromard, F., & Karam, M. a. (2000). Interpretation of polarimetric radar signatures of mangrove forests. *Remote Sensing of Environment*, *71*(1), 56–66. https://doi.org/10.1016/S0034-4257(99)00064-4

Proisy, Christophe, Lrt, I. R. D., Amap, U. M. R., Française, G., Mitchell, A., & Lucas, R. (2003). Estimation of Mangrove Biomass using Multifrequency Radar Data. Application to Mangroves of French Guiana and Northern Australia. *Proceeding of the Mangrove 2003 Conference*, (May 2003), 20–24.

Quiñones, M. J., & Hoekman, D. H. (2004). Exploration of factors limiting biomass estimation by polarimetric radar in tropical forests. *IEEE Transactions on Geoscience and Remote Sensing*, *42*(1), 86–104. https://doi.org/10.1109/TGRS.2003.815402

Ranson, K. J., Sun, G., Lang, R. H., Chauhan, N. S., Cacciola, R. J., & Kilic, O. (1997). Mapping of boreal forest biomass from spaceborne synthetic aperture radar the SIR-C image components and foliage. *Journal of Geophysical Research*, *102*, 29599–29610.

Salem, M. E., & Mercer, D. E. (2012). The economic value of mangroves: A meta-analysis. *Sustainability*, *4*(3), 359–383. https://doi.org/10.3390/su4030359

Shimada, M., Isoguchi, O., Tadono, T., & Isono, K. (2009). PALSAR radiometric and geometric calibration. *IEEE Transactions on Geoscience and Remote Sensing*, *47*(12), 3915–3932. https://doi.org/10.1109/TGRS.2009.2023909

Shimada, M., & Ohtaki, T. (2010). Generating Large-Scale High-Quality SAR Mosaic Datasets: Application to PALSAR Data for Global Monitoring. *IEEE Journal of Selected Topics in Applied Earth Observations and Remote Sensing*, *3*(4), 637–656.

https://doi.org/10.1109/JSTARS.2010.2077619

Thomas, N., Lucas, R., Bunting, P., Hardy, A., Rosenqvist, A., & Simard, M. (2017). Distribution and drivers of global mangrove forest change, 1996-2010. *PLoS ONE*, *12*(6), 1–14. https://doi.org/10.1371/journal.pone.0179302

Wang, M., Madden, M., Hendy, I., Estradivari, & Ahmadia, G. N. (2017). Modeling projected changes of mangrove biomass in different climatic scenarios in the Sunda Banda Seascapes. *International Journal of Digital Earth*, *10*(4), 457–468. https://doi.org/10.1080/17538947.2016.1190411

Chapter 6

Discussion

The objective of this thesis was to understand the dynamics of mangrove forest structure and biomass in the Niger Delta. I provided local knowledge on how wood harvesting is affecting mangrove stand structure, canopy features and aboveground biomass within the region. I established the trend in biomass across a tidal gradient and a possible connection between the colonization of an invasive species and mangrove clearance. I also established a relationship between mangrove area and biomass using earth observation satellites. I specifically established a relationship between surface reflectance and canopy features; and radar backscatter and AGB. Using these relationships I estimated mangrove area and AGB over the Niger Delta for 2007 and 2017. A common theme throughout this thesis has been to understand the trend of mangrove cover, structure and AGB through field surveys and earth observations. In this chapter, I now review the key findings of this thesis and discuss the implications for 1) the control of local mangrove forests harvesting and 2) a national mangrove monitoring system.

6.1 Mangrove Forest Biomass and Structure

Mangrove forests are shaped and modified by a combination of various factors as a result of their transitory nature. Mangrove forests are not only a transition between land and sea, they also lie in transition between fresh and oceanic waters; hence their estuarine nature. The characteristics of these zones which border mangrove forest are somewhat mixed creating the peculiar nature of mangrove forests (Alongi, 2009). Mangrove forests are also shaped based on their provisional ecosystem services which results in high population density along coastal zones due to fisheries production and development. This human population in turn shapes this coastal ecosystem. Mangrove forests in the Niger Delta provide services such as shell fishes, sand for construction, wood for fuel and construction, and aesthetic purposes (Akanni *et al.,* 2017). However, unsustainable utilisation of mangrove resources can result in altering the ecosystem balance. The interaction of natural and

anthropogenic factors with mangroves results in the modification of their forests structure and biomass. The third chapter of my thesis addresses the natural variation of mangrove biomass across a tidal, distance from sea and settlement gradient. I showed evidence of a strong positive tidal influence on mangrove productivity in the Niger Delta but a negative influence from human settlements. My third chapter also showed the reduction of stand contribution to AGB due to harvesting target size of mangrove stand. This harvesting also indicated encroachment of nipa palm invasive species to affected regions.

6.1.1 Understanding the Natural Variation of Mangrove Forest Productivity

Mangrove forests show a trend in spatial distribution based on regional characteristics which is determined by the ocean basin where they are located and the geologic form of the coastal zone where they are located (Twilley *et al.*, 2018). Understanding the trend in mangrove productivity in the Niger Delta can assist in planning conservation activities which focus on highly productive regions. Mangrove forests in the Niger Delta is largely understudied in terms of productivity and its relationship with environmental gradients. This is the first study of mangroves in the Niger Delta that gives evidence of biomass across multiple gradients-tide, settlement and disturbance. I gave evidence mangrove forests structure, AGB and productivity amongst different sites differ in terms of distance from tidal ecotone and from the ocean. I also showed a potential to monitor the productivity of mangrove forests by establishing a relationship between canopy and wood properties. The rationale behind this was to give a baseline for long term monitoring of mangrove productivity from local knowledge of the ecosystem.

My thesis indicated a limiting factor to AGB in mangrove forests in the Niger Delta along a tidal gradient (**3.4.1**). Mangrove forest landscape have been shown to show a pattern along environmental gradients in Florida (Castañeda-Moya *et al.*, 2013). Castañeda-Moya *et al.*,

(2013) showed that biomass and NPP of mangrove forest showed a pattern with environmental gradients such as hydro period of tides, sulphide concentration and soil phosphorus. Although, hydro period and sulphide concentrations were not measured during my thesis, other studies in the Niger Delta have shown a gradient of soil nitrogen and phosphorus relation to mangrove species zonation (Ukpong, 2000a). The next step in this study is to include the species diversity, tidal period and soil nutrients as added parameters in understanding the trend of mangrove biomass in the Niger Delta. The establishment of permanent sampling plots (PSP) can also create a means for a long term monitoring in ecosystem productivity in mangrove forests in the Niger Delta to establish its spatial and temporal relationship with environmental factors.

My thesis indicated a weak relationship between LAI and AGB (**3.4.2**) and a stronger relationship between NDVI, LAI and AGB (**3.4.3**). These results shows a possibility in modelling carbon cycle in mangrove forests of the Niger Delta. To predict future impact of local laws, management and conservation plans; modelling carbon cycle and hence productivity of mangrove forests provides a means to merge field surveys and satellite imagery in understanding mangrove forests dynamics. However, care should always be taken when extrapolating local research to a landscape as was the case in this study. There is limited research on modelling carbon cycle in mangrove forests as a result of the complex characters involved in shaping mangrove forests. Model data fusion is a method of incorporating various models and datasets in order to better understand ecosystem functioning. Multiple source of data helps in better constraining range of input data for predicting carbon cycle pathways (Bloom and Williams, 2015). MDF has an advantage to other model techniques as it takes into account observational data together with modelled data in order to provide uncertainties and data synonymous with observations (Fox *et al.*, 2009; Williams *et al.*, 2005). My Ph. D. has presented the possibility of MDFs in carbon cycle

of mangrove forests in Nigeria. Modelled LAI-AGB, radar-AGB, NDVI-LAI and land cover classification are all viable input for ecosystem modelling of carbon cycle. Initial conditions of a spatial model may include parameters such as foliar nitrogen, canopy height, stand age, land cover, LAI and biomass (Turner *et al.*, 2004). However, this research is still limited in the relationship between nutrients and productivity, but this can be achieved by pooling various research in the region.

6.1.2 Local Wood Exploitation Effects on Mangrove Forest Structure

The economic activity within various communities surrounding mangrove forests depends on the regional ecosystem services offered by the ecosystem. A study in the Niger Delta has shown that different communities differ in the level of ecosystem services provided by mangroves which ranged from regulatory, provisioning to supporting values (Akanni *et al.*, 2017). Wood exploitation is a means of income in most coastal rural communities surrounded by forests. In **Chapter 3**, I investigated one of the rarely studied effect of wood exploitation, what is the effect of wood harvesting on mangrove stand and canopy structure? This question was motivated by both the observed wood exploitation and nipa colonisation ongoing within the study region and if a similar effect resulted when compared to other regions. Similar studies have related disturbance in mangrove forests to stand structure (Amir and Duke, 2009; Wan Norilani *et al.*, 2014). The disturbance regime was based primarily on visual evidence of current and historical mangrove clearance, and presence of indicator species (**3.2.7**). A similar disturbance classification has been done in Cameroun where branching intensity was also an included criteria for level of disturbance (Ajonina, 2008). I implied that a significant difference in contribution of different DBH size classes to AGB amongst disturbance regime would mean an effect of wood exploitation on mangrove structure, and a higher LAI variation within field plots implied uneven canopy cover resulting from disturbance. The premise that the mangrove stem size structure in undisturbed plots

showed a natural trend was based on comparison with natural forest stand dynamics from previous studies (Clarke and Kerrigan, 2000; McNicol *et al.*, 2017; Wan Norilani *et al.*, 2014). **Chapter 3** also explored another question of a likely link between wood exploitation and nipa palm colonization. I implied that the number of nipa stand within each plot would be related to the basal area removed and class size contribution to AGB. My motivation for this question was based on the absence of data and research on a critical non-native invasive species in the Niger Delta threatening extinction of mangrove forests in the Atlantic coast of West Africa.

Evidence from my thesis showed a significant effect of local wood exploitation on mangrove stand structure (**3.3.6.2**). I established that the DBH class size 15-20 cm is the target size class for harvesting in the Delta by local communities owing to its reduced contribution to AGB in disturbed plots (**3.4.4**). I also established that reduction in size class 10 to 20 cm in mangrove forests was increasing their vulnerability to nipa palm invasion (**3.4.5**). The implication of mangrove wood exploitation in the Niger Delta is that unsustainable harvesting over time will result in a complete change of mangrove ecosystem to a coastal palm vegetation. The connection between over-exploitation of forest wood products and invasion of non-native species has always existed (Moore, 2005). Change in forest structure and stand dynamics can result in the penetration of invasive species. Establishment of non-invasive species in mangrove forests can result in the difficulty of mangrove recovery long after logging has stopped (Brown and Gurevitch, 2004). Despite mangrove forests being tough ecosystems to be invaded (Lugo, 1998), Niger Delta mangroves are faced with various stressors which makes them susceptible to nipa palm which has no wide scale use within the region. Further research endeavours aimed at understanding the relationship between wood harvesting and mangrove forest structure could take into account the effect on soil nutrient and how wood exploitation affects mixed mangrove species stands. There is a huge knowledge gap between

the effects of disturbance on mangrove soil structure owing to the difficulty in sampling flooded mangrove soil.

6.2 Remote Sensing Application in Mangrove Forest Monitoring

The extensive nature of forested landscape entails the use of remote means in extracting characteristics in relation to visual and field observation. Mangrove forests have a complicated structure in both the trees and surrounding environment. The adaptive structures of mangrove trees including prop roots and aerial roots and their dense nature restricts movement and hence field surveys are difficult. The remote location of mangrove forests along the coasts also makes access to mangrove forests difficult. Further complication about field work in Niger Delta is the rural nature of the communities which makes communication of research plans difficult. However, earth observation satellites can detect leaf and woody characteristics of mangroves enabling the possibility to monitor the extent and biomass of these coastal forests spatially and temporally. Chapters 3, 4 and 5 of my thesis utilised earth observation satellites in order to estimate mangrove and nipa area in the Niger delta and estimate productivity within the region using 2007 and 2017 earth observation data.

6.2.1 Earth Observation Monitoring of Mangrove Forest Loss

Remote sensing options make use of land surface properties which makes detection of various land cover types and hence monitor change in land use viable. Mangrove forests are distinguishable in earth observation satellite because they are among the first vegetation along the coast. Mangrove forests are also intertidal ecosystems, hence the influence of coastal water also make them a little more distinguishable from more inland forests with similar foliage surface reflectance. In **chapter 4**, I attempted to estimate the current area of mangrove and nipa palm vegetation in the Niger Delta using a combination of elevation, radar and optical data. Previous estimates of mangrove biomass are from global datasets and unsupervised classification attempts (Bunting *et al.*, 2018; Fatoyinbo and Simard, 2013; Giri *et al.*, 2011; James *et al.*, 2007; Spalding *et al.*, 2010). I used over 500 GCPs as training

and test data for a supervised classification comparing two different techniques. I showed that the use of combined radar and optical data improved classification. This implies that local and regional land cover maps can be generated using different methods and compared for best accuracy with reference to land use planning in the future. Furthermore, improving the spatial resolution of the satellite products holds potential for the future of detecting fringe vegetation.

In my fourth chapter, I estimated mangrove forests and nipa palm cover in the Niger Delta in 2007 and 2017. Nipa palm cover in the Niger Delta has never been estimated using satellite imagery. My classification results confirm the relationship between mangrove structure and distance from closest settlement in my previous section where I established a link between local disturbance of mangrove forest and settlement proximity (**3.4.1; 4.4.3**). Land cover maps generated in my thesis show a similar trend compared to global mangrove cover maps (Bunting *et al.*, 2018), however I recorded about 10% higher mangrove cover. Despite, the fringing nature of nipa palm, I estimated the current cover and confirmed the spread of this mangrove palm in the delta. However, due to the influence of tide and the vegetation continuum with mangrove forests, there was high error in terms of omission and commission (**4.3.1**). The transitional nature of some land cover classes poses a problem in their identification in land cover classification (Villarreal *et al.*, 2012). Despite having GCPs from nipa and mangroves, some of nipa fringes are less than 30m in span thereby limiting the classification power of the data with base resolution 30m. This can be reduced using specific satellite products taken during low tide and finer resolution such as drones or local planes fitted with remote sensors. Future research can include the use of satellite products such as hyperspectral imagery and random forest classification methods to produce more accurate land cover maps.

I also carried out a change detection of mangrove and nipa cover between 2007 and 2017. Change detection maps showed a gradual loss of mangrove from the landward margin (4.3.3). The gradual loss of mangrove is not only linked to local disturbance but also as a result of development in the Niger Delta and increase of agricultural land in order to support the increasing population (4.4.3). Furthermore, the exponential increase of nipa area in the change detection analysis is indicative of the risk of losing mangrove forests in the Niger Delta. Future research can combine land cover maps, change detection and nipa cover with population density, logging data and development hotspots, thereby generating a vulnerability map of mangrove forests in the Niger Delta.

6.2.2 Radar Sensor Prediction of Mangrove Biomass

The ability of radar sensors to penetrate the canopy cover of forests helps in the prediction of woody biomass. In **Chapter 5**, I established the relationship between ground estimates of AGB (Chapter 3) and ALOS PALSAR backscatter. This is the first assessment of radar backscatter-AGB relationship in Nigeria. Previous biomass studies in mangrove forests in the Niger Delta has been limited to field studies (Numbere and Camilo, 2018; Nwigbo *et al.*, 2013) and global biomass maps (Avitabile *et al.*, 2015; Baccini *et al.*, 2007; Hutchison *et al.*, 2014; Saatchi *et al.*, 2011). I discovered a peculiar relationship in my thesis as there was no significant relationship with the individual bands (HH and HV) compared with other studies (Carreiras *et al.*, 2012; Cohen, 2014; Hamdan *et al.*, 2014; Mitchard *et al.*, 2012). However, I found significant relationship between AGB and HV HH ratio explaining about 55% of the variation (5.4.1). One of the reasons for the insignificant relationship with the individual bands could be as a result of the monospecific nature (*Rhizophora* spp.) of field estimates of AGB. Tidal influence and loss of forests structure resulting in reduced double bounce of the radar signal could have affected the relationship with the individual bands. To further analyse the radar-AGB relationship in chapter 5, inclusion of other mangrove species native to the

Atlantic coast of Africa can account for a wider cover of mangrove variation. Secondly, use of temporally-stamped radar signals can account for the effect of tidal influence on radar backscatter.

I applied the best relationship (a ratio of both the HV and the HV HH ratio bands) across the mangrove area in the Niger Delta I estimated in chapter 4 for both 2007 and 2017 (5.3.3). The RMSE I estimated shows the uncertainty in estimating biomass using radar backscatter. This uncertainty could be as a result of the plot size (0.25 ha) used in field plot AGB which may have not accounted for the noise (Cohen, 2014). I used a buffer of 5m to account for the noise in radar backscatter (25m resolution). Also, application of the radar-AGB relationship of certain year (2017) to a data product of a previous year (2007) may account for some backscatter error. Further research in estimating AGB from radar backscatter could make use of larger plots ~ 1ha and account for the similarity of radar backscatter of different year of collection. I restrained AGB over the mangrove landscape to 200 t ha^{-1} to avoid over-estimation of the AGB in the region. Future biomass studies should include plots with higher biomass in order to get a wider range of biomass in the region.

I recorded a reduction in total and mean AGB between 2007 and 2017 implying effect of mangrove disturbance and land use change on mangrove forests biomass (5.3.4). The objectives I set out to achieve in chapter 5 have filled a huge knowledge gap in mangrove forest biomass research in the Niger Delta. The inclusion of spatial and temporal dynamics of mangrove forests biomass can act as an input for modelling carbon cycle modelling in the Niger Delta. Secondly, carbon sequestration from restoration plans and loss from deforestation can be monitored using remote sensing means thereby generating a baseline for reporting national carbon balance.

Remote sensing of mangrove forests offers a platform for large scale monitoring of cover and biomass over time. However, my thesis encountered various setback from resolution,

cloud cover and GCPs. Future research into land cover classifications can target GCPs in transitory land classes which can make for a better differentiation quality. Secondly, the use of higher penetrative radar bands such as P-band radar which is being planned by ESA scheduled to launch in 2022 can provide a means of monitoring forest carbon (de Selding, 2016). Hyperspectral imagery can also improve the differentiation of mangrove and nipa palm and can considered in future research. However, spatial analysis is only as good as the ground data used as input (Hussain *et al.*, 2013). Hence, field plots used in establishing radar-biomass models should have enough information by increasing the area of the plots.

6.3 Future Implications for Mangrove Forests Research in the Niger Delta

The global community has shown interests in mangrove forests as a viable means for climate change mitigation because of their potential in storing carbon within their biomass and soil. Mangrove forests can play a huge role in the global carbon balance because conservation and restoration efforts can result in boosting carbon sink over time. However, mangrove loss from land use change and invasive species can result in the loss of carbon stored over longer timescales (Murray and Vegh, 2012). The Niger Delta is poised for more loss of mangrove due to the plethora of factors affecting mangrove forests. Local laws can be put in place to control unsustainable mangrove harvesting while on a regional context, a national mangrove action plan can monitor mangrove loss and threat and hence vulnerability.

6.3.1 Control of Local Mangrove Forests Harvesting

Managing the harvesting of wood products is difficult in communities where their main economy is generated from the sale of fuel wood. Some of the ecosystem services provided by mangrove forests is timber products and fuelwood (Miththapala, 2008). However, the threat exists in the unsustainable harvesting of mangrove wood resources in the Niger Delta. The unsustainable use of wood products could have been as a result of a shift in economic activity resulting from over-exploitation of a previous resource. This shift in economic activity has also been linked with impoverished communities looking for a means of survival (Polidoro *et al.*, 2010). Countries have established laws in order to manage the vulnerability of mangrove forests to deforestation (Lugo *et al.*, 2014). As an example, Fiji Forest Policy Statement of 2007 prohibits the commercial harvesting of mangrove trees by the department of Forestry (Momoemausu-Siamomua, 2013). Another example is the target diameter harvesting (TDH) system; a method of continuous cover forestry (CCF) which has been employed in various natural forests (Drössler *et al.*, 2017; Perry, 2013; Sterba and Zingg,

2001). This law can control mangrove stand harvesting maximizing both economic and ecological benefits. The combined effect of the high quality timber product from mangrove species, over-exploitation and the situation of mangrove forests in local communities requires a means of managing mangrove harvesting especially in areas with no laws.

The current environmental law guiding Nigeria is the National Environmental Standards and Regulations Enforcement Agency (NESREA) which is an offshoot of the Federal Ministry of Environment, established in 2007. NESREA replaced the Federal Environmental Protection Agency (FEPA) Act Decree in 1988 but repealed in 2004. However, there is no mention of mangrove forests or coastal vegetation within its regulations considering Nigeria having the fourth largest mangrove in the world. The NESREA act also doesn't take part in oil spills monitoring which could be a flaw on laws governing mangrove forest management in Nigeria (Stevens, 2011). State governments have liaised with international organisations such as the Centre for Information and Development in Cross River State liaising with the UN-REDD programme, the United Nations Development Programme (UNDP)- Global Environment Facility (GEF) Small Grants Programme (SGP) in mangrove replanting, generating by-laws and alternative income source (Edet, 2018). Despite the efforts of the government, mangrove harvesting laws may be best managed by local communities.

Community-based mangrove forest management may offer the best means of creating laws or restrictions for mangrove harvesting. This local means of management stems from most ownership rights of mangrove forests belonging to local communities (Lugo *et al.*, 2014). Support from local and international environmental agencies can assist in the training, funding and monitoring of the processes involved in restoration and conservation. Local community knowledge of mangrove benefits are scarce resulting in poor management plans and decisions. Some communities in Ete eventually get stipend for a certain mangrove region to be cleared for commercial purposes (verbal communication, 2017). This location during

my field survey of thesis understood the importance of mangrove forests but complained of the unavailability of an alternative source of income, hence, their fear on having some restriction on mangrove wood exploitation. Feka *et al.*, (2011) suggested education of local communities and providence of alternative source of income in order to sustain mangroves (Feka *et al.*, 2011). However, most local communities have little access to other sources of income in rural communities in the Niger Delta especially in regions with families to feed. Hence, the need to proffer sustainable harvesting of mangrove stands in a sort of silviculture may be the only alternative to control mangrove wood overexploitation.

6.3.2 National Mangrove Monitoring System

The term blue carbon has been coined for carbon sink in the oceans including coastal vegetation such as sea grasses, tidal marshes and mangrove forests. The term was an attempt by the internal community to call to attention the risk of releasing carbon stored within these ecosystems as a result of deforestation. They intended to achieve this by providing options for funding, management and strategies in order to protect these ecosystems (Nellemann *et al.*, 2009). The International Blue Carbon Initiative is a global program established to provide both scientific and policy advise to regional projects. In order to disseminate this advice, various blue carbon projects aimed at a regional assessment of mangrove resources were established by the initiative. These projects aim to mitigate climate change in these ecosystems while also implementing carbon finance mechanisms such as the REDD+ and UNFCCC mechanisms (Wylie *et al.*, 2016). Wylie *et al.*, (2016) analysed four of these projects in Kenya, Vietnam, Madagascar and India, and discovered a common theme of livelihood aspect inclusion and ensured that leakages didn't occur. However, their analysis showed that these projects are properly shaped based on the regional assessments of the needs within each region.

Regional management of mangrove forests is the most promising route in terms of conservation and restoration of this ecosystem because of the local properties. Mangrove forests show a latitudinal trend in species diversity, biomass and area (Twilley *et al.*, 1992). Also, mangrove forests outline the coasts of various ocean basins hence are characterised by inherent coastal structures, tidal regime, population densities and nutrient loading (Twilley *et al.*, 2018). These various regional characteristic combine to shape the dynamics of productivity, threats, anthropogenic effects and climate change effects. Hence, the most effective means is following a regional approach in managing the threats, plan conservation plans and execute restoration projects in mangrove forests. However, there is no report of a blue carbon project in Nigeria despite the number of threats being faced by the largest mangrove area in Africa.

There is a huge potential for mangrove REDD+ activities in the Nigeria using a blue carbon project baseline. The potential can make use of a diverse stakeholder involvement- local communities, the government and oil exploration companies. My thesis extended over five states of the coastal zone out of six where mangroves are found. This spatial coverage of my thesis with the involvement of local communities and the government poses a possibility for future liaising for a national monitoring system. This potential is further heightened by the diverse coastal geomorphology of the Nigerian coastline ranging from lagoonal system in the west, deltaic formations in central coasts and estuarine morphology in the east (Hughes and Hughes, 1992). However, the only hindrance to regional mangrove forest management is understanding the underlying ecosystem function of these coastal forests.

6.4 Concluding Remarks

To predict future impact of local laws, management and conservation plans, modelling carbon cycle and hence productivity of mangrove forests provides a means to merge field surveys and satellite imagery in understanding mangrove forests dynamics. Modelling carbon cycle of Nigerian mangrove forests requires a technique that incorporates various type and forms of data in building an ecosystem model. Model data fusion is a method of incorporating various models and datasets in order to better understand ecosystem functioning. Multiple source of data helps in better constraining range of input data for predicting carbon cycle pathways (Bloom and Williams, 2015). My Ph. D. has presented the possibility of MDFs in carbon cycle of mangrove forests in Nigeria. Modelled LAI-AGB, radar-AGB, NDVI-LAI and land cover classification are all viable input for ecosystem modelling of carbon cycle.

Future research on mangrove forests can incorporate long term monitoring of mangrove forest structure and its relationship with nutrients. Secondly, the use of earth observation satellite with finer resolution can assist in intricate analysis on the drivers of mangrove forest change.

6.5 References

Ajonina, G. N. (2008). Inventory and Modelling Mangrove Forest Stand Dynamics Following Different Levels of Wood Exploitation Pressures in the Douala-Edea Atlantic Coast of Cameroon, Central Africa, 215. Retrieved from http://www.freidok.uni-freiburg.de/volltexte/6132/pdf/Gordon_N._Ajonina_Thesis.pdf

Akanni, A., Onwuteaka, J., Uwagbae, M., Mulwa, R., & Elegbede, I. O. (2017). *The Values of Mangrove Ecosystem Services in the Niger Delta Region of Nigeria*. *The Political Ecology of Oil and Gas Activities in the Nigerian Aquatic Ecosystem* (Vol. 1980). Elsevier Inc. https://doi.org/10.1016/B978-0-12-809399-3.00025-2

Alongi, D. M. (2009). *The energetics of mangrove forests*. *The Energetics of Mangrove Forests*. https://doi.org/10.1007/978-1-4020-4271-3

Amir, A., & Duke, N. (2009). A forever young ecosystem: light gap creation and turnover of subtropical mangrove forests in Moreton Bay, Southeast Queensland, Australia. *11th Pacific Science Inter-Congress in Conjunction with the 2nd Symposium on French Research in the Pacific*, 1–5.

Avitabile, V., Herold, M., Heuvelink, G. B. M., Lewis, S. L., Phillips, O. L., Asner, G. P., … Willcock, S. (2015). An integrated pan-tropical biomass map using multiple reference datasets. *Global Change Biology*, n/a-n/a. https://doi.org/10.1111/gcb.13139

Baccini, a, Friedl, M. a, Woodcock, C. E., & Zhu, Z. (2007). Scaling field data to calibrate and validate moderate spatial resolution remote sensing models. *Photogrammetric Engineering Remote Sensing*, *73*(8), 945–954. https://doi.org/10.14358/PERS.73.8.945

Bloom, a. a., & Williams, M. (2015). Constraining ecosystem carbon dynamics in a data-limited world: integrating ecological “common sense” in a model–data fusion

framework. *Biogeosciences*, *12*(5), 1299–1315. https://doi.org/10.5194/bg-12-1299-2015

Brown, K. A., & Gurevitch, J. (2004). Long-term impacts of logging on forest diversity in Madagascar. *Proceedings of the National Academy of Sciences*, *101*(16), 6045–6049. https://doi.org/10.1073/pnas.0401456101

Bunting, P., Rosenqvist, A., Lucas, R. M., Rebelo, L.-M., Hilarides, L., Thomas, N., … Finlayson, C. M. (2018). The Global Mangrove Watch-A New 2010 Global Baseline of Mangrove Extent, *10*, 1669. https://doi.org/10.3390/rs10101669

Carreiras, J. M. B., Vasconcelos, M. J., & Lucas, R. M. (2012). Understanding the relationship between aboveground biomass and ALOS PALSAR data in the forests of Guinea-Bissau (West Africa). *Remote Sensing of Environment*, *121*, 426–442. https://doi.org/10.1016/j.rse.2012.02.012

Castañeda-Moya, E., Twilley, R. R., & Rivera-Monroy, V. H. (2013). Allocation of biomass and net primary productivity of mangrove forests along environmental gradients in the Florida Coastal Everglades, USA. *Forest Ecology and Management*, *307*, 226–241. https://doi.org/10.1016/j.foreco.2013.07.011

Clarke, P. J., & Kerrigan, R. A. (2000). Do forest gaps influence the population structure and species composition of mangrove stands in northern Australia? *Biotropica*, *32*(4), 642–652. https://doi.org/10.1111/j.1744-7429.2000.tb00511.x

Cohen, R. (2014). Estimating the above-ground biomass of mangrove forests in Kenya. *Ph.D. Thesis*, 122.

de Selding, P. (2016). Airbus UK to build Europe's Biomass satellite, featuring first use of P-band radar. Retrieved January 29, 2019, from http://spacenews.com/airbus-uk-to-

build-europes-biomass-satellite-featuring-first-use-of-p-band-radar/

Drössler, L., Fahlvik, N., Wysocka, N. K., Hjelm, K., & Kuehne, C. (2017). Natural regeneration in a multi-layered Pinus sylvestris-Picea abies forest after target diameter harvest and soil scarification. *Forests*, *8*(2), 1–14. https://doi.org/10.3390/f8020035

Edet, C. (2018). Preserving mangrove forest ecosystem in Cross River – EnviroNews Nigeria –. Retrieved December 16, 2018, from https://www.environewsnigeria.com/preserving-mangrove-forest-ecosystem-in-cross-river/

Fatoyinbo, T. E., & Simard, M. (2013). Height and biomass of mangroves in Africa from ICESat/GLAS and SRTM. *International Journal of Remote Sensing*, *34*(2), 668–681. https://doi.org/10.1080/01431161.2012.712224

Feka, N. Z., Manzano, M. G., & Dahdouh-Guebas, F. (2011). The effects of different gender harvesting practices on mangrove ecology and conservation in Cameroon. *International Journal of Biodiversity Science, Ecosystem Services and Management*, *7*(2), 108–121. https://doi.org/10.1080/21513732.2011.606429

Fox, A., Williams, M., Richardson, A. D., Cameron, D., Gove, J. H., Quaife, T., … Van Wijk, M. T. (2009). The REFLEX project: Comparing different algorithms and implementations for the inversion of a terrestrial ecosystem model against eddy covariance data. *Agricultural and Forest Meteorology*, *149*(10), 1597–1615. https://doi.org/10.1016/j.agrformet.2009.05.002

Giri, C., Ochieng, E., Tieszen, L. L., Zhu, Z., Singh, A., Loveland, T., … Duke, N. (2011). Status and distribution of mangrove forests of the world using earth observation satellite

data. *Global Ecology and Biogeography*, *20*(1), 154–159. https://doi.org/10.1111/j.1466-8238.2010.00584.x

Hamdan, O., Khali Aziz, H., & Mohd Hasmadi, I. (2014). L-band ALOS PALSAR for biomass estimation of Matang Mangroves, Malaysia. *Remote Sensing of Environment*, *155*, 69–78. https://doi.org/10.1016/j.rse.2014.04.029

Hughes, R. H., & Hughes, J. S. (1992). *A Directory of African Wetlands* (34th ed.). IUCN, Gland Switzerland and Cambridge, UK; UNEP, Nairobi, Kenya and WCMC, Cambridge, UK.

Hussain, M., Chen, D., Cheng, A., Wei, H., & Stanley, D. (2013). Change detection from remotely sensed images: From pixel-based to object-based approaches. *ISPRS Journal of Photogrammetry and Remote Sensing*, *80*, 91–106. https://doi.org/10.1016/j.isprsjprs.2013.03.006

Hutchison, J., Manica, A., Swetnam, R., Balmford, A., & Spalding, M. (2014). Predicting global patterns in mangrove forest biomass. *Conservation Letters*, *7*(3), 233–240. https://doi.org/10.1111/conl.12060

James, G. K., Adegoke, J. O., Saba, E., Nwilo, P., & Akinyede, J. (2007). Satellite-Based Assessment of the Extent and Changes in the Mangrove Ecosystem of the Niger Delta. *Marine Geodesy*, *30*(3), 249–267. https://doi.org/10.1080/01490410701438224

Lugo, A. E., Medina, E., & McGinley, K. (2014). Issues and challenges of mangrove conservationin the anthropocene. Desafíos de la conservación del mangle en el Antropoceno. *Madera y Bosques*, *20*, 11–38. Retrieved from http://www1.inecol.edu.mx/myb/resumeness/no.esp.2014/myb20esp1138.pdf

Lugo, Ariel E. (1998). Mangrove Forests: a Tough System to Invade but an Easy one to

Rehabilitate. *Marine Pollution Bulletin*, *37*(8–12), 427–430. https://doi.org/10.1002/jssc.201700030

McNicol, I. M., Ryan, C. M., Dexter, K. G., Ball, S. M. J., & Williams, M. (2017). Aboveground Carbon Storage and Its Links to Stand Structure, Tree Diversity and Floristic Composition in South-Eastern Tanzania. *Ecosystems*. https://doi.org/10.1007/s10021-017-0180-6

Mitchard, E. T. a., Saatchi, S. S., White, L. J. T., Abernethy, K. a., Jeffery, K. J., Lewis, S. L., … Meir, P. (2012). Mapping tropical forest biomass with radar and spaceborne LiDAR in Lopé National Park, Gabon: overcoming problems of high biomass and persistent cloud. *Biogeosciences*, *9*(1), 179–191. https://doi.org/10.5194/bg-9-179-2012

Miththapala, S. (2008). *Mangroves. Coastal Ecosystems Series Volume 2* (Vol. 2). https://doi.org/10.1016/B978-012374473-9.00090-4

Momoemausu-Siamomua, M. (2013). *Review of Policy and Legislation Relating to the Use and Management of Mangrove Ecosystems in Samoa*.

Moore, B. a. (2005). *Alien invasive species: impacts on forests and forestry*.

Murray, B. C., & Vegh, T. (2012). Incorporating Blue Carbon as a Mitigation Action under the United Nations Framework Convention on Climate Change Technical Issues to Address. *Nicholas Institute Report*, (November).

Nellemann, C., Corcoran, E., Duarte, C. M., Valdés, L., De Young, C., Fonseca, L., & Grimsditch, G. (2009). *Blue Carbon - The Role of Healthy Oceans in Binding Carbon*. *Environment*. Retrieved from http://books.google.com/books?id=onCVCHQl4RoC

Numbere, A. O., & Camilo, G. R. (2018). Structural characteristics, above-ground biomass and productivity of mangrove forest situated in areas with different levels of pollution

in the Niger Delta, Nigeria. *African Journal of Ecology*, (March), 1–11. https://doi.org/10.1111/aje.12519

Nwigbo, S. C., Azaka, O. A., Chukwuneke, J. L., & Nwadike, C. E. (2013). Establishing Allometric Relationships Using Crown Diameter for Estimating Above Ground Combustible Fuels in Southern Nigerian Mangrove Vegetations. *International Journal of Multidisciplinary Sciences and Engineering*, *4*(7), 43–52.

Perry, B. C. (2013). Economic analysis of a target diameter harvesting system in radiata pine.

Polidoro, B. a., Carpenter, K. E., Collins, L., Duke, N. C., Ellison, A. M., Ellison, J. C., … Yong, J. W. H. (2010). The loss of species: Mangrove extinction risk and geographic areas of global concern. *PLoS ONE*, *5*(4), e10095. https://doi.org/10.1371/journal.pone.0010095

Saatchi, S. S., Harris, N. L., Brown, S., Lefsky, M., Mitchard, E. T. a., Salas, W., … Morel, A. (2011). Benchmark map of forest carbon stocks in tropical regions across three continents. *Proceedings of the National Academy of Sciences*, *108*(24), 9899–9904. https://doi.org/10.1073/pnas.1019576108

Spalding, M., Kainuma, M., & Collins, L. (2010). Book review: World atlas of mangroves. *Wetlands*. https://doi.org/10.1007/s13157-011-0224-1

Sterba, H., & Zingg, A. (2001). Target diameter harvesting - A strategy to convert even-aged forests. *Forest Ecology and Management*, *151*(1–3), 95–105. https://doi.org/10.1016/S0378-1127(00)00700-3

Stevens, L. (2011). the Illusion of Sustainable Development : How Nigeria ’ S Environmental Laws Are Failing the Niger Delta. *The Vermont Law Review*, *36*(2009), 388–407.

Retrieved from http://lawreview.vermontlaw.edu/wp-content/uploads/2012/02/15-Stevens-Book-2-Vol.-36.pdf

Turner, D. P., Ollinger, S. V., & Kimball, J. S. (2004). Integrating Remote Sensing and Ecosystem Process Models for Landscape- to Regional-Scale Analysis of the Carbon Cycle. *BioScience*, *54*(6), 573. https://doi.org/10.1641/0006-3568(2004)054[0573:IRSAEP]2.0.CO;2

Twilley, R. R., Chen, R. H., & Hargis, T. (1992). Carbon sinks in mangroves and their implications to carbon budget of tropical coastal ecosystems. *Water, Air, and Soil Pollution*, *64*(1–2), 265–288. https://doi.org/10.1007/BF00477106

Twilley, Robert R., Rovai, A. S., & Riul, P. (2018). Coastal morphology explains global blue carbon distributions. *Frontiers in Ecology and the Environment*, *16*(9), 503–508. https://doi.org/10.1002/fee.1937

Ukpong, I. E. (2000). Ecological classification of Nigerian mangrove using soil nutrient gradient analysis. *Wetland Ecology and Management*, (8), 263–272.

Villarreal, M. L., van Leeuwen, W. J. D., & Romo-Leon, J. R. (2012). Mapping and monitoring riparian vegetation distribution, structure and composition with regression tree models and post-classification change metrics. *International Journal of Remote Sensing*, *33*(13), 4266–4290. https://doi.org/10.1080/01431161.2011.644594

Wan Norilani, W. I., Wan Juliana, W. A., Latiff, A., & Salam, M. R. (2014). Community structure at two compartments of a disturbed mangrove forests at pulau langkawi. *AIP Conference Proceedings*, *1614*, 790–794. https://doi.org/10.1063/1.4895303C

Williams, M., Schwarz, P. A., Law, B. E., Irvine, J., & Kurpius, M. R. (2005). An improved analysis of forest carbon dynamics using data assimilation. *Global Change Biology*,

11(1), 89–105. https://doi.org/10.1111/j.1365-2486.2004.00891.x

Wylie, L., Sutton-Grier, A. E., & Moore, A. (2016). Keys to successful blue carbon projects: Lessons learned from global case studies. *Marine Policy*, *65*, 76–84. https://doi.org/10.1016/j.marpol.2015.12.020

Appendices

Appendix I: Summary of Plot data (Disturbance regime as summarized in Table 3.1)

Plot ID	Site	Transects	Distance from sea (km)	Distance from Tidal Channel (m)	Distance from Closest settlement (km)	Disturbance Regime	Mean height (m)	Leaf Area Index mean (variance)	Canopy Cover (%)	Stem Density (trees ha^{-1})	Basal Area (m^2 ha^{-1})	Proportion Removed	Aboveground Biomass (t ha^{-1})
E1A	Ete	Ete1	18.6	85	1.6	HE	13.0	1.14 (1.17)	57.12	739	5.21	0.81	44.60
E1B	Ete	Ete1	18.7	105	1.7	HE	13.0	0.89 (0.48)	53.27	547	5.77	0.79	57.15
E1C	Ete	Ete1	18.7	110	1.7	HE	11.8	2.41 (0.11)	82.94	899	7.44	0.73	66.30
E2A	Ete	Ete2	18.2	35	1.1	HE	9.9	1.27 (1.08)	60.89	430	4.83	0.82	50.22
E2B	Ete	Ete2	18.0	50	1.0	HE	10.8	1.62 (1.40)	69.39	650	6.34	0.77	63.24
E3A	Ete	Ete3	18.9	35	2.0	Und	17.2	2.08 (0.21)	80.06	4037	27.24	0.00	241.23
E3B	Ete	Ete3	18.9	100	2.0	Und	17.6	2.06 (0.10)	81.96	1571	14.16	0.48	137.87
E3C	Ete	Ete3	19.0	130	1.9	Und	16.6	2.08 (0.02)	81.94	1380	15.3	0.44	152.19
E4A	Ete	Ete4	18.9	35	2.0	Und	12.4	2.40 (0.05)	84.32	1988	9.58	0.65	75.33
E4B	Ete	Ete4	18.9	100	1.9	Und	16.6	1.88 (0.29)	76.20	1938	14.35	0.47	127.78

E5A	Ete	Ete5	18.9	30	1.8	ME	12.4	1.42 (0.33)	70.28	1439	15.98	0.41	166.02
E5B	Ete	Ete5	19.0	75	1.7	ME	14.1	1.62 (0.68)	72.28	2122	15.05	0.45	127.95
K1A	Kono	Kono	20.9	30	0.1	Und	17.7	1.78 0.01)	75.23	1089	15.24	0.00	159.33
K1B	Kono	Kono	20.9	30	0.1	Und	17.9	1.56 (0.01)	73.24	698	11.93	0.24	125.83
O1A	Oproama	Oproama1	67.5	45	0.8	HE	10.6	2.02 (0.70)	78.71	218	2.06	0.57	18.97
O1B	Oproama	Oproama1	67.5	105	0.9	HE	8.4	1.07 (0.52)	60.16	234	2.07	0.57	18.73
O1C	Oproama	Oproama1	67.6	185	1.0	HE	6.8	0.46 (0.08)	38.67	204	1.36	0.60	11.06
O2A	Oproama	Oproama2	67.3	45	0.7	HE	11.9	1.48 (0.06)	73.45	516	3.82	0.49	32.99
O2B	Oproama	Oproama2	67.4	105	0.8	HE	12.9	0.59 (0.26)	45.64	555	3.67	0.50	30.15
O2C	Oproama	Oproama2	67.5	170	0.9	HE	7.0	0.59 (0. 09)	46.69	299	1.78	0.58	14.20
O3A	Oproama	Oproama3	68.2	42	0.3	ME	11.8	0.73 (0.21)	51.33	530	4	0.49	34.64
O3B	Oproama	Oproama3	68.2	125	0.4	ME	9.7	0.58 (0.01)	44.17	663	5.04	0.44	43.16
O4A	Oproama	Oproama4	67.5	40	0.9	Und	19.6	1.43 (0.54)	71.06	1187	15.65	0.00	157.61
O4B	Oproama	Oproama4	67.6	112	1.0	Und	14.2	2.25 (0.46)	82.37	822	9.95	0.24	97.52
O4C	Oproama	Oproama4	67.7	171	1.1	ME	10.6	0.82 (0.06)	52.06	559	4.45	0.47	39.28

Appendix II: Plot classification into different disturbance regime with criteria involved in classification.

Plot ID	Location	Evidence of disturbance	Canopy Openness	Undergrowth	The density of stem ≥ 20cm DBH	Nipa (ratio)	Basal Area (m^2 ha^{-1})	The proportion of basal area removed	Aboveground Biomass (t ha^{-1})	Disturbance Regime
E1A	Ete	Yes	42.88	Present	1.1	25 (13%)	5.21	0.81	44.60	**HE**
E1B	Ete	Yes	46.73	Present	2.7	27 (15%)	5.77	0.79	57.15	**HE**
E1C	Ete	Yes	17.06	Present	1.2	33 (13%)	7.44	0.73	66.30	**HE**
E2A	Ete	Yes	39.11	Present	9.3	23 (20%)	4.83	0.82	50.22	**HE**
E2B	Ete	Yes	30.61	Present	4.6	31 (18%)	6.34	0.77	63.24	**HE**
E3A	Ete	No	19.94	Absent	1.7	2(0.4%)	27.24	0.00	241.23	**Und**
E3B	Ete	No	18.04	Absent	3.8	3 (0.6%)	14.16	0.48	137.87	**Und**
E3C	Ete	No	18.06	Absent	3.8	0 (0%)	15.3	0.44	152.19	**Und**
E4A	Ete	No	15.68	Absent	0.3	5 (1.3%)	9.58	0.65	75.33	**Und**
E4B	Ete	No	23.8	Absent	1.2	3 (0.7%)	14.35	0.47	127.78	**Und**
E5A	Ete	Yes	29.72	Present	5.8	6 (1.9%)	15.98	0.41	166.02	**ME**
E5B	Ete	Yes	27.72	Present	0.2	15(2.7%)	15.05	0.45	127.95	**ME**
K1A	Kono	No	24.77	Absent	5	0 (0%)	15.24	0.00	159.33	**Und**
K1B	Kono	No	26.76	Absent	9.7	6 (3.1%)	11.93	0.24	125.83	**Und**
O1A	Oproama	Yes	21.29	Present	1.4	0 (0%)	2.06	0.57	18.97	**HE**
O1B	Oproama	Yes	39.84	Present	3.0	0 (0%)	2.07	0.57	18.73	**HE**
O1C	Oproama	Yes	61.33	Present	0	0 (0%)	1.36	0.60	11.06	**HE**
O2A	Oproama	Yes	26.55	Present	0.6	0 (0%)	3.82	0.50	32.99	**HE**
O2B	Oproama	Yes	54.36	Present	0	0 (0%)	3.67	0.50	30.15	**HE**
O2C	Oproama	Yes	53.31	Present	0	0 (0%)	1.78	0.58	14.20	**HE**
O3A	Oproama	No	48.67	Present	0.9	0 (0%)	4	0.49	34.64	**ME**
O3B	Oproama	No	55.83	Present	0	0 (0%)	5.04	0.44	43.16	**ME**

O4A	Oproama	No	28.94	Absent	6.1	0 (0%)	15.65	0.00	157.61	**Und**
O4B	Oproama	No	17.63	Absent	3	0 (0%)	9.95	0.24	97.52	**Und**
O4C	Oproama	No	47.94	Absent	0.5	0 (0%)	4.45	0.47	39.28	**ME**

Appendix III: Confusion Matrix of the 2017 SVM Radial Basis Function kernel Land Cover Classification of the Niger Delta.

	Ground Truth (Pixels)						
Class	**surface water**	**agricultural land**	**rain forest**	**mangrove forest**	**nipa palm**	**built up areas**	**Total**
Unclassified	0	0	0	0	0	0	0
surface water	**399**	0	0	33	48	0	480
agricultural land	0	**296**	0	0	0	0	296
rain forest	0	0	**476**	9	7	0	492
mangrove forest	0	0	2	**343**	210	0	555
nipa palm	0	0	0	7	**52**	0	59
built up areas	0	2	0	1	1	**305**	309
Total	399	298	478	393	318	305	**2191**
	Ground Truth (Percent)						
Class	**surface water**	**agricultural land**	**rain forest**	**mangrove forest**	**nipa palm**	**built up areas**	**Total**
Unclassified	0	0	0	0	0	0	0
surface water	**100**	0	0	8.4	15.09	0	21.91
agricultural land	0	**99.33**	0	0	0	0	13.51
rain forest	0	0	**99.58**	2.29	2.2	0	22.46
mangrove forest	0	0	0.42	**87.28**	66.04	0	25.33
nipa palm	0	0	0	1.78	**16.35**	0	2.69
built up areas	0	0.67	0	0.25	0.31	**100**	14.1
Total	100	100	100	100	100	100	**100**

Appendix IV: Confusion Matrix of the 2017 SVM Polynomial kernel Land Cover Classification of the Niger Delta.

	Ground Truth (Pixels)						
Class	**surface water**	**agricultural land**	**rain forest**	**mangrove forest**	**nipa palm**	**built up areas**	**Total**
Unclassified	0	0	0	0	0	0	0
surface water	**399**	0	0	33	52	0	484
agricultural land	0	**296**	0	0	0	0	296
rain forest	0	0	**476**	9	7	0	492
mangrove forest	0	0	2	**344**	209	0	555
nipa palm	0	0	0	6	**50**	0	56
built up areas	0	2	0	1	0	**305**	308
Total	399	298	478	393	318	305	**2191**
	Ground Truth (Percent)						
Class	**surface water**	**agricultural land**	**rain forest**	**mangrove forest**	**nipa palm**	**built up areas**	**Total**
Unclassified	0	0	0	0	0	0	0
surface water	**100**	0	0	8.4	16.35	0	22.09
agricultural land	0	**99.33**	0	0	0	0	13.51
rain forest	0	0	**99.58**	2.29	2.2	0	22.46
mangrove forest	0	0	0.42	**87.53**	65.72	0	25.33
nipa palm	0	0	0	1.53	**15.72**	0	2.56
built up areas	0	0.67	0	0.25	0	**100**	14.06
Total	100	100	100	100	100	100	**100**

Appendix V: Change Detection Statistics in area and percentage cover of the land cover classes between 2007 and 2017.

Area (Hectares)									
Year		**2007**						**Row Total**	**Class Total**
	Land Cover Classes	**Surface water**	**Agricultural land**	**Tropical Forest**	**Mangrove forest**	**Nipa palm**	**Built up areas**		
2017	**Surface water**	1,771,499	4,777	15,490	23,623	268	8,794	1,824,452	1,824,452
	Agricultural land	4,696	1,674,915	580,392	11,821	40	146,065	2,417,929	2,417,928
	Tropical Forest	4,744	257,419	2,030,743	223,528	465	33,020	2,549,919	2,549,919
	Mangrove forest	33,277	8,682	114,983	629,668	355	14,810	801,774	801,774
	Nipa palm	1,427	1,284	1,256	5,715	29	1,733	11,444	11,444
	Built up areas	12,862	226,639	146,221	17,192	283	190,563	593,759	593,759
Class Total		1,828,504	2,173,716	2,889,083	911,548	1,441	394,985		
Class Changes		57,005	498,802	858,340	281,880	1,412	204,422		
Image Difference		- 4,053	244,212	- 339,164	-109,774	10,004	198,774		
Percentages (%)									
2017	**Surface water**	96.88	0.22	0.54	2.59	18.62	2.23	100.00	100.00
	Agricultural land	0.26	77.05	20.09	1.30	2.79	36.98	100.00	100.00
	Tropical Forest	0.26	11.84	70.29	24.52	32.31	8.36	100.00	100.00

	Mangrove forest	1.82	0.40	3.98	69.08	24.62	3.75	100.00	100.00
	Nipa palm	0.08	0.06	0.04	0.63	2.01	0.44	100.00	100.00
	Built up areas	0.70	10.43	5.06	1.89	19.66	48.25	100.00	100.00
Class Total		100.00	100.00	100.00	100.00	100.00	100.00	0.00	0.00
Class Changes		3.12	22.95	29.71	30.92	97.99	51.75	0.00	0.00
Image Difference		-0.22	11.24	-11.74	-12.04	694.43	50.33	0.00	0.00

Appendix VI: Percentage change of AGB classes in Niger Delta between 2007 and 2017.

AGB (Mg ha^{-1})		2007 (%)					
		AGB 0-50	**AGB 50-100**	**AGB 100-150**	**AGB 150-200**	**Row Total**	**Class Total**
2017 (%)	**Deforestation**	23	30	41	35	4	100
	AGB 0-50	36	12	7	8	71	100
	AGB 50-100	31	40	25	18	79	100
	AGB 100-150	6	11	14	14	89	100
	AGB 150-200	4	7	13	24	90	100
	Class Total	100	100	100	100	0	0
	Class Changes	64	60	86	76	0	0
	Percentage change	-14	7	-32	-37	0	0

Appendix VII: Net loss of Percentage change of AGB classes in Niger Delta between 2007 and 2017.

Region	2007 Total AGB ($X10^6$ Mg)	Net loss ($X10^6$ Mg)	Total Regrowth $X10^6$ Mg (Median ± SD Mg ha^{-1} yr^{-1})	Total Minor Losses $X10^6$ Mg % of total loss (Median ± SD Mg ha^{-1} yr^{-1})	Total Degradation $X10^6$ Mg % of total loss (Median ± SD Mg ha^{-1} yr^{-1})	Total Deforestation $X10^6$ Mg % of total loss (Median ± SD Mg ha^{-1} yr^{-1})	Total loss $X10^6$ Mg
Akwa Ibom	2.5	1.8	0.1 (1.9± 1.9)	0.01- 1 (0.5 ± 0.7)	0.3- 13 (3.8 ± 3.8)	1.6- 86 (8 ± 5.3)	1.9
Bayelsa	27.5	10.8	2.3- (2.4± 2.0)	0.3- 2 (0.5± 0.8)	3.0- 23 (4.5± 3.6)	9.8- 75 (10 ± 5.4)	13.1
Cross River	2.8	1.5	0.1 (2.3± 2.0)	0.03- 2 (0.7± 0.9)	0.3- 21 (4.8± 3.4)	1.3- 78 (9.2 ± 4.9)	1.7
Delta	25.7	12.2	2.2 (2.2± 1.9)	0.2- 1 (0.5± 4.1)	3.0- 21 (4.6± 4.1)	11.2- 78 (9.3 ± 5.6)	14.4
Rivers	21	11.7	2.7 (2.5± 1.9)	0.2- 3 (0.7± 0.8)	2.9- 33 (4.7± 3.7)	5.6- 64 (8.6 ± 5.8)	8.8
Niger Delta	82.4	27.5	7.7 (2.2± 2.0)	0.7- 2 (0.6 ± 0.8)	10- 28 (13.3 ± 3.8)	24.4- 69 (9.3 ± 5.6)	35.1

Appendix VIII: AGB Contribution of Mangrove forests classes in the Niger Delta for 2007 and 2017.

	Percentage Reduction from 2007	Total Loss	Total gain	Net change	Percentage Deforestation	Percentage Degradation	Percentage Gain
>100 Mg ha^{-1}	61%	- 29,205,325	1,071,368	- 28,133,957	71%	27%	2%
50- 100 Mg ha^{-1}	30%	- 9,862,112	2,639,589	- 7,222,522	80%	17%	11%
<50 Mg ha^{-1}	9%	- 2,188,857	3,901,289	1,712,432	83%	14%	53%

	Year	Area coverage (ha)	Percentage Area	Total AGB (Mg)	Percentage AGB contribution	Mean (Mg ha^{-1})	Standard deviation (Mg ha^{-1})	Median (Mg ha^{-1})
>100 Mg ha^{-1}	**2017**	213,234	27%	32,810,379	50%	154.0	37.9	148.2
	2007	326,344	36%	50,760,250	61%	155.7	37.0	151.8
50- 100 Mg ha^{-1}	**2017**	357,705	46%	26,595,873	41%	74.4	13.3	74.9
	2007	333,165	37%	24,513,929	30%	73.7	14.1	72.9
<50 Mg ha^{-1}	**2017**	214,805	27%	5,848,470	9%	27.3	14.9	28.8
	2007	251,412	28%	7,329,047	9%	29.2	13.4	30.6